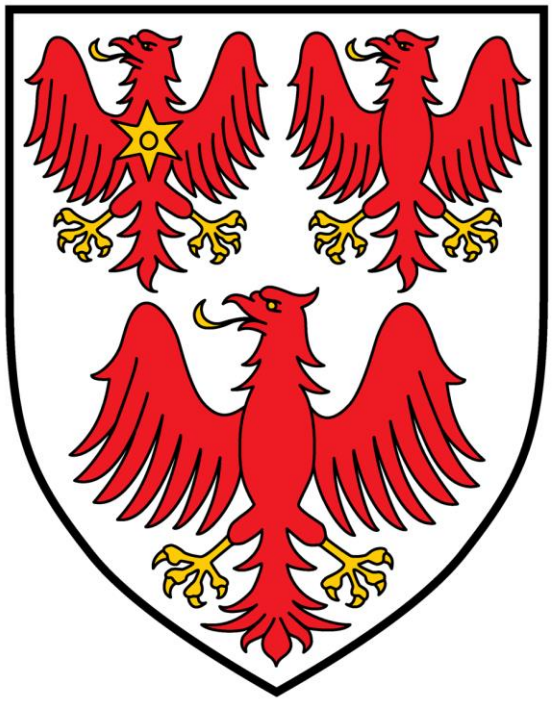
AMINO-FUNCTIONALISED β-DIKETIMINATE LIGANDS ("*N*-NACNACS"): SYNTHESIS AND COORDINATION CHEMISTRY WITH MAIN GROUP ELEMENTS





Dinh Cao Huan Do

The Queen's College

Thesis submitted for the Degree of Doctor of Philosophy

November 2018

ACKNOWLEDGEMENTS

It has been a privilege for me to have been part of the Aldridge Group in the past four years, doing one of the two things I enjoy the most during my time in Oxford – and I am not sure if I have accidentally enjoyed cricket slightly more than my own chemistry. In any case, I wish to honour the valuable contribution from these following people to my research life; the list is definitely not exhaustive by any means.

First and foremost, I would like to express my gratitude to my supervisor – Professor Simon Aldridge – for his continuous guidance and support, the relentless motivation through the timeless saying "*The world is your oyster*" whenever I was in doubt of my *level of talent*, and for never questioning my absence from the lab every Wednesday afternoon in Trinity. *Whatismore*, the completion of this thesis would not be possible without his constructive advice and patient proofreading; I have learnt a great deal about the English language from his corrections.

Credit also goes to my wonderful Part II students: Ailsa Keyser (2015/16) for her great assistance in various aspects of my research, and Dafydd Jones (2016/17) for heavily scrutinising the true electronic nature of *our* ligand.

A big thank-you goes to all the crystallographers, in particular Drs Evgeny Kolychev, Christian Sindlinger, Jamie Hicks, and Maria Ángeles-Fuentes, for those long and tiring hours down in the cold X-ray room. Their perseverance is second to none, given the fact that more often than not, my "crystals" are either too small to diffract, or not crystalline at all. This thesis would certainly be less colourful without their magnificent effort.

Basic knowledge of computational chemistry has been bestowed upon me, firstly by Dr Sindlinger, and more intensively later on by Dr Petra Vasko. Although I did try my best to learn, it is very likely that their patience has been tested on numerous occasions. For this reason, I am extremely grateful for your dedication towards my DFT education.

Dr Nick Rees has kindly helped me with everything NMR-related, especially setting up new experiments on the spectrometers – I am sorry that sometimes my sample was *not concentrated enough*.

I was blessed with the immense support from my colleagues in S12 during the drafting of this thesis: Alexa, Anna, Jamie, Petra, and Ying Kai have provided me with useful suggestions and motivational small talks. Furthermore, Alexa has kindly helped me proofread virtually all of my chapters despite her being occupied with her own thesis, and Ying Kai has bombarded me with numerous brilliant ideas along the way – I only wish I would have time to try all of them.

Other past and present members of the group have provided a delightful working environment in the lab (with a hint of questionable music taste), as well as an endless source of humour in the 11-ish and half-3-ish tea-breaks. I shall never forget the global delicacies we had, from the Nordic nations to the Far East, not to mention the occasional sumptuous cake *from* Jamie.

In addition, I would like to thank S11 lab – particularly Drs. Alexander Hinz, Frank Tamborino, and Stefan Mitzinger – and Dr. Antonio Martinez-Martinez from the Weller Group for being wonderful neighbours to ours and helping me in one way or another.

Needless to say, I would not be able to embark on this amazing four-year journey in Oxford without the valuable financial support from the Jardine Foundation and the University of Oxford *via* the Jardine-Oxford Graduate Scholarship, and especially the initial encouragement from Dr Dragoslav (Drasko) Vidović – my undergraduate research Supervisor in NTU (Singapore).

Lastly, I would like to dedicate this paragraph to my family, whose immeasurable support has helped me get through tough times; no words can describe how much I love them. And to my fiancée, Trân: Thank you for having put up with me during the last seven years and counting – our long-distance relationship never seems that long with you. I am very much looking forward to us sharing the same time zone again.

ABSTRACT

This thesis examines the synthesis of a series of novel amino-functionalised β-diketiminate protio-ligands ("*N*-nacnacH"), and the subsequent application of these *N*-nacnac ligands in the coordination chemistry of Main Group elements, with the main focus being on the heavier Group 14 elements (Si, Ge, Sn). Comparison between the novel *N*-nacnac complexes and their classical β-diketiminate "Nacnac" analogues are drawn wherever possible, in order to highlight the differences in molecular properties brought about by the introduction of the σ-electron withdrawing/π-electron donating NMe_2 functions at the ligand backbone.

Chapter 3 introduces an optimised synthetic protocol for the preparation of *N*-nacnacH protio-ligands of the form (**1-Ar**)H (Ar = Ph, *o*-Xyl, Dipp). Attempts to synthesise (**1-^{t}Bu**)H and (**1-Mes**)H are frustrated by the formation of the rearranged products **2-^{t}Bu** and **3**, while modifying the work-up method eventually allows access to (**1-^{t}Bu**)H, albeit in low yield. The isolated protio-ligands (**1-Ar**)H exist in the diimine configuration in both solid- and solution-state, in contrast to the imino-enamine form typical of most NacnacH systems. Direct metallation of (**1-Ar**)H by ^{n}BuLi or $AlMe_3$ generates the corresponding lithiated and aluminated complexes, respectively; the former are of synthetic significance as useful reagents for the synthesis of more exotic *N*-nacnac Main Group species *via* transmetallation. Spectroscopically, the donor capability of the NMe_2 functions is demonstrated by ^{1}H NMR resonances of the backbone γ-CH protons in the metallated compounds, which are shifted significantly upfield compared to their Nacnac counterparts.

In **chapter 4**, the formation of *N*-nacnac-ligated monochlorotetrelenes of the generic form (**1-Ar**)ECl (E = Si, Ge, Sn) is discussed. The establishment of a library of germylenes and stannylenes bearing different *N*-bound aromatic substituents with varying degrees of steric bulk allows for a systematic study of the steric effects of the flanking aryl groups on the overall molecular metrics of these complexes. Most importantly, (**1-Dipp**)SiCl represents one of the first examples of a β-diketiminate-stabilised chlorosilylene. Preliminary reactivity studies have then been carried out with the bulky chlorotetrelene systems (**1-Dipp**)ECl

(E = Si, Ge, Sn): chloride abstraction leads to the isolation of the corresponding cationic species [(**1-Dipp**)E][Al{OC(CF_3)$_3$}$_4$].

Chapter 5 reports on further investigations into the reactivities of (**1-Dipp**)ECl (E = Ge, Sn). The syntheses and characterisation of the hydrido- ((**1-Dipp**)EH) and phosphaketenyl-tetrelenes ((**1-Dipp**)E(PCO)) *via* salt metathesis are reported, and the photochemistry of (**1-Dipp**)Ge(PCO) subsequently explored. UV-induced P─C bond cleavage generates the bicyclic germylene **4**; the formation of which is proposed by DFT calculations to proceed *via* either a concerted mechanism (attack of the backbone C─C bond on phosphorus with accompanied loss of CO), or a step-wise pathway involving a germaphosphinidene intermediate.

Chapter 6 presents the chemistry of the *N*-nacnac-stabilised chlorosilylene. Mild oxidation of (**1-Dipp**)SiCl affords the first example of a Lewis-acid-free *sila*-acyl chloride (**1-Dipp**)Si(O)Cl, which undergoes nucleophilic *sila*-acyl substitution to yield the *sila*-aldehyde (**1-Dipp**)Si[O(BEt_3)]H and *sila*-ester (**1-Dipp**)Si(O)(O^{t}Bu). Notably, this substitution chemistry – while well known in carbonyl chemistry – is demonstrated for the first time to be compatible with heavier Group 14 carbonyl analogues. Crystallographic studies reveal very short Si=O bonds in the Lewis-acid-free siliconyl systems, which hint at marked multiple bond character of the Si=O function. On the other hand, metathesis reactions of (**1-Dipp**)SiCl with sources of H$^-$ or ^{t}BuO$^-$ are found to result in a ring contraction process, generating five-membered aza-butadienyl Si^{IV}-complexes of the form (**5-Dipp**)Si(NDipp)R (R = H, ^{t}BuO). Intrigued by this mode of intramolecular rearrangement, and based on related examples with Nacnac-stabilised low-valent metal complexes, the relationship between the σ-donor capability of the R substituent and the tendency for compounds of the form (**1-Dipp**)SiR to undergo ring contraction has been probed, both experimentally and computationally. The proposed mechanism suggests that in most cases, strong σ-donating groups favour the *N,C*-chelate aza-butadienyl configuration under ambient conditions. This is broadly in line with the experimental findings, with the exception of the R = P($SiMe_3$)$_2$ system which, together with the σ-withdrawing R = Cl system, exists in the *N*-nacnac-chelate form at room temperature.

LIST OF ABBREVIATIONS

The following abbreviations will be employed throughout this Thesis

^{Ar}*N*-nacnac = **1-Ar** = [HC{C(NMe$_2$)(NAr)}$_2$]$^-$

^{Ar}Nacnac = [HC{C(Me)(NAr)}$_2$]$^-$

^{R,Ar}Nacnac = [HC{C(R)(NAr)}$_2$]$^-$

Ad = 1-adamantyl

Ar = aryl

Ar* = C$_6$H$_2$[C(H)Ph$_2$]$_2$Me-2,6,4

calc. = calculated

COSY = correlation spectroscopy

Cy = cyclohexyl = C$_6$H$_{11}$-

δ = chemical shift

d = days

DFT = Density Functional Theory

Dipp = 2,6-diisopropylphenyl = 2,6-^{i}Pr$_2$-C$_6$H$_3$

EI = Electron Impact Ionisation

equiv. = equivalent

ESI = Electrospray Ionisation

h = hours

HMBC = Heteronuclear Multiple Bond Correlation

HOMO = Highest Occupied Molecular Orbital

HSQC = Heteronuclear Single Quantum Correlation

^{i}Pr = C(H)Me$_2$

IDipp = 1,3-bis-(2,6-diisopropylphenyl)imidazol-2-ylidene = (HCDippN)$_2$C:

I^{t}Bu = 1,3-di-(*tert*-butyl)imidazol-2-ylidene = (HC^{t}BuN)$_2$C:

Int = intermediate

J = coupling constant

L = neutral, two-electron donor (unless otherwise stated)

LUMO = Lowest Unoccupied Molecular Orbital

Me = CH_3

meas. = measured

Mes = 2,4,6-trimethylphenyl = 2,4,6-Me_3-C_6H_2

MO = Molecular Orbital

MS = Mass Spectroscopy

ν = frequency

Nacnac = β-diketiminate ligand

NHC = *N*-heterocyclic carbene

NMR = Nuclear Magnetic Resonance

N-nacnac = amino-functionalised β-diketiminate ligand

Ph = phenyl = C_6H_5

ppm = parts per million

py = pyridine = C_5H_5N

R = monoanionic, one-electron donor (unless otherwise stated)

R^F = $C(CF_3)_3$

r.t. = room temperature

^{t}Bu = *tert*-butyl = Me_3C

Tbt = 2,4,6-[$CH(Me_3Si)_2]_3$-C_6H_2

TMEDA = tetramethylethylenediamine = $(Me_2NCH_2)_2$

Tolyl = 2-Me-C_6H_4- (*o*-Tol), 3-Me-C_6H_4- (*m*-Tol), or 4-Me-C_6H_4- (*p*-Tol)

Tripp = 2,4,6-triisopropylphenyl = 2,4,6-^{i}Pr_3-C_6H_2

TS = transition state

XRD = X-ray diffraction

Xyl = *o*-Xyl (unless otherwise stated) = 2,6-dimethylphenyl = 2,6-Me_2-C_6H_3

TABLE OF CONTENTS

CHAPTER 1 – INTRODUCTION **1**
1.1 Preamble **1**
1.1.1 From cacodyl to carboranes: The first two centuries of Main Group chemistry *1*
1.1.2 The field of stable heavier Group 14 carbene analogues (1970s-now) *4*
1.1.3 Heavier group 14 analogues of alkenes, imines, and ketones *14*
1.2 ***N,N'*-chelating ligands: Privileged bidentate donors in Main Group chemistry** **25**
1.2.1 Three-membered N,N'-chelates *26*
1.2.2 Four-membered N,N'-chelates *31*
1.2.3 Five-membered N,N'-chelates *34*
1.3 Project Aims **38**
1.4 References **40**
CHAPTER 2 – GENERAL EXPERIMENTAL AND COMPUTATIONAL METHODS **52**
2.1 Manipulation of air- and moisture-sensitive materials **52**
2.2 Analytical techniques **54**
2.2.1 NMR spectroscopy *54*
2.2.2 X-ray crystallography *54*
2.2.3 Infrared spectroscopy *55*
2.2.4 Mass spectrometry *55*
2.2.5 Elemental (C,H,N) analyses *56*
2.3 Preparation and purification of chemicals **56**
2.3.1 Solvents *56*
2.3.2 Starting materials *57*
2.4 Computational details **57**
2.5 References **59**
CHAPTER 3 - SYNTHESIS AND METALLATION OF AMINO-FUNCTIONALISED NACNAC-LIGANDS **61**
3.1 Introduction **61**
3.2 Results and Discussion **67**
3.2.1 Protio-ligand synthesis (Ar = Ph, o-Xyl, Dipp) *67*
3.2.2 Attempts at protio-ligand synthesis with $^{t}BuNH_2$ *71*
*3.2.3 Attempted synthesis of **(1-Mes)**H* *74*
3.2.4 Direct metallation of N-nacnac ligands with lithium and aluminium alkyls *77*
3.3 Conclusions **83**
3.4 Synthesis of Novel Compounds **84**

3.5 References and notes 91
CHAPTER 4 - COMPLEXATION STUDIES OF HEAVIER GROUP 14 ELEMENTS WITH *N*-NACNAC LIGANDS 96
4.1 Introduction 96
4.2 Results and Discussion 101
4.2.1 Synthesis and characterisation of N-nacnac-ligated chlorotetrelenes (^{Ar}N-nacnac)ECl (E = Ge, Sn) 101
4.2.2 Synthesis and characterisation of the chlorosilylene (^{Dipp}N-nacnac)SiCl 108
4.2.3 Formation of cationic tetrelenes via chloride abstraction 112
4.3 Conclusions 116
4.4 Synthesis of novel compounds 118
4.5 References 123
CHAPTER 5 - SYNTHESIS AND REACTIVITY STUDIES OF *N*-NACNAC STABILISED HYDRIDO- AND PHOSPHAKETENYL-TETRELENES 126
5.1 Introduction 126
5.2 Results and Discussion 133
5.2.1 Synthesis and characterisation of the hydridogermylenes and stannylenes 133
5.2.2 Synthesis and reactivity studies of the phosphaketenylgermylenes and stannylenes 136
5.3 Conclusions 149
5.4 Synthesis of novel compounds 150
5.5 References 154
CHAPTER 6 – THE OXIDATION AND SUBSTITUTION CHEMISTRY OF A *N*-NACNAC STABILISED CHLOROSILYLENE 157
6.1 Introduction 157
6.2 Results and Discussion 164
6.2.1 Syntheses of sila-carbonyl species by oxidation-substitution 164
6.2.2 Ring-contraction chemistry initiated by ligand exchange with the chlorosilylene 173
6.2.3 The rearrangement of N-nacnac ligands: Effects of silicon-bound substituents 177
6.2.4 Computational investigation of the rearrangement process 185
*6.2.5 Investigation of the thermal stabilities of (**1-Dipp**)Si{P(SiMe$_3$)$_2$} and (**1-Dipp**)SiCl 190*
6.5 Conclusions 194
6.6 Syntheses of novel compounds 197
6.7 References 206
CHAPTER 7 – CONCLUSIONS 210

CHAPTER 1

INTRODUCTION

1.1 Preamble

1.1.1 From cacodyl to carboranes: The first two centuries of Main Group chemistry

Main Group chemistry – a sub-discipline of inorganic chemistry – is generally defined as the studies of the chemical behaviour of *s*- and *p*-block elements and their compounds. In practice, this definition usually comprises the elements from Groups 1, 2, and 13-18 of the Periodic Table, with the exclusion of radioactive elements (heavier than bismuth *i.e.* Z > 83), and carbon-containing molecules which are traditionally considered as part of the domain of organic chemistry. Many of these elements were discovered even before the first millennium BC, including carbon, tin, and lead from Group 14, antimony from Group 15, and sulphur from Group 16.[1] In modern era, *p*-block element-containing compounds have accounted for a significant proportion of the manufacture of inorganic chemicals, with notable examples including electronic-grade silicon (EGS) and indium tin oxide (ITO), both finding wide applications in materials industries.[2]

Historically, one of the earliest attempts to study the nature of Main Group compounds can be traced back to late 18th-century France, when Louis Claude Cadet de Gassicourt isolated a foul-smelling product by heating arsenic trioxide with potassium acetate, followed by distillation.[3] The product was simply described as *une liqueur fumante* ("a fuming liquid"), without Gassicourt knowing its exact composition. Subsequent investigations – mainly by Frankland and Bunsen –

suggested that the main components of such a liquid might have been the two species $(Me_2As)_2O$ and $(Me_2As)_2$; the latter was also referred to as *cacodyl* by Bunsen.[3,4] Later on, advances in laboratory practices allowed for the rapid evolution of Main Group chemistry during the 19th century, which continued into the early decades of the 20th century. These advances included efforts towards isolating the remaining (non-radioactive) members of the Main Group family in their elemental forms - which was successfully completed in 1886 with the simultaneous discoveries of fluorine (by Moissan) and germanium (by Winkler).[5] Additionally, the foundations of Main Group *organometallic* chemistry (featuring compounds with carbon-Main Group metal bond(s)) was firmly established in the period 1840-70, when notable works by Schafarik, Frankland, and Löwig on organoaluminium ($EtAlI_2$ and Et_2AlI), organotin (Et_2SnI_2), and heavy organo-pnictogen compounds (Et_3Pn, Pn = As, Sb, Bi) were published.[3,4h,6,7] *S*-block chemistry (Groups 1 and 2) had its own breakthrough when Grignard reported the preparation of organomagnesium reagents in 1900, followed by the optimisation of synthetic methodologies for the lithium and sodium analogues, mainly by Schlenk, Gilman, and Ziegler, over the next 30 years.[8] At a more macroscopic scale, the contemporary social demands during the Industrial Revolution era (*ca.* 1760 - 1840) provided the impetus for the design and implementation of novel industrial chemical processes; some of which manufactured Main Group-based commodity chemicals, such as sulphuric acid (*via* the contact process, patented in 1831), sodium carbonate (Solvay process, 1860s), nitric acid (Ostwald process, 1902), and ammonia

(Haber-Bosch process, 1911).[2] The impact of these accomplishments, both in the laboratory and in industry, on the discipline of chemistry and on society as a whole was recognised by the scientific community through three Nobel Prizes awarded in the years 1906 (Moissan, for works on the discovery of fluorine), 1912 (Grignard, organomagnesium reagents), and 1918 (Haber, the synthesis of ammonia *via* Haber-Bosch process).[9]

Arguably, the inter-war period marked the beginning of the heyday of *applied* Main Group chemistry. In 1922, Midgley and Boyd demonstrated the pioneering use of tetraethyl lead (Et_4Pb) as an effective anti-knock additive in petrol, more than 60 years after the first reported isolation and characterisation of this compound by Buckton, although its usage has been recently phased out due to health and environmental concerns.[10] The global manufacture of polysiloxanes (*silicones*) – a family of extraordinarily robust and versatile polymeric materials containing Si—O—Si bridges – was revolutionalised in the early 1940s, thanks to the invention of the Direct Process by Rochow.[11] This offers a cost-effective synthetic route to methylchlorosilanes of the form Me_nSiCl_{4-n} (n = 1-3), which can subsequently be hydrolysed to generate silicone polymers on a large scale. With regards to applications in the laboratory, a plethora of Main Group-based reagents had started to find use in organic synthesis, not least thanks to their increasingly facile preparation; among numerous examples are Group 1 compounds as strong bases for deprotonation, Grignard reagents for C—C bond formation, and Group 13 compounds as potent Lewis acid catalysts.[11] In particular, the merits of the research

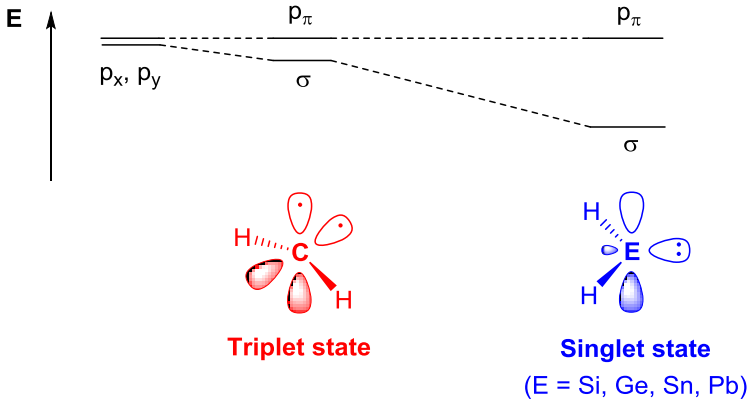
on boranes as powerful reducing agents by Brown, and phosphorus-ylides for constructing C=C double bonds by Wittig, were reflected by their joint Nobel Prizes in 1979.[8] Furthermore, investigations on boron-based clusters (*carboranes*) largely by Hawthorne and Lipscomb in the 1960-70s, especially the nature of the B─H bonds in those macromolecules, have not only strongly influenced Main Group chemistry, but also revealed enormous potential applications in metal-organic frameworks (MOFs), molecular machines, and cancer treatment, to name a few.[12]

In stark contrast to the rapid progress of applied Main Group chemistry highlighted above, fundamental studies of the chemistries of the Main Group elements at the time were still heavily restrained by classical bonding concepts, which (prematurely) predicted the instability (or even the non-existence) of whole classes of compounds not adhering to these rules.[13] Notable examples include the *octet rule*, whereby the most stable electronic configuration of an atom generally consists of eight valence electrons, and the *double bond rule*, which describes the inability of Main Group elements with a principal quantum number $n \geq 3$ to construct stable multiple bonds.[14] The challenges of defying these prevailing dogmas has been reflected in the development of Main Group chemistry in recent decades, and has undoubtedly re-ignited chemical interest in the field.

1.1.2 The field of stable heavier Group 14 carbene analogues (1970s-now)

Heavier Group 14 carbene analogues (silylenes, germylenes, stannylenes, and plumbylenes), also collectively referred to as *tetrelenes* (from the Greek word *tetra* for four), are compounds featuring a divalent tetrel centre with two associated

non-bonding electrons. As such, these systems are intrinsically *electrophilic* for having only six valence electrons – two short of a stable configuration according to the octet rule. Computational investigations of the prototypical tetrelenes, H_2E (E = C – Pb), hinted at an energetically favourable *singlet* ground state for all heavier tetrels (E = Si to Pb), in which the two non-bonding electrons pair up and occupy a σ-type orbital, leaving a vacant p_π-type orbital; the geometry around the tetrel centre is bent (*ca.* 90°, Figure 1.1).[15] This contrasts with the *triplet* ground state observed for methylene, H_2C, which acquires biradicaloid character from the two unpaired electrons in the σ- and p_π-orbitals, with the H—C—H angle being more obtuse (*ca.* 129°). Most importantly, the frontier orbital configuration of the heavier tetrelenes suggests that – while the parent species H_2E are not stable under ambient conditions – derivatives of the type R_2E should be isolable if the R groups are (i) strongly π-donating, to quench the electronic deficiency arising from the vacant p_π-type orbital, and/or (ii) sterically demanding, to reduce the tendency towards aggregation.



Compound	$\Delta E_{S\rightarrow T}$
H_2C:	-65
H_2Si:	74
H_2Ge:	96
H_2Sn:	97
H_2Pb:	143

Figure 1.1 Frontier orbitals of H_2C and its heavier analogues (*left*); singlet-triplet gaps of the dihydridotetrelenes in kJ mol^{-1} (*right*), $\Delta E_{S\rightarrow T}$ = E(triplet) – E(singlet)

In response to the dearth of stable low-valent species, research on the heavier Group 14 elements (Si, Ge, Sn, Pb) by the group of Lappert from the early 1970s onwards opened up a new dimension to the fundamental aspects of Main Group chemistry. This led to the synthesis of the first examples of low-coordinate tetrelenes of the form R_2E (E = Ge, Sn, Pb) which are *stable at ambient temperature* (Figure 1.2).[16] The thermodynamic and kinetic stability of these compounds can be attributed to the use of strongly-donating and sterically bulky alkyl, amido, or alkoxo ligands. In each of these tetrelenes, the geometry at the Group 14 metal centre is bent (Table 1.1), a finding which is consistent with a singlet ground state *i.e.* having a lone pair of electrons and a vacant p_π-type orbital at the tetrel centre (*vide supra*). Consistently, early reactivity studies corroborated this frontier orbital feature, in part through the synthesis of a range of Transition Metal-tetrelene complexes, in which the tetrelene molecule acts as a neutral 2-electron donor *via* the σ-type lone pair and, to a lesser extent, as a π-acceptor *via* the empty n*p* orbital.[16a,16e,17] Moreover, these heavier Group 14 carbenoid species were found to undergo oxidative addition at the tetrel centre with H—X (X = F, O, Cl), C—X (X = Cl, Br, I) bonds and halogens (Cl_2, Br_2), a chemical behaviour which had previously been associated only with Transition Metal complexes, or *transient* low-valent Main Group species (Scheme 1.1).[18] From a fundamental viewpoint, these results certainly sparked an interest in the chemistry of stable heavier group 14 carbene analogues, and low-valent Main Group compounds as a whole.

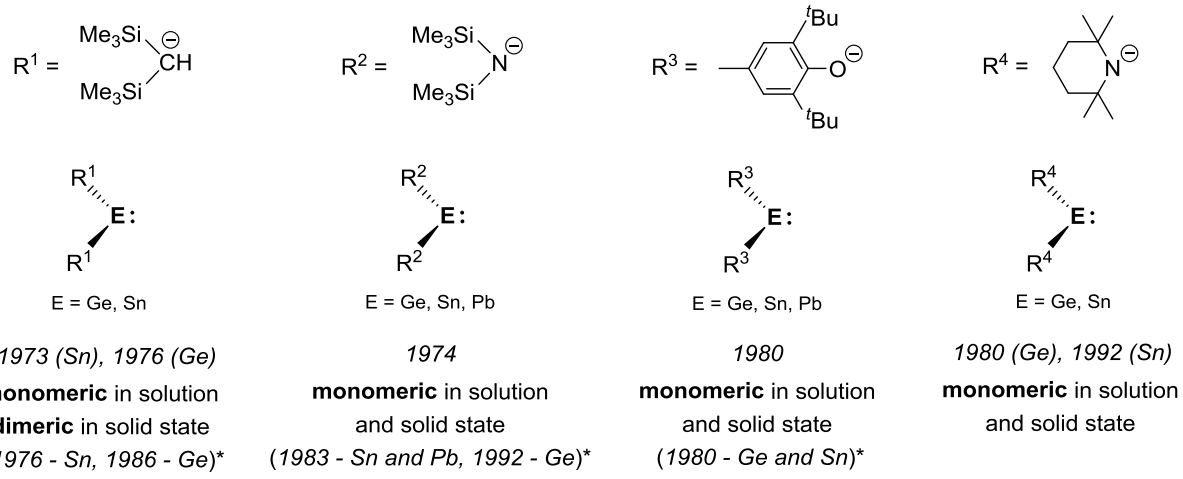
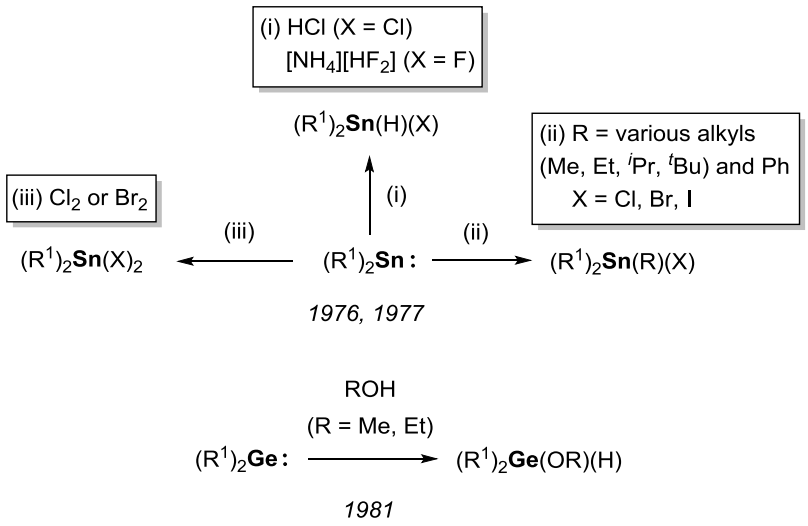


Figure 1.2 Prominent examples of stable low-coordinate heavier Group 14 metallylene complexes, synthesised by Lappert and co-workers in the 1970s and early 80s. The asterisk (*) denotes the year when structural elucidation was made possible by X-ray crystallography.

Germylene	Bite angle	Stannylene	Bite angle	Plumbylene	Bite angle
$(R^1)_2Ge$:	112.5(3)	$(R^1)_2Sn$:	109.2(2)	$(R^1)_2Pb$:	N/A
$(R^2)_2Ge$:	107.1(2)	$(R^2)_2Sn$:	104.7(2)	$(R^1)_2Pb$:	103.6(7)
$(R^3)_2Ge$:	92.0(4)	$(R^3)_2Sn$:	88.8(2)	$(R^3)_2Pb$:	N/A
$(R^4)_2Ge$:	111.4(5)	$(R^4)_2Sn$:	109.7(2)	$(R^4)_2Pb$:	N/A

Table 1.1 Bite angles (°) of the tetrelene compounds outlined in Figure 1.2, as determined by X-ray crystallography



Scheme 1.1 Selected early reports of bond activation with Lappert's tetrelenes

Since these seminal discoveries in the 1970s, research on stable heavier tetrelenes has received significant attention, which is reflected by a large number of subsequent reports on these low-valent species.[19] Arguably, rapid development of the field has been heavily associated with increasingly innovative ligand design. For instance, common bulky anionic monodentate carbon- and nitrogen-based donors have evolved from the trimethylsilyl-substituted systems, employed by Lappert nearly five decades ago (Figure 1.2), to the extremely sterically-encumbered *m*-terphenyl and "Rind" groups (*C*-based representatives), as well as the bulky amides "[(Ar*)(R)N]-" (*N*-based), which have gained popularity in recent times (Figure 1.3).[20]

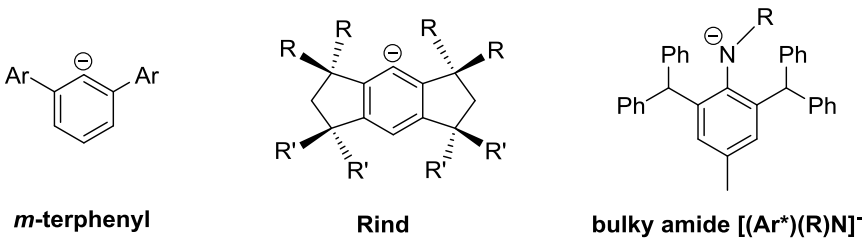


Figure 1.3 Prominent monoanionic, monodentate ligands employed in Main Group chemistry

Systematic modification of the electronic profile of the supporting ligands is also of great interest, in order to manipulate the HOMO-LUMO gap of the resulting tetrelenes, and potentially access complexes with enhanced reactivity towards small molecules. According to a qualitative description of the frontier orbital interactions between the Group 14 atom E and two uninegative ligands R in a model tetrelene complex, R_2E, σ-withdrawing R groups can be envisaged to lower the energy of the HOMO, which is essentially the lone pair of electrons on the tetrel centre with high *s*-character, and π-donating R substituents raise the energy of the LUMO, which is

generally the vacant *p*-type orbital of the tetrel atom (Figure 1.4).[21] A combination of these two effects would result in a wider HOMO-LUMO gap, and consequently a more stable divalent species in the singlet ground state. In part, this orbital description reflects the widespread uses of amido and alkoxo donors, which are both σ-withdrawing and π-donating. On the other hand, the reverse set-up involving an electropositive R substituent with π-accepting capability, such as the boryl ligand $[B(NDippCH)_2]^-$ (*vide infra*), would conceivably lead to a narrower HOMO-LUMO gap, and render the resulting complex more reactive. In addition, the HOMO-LUMO gap is also affected by the angle defined at the tetrel centre by the bonds to the R substituents: a narrower angle is associated with a lower-energy HOMO with high *s*-character, and consequently a wider HOMO-LUMO gap. Thus, in general, heavier tetrelenes stabilised by a cyclic backbone are more robust than their acyclic counterparts, due to the ability of the former to maintain a narrower bite angle at the Group 14 element centre (*vide infra*).

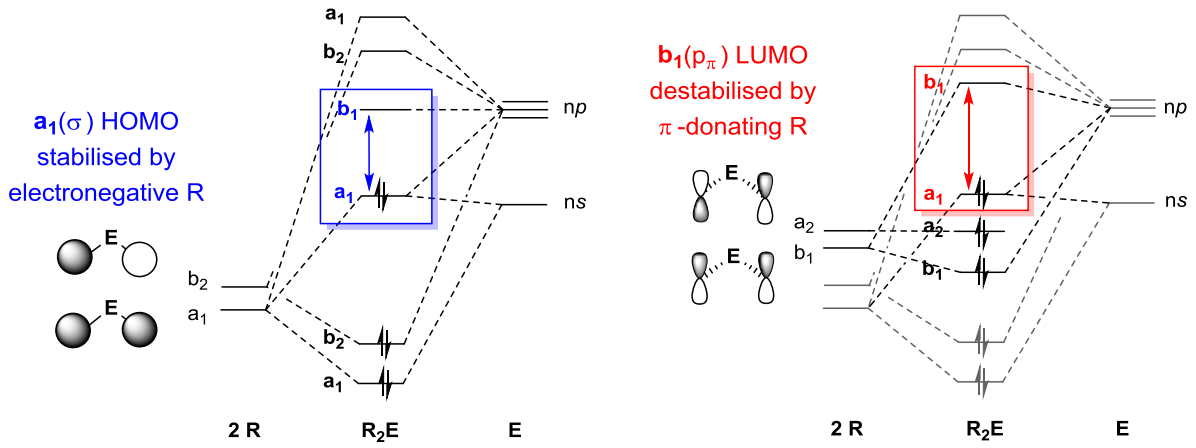


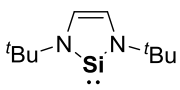
Figure 1.4 Frontier orbital energy perturbation of heavier tetrelenes R_2E induced by the electronic profile of R substituents

The increased thermodynamic stability of the +2 oxidation state on descending Group 14 presumably also contributes to the observation that, by the end of the 1980s, stable germylenes, stannylenes, and plumbylenes were no longer seen as synthetic curiosities, while two-coordinate silylenes had yet to be structurally characterised. That said, the thermodynamic robustness of the heavier tetrelenes hints at a diminished ability to activate strong, relatively non-polar bonds, such as H─H and C─H *via* oxidative addition chemistry.[22] As a result, two significant challenges remained in this area: (i) to isolate stable low-coordinate silylenes, and (ii) to construct highly reactive heavier tetrelenes (Ge, Sn, Pb) which can undergo oxidative addition with unactivated σ-bonds in "building-block" molecules. Based on the frontier orbital perturbation diagram (Figure 1.4), the key to tackle these challenges would owe much to the fine-tuning of the electronic and steric properties of the ligand scaffold. Namely, a balance needs to be struck between amplifying their Transition Metal-like reactivity (by having partially-occupied frontier orbitals with narrow energy gaps), while maintaining a workable degree of stability in the complexes themselves (wide HOMO-LUMO gaps).

With regards to the chemistry of stable silylenes, a landmark was finally reached in 1994 when West and co-workers successfully accessed the cyclic silylene $\{(^{t}BuN)HC\}_2Si$ from the corresponding dichlorosilane precursor, *via* potassium metal reduction (Figure 1.5).[23] Interestingly, a similar diaza-butadienyl ligand backbone, albeit bearing slightly different *N*-substituents ($[RN{-}C(H){=}C(H){-}NR]^{2-}$, R = Ad) was also employed by Arduengo for the stabilisation of the first crystallographically

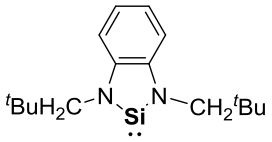
characterised stable carbene.[24] Given the more reactive nature of silylenes compared to their heavier Group 14 analogues, the majority of structurally characterised examples of silylenes reported thereafter were cyclic, typically with π-donor(s) attached to the silicon centre (Figure 1.5).[19b,19c,25] Besides "traditional" amino substiuents, phosphorus-based ylide moieties have also been employed in this regard.[25f,25h] As noted, the chelate effect decreases the central atom-ligand bite angle, which increases the *s*-character of the non-bonding σ-type orbital (formally the lone pair on the silicon centre). Moreover, π-donating Si-bound substituents help to alleviate the unsaturated nature of the vacant *p*-type orbital on the silicon centre, and typically widen the HOMO-LUMO gap through elevation of the LUMO (Figure 1.4). The importance of this π-overlap is reflected in the thermally sensitive nature of Kira's five-membered cyclic dialkylsilylene (Scheme 1.2), where such a π-donor effect is precluded.[26a] This silylene is found to be stable at 0°C, but slowly undergoes 1,2-silyl migration at room temperature in solution to the corresponding silaethene. Circumventing such side reactions was discovered to be feasible by modifying the silyl substituents, which increased the steric bulk around the Si^{II} centre. Thus, the new cyclic dialkylsilylene bearing 1,3-disilaindane functions was isolated and fully characterised in the solid state, while an equilibrium with its disilene form was detected at low temperature.[26b]

AMIDOSILYLENES



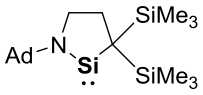
Bite angle (°) **90.5(1)**

West, 1994



88.2(1)

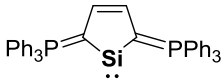
Lappert, 1995



92.64(8)

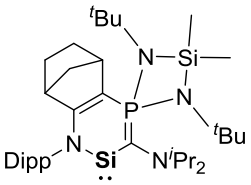
Iwamoto, 2016

YLIDE-INCORPORATED SILYLENES



Bite angle (°) **86.9 (calculated)**

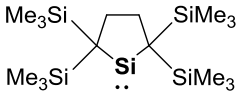
Driess, 2011



104.08(7)

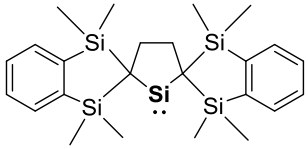
Baceiredo and Kato, 2016

DIALKYLSILYLENES



Bite angle (°) **93.88(7)**

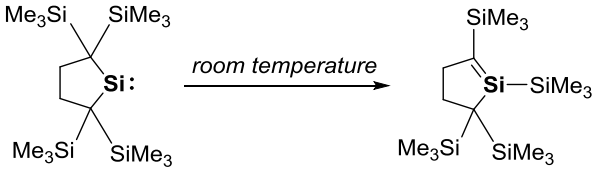
Kira, 1999



92.56(8)

Iwamoto, 2012

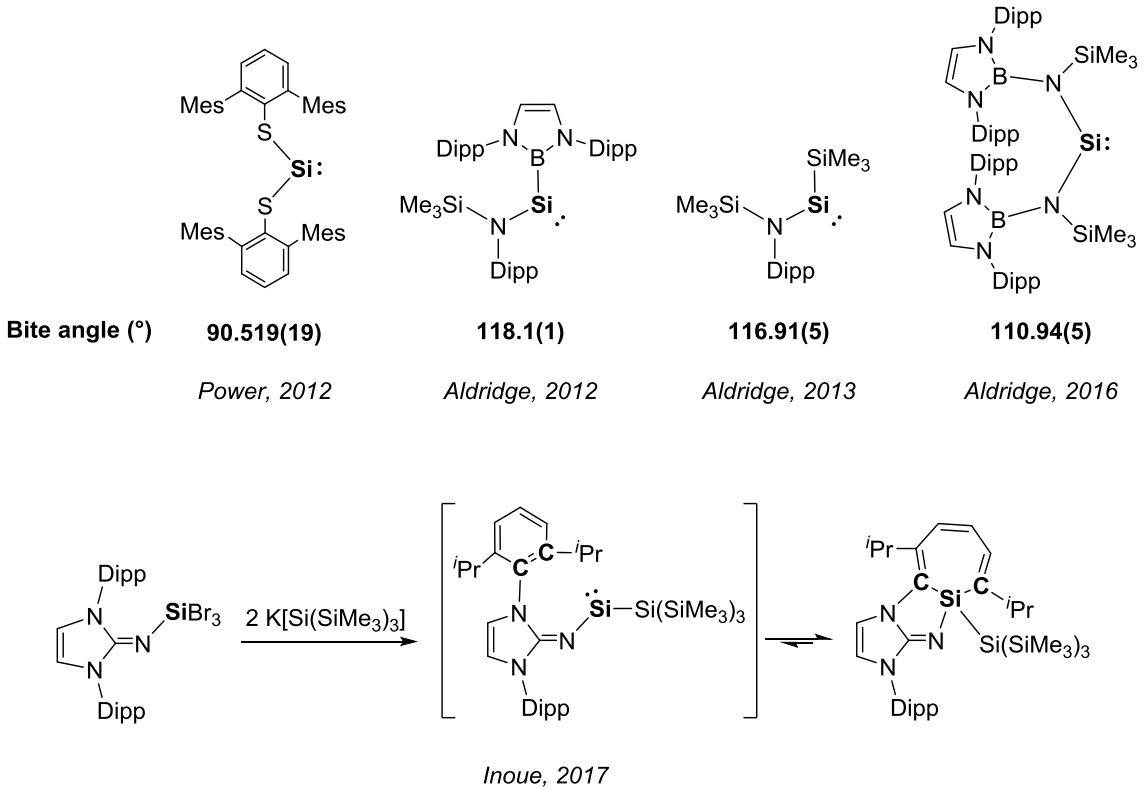
Figure 1.5 Prominent examples of stable two-coordinate cyclic silylenes in literature



Scheme 1.2 1,2-Silyl migration observed with Kira's dialkylsilylene

Not being restricted to the cyclic configurations, a handful of stable *two-coordinate acyclic* silylenes have, however, been reported in recent years, with the first two examples reported in 2012 by the groups of Aldridge and Power.[27] These examples utilise either a combination of boryl/amido ligands,[27a] or two terphenyl-substituted thiolates.[27b] Interestingly, a recent attempt to isolate an acyclic

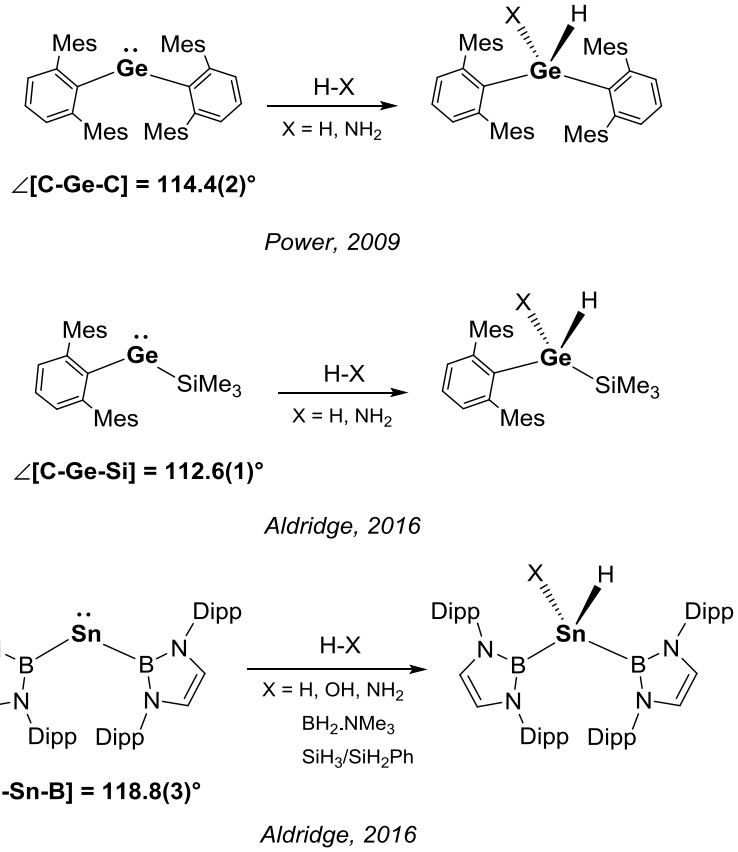
silylene featuring an *N*-heterocyclic imine donor and a bulky silyl group, is characterised by (reversible) insertion of the silicon centre into a proximal Dipp C=C bond, even at low temperatures (-78°C) (Scheme 1.3).[28] Presumably, this highlights the enhanced reactivity of acyclic silylenes compared to their cyclic counterparts.



Scheme 1.3 Prominent examples of stable two-coordinate acyclic silylenes (*top*); observed intramolecular dearomatisation by a transient iminato(silyl)silylene (*bottom*).

On the other hand, the opposite strategy in ligand selection has been employed with germylene and stannylene complexes, with the idea of decreasing the HOMO-LUMO gap and producing tetrelene systems capable of interesting small molecule activation. Accordingly, strongly σ-donating and π-accepting (or weakly π-donating) substituents (*e.g* aryl, boryl, or silyl groups) have been employed in landmark examples of two-coordinate Ge^{II}/Sn^{II} species, which can oxidatively add

small molecules (H_2, NH_3, H_2O, SiH_4 etc.) in a controlled manner (Scheme 1.4).[29] It is worth noting that very recently, the 45-year-old stannylene $\{(Me_3Si)_2CH\}_2Sn$ was discovered to undergo base-induced reversible H_2 addition at the metal centre, *via* a proposed "frustrated Lewis pair" mechanism.[30]



Scheme 1.4 Landmark discoveries of small-molecule activation by germylenes/stannylenes

1.1.3 Heavier group 14 analogues of alkenes, imines, and ketones

Alkenes, imines, and ketones are ubiquitous functional groups in organic chemistry. By contrast, their heavier Group 14 derivatives bearing E=X double bonds (E = Si, Ge, Sn, Pb; X = C, N, O) are not traditionally as well-represented. In part, this can be attributed to the more pronounced difference in electronegativity between the second row elements and the heavy tetrels[1] – especially in the cases of nitrogen and

oxygen – which imparts significant polarisation across the E=X bond ($E{=}X \leftrightarrow E^{\delta+}{-}X^{\delta-}$, Table 1.2). As a result, these systems are more prone to oligo-/polymerisation, and often trapping experiments are required to confirm their fleeting existence.[31]

Element (electronegativity)	**C (2.55)**	**N (3.04)**	**O (3.44)**
Si (1.90)	0.65	1.14	1.54
Ge (2.01)	0.54	1.03	1.43
Sn (1.96)	0.59	1.08	1.48
Pb (2.33)	0.22	0.71	1.11

Table 1.2 The absolute differences in electronegativities (Pauling scale) between heavier tetrels and the 2nd-row elements carbon, nitrogen, and oxygen

$H_2E{=}CH_2$	**E = C**	**E = Si**	**E = Ge**	**E = Sn**	**E = Pb**
E=C bond energy	739	462	357	280	191

Table 1.3 The energies of E=C double bonds (kJ mol^{-1}) in the prototype model $H_2E{=}CH_2$ (calculated by Jacobsen and Ziegler)

$H_2E{=}O$	**E = C**	**E = Si**	**E = Ge**	**E = Sn**	**E = Pb**
E=O bond energy	791	746	617	534	460

Table 1.4 The energies of E=O double bonds (kJ mol^{-1}) in the prototype model $H_2E{=}O$ (calculated by Suzuki, Tokitoh, Okazaki *et al.*)

Theoretical investigations confirm the weaker nature of E=C and E=O bonds going from E = C to E = Pb - for the prototype ethene ($H_2E{=}CH_2$) and formaldehyde ($H_2E{=}O$) models - through their respective bond energies (Tables 1.3 and 1.4).[15,32] Using a simple bonding concept, this can be attributed to less effective π-overlap between the n*p* (n = 3 to 6) orbital of the tetrel atom and the 2*p* orbital of the second row element. Although corresponding systematic studies with heavier imine

analogues are not yet available, calculations from Schleyer suggest that the double bond energy in the simplest silaimine $H_2Si=NH$ is 206 kJ mol^{-1}, which is 231 kJ mol^{-1} lower than that of $H_2C=NH$, and consistent with the idea of weaker E=N bonds for the heavier tetrels.[33]

As briefly mentioned in section 1.1.1, until the end of the 1970s, the paucity of stable heavier Group 14 alkene, imine, and ketone analogues underpinned the "double bond rule" in Main Group chemistry. In 1981, this dogma was debunked for good when three landmark compounds bearing Si=Si, P=P, and Si=C bonds were isolated and characterised at ambient conditions by the groups of West, Yoshifuji, and Brook respectively (Figure 1.6).[34] These examples provided critical impetus for the study of multiple bonding with heavy Main Group elements, which until the present day has been a continuing major research theme in Main Group chemistry.[35]

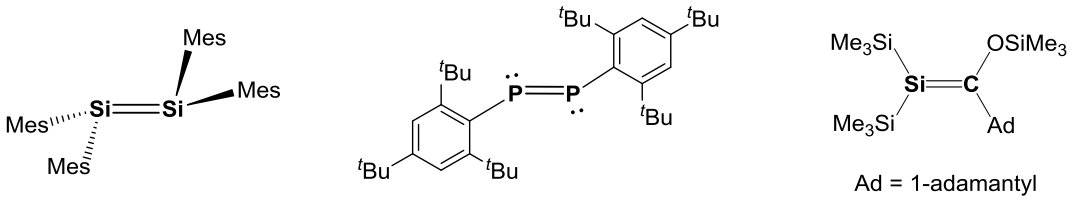


Figure 1.6 The first examples of stable compounds featuring Si=Si, P=P, and Si=C double bonds

Following the seminal discovery by Brook, the number of reported silicon analogues of alkenes featuring a Si=C bond has rocketed in the past 30 years.[35b] The majority of these compounds utilise extremely bulky ligands at silicon and/or carbon to prevent unwanted aggregation. Moreover, electronic stabilisation can also be achieved by additional coordination of neutral donors to silicon, which partially

neutralises the $Si^{\delta+}—C^{\delta-}$ polarisation, and concomitantly elongates the silicon-carbon linkage (Figure 1.7).[36] As a consequence, Si=C bond distances are found in the range 1.703(5) – 1.926(3) Å (*cf.* 1.87 – 1.91 Å for Si—C single bonds), with the longer end of this range (*ca.* 1.76 Å and above) generally being occupied by *silenoates* with a carbon-bound oxygen-based substituent.[34d,37] Notably, unusual strained ring systems featuring exo-/endocyclic Si=C bonds have been isolated and characterised by the groups of Kira and Sekiguchi.[38] These represent rare examples of silicon analogues of triafulvenes and cyclopropenes.

In addition, a handful of stable germenes, stannenes, and plumbenes have been reported, although in general their chemistries still remain rather under-developed compared to silenes (Figure 1.8).[35b] The majority of tetrel-carbon "double" bonds in these examples can be envisaged to be relatively more zwitterionic in nature ($E^{\delta+}—C^{\delta-}$), which is in line with the prediction of weaker E=C bonds and poorer n*p*-2*p* π-overlap on descending Group 14 (Table 1.3). To partially mitigate such polarisation, ligands which can induce extended π-delocalisation (*e.g* fluorenyl, diboryl) are often employed in coordination to the nucleophilic carbon centres.[39]

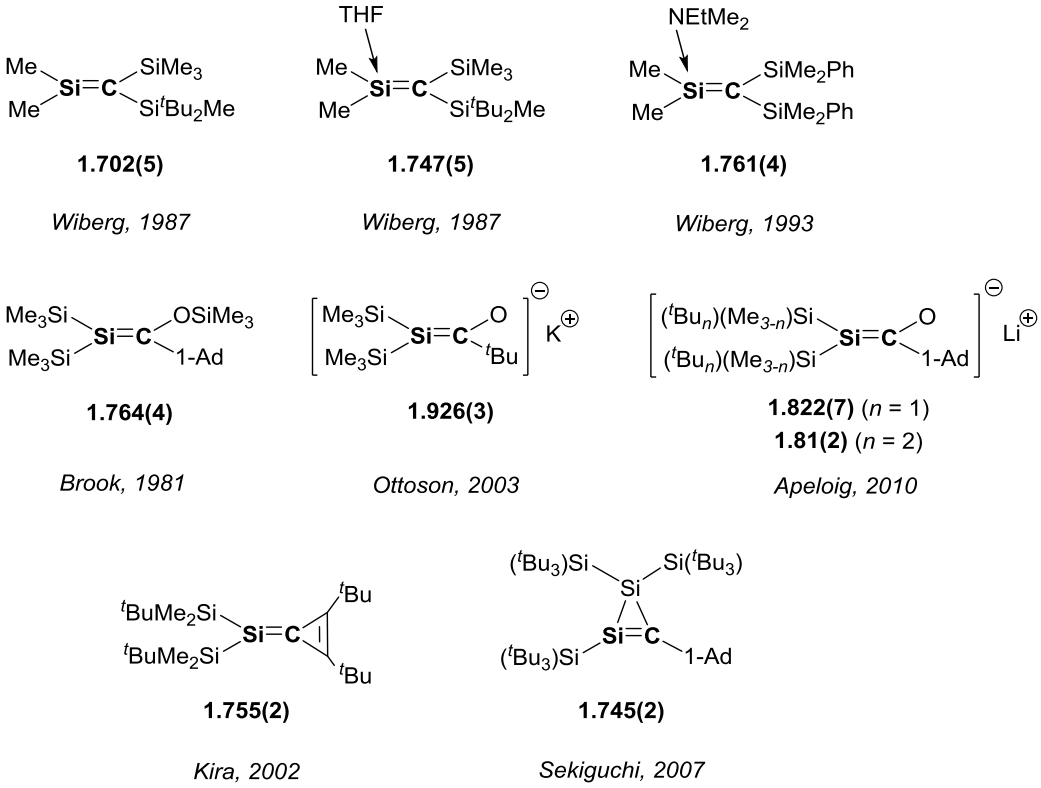


Figure 1.7 Selected examples of reported silenes

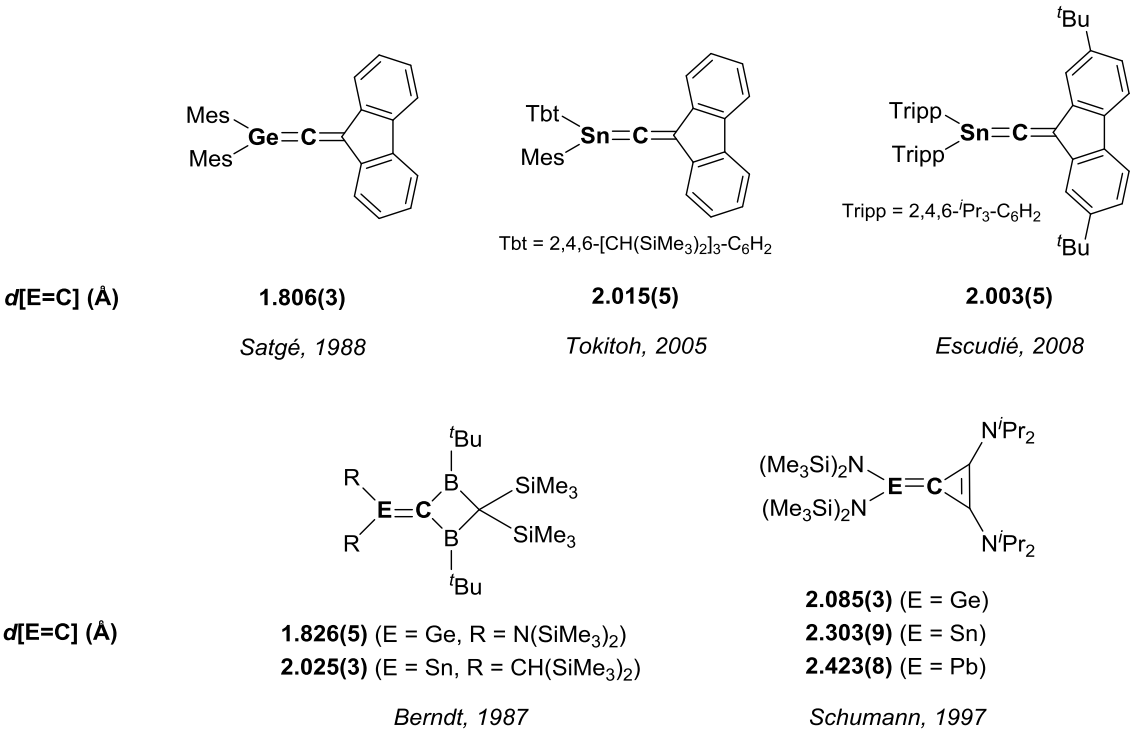
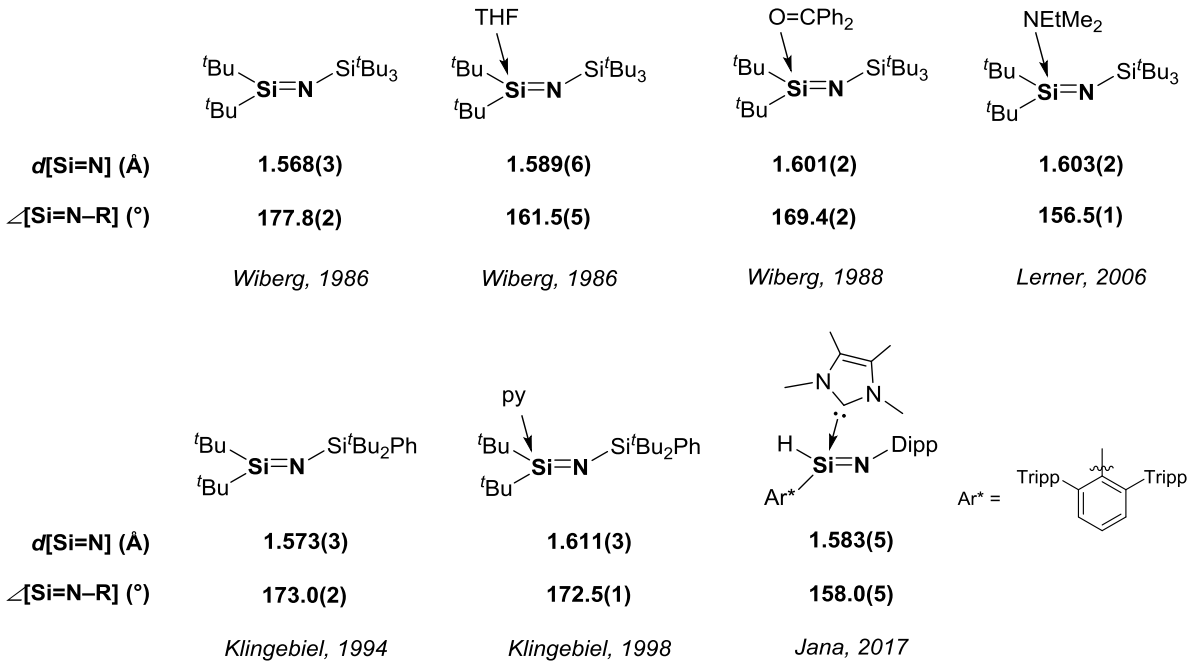


Figure 1.8 Selected examples of previously reported germenes, stannenes, and plumbenes

As per the case of heavier Group 14 alkene analogues, silaimines stand out as the best-studied class of imine derivative.[35b] The first example of a stable silaimine (^{t}Bu$_2$Si=N─Si^{t}Bu$_3$) was reported in 1986 by Wiberg and co-workers, which was followed shortly by another example from the group of Klingebiel in the same year (^{i}Pr$_2$Si=N─C$_6$H$_2$(2,4,6-^{t}Bu$_3$)).[40] Crystallographically-determined Si=N double bond distances are typically found between 1.568(3) and 1.678(2) Å (*cf.* 1.64 – 1.81 Å for Si─N single bonds,[41] and the geometry around nitrogen approaches linearity, with most angles at N measured as 156.5(1)° to 177.8(2)°. Computationally, this is reflected by a low-energy isomerisation barrier about the Si=N axis *via* a linear transition state, which was calculated for the prototype H$_2$Si=NH system to like *ca.* 23 kJ mol^{-1}.[42] Additional coordination of a Lewis base to the silicon centre is more frequently observed in silaimines compared to silenes, presumably due to the more highly-polarised Si=N (Si$^{\delta+}$─N$^{\delta-}$) linkage. This generally leads to slightly longer Si=N distances in the donor-stabilised silaimine (by *ca.* 0.02 – 0.05 Å), with respect to the corresponding uncomplexed species (Figure 1.9).[40,43] For instance, the molecular metrics of three donor-stabilised silaimines of the form ^{t}Bu$_2$(L)Si=N─Si^{t}Bu$_3$ (L = THF, Ph$_2$C=O, EtMe$_2$N) suggest a ≈ 2 % elongation in the Si=N bond relative to the free silaimine. It is also worth mentioning that very recently, two remarkable examples of stable NHC-stabilised 1-hydrosilaimines have been reported.[43f,43g]

Examples of the heavier derivatives (germaimines and stannaimines) have also been structurally characterised (Figure 1.10).[44] In these species, the bending

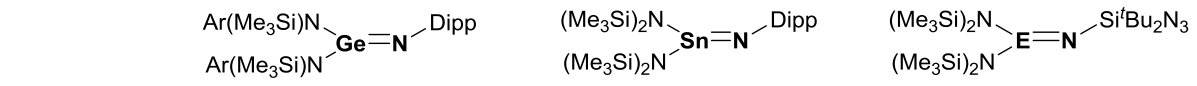
angles at nitrogen are narrower (120.5(2)° to 139.0(2)°) than those in silaimines, which can be attributed to the poorer π-overlap between the tetrel atom and nitrogen. While the majority of these compounds are thermally robust, the tin species $\{(Me_3Si)_2N\}_2Sn{=}NDipp$ was discovered to undergo C─H activation of one of the ^{i}Pr groups in a hexane solution within two weeks (Scheme 1.5).[44b] This presumably highlights the weakened tetrel-nitrogen double bond descending Group 14.



***d*[Si=N] (Å)**	**1.568(3)**	**1.589(6)**	**1.601(2)**	**1.603(2)**
∡[Si=N–R] (°)	**177.8(2)**	**161.5(5)**	**169.4(2)**	**156.5(1)**
	Wiberg, 1986	*Wiberg, 1986*	*Wiberg, 1988*	*Lerner, 2006*

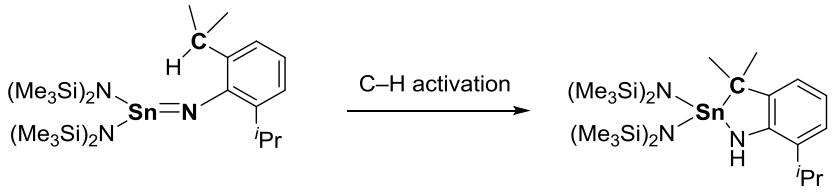
***d*[Si=N] (Å)**	**1.573(3)**	**1.611(3)**	**1.583(5)**
∡[Si=N–R] (°)	**173.0(2)**	**172.5(1)**	**158.0(5)**
	Klingebiel, 1994	*Klingebiel, 1998*	*Jana, 2017*

Figure 1.9 Selected examples of reported silaimines



***d*[E=N] (Å)**	**1.690(4)** (Ar = Mes) **1.703(2)** (Ar = Dipp)	**1.921(3)**	**1.703(5)** (E = Ge) **1.905(5)** (E = Sn)
∡[E=N–R] (°)	**139.0(2)** (Ar = Mes) **134.2(2)** (Ar = Dipp)	**120.5(2)**	**136.0(4)** (E = Ge) **130.6(3)** (E = Sn)
	Meller, 1991	*Meller, 1993*	*Ando, 1994*

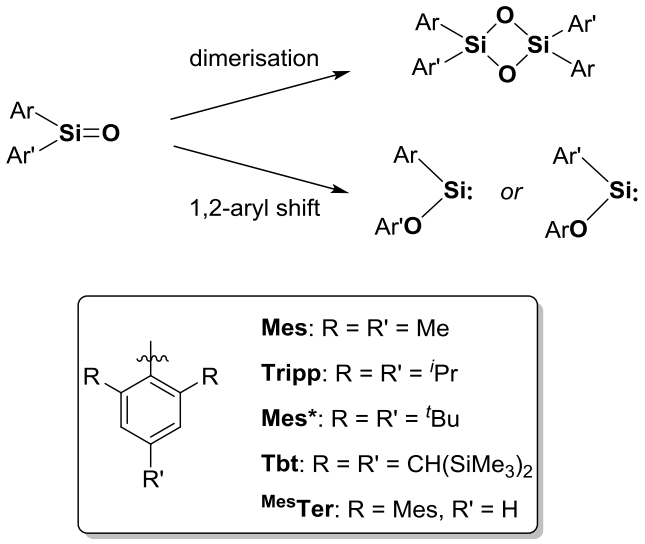
Figure 1.10 Selected examples of reported germa- and stannaimines



Scheme 1.5 C─H activation of a thermally-sensitive stannaimine

With regards to the chemistry of heavier ketone analogues, literature records show that compounds of the form $(R_1)(R_2)E{=}O$ readily undergo oligo-/polymerisation, or other decomposition pathways, even at low temperatures.[19c,31a,31c,35a-c] As such, early attempts to ratify the existence of E=O double bonds (E = Si, Ge) by spectroscopic means often relied on matrix trapping techniques under cryogenic conditions.[45] By the end of the 1990s, additional evidence for *silanones* and *germanones* (silicon and germanium analogues of ketones) had been reported - as fleeting intermediates in solution phase.[46] Moreover, popular theoretical viewpoints at that time remained positive about the possibility of isolating and characterising silanones and germanones under ambient conditions by making use of sufficient steric and/or electronic stabilisation. By contrast, stannanones and plumbanones were proposed to be too unstable to exist.[47] A comprehensive computational study by Kimura and Nagase suggested that the use of extremely bulky aryl substituents should allow for the kinetic stabilisation of the elusive silanone.[47d] Thus, quantum chemical probes of a series of diarylsilanones hinted at (i) an increasingly endothermic head-to-tail dimerisation process for bulkier aryl substituents, and (ii) a high energy barrier for the 1,2-aryl shift

necessary for the isomerisation from a silanone to the corresponding sila-ether (Scheme 1.6 and Table 1.5).



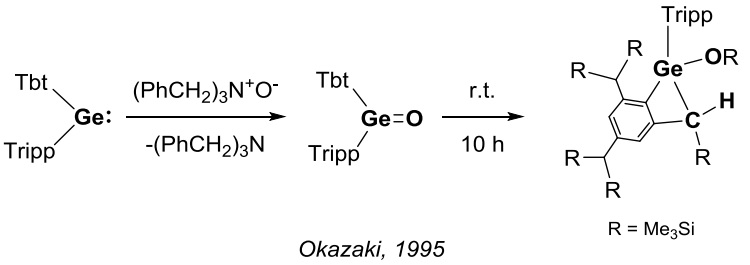
Scheme 1.6 The proposed chemical transformations of silanones (Ar)(Ar')Si=O; of which the energy profiles were calculated by Kimura and Nagase

Ar	Ar′	Dimerisation energy	Energy barrier for 1,2-aryl shift
Tripp	Tripp	-352	
Tripp	Tbt	-301	
Mes*	Tbt	-42	
Tbt	**Tbt**	**+192**	**+213**
^{Mes}Ter	**Tbt**	**+201**	**+234** (*^{Mes}Ter shift*) **+251**(*Tbt shift*)

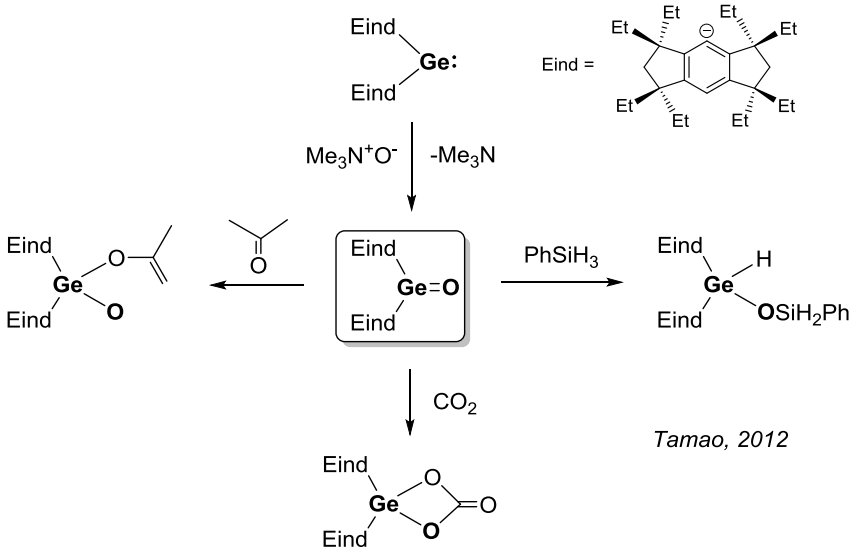
Table 1.5 Calculated dimerisation energies and the energetic barriers for 1,2-aryl shift (in kJ mol^{-1})

Inspired by these theoretical predictions, the use of a combination of kinetic stabilisation (steric protection around the Si=O unit) and thermodynamic stabilisation (by manipulating the electron density in the E=O bond to offset its intrinsic polarity) has indeed allowed for the isolation of a handful of stable

compounds bearing a formal Si=O bond.[31c] Accordingly, these species typically feature electron-donating fragments (*e.g* Group 15-based ligands, NHCs, electron-rich Transition Metal fragments) bound to the silicon centre, and/or a Lewis-acidic "cap" bound at the nucleophilic oxygen. Moreover, additional electronic stabilisation brought about by the coordination of a further electron-rich neutral donor at silicon is reflected by the larger number of reported base-stabilised silanones of the form $(R_1)(R_2)(L)Si=O$ compared to "free" silanones. A more detailed discussion of the synthesis and reactivity of silanones and related derivatives is provided in chapter 6 of this thesis (*vide infra*).



Scheme 1.7 Intramolecular cyclisation of the *quasi*-stable germanone (Tbt)(Tripp)Ge=O



Scheme 1.8 The formation of the stable germanone $(Eind)_2Ge=O$, and its reactivity towards acetone, phenylsilane, and carbon dioxide

Intriguingly, the kinetic stabilisation strategy proposed by Kimura and Nagase for silanones (Scheme 1.6) has been extended to germanium chemistry. Thus, the germanone (Tbt)(Tripp)Ge=O was synthesised *via* the oxidation of the corresponding germylene; however, this species was found to slowly undergo intramolecular cyclisation involving a proximal $CH(SiMe_3)_2$ group, over the course of 10 h (Scheme 1.7).[46f] The change to the more rigid ligand framework Eind (1,1,3,3,5,5,7,7-octaethyl-*s*-hydrindacen-4-yl), however, allowed for the isolation of the first stable germanone with a *three-coordinate* germanium centre $(Eind)_2Ge=O$ (Scheme 1.8).[48] This compound decomposes only at *ca.* 200°C under an argon atmosphere, and no change was detected in ^1H NMR spectrum of a sample heated at 80°C over three days. Structurally, it features a near-planar geometry around the tetrel atom (sum of all angles = 359.8°), and the Ge=O bond distance (1.6468(5) Å) is shorter than the typical Ge—O single bond length in four-coordinate Ge^{IV} complexes (1.76 Å). Reactivity studies on the other hand highlight the distinct zwitterionic nature of the Ge=O bond, compared to the C=O unit in ketones. Thus, $(Eind)_2Ge=O$ was found to activate acetone, phenylsilane, and carbon dioxide – reagents which generally do not react with ketones – and the isolated products from these reactions are suggestive of chemistry involving interaction between the extremely nucleophilic oxygen and the electrophilic carbon/silicon centres (Scheme 1.8).

In addition, examples of base-stabilised germanones – with oxygen-capping Lewis acids in some cases – have also been reported (Figure 1.11).[49] Due to the slight decrease in ionic character of the germanium-oxygen linkage and the

pyramidalisation of the tetrel centre, the Ge=O bond distances in these species are generally longer than that found in $(Eind)_2Ge=O$. However, an exception can be found in the DMAP-coordinated *N,N'*-diamidogermanone (*d*(Ge=O) = 1.646(2) Å, DMAP = 4-dimethylaminopyridine),[49b] where the Ge=O distance is statistically identical to that observed in Tamao's germanone. Presumably, this reflects a less perturbed Ge=O multiple bond, compared to NHC-stabilised counterparts, due to DMAP being a weaker donor (Figure 1.11).

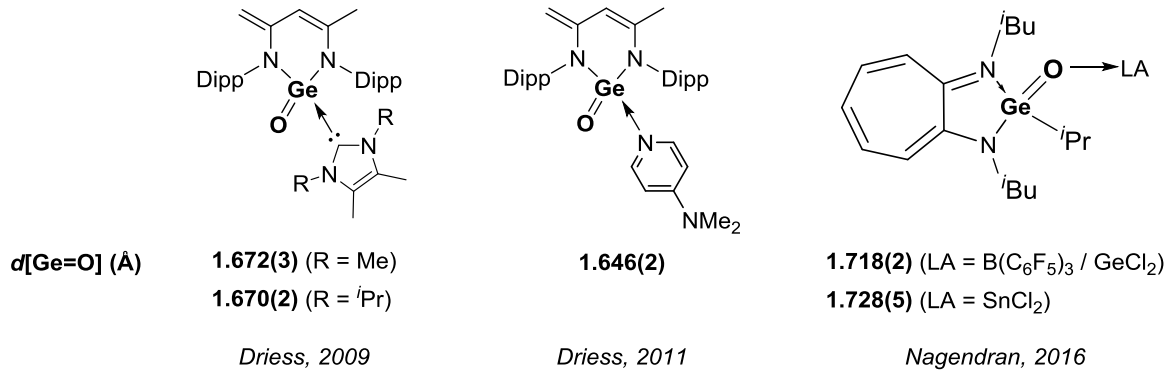


Figure 1.11 Reported base-stabilised germanones

1.2 *N,N'*-chelating ligands: Privileged bidentate donors in Main Group chemistry

Various examples from sections 1.1.2 and 1.1.3 have illustrated the need for suitable ligand design in the isolation of highly reactive Main Group compounds. Especially in the case of low-coordinate complexes featuring low-valent Main Group elemental centres – the need to overcome innate electronic deficiency and the propensity to aggregate/decompose requires bulky, strongly-donating supporting ligands. In this regard, *N,N'*-chelating donors have stood out as ideal candidates thanks to the π-donor capability of the nitrogen atoms, the steric protection offered by the flanking bulky *N*-bound substituents (which are also readily tunable), and the

intrinsic chelate effect.[50] Within the realm of Main Group chemistry, perhaps the most commonly-encountered ligand systems are (i) amidinates/guanidinates, (ii) diazabutadienyl-derived diamides and ethylenediamides, and (iii) β-diketiminates "Nacnacs".

1.2.1 Three-membered N,N'-chelates

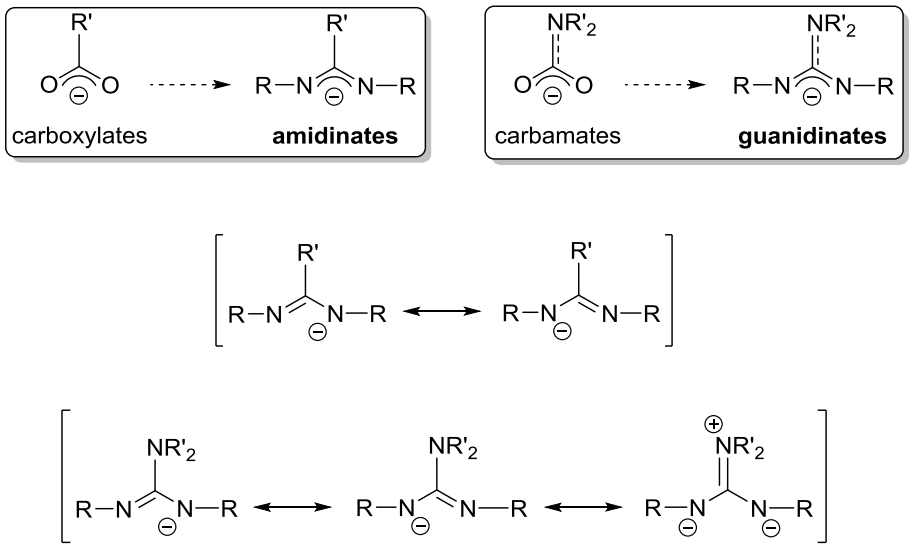
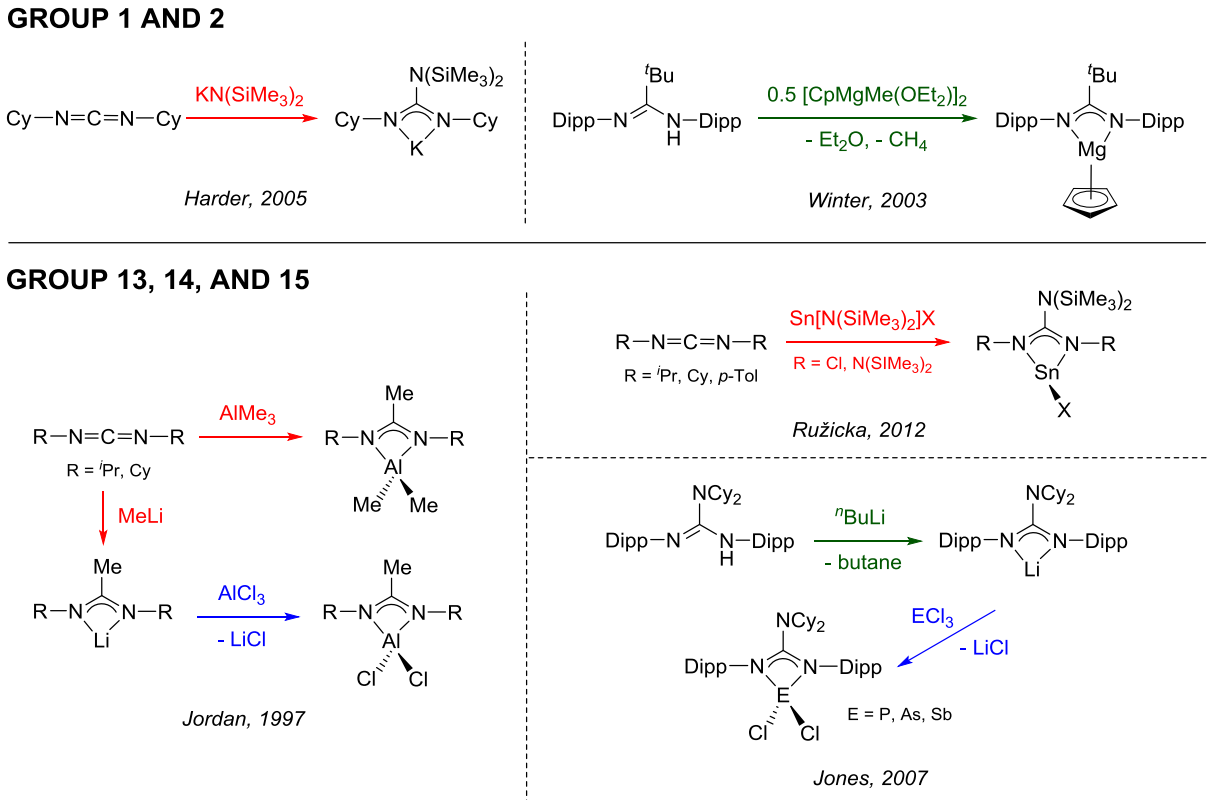


Figure 1.12 Amidinates, guanidinates, and their respective canonical resonance forms

Monoanionic amidinate (of the generic form $[C(R')(NR)_2]^-$) and guanidinate ($[C(NR'_2)(NR)_2]^-$) donors can be thought of as nitrogen analogues of carboxylates and carbamates, respectively (Figure 1.12).[51] By virtue of resonance, the negative charge is delocalised over the NCN backbone; notably, the incorporation of a C-bound amino group in the guanidinate ligand family induces an additional "doubly amido" canonical structure, which is thought to render them stronger donors than amidinates. Main Group complexes featuring these supporting ligands are commonly accessible by (i) insertion of a carbodiimide into a metal-carbon (for amidinates) or metal-amide bond (for guanidinates), (ii) deprotonation of an

amidine or guanidine protio-ligand by a strong base, and (iii) transmetallation between a Group 1 complex and a metal halide (Scheme 1.9).[52]

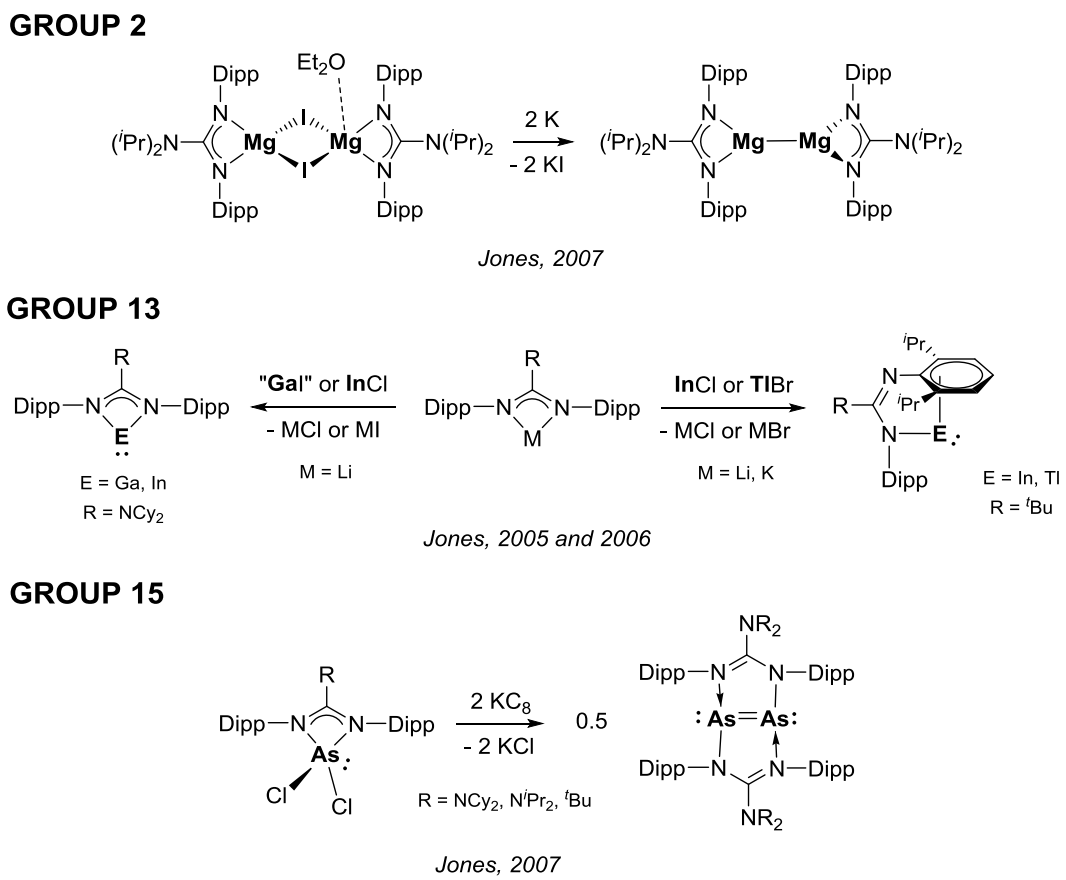


Scheme 1.9 Some examples of Main Group complexes with amidinate/guanidinate ligands, prepared *via* route (i) (*in red*), route (ii) (*in green*), and route (iii) (*in blue*).

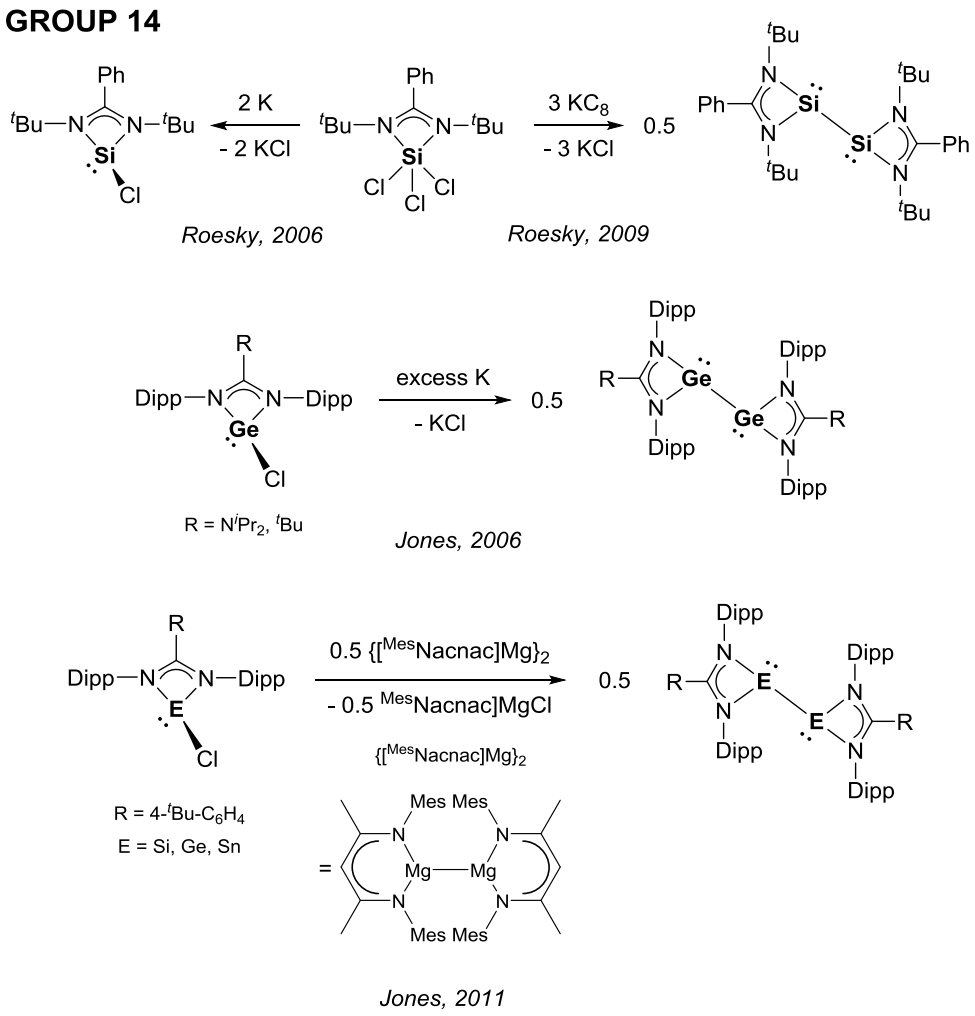
Since the mid-2000s, a handful of landmark low-valent Main Group compounds featuring amidinate/guanidinate ligands have been reported (Schemes 1.10 and 1.11).[53] The group of Jones pioneered the use of the bulky guanidinate donor $[(Cy_2N)C(NDipp)_2]^-$ to support complexes featuring monovalent Group 13 elements (Ga^I, In^I, Tl^I).[53a] This ligand displays a "conventional" *N,N'*-chelated bonding motif with gallium and indium, while *N*,(η^3-arene)-coordination is preferred in the case of thallium. By means of comparison, this *N*-arene coordination mode was found to predominate in the

amidinate complexes of both indium and thallium (Scheme 1.10).[53b] A possible explanation for these observations can be proposed based on the difference in the donor capabilities of these two classes of ligand. Guanidinates – the stronger donors (Figure 1.12) – are associated with more robust N─E bonds (E = Group 13 element), which in turn renders the *N,N'*-chelated conformation more thermodynamically stable compared to that in amidinates. With respect to the Group 14 elements, ligand systems of the form $[(R)C(NDipp)_2]^-$ (R = ^{t}Bu, N^{i}Pr$_2$) have proved to be effective in stabilizing Ge^I-dimers with bonding between two germanium atoms in a *trans*-bent configuration (Scheme 1.11).[53c] In the same year (2006), Roesky and co-workers employed an amidinate ligand to isolate the first example of a base-stabilised monochlorosilylene, by treating the trichlorosilyl precursor $\{(Ph)C(N^tBu)_2\}SiCl_3$ with two equivalents of potassium metal.[53d] Moreover, the corresponding reduction process with three equivalents of potassium graphite was found to generate a Si^I-dimer, $[\{(Ph)C(N^tBu)_2\}Si]_2$, featuring a Si─Si bond, which features a similar molecular geometry to that of the germanium analogue.[53e] Notably, beyond the realm of low-valent Main Group complexes, the silylene $\{PhC(N^tBu)_2\}SiCl$ also acts as a versatile starting material for numerous bidentate bis(*N*-heterocyclic silylene) ligands, whose Transition Metal complexes have been investigated in a range of catalytic processes.[53f] In Group 15, the reduction of the amidinate/guanidinate stabilised dichloroarsines has been shown to result in the formation of a donor-stabilised diarsene (Scheme 1.10).[52d] In this compound, the ligand bonding motif was shown to have changed from κ^2-*N,N'*-chelated to

μ²-*N,N'*-bridged, and crystallographic data hinted at multiple bonding character in the As─As linkage. With regards to *s*-block elements, in particular those of Group 2, Jones *et al.* have isolated two remarkable dimeric Mg^{I} complexes with unprecedented Mg─Mg bonds, stabilised by either a guanidinate $[(^{i}Pr_2N)C(NDipp)_2]^-$ or a β-diketiminate ("Nacnac") $[HC\{C(Me)(NMes)\}_2]^-$ ligand, from the reduction of the corresponding iodo precursors with potassium metal.[53g] Interestingly enough, the Mes-substituted Nacnac-ligated Mg^{I}-dimer itself was later employed as a reducing agent in the synthesis of a series of sterically-encumbered amidinate-supported monovalent tetrel dimers (Si, Ge, Sn), which notably featured the first example of a dimeric Sn^{I}-species stabilised by an amidinate donor (Scheme 1.11).[53h]



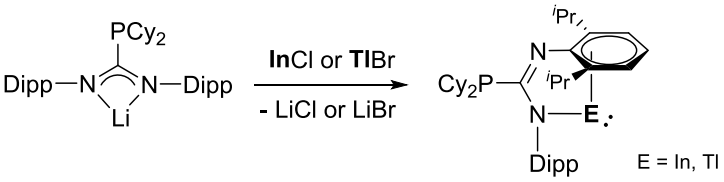
Scheme 1.10 Prominent examples of low-valent Group 2/13/15 elemental complexes featuring amidinate/guanidinate ligands



Scheme 1.11 Prominent examples of low-valent Group 14 elemental complexes featuring amidinate/guanidinate ligands

Besides amidinates and guanidinates, three-membered NC*N*-chelate ligands which feature C-bound *phosphido* functions (*phospha*-guanidinates) have been synthesised, and their coordination chemistry with low-valent heavier Group 13 elements probed using conventional synthetic methodologies (Scheme 1.12).[54] Thus, the lithiated ligand {(Cy_2P)C($NDipp)_2$}Li reacts with a monovalent metal halide (InCl or TlBr), to afford the corresponding In^I and Tl^I complexes, featuring *N*,(η^3-arene)-metal interaction in both cases.[54c] Presumably, compared to NCy_2, the lone pair on the pnictogen centre in PCy_2 is more pyramidalised, which hampers

effective π-delocalisation into the three-membered NCN ligand scaffold and thereby reduces the contribution of the "doubly amido" resonance form. As a result, the donor capability of phospha-guanidinates can be envisaged to be less than that of guanidinates, which – in a similar fashion to amidinate-based systems – disfavours the *N,N'*-chelated bonding mode.[53b] Thus, it is understandable that other examples of low-valent phospha-guanidinate-stabilised Main Group complexes remain elusive to date.

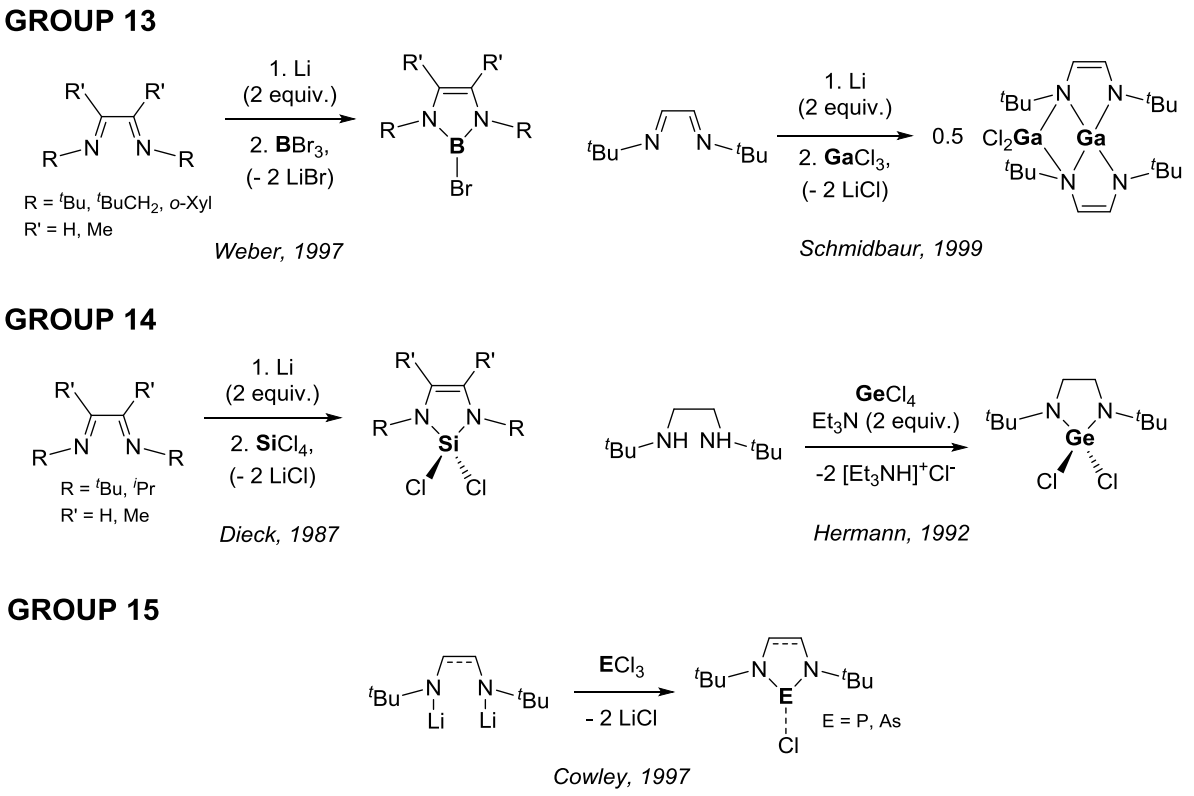


Jones, 2008

Scheme 1.12 Examples of phospha-guanidinate-stabilised low-valent Main Group complexes

1.2.2 Four-membered N,N'-chelates

1,4-Diazabutadienes, of the generic form RN=C(H)─C(H)=NR, generally undergo two-electron reduction with a Group 1 or Group 2 metal to afford the dianionic diazabutadienyl ligands $[RN{-}C(H){=}C(H){-}NR]^{2-}$. On the other hand, the preparation of the saturated ethylenediamide analogues, $[RN{-}C(H)_2{-}C(H)_2{-}NR]^{2-}$, typically requires double-deprotonation of the corresponding diamine starting material. In either case, coordination to a *p*-block element centre can be facilitated by the reaction of the dianionic ligand (commonly generated *in situ*) with a metal halide source, which results in the extrusion of the corresponding Group 1/Group 2/ammonium halide salt (Scheme 1.13).[55]

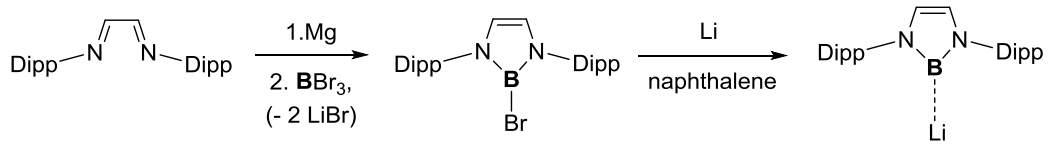


Scheme 1.13 Some examples of Main Group complexes stabilised by four-membered *N,N'*-chelates, prepared by metathesis with either Group 1 metal complexes or *in situ*-deprotonated ligands

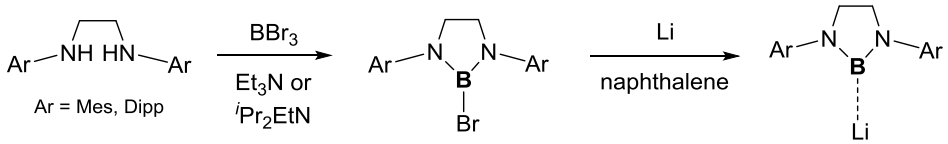
In part, the interest in low-valent Main Group complexes stabilised by these two classes of ligands (and in particular those featuring Group 13 and Group 14 elements) can be attributed to the structural resemblance and isoelectronic relationship with *N*-heterocyclic carbenes, which hints at a degree of electronic stabilisation for the resulting complexes.[50,56] With regards to carbene analogues of the heavier tetrels, these neutral compounds can be accessed *via* facile metathesis between the doubly-lithiated ligand and a readily available source of a divalent halide (for germanium and tin), or by reduction of the corresponding E^{IV} precursor (for silicon, Scheme 1.14).[23,55b,55f] Perhaps more remarkable are the syntheses of the anionic Group 13 counterparts (boryl and gallyl),[55e,57] which belong to the exotic class of complexes bearing a nucleophilic triel element centre. In particular, the

boryl ligand has played a pivotal role as a strongly σ-donating and π-withdrawing donor in supporting divalent silicon and tin species which display unusual reactivity towards small molecules (Schemes 1.3 and 1.4).[27a,27c,27d,29c] It is also worth mentioning that additional incorporation of an aromatic fragment at the ligand backbone is also possible – several examples of low-valent Group 13 and Group 14 complexes supported by benzannulated derivatives of the four-membered *N,N′*-chelates have been reported (Figure 1.13).[25a,57b,58]

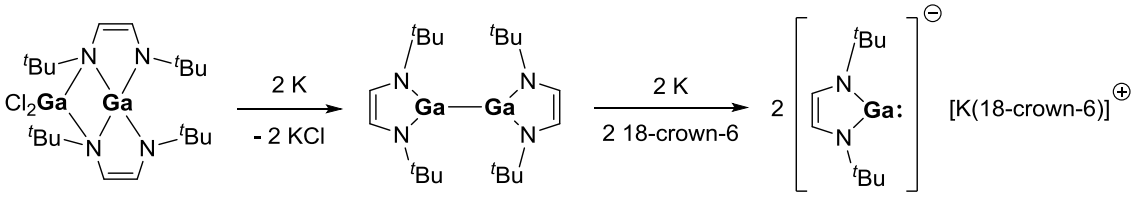
GROUP 13



Yamashita and Nozaki, 2006

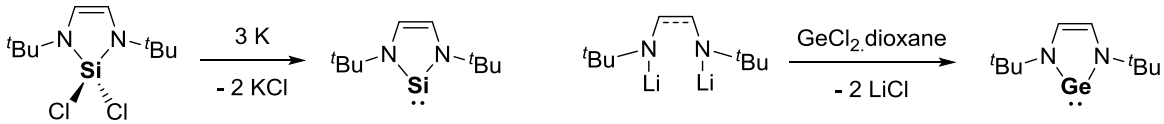


Yamashita and Nozaki, 2008



Schmidbaur, 1999

GROUP 14



West, 1994 *Herrmann, 1992*

Scheme 1.14 Prominent examples of low-valent Group 13/14 complexes featuring four-membered *N,N′*-chelating ligands

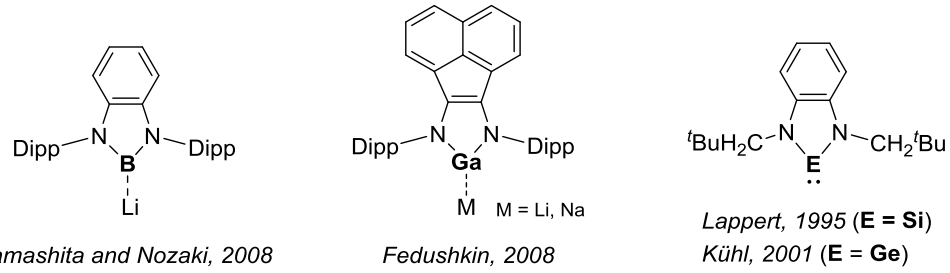


Figure 1.13 Some examples of low-valent Main Group complexes stabilised by backbone-annulated four-membered *N,N'*-chelates

1.2.3 Five-membered N,N'-chelates

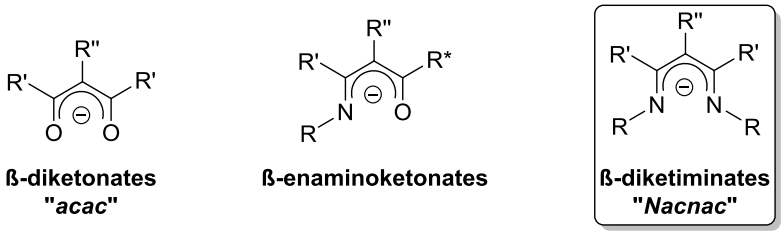


Figure 1.14 Commonly employed chelate ligands in coordination chemistry: (*from left*) β-diketonates, β-enaminoketonates, and β-diketiminates

Over the last 20 years, β-diketiminate ligands ("Nacnac", [R''{C(R')(NR)}$_2$]$^-$) have acquired a reputation as a versatile class of monoanionic bidentate donor, which has been widely employed across almost all stable elements in the Periodic Table.[50,59] Compared to their "predecessors" β-diketonates and β-enaminoketonates (Figure 1.14),[60] the complete substitution of oxygen atoms by NR functions in Nacnac ligands has two main advantages. On electronic grounds, the donor capabilities generally increase, which can be attributed to nitrogen (3.04) being less electronegative than oxygen (3.44, Pauling scale).[1] Furthermore, significant variation in the *N*-bound R substituents is possible, in order to achieve a tailored steric and/or electronic profile for the resulting ligand; in these regards, Nacnac donors are rather reminiscent of amidinates (Figure 1.12). These factors have rendered Nacnacs a

particularly attractive class of ligands for the stabilisation of low-coordinate, low-valent Main Group complexes (Figures 1.15 and 1.16);[53g,53h,62-65] a detailed discussion on this topic will be provided in chapter 3.

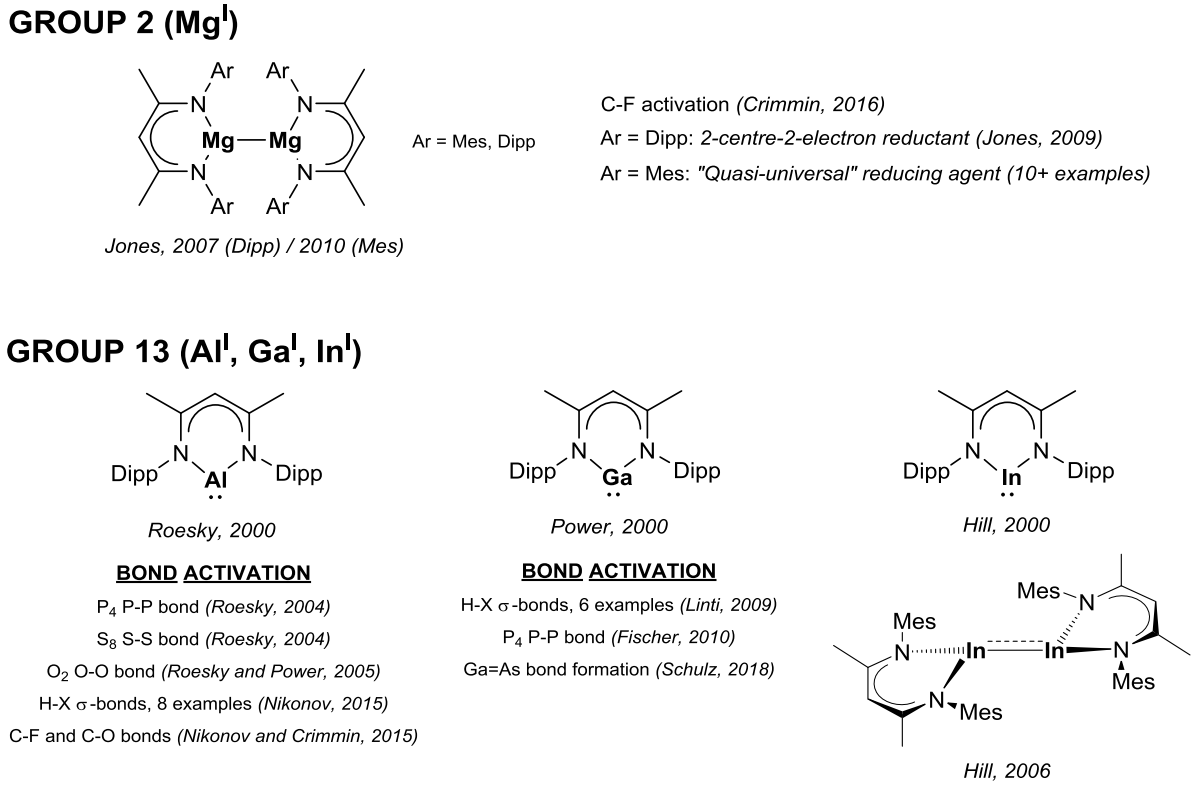


Figure 1.15 Examples of Nacnac-stabilised sub-valent Group 2 and Group 13 compounds (and their associated reactivities)

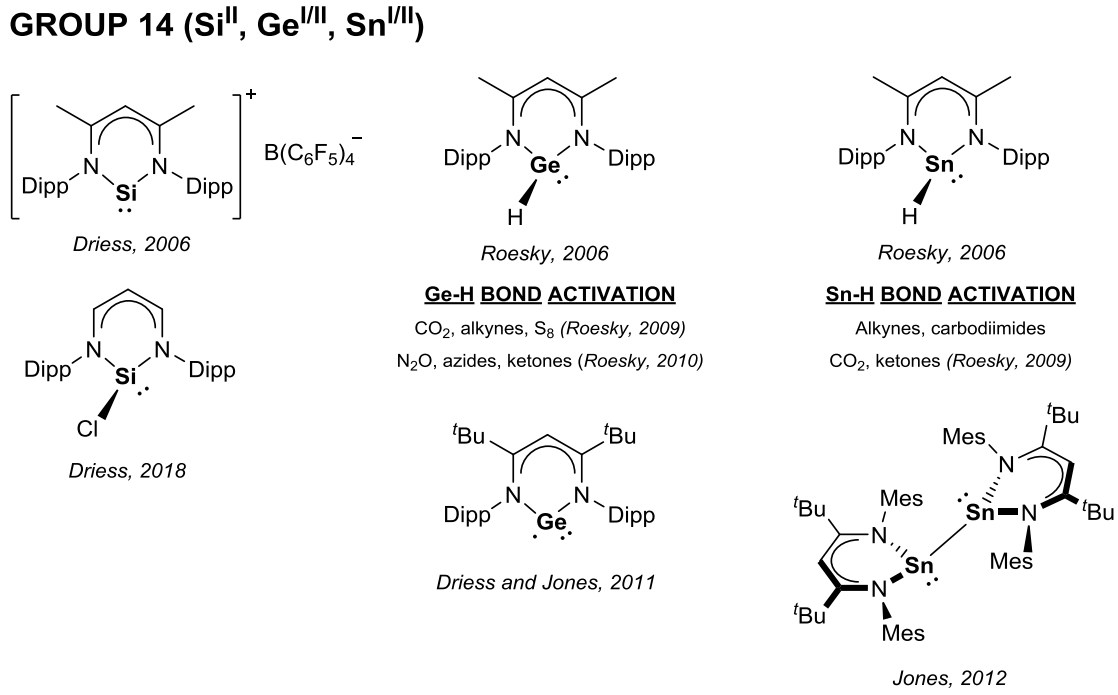
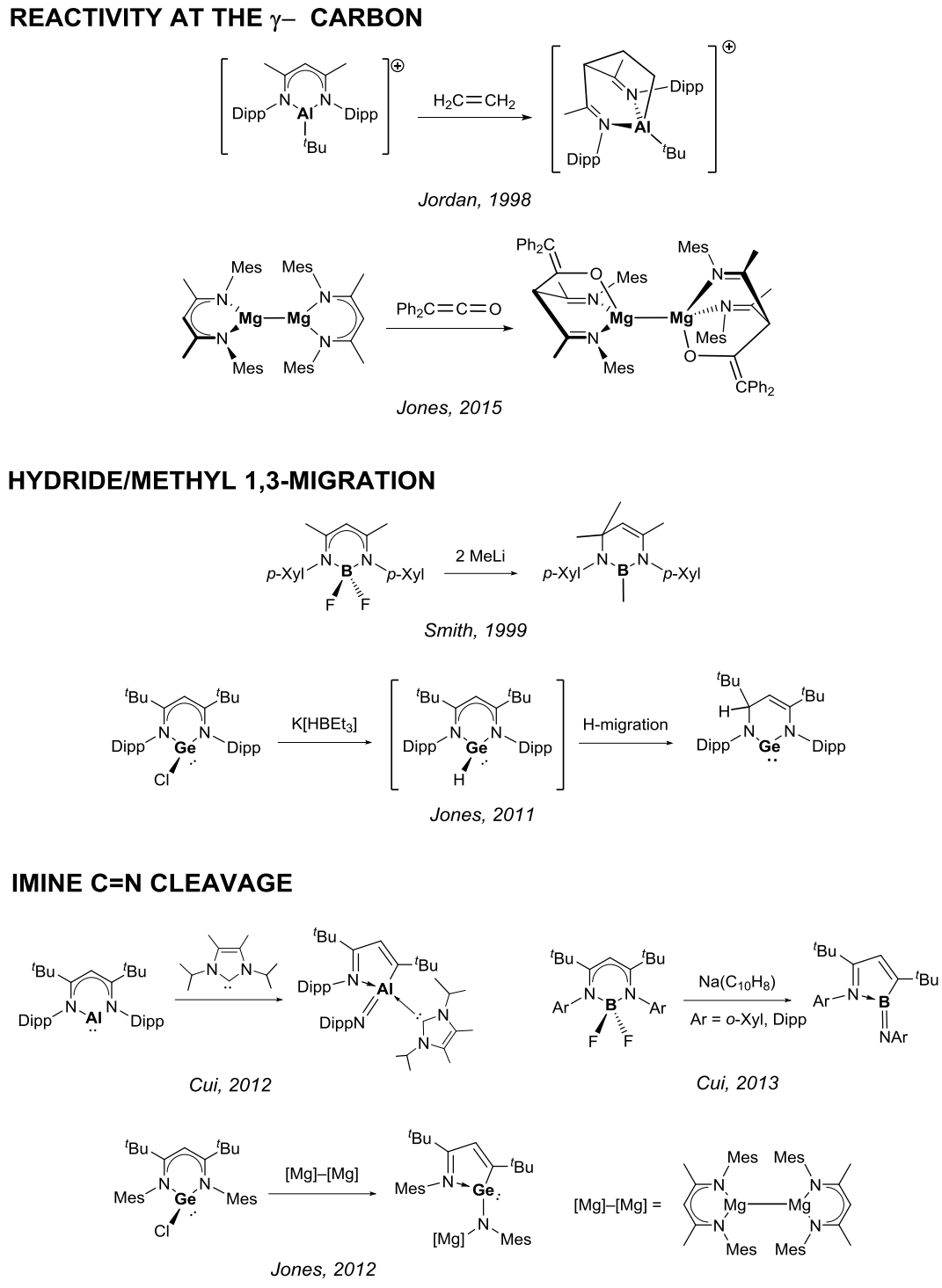


Figure 1.16 Examples of Nacnac-stabilised sub-valent Group 14 compounds (and their associated reactivities)

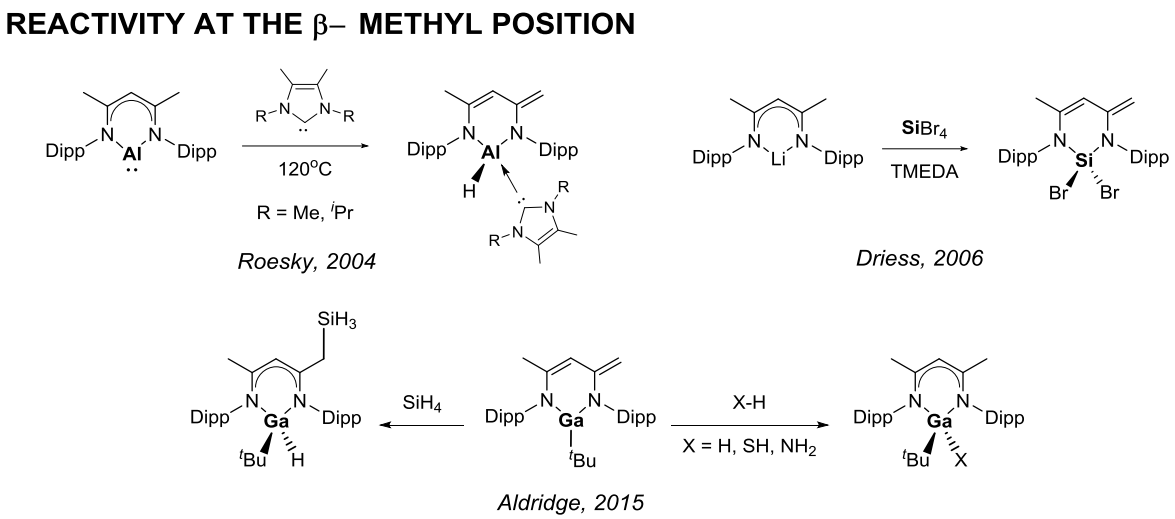
Notably, the modes of reactivity outlined in Figures 1.15 and 1.16 are predominantly observed at the associated Main Group elemental centres. This highlights the robustness nature of Nacnac ligands, which are by-and-large considered as "innocent" spectator donors in coordination chemistry.[59a,59d] Nonetheless, a number of examples of chemical transformations that occur at backbone ligand sites of Main Group complexes have been documented.[66] Such chemistry typically involves the γ-carbon (in tandem with the electrophilic metal centre),[67] or substituent migration from the Main Group element centre to the β-carbon position (Scheme 1.15).[68] Furthermore, a pathway which severely disrupts the five-membered backbone – and is frequently associated with low-valent Main Group complexes – is imine C=N cleavage. This process affords an aza-butadienyl *N,C*-chelate (or the reduced monoanionic derivative), with accompanying formation

of a nitrogen-heteroelement multiple bond in most cases.[65e,69] These observations hint at alternating polarisation in the NC_3N unit, which gives rise to the electrophilicity of the β-carbon and the nucleophilicity of the γ-carbon.



Scheme 1.15 Examples of ligand-based reactivity in Nacnac complexes of Main Group elements

In addition, a type of chemical transformation at the Nacnac ligand backbone that is exclusive to the "traditional" β-methylated Nacnac ligand $[HC\{C(Me)(NR)\}_2]^-$ is the deprotonation of the β-carbon-bound methyl group, which is acidic enough to be attacked by strong bases (Scheme 1.16).[70] The resulting dianionic bis(amido) ligand was observed to participate in metal-ligand cooperative reactivity, which often involved the "regeneration" of the monoanionic Nacnac ligand scaffold *via* a formal 1,4-addition process.



Scheme 1.16 Some examples of reactivity observed at the backbone methyl position in Nacnac complexes of Main Group elements

1.3 Project Aims

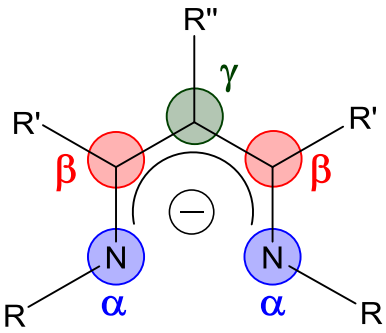


Figure 1.17 Commonly used labelling scheme for substituent positions on the NC_3N skeleton in a typical (symmetrical) Nacnac ligand

Prior to the beginning of this project, tailoring the steric and/or electronic profiles of Nacnac ligands had predominantly been carried out by varying the (α-position) *N*-bound substituents and (less commonly) the β- and γ-carbon-bound functions (see Figure 1.17 for labelling scheme). In particular, while Nacnac ligands featuring either Me, ^{t}Bu, CF_3, or H groups at the β-position are near ubiquitous in Main Group chemistry, complexation studies with those bearing π-donating substituents (*e.g* amido or alkoxido) at the same position have not been explored in any depth. Thus, the synthesis of these amido/alkoxo-functionalised Nacnacs would be potentially beneficial to the field of Main Group chemistry; due to the electronic perturbation brought about by these electron-rich functions, unconventional electronic properties of the resulting complexes could be induced. Drawing inspiration from pioneering works by Viehe *et al.* in the late 1970s and further recent insights by Clyburne group,[61] the synthesis and characterisation of a series of *(dimethyl)amino-functionalised* β-diketiminate protio-ligands *N*-nacnac(H) was targeted. The ligand synthesis strategy will be discussed in chapter 3, together with the complexation of these protio-ligands with lithium and aluminium *via* direct metallation. Most importantly, chapters 4, 5, and 6 showcase the focal research theme of this thesis: the coordination chemistry of *N*-nacnac ligands with heavier Group 14 elements (Si, Ge, Sn). Chapter 4 discusses the synthesis of the chlorotetrelene complexes (with silicon, germanium, and tin) as versatile precursors to systems with more exotic reactivities, which is then demonstrated by a preliminary study of the corresponding cationic tetrelenes formed by chloride

abstraction. Chapter 5 examines the formation of the phosphaketenyl-germylenes and stannylenes, with the emphasis on the photochemical behaviour of the former. Lastly, chapter 6 explores the chemistry of the chlorosilylene, with regards to (i) oxidation-substitution chemistry, which affords a series of silicon analogues of classical carbonyl compounds, and (ii) the effect of ligand substitution on the propensity for C=N cleavage.

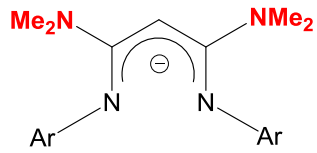


Figure 1.18 Generic form of amino-functionalised β-diketiminate ligand (*N*-nacnac) – the ligand of choice in complexation studies with Main Group elements in this thesis

1.4 References

[1] J. Emsley in *The Elements* 3rd ed., Clarendon Press, Oxford, **1998**.

[2] R. Thomson in *Industrial Inorganic Chemicals: Production and Uses*, The Royal Society of Chemistry, Cambridge, **1995**.

[3] For a more modern perspective on the event: a) D. Seyferth, *Organometallics* **2001**, *20*, 1488–1498; b) D. Seyferth, *Organometallics* **2001**, *20*, 2940–2955.

[4] a) R. W. Bunsen, *Poggendorf's Ann.* **1837**, *40*, 219-233; b) R. W. Bunsen, *Poggendorf's Ann.* 1837, 42, 145-158; c) R. W. Bunsen, *Ann. Pharm.* **1837**, *24*, 271-286; d) R. W. Bunsen, *Ann. Pharm.* **1839**, *31*, 175-180; e) R. W. Bunsen, *Justus Liebigs Ann. Chem.* **1841**, *37*, 1-57; f) R. W. Bunsen, *Justus Liebigs Ann. Chem.* **1842**, *42*, 14-46; g) R. W. Bunsen, *Justus Liebigs Ann. Chem.* **1843**, *46*, 1-48; h) E. Frankland, *Justus Liebigs Ann. Chem.* **1849**, *71*, 213-216; i) E. Frankland, *Philos. Trans.* **1852**, *142*, 417-444.

[5] a) H. Moissan, *C. R. Hebd. Seances Acad. Sci.* **1886**, *102*, 1543 – 1544; b) H.Moissan, *C. R. Hebd. Seances Acad. Sci.* **1886**, *103*, 202 – 205; c) H. Moissan, *C. R.*

Hebd. Seances Acad. Sci. **1886**, *103*, 256 – 258; d) C. Winkler, *Ber. Dtsch. Chem. Ges.* **1886**, *19*, 210–211.

[6] a) W. Hallwachs, A. Schafarik, *Justus Liebigs Ann. Chem.* **1859**, *109*, 206-209; b) E. Frankland, *Justus Liebigs Ann. Chem.* **1853**, *85*, 329-373; c) C. Löwig, M. E. Schweizer, *Justus Liebigs Ann. Chem.* **1850**, *75*, 315-355.

[7] a) V. Grignard, *C. R. Hebd. Seances Acad. Sci.* **1900**, 130, 1322-1324; b) W. Schlenk, J. Holtz, *Ber. Dtsch. Chem. Ges.* **1917**, *50*, 262-274; c) K. Ziegler, H. Colonius, *Liebigs Ann. Chem.* **1930**, *476*, 135-149; d) H. Gilman, E. A. Zoellner, W. M. Selby, *J. Am. Chem. Soc.* **1932**, *54*, 1957-1962; e) H. Gilman, E. A. Zoellner, W. M. Selby, *J. Am. Chem. Soc.* **1933**, *55*, 1252-1257.

[8] Winners of the Nobel Prizes in Chemistry, http://nobelprizes.com/nobel/chemistry/chemistry.html. Note that in 1912 Grignard was co-awarded the prize with Paul Sabatier.

[9] a) G. B. Buckton, *Proc. R. Soc. Lond.* **1859**, *9*, 685-690; b) G. B. Buckton, *Philos. Trans. R. Soc. London* **1859**, *149*, 417-435; c) G. B. Buckton, *Justus Liebigs Ann. Chem.* **1859**, *109*, 218-227; d) G. B. Buckton, *Justus Liebigs Ann. Chem.* **1859**, *112*, 220-227; e) T. Midgley, Jr.; T. A. Boyd, *Ind. Eng. Chem.* **1922**, *14*, 897-901.

[10] a) E. G. Rochow, W. F. Gilliam, *J. Am. Chem. Soc.* **1941**, *63*, 798-800; b) E. G. Rochow, *J. Am. Chem. Soc.* **1945**, *67*, 963-965; c) E. G. Rochow in *An Introduction to the Chemistry of the Silicones (2nd ed.)*, Wiley, New York, **1951**. A modern review on the chemistry of silicones can be found at: d) D. Seyferth, *Organometallics* **2001**, *20*, 4978–4992.

[11] a) H. Yamamoto in *Lewis Acids in Organic Synthesis*, Wiley-VCH, Weinheim, **2000**; b) H. Yamamoto, K. Oshima, *Main Group Metals in Organic Synthesis*, Wiley-VCH, Weinheim, **2004**.

[12] a) W. N. Lipscomb, *Acc. Chem. Res.* **1973**, *6*, 257–262; b) K. P. Callahan, M. F. Hawthorne, *Adv. Organomet. Chem.* **1976**, *14*, 145–186; c) W. N. Lipscomb, *Science* **1977**, *196*, 1047–1055. A more recent micro-review by Russell Grimes (who worked

with both Lipscomb and Hawthorne) on modern applications of carboranes can be found at: d) R. N. Grimes, *Dalton Trans.* **2015**, *44*, 5939–5956.

[13] W. E. Dasent in *Nonexistent Compounds*, Marcel Dekker, Inc.: New York, **1965**.

[14] Early discussions on the rule can be found at: a) J. J. Goubeau, *Angew. Chem.* **1957**, 69, 77-82; b) P. Jutzi, *Angew. Chem. Int. Ed.* **1975**, *14*, 232–245; c) L.E. Guseln'ikov, N. S. Nametkin, *Chem. Rev.* **1979**, 79, 529 (and references cited therein).

[15] H. Jacobsen, T. Ziegler, *J. Am. Chem. Soc.* **1994**, *116*, 3667–3679.

[16] a) P. J. Davidson, M. F. Lappert, *J. Chem. Soc. Chem. Commun.* **1973**, 317a–317a; b) D. H. Harris, M. F. Lappert, *J. Chem. Soc. Chem. Commun.* **1974**, 895–896; c) D. E. Goldberg, D. H. Harris, M. F. Lappert, K. M. Thomas, *J. Chem. Soc. Chem. Commun.* **1976**, 261–262; d) P. J. Davidson, D. H. Harris, M. F. Lappert, *J. Chem. Soc. Dalton Trans.* **1976**, 2268–2274; e) J. D. Cotton, P. J. Davidson, M. F. Lappert, *J. Chem. Soc. Dalton Trans.* **1976**, 2275–2286; f) M. J. S. Gynane, D. H. Harris, M. F. Lappert, P. P. Power, P. Rivière, M. Rivière-Baudet, *J. Chem. Soc. Dalton Trans.* **1977**, 2004–2009; g) B. Cetinkaya, I. Gumrukcu, M. F. Lappert, J. L. Atwood, R. D. Rogers, M. J. Zaworotko, *J. Am. Chem. Soc.* **1980**, *102*, 2088–2089; h) M. F. Lappert, M. J. Slade, J. L. Atwood, M. J. Zaworotko, *J. Chem. Soc. Chem. Commun.* **1980**, 621–622. Note: the monomeric structure of the bis(amido)tetrelenes reported in ref. 13b were confirmed by X-ray crystallography later – see: i) T. Fjeldberg, H. Hope, M. F. Lappert, P. P. Power, A. J. Thorne, *J. Chem. Soc. Chem. Commun.* **1983**, 639–641 (stannylene and plumbylene); j) R. W. Chorley, P. B. Hitchcock, M. F. Lappert, W.-P. Leung, P. P. Power, M. M. Olmstead, *Inorganica Chim. Acta* **1992**, *198–200*, 203–209 (germylene). The dimeric structure of the bis(alkyl)germylene reported in ref 13c were confirmed by X-ray crystallography in: k) D. E. Goldberg, P. B. Hitchcock, M. F. Lappert, K. M. Thomas, A. J. Thorne, T. Fjeldberg, A. Haaland, B. E. R. Schilling, *J. Chem. Soc. Dalton Trans.* **1986**, 2387–2394.

[17] M. F. Lappert, S. J. Miles, P. P. Power, A. J. Carty, N. J. Taylor, *J. Chem. Soc. Chem. Commun.* **1977**, 458–459.

[18] a) M. J. S. Gynane, M. F. Lappert, S. J. Miles, P. P. Power, *J. Chem. Soc. Chem. Commun.* **1976**, 256–257; b) M. J. S. Gynane, M. F. Lappert, S. J. Miles, A. J. Carty, N. J. Taylor, *J. Chem. Soc. Dalton Trans.* **1977**, 2009–2015; c) M. F. Lappert, S. J. Miles, J. L. Atwood, M. J. Zaworotko, A. J. Carty, *J. Organomet. Chem.* **1981**, *212*, C4–C6. Note: nearly 20 years after the report on O─H activation with the bis(alkyl)germylene (ref. 14c), the corresponding chemistry with bis(alkyl)stannylene was explored – see: d) F. Schager, R. Goddard, K. Seevogel, K.-R. Pörschke, *Organometallics* **1998**, *17*, 1546–1551.

[19] Selected reviews: a) W. P. Neumann, *Chem. Rev.* **1991**, *91*, 311–334; b) N. Tokitoh, R. Okazaki, *Coord. Chem. Rev.* **2000**, *210*, 251–277; c) Y. Mizuhata, T. Sasamori, N. Tokitoh, *Chem. Rev.* **2009**, *109*, 3479–3511.

[20] Selected reviews: a) J. A. C. Clyburne, N. McMullen, *Coord. Chem. Rev.* **2000**, *210*, 73–99; b) P. P. Power, *J. Organomet. Chem.* **2004**, *689*, 3904–3919; c) E. Rivard, P. P. Power, *Inorg. Chem.* **2007**, *46*, 10047–10064; d) T. Matsuo, K. Tamao, *Bull. Chem. Soc. Jpn.* **2015**, *88*, 1201–1220; e) D. L. Kays, *Chem. Soc. Rev.* **2016**, *45*, 1004–1018.

[21] M. Usher, A. V Protchenko, A. Rit, J. Campos, E. L. Kolychev, R. Tirfoin, S. Aldridge, *Chem. Eur. J.* **2016**, *22*, 11685–11698.

[22] a) P. P. Power, *Nature* **2010**, *463*, 171–177; b) T. Chu, G. I. Nikonov, *Chem. Rev.* **2018**, *118*, 3608–3680.

[23] M. Denk, R. Lennon, R. Hayashi, R. West, A. V Belyakov, H. P. Verne, A. Haaland, M. Wagner, N. Metzler, *J. Am. Chem. Soc.* **1994**, *116*, 2691–2692.

[24] A. J. Arduengo, R. L. Harlow, M. Kline, *J. Am. Chem. Soc.* **1991**, *113*, 361–363.

[25] a) B. Gehrhus, M. F. Lappert, J. Heinicke, R. Boese, D. Bläser, *J. Chem. Soc. Chem. Commun.* **1995**, 1931–1932; b) R. West, M. Denk, *Pure Appl. Chem.* **1996**, *68*, 785–788; c). Li, N. J. Hill, A. C. Tomasik, G. Bikzhanova, R. West, *Organometallics* **2006**, *25*, 3802–3805; d) A. C. Tomasik, A. Mitra, R. West, *Organometallics* **2009**, *28*, 378–381; e) P. Zark, A. Schäfer, A. Mitra, D. Haase, W. Saak, R. West, T. Müller, *J. Organomet. Chem.* **2010**, *695*, 398–408; f) M. Asay, S. Inoue, M. Driess, *Angew. Chem.*

Int. Ed. **2011**, *50*, 9589–9592; g) i) T. Kosai, S. Ishida, T. Iwamoto, *Angew. Chem. Int. Ed.* **2016**, *55*, 15554–15558; h) I. Alvarado-Beltran, A. Baceiredo, N. Saffon-Merceron, V. Branchadell, T. Kato, *Angew. Chem. Int. Ed.* **2016**, *55*, 16141–16144; i) H. Wang, T. L. Chan, Z. Xie, *Chem. Commun.* **2018**, *54*, 385–388. Some reviews can also be found at: j) M. Haaf, T. A. Schmedake, R. West, *Acc. Chem. Res.* **2000**, *33*, 704–714; k) N. J. Hill, R. West, *J. Organomet. Chem.* **2004**, *689*, 4165–4183.

[26] a) M. Kira, S. Ishida, T. Iwamoto, C. Kabuto, *J. Am. Chem. Soc.* **1999**, *121*, 9722–9723; b) T. Abe, R. Tanaka, S. Ishida, M. Kira, T. Iwamoto, *J. Am. Chem. Soc.* **2012**, *134*, 20029–20032.

[27] a) A. V Protchenko, K. H. Birjkumar, D. Dange, A. D. Schwarz, D. Vidovic, C. Jones, N. Kaltsoyannis, P. Mountford, S. Aldridge, *J. Am. Chem. Soc.* **2012**, *134*, 6500–6503; b) B. D. Rekken, T. M. Brown, J. C. Fettinger, H. M. Tuononen, P. P. Power, *J. Am. Chem. Soc.* **2012**, *134*, 6504–6507; c) A. V. Protchenko, A. D. Schwarz, M. P. Blake, C. Jones, N. Kaltsoyannis, P. Mountford, S. Aldridge, *Angew. Chem. Int. Ed.* **2013**, *52*, 568–571; d) T. J. Hadlington, J. A. B. Abdalla, R. Tirfoin, S. Aldridge, C. Jones, *Chem. Commun.* **2016**, *52*, 1717–1720.

[28] D. Wendel, A. Porzelt, F. A. D. Herz, D. Sarkar, C. Jandl, S. Inoue, B. Rieger, *J. Am. Chem. Soc.* **2017**, *139*, 8134–8137.

[29] a) Y. Peng, J.-D. Guo, B. D. Ellis, Z. Zhu, J. C. Fettinger, S. Nagase, P. P. Power, *J. Am. Chem. Soc.* **2009**, *131*, 16272–16282; b) M. Usher, A. V Protchenko, A. Rit, J. Campos, E. L. Kolychev, R. Tirfoin, S. Aldridge, *Chem. Eur. J.* **2016**, *22*, 11685–11698; c) A. V. Protchenko, J. I. Bates, L. M. A. Saleh, M. P. Blake, A. D. Schwarz, E. L. Kolychev, A. L. Thompson, C. Jones, P. Mountford, S. Aldridge, *J. Am. Chem. Soc.* **2016**, *138*, 4555–4564.

[30] R. Turnell-Ritson, J. Sapsford, R. Cooper, S. Lee, T. Földes, P. Hunt, I. Pápai, A. E. Ashley, *Chem. Sci.* **2018**, *13*, 2–4.

[31] Selected reviews: a) J. Barrau, J. Escudie, J. Satgé, *Chem. Rev.* **1990**, *90*, 283–319; b) A. G. Brook, M. A. Brook, .*Adv. Organomet. Chem.* **1996**, *39*, 71-158; c) Y. Xiong, S. Yao, M. Driess, *Angew. Chem. Int. Ed.* **2013**, *52*, 4302–4311.

[32] H. Suzuki, N. Tokitoh, R. Okazaki, S. Nagase, M. Goto, *J. Am. Chem. Soc.* **1998**, *120*, 11096–11105.

[33] P. V. R. Schleyer, P. D. Stout, *J. Chem. Soc. Chem. Commun.* **1986**, 1373–1374.

[34] a) A. G. Brook, F. Abdesaken, B. Gutekunst, G. Gutekunst, R. K. Kallury, *J. Chem. Soc. Chem. Commun.* **1981**, 191–192; b) R. West, M. J. Fink, J. Michl, *Science* **1981**, *214*, 1343–1344; c) M. Yoshifuji, M. Yoshifuji, I. Shima, I. Shima, N. Inamoto, N. Inamoto, K. Hirotsu, K. Hirotsu, T. Higuchi, T. Higuchi, *J. Am. Chem. Soc.* **1981**, *103*, 4587–4589. Note: Structural elucidation of the silaethene was made available by X-ray crystallography a year after its report: d) A. G. Brook, S. C. Nyburg, F. Abdesaken, B. Gutekunst, G. Gutekunst, R. Krishna, M. R. Kallury, Y. C. Poon, Y. M. Chang, W. Wong-Ng, *J. Am. Chem. Soc.* **1982**, *104*, 5667–5672.

[35] Selected reviews: a) P. P. Power, *Chem. Rev.* **1999**, *99*, 3463–3503; b) R. C. Fischer, P. P. Power, *Chem. Rev.* **2010**, *110*, 3877–3923; c) V. Y. Lee, A. Sekiguchi, J. Escudié, H. Ranaivonjatovo, *Chem. Lett.* **2010**, *39*, 312–318; d) P. P. Power, *Acc. Chem. Res.* **2011**, *44*, 627–637.

[36] a) N. Wiberg, G. Wagner, J. Riede, G. Müller, *Organometallics* **1987**, *6*, 32–35; b) N. Wiberg, G. Wagner, G. Reber, J. Riede, G. Müller, *Organometallics* **1987**, *6*, 35–41; c) N. Wiberg, K.-S. Joo, K. Polborn, *Chem. Ber.* **1993**, *126*, 67–69.

[37] a) T. Guliashvili, I. El-Sayed, A. Fischer, H. Ottosson, *Angew. Chem. Int. Ed.* **2003**, *42*, 1640–1642; b) R. Dobrovetsky, L. Zborovsky, D. Sheberla, M. Botoshansky, D. Bravo-Zhivotovskii, Y. Apeloig, *Angew. Chem. Int. Ed.* **2010**, *49*, 4084–4087.

[38] a) K. Sakamoto, J. Ogasawara, Y. Kon, T. Sunagawa, C. Kabuto, M. Kira, *Angew. Chem. Int. Ed.* **2002**, *41*, 1402–1404; b) M. Igarashi, M. Ichinohe, A. Sekiguchi, *J. Am. Chem. Soc.* **2007**, *129*, 12660–12661.

[39] Selected examples: a) H. Meyer, G. Baum, W. Massa, A. Berndt, *Angew. Chem. Int. Ed.* **1987**, *26*, 798–799; b) H. Meyer, G. Baum, W. Massa, S. Berger, A. Berndt, *Angew. Chem. Int. Ed.* **1987**, *26*, 546–548; c) M. Lazraq, J. Escudié, C. Couret, J. Satgé, M. Dräger, R. Dammel, *Angew. Chem. Int. Ed.* **1988**, *27*, 828–829; d) H. Schumann, M. Glanz, F. Girgsdies, F. E. Hahn, M. Tamm, A. Grzegorzewski, *Angew. Chem. Int. Ed.* **1997**, *36*, 2232–2234; e) M. Stürmann, W. Saak, M. Weidenbruch, A. Berndt, D. Sclesclkewitz, *Heteroat. Chem.* **1999**, *10*, 554–558; f) Y. Mizuhata, N. Takeda, T. Sasamori, N. Tokitoh, *Chem. Commun.* **2005**, 5876–5878; g) A. Fatah, R. El Ayoubi, H. Gornitzka, H. Ranaivonjatovo, J. Escudié, *Eur. J. Inorg. Chem.* **2008**, 2007–2013.

[40] a) N. Wiberg, K. Schurz, G. Reber, G. Müller, *J. Chem. Soc. Chem. Commun.* **1986**, 591–592; b) M. Hesse, U. Klingebiel, *Angew. Chem.* **1986**, *98*, 638–639.

[41] M. Veith, H. Bärnighausen, *Acta Crystallogr. Sect. B* **1974**, *30*, 1806–1813.

[42] a) T. N. Truong, M. S. Gordon, *J. Am. Chem. Soc.* **1986**, *108*, 1775–1778; b) M. W. Schmidt, P. N. Truong, M. S. Gordon, *J. Am. Chem. Soc.* **1987**, *109*, 5217–5227.

[43] Selected examples: a) N. Wiberg, K. Schurz, G. Müller, J. Riede, *Angew. Chem. Int. Ed.* **1988**, *27*, 935–936; b) S. Walter, U. Klingebiel, D. Schmidt-Bäse, *J. Organomet. Chem.* **1991**, *412*, 319–326; c) D. Grosskopf, L. Marcus, U. Klingebiel, M. Noltemeyer, D. Grosskopf, L. Marcus, U. Klingebiel, *Phosphorus, Sulfur Silicon Relat. Elem.* **1994**, *97*, 113–123; d) J. Niesmann, U. Klingebiel, M. Schäfer, R. Boese, *Organometallics* **1998**, *17*, 947–953; e) H. W. Lerner, M. Bolte, K. Schurz, N. Wiberg, G. Baum, D. Fenske, J. W. Bats, M. Wagner, *Eur. J. Inorg. Chem.* **2006**, *2*, 4998–5005; f) H. Cui, C. Cui, *Chem. Asian J.* **2011**, *6*, 1138–1141; g) D. Dhara, T. Vijayakanth, M. K. Barman, K. P. K. Naik, N. Chrysochos, C. B. Yildiz, R. Boomishankar, C. Schulzke, V. Chandrasekhar, A. Jana, *Chem. Commun.* **2017**, *53*, 8592–8595.

[44] a) A. Meller, G. Ossig, W. Maringgele, D. Stalke, R. Herbst-Irmer, S. Freitag, G. M. Sheldrick, *J. Chem. Soc. Chem. Commun.* **1991**, 1123–1124; b) G. Ossig, A. Meller, S. Freitag, R. Herbst-Irmer, *J. Chem. Soc. Chem. Commun.* **1993**, 497–499; c) T. Ohtaki, Y.

Kabe, W. Ando, *Heteroat. Chem.* **1994**, *5*, 313–320; d) W. Ando, T. Ohtaki, Y. Kabe, *Organometallics* **1994**, *13*, 434–435.

[45] Selected examples: a) J. W. Hastie, R. H. Hauge, J. L. Margrave, *Inorganica Chim. Acta* **1969**, *3*, 601–606; b) J. S. Anderson, J. S. Ogden, *J. Chem. Phys.* **1969**, *51*, 4189-4196; c) H. Z. Schnöckel, *Z. Anorg. Allg. Chem.* **1980**, *460*, 37-50; d) H. Schnöckel, *J. Mol. Struct.* **1980**, *65*, 115-123; e) C. A. Arrington, J. Michl, R. West, *J. Am. Chem. Soc.* **1983**, *105*, 6176–6177; f) R. Withnall, L. Andrews, *J. Am. Chem. Soc.* **1985**, *107*, 2567–2568; g) D. A. Dixon, J. L. Gole, *Chem. Phys. Lett.* **1986**, *125*, 179–183; h) R. Withnall, L. Andrews, *J. Phys. Chem.* **1988**, *92*, 594–602; i) R. Withnall, L. Andrews, *J. Phys. Chem.* **1990**, *94*, 2351–2357; j) V. N. Khabashesku, K. N. Kudin, J. L. Margrave, L. Fredin, *J. Organomet. Chem.* **2000**, *595*, 248–260. A more recent example can be found at: k) M. M. Linden, H. P. Reisenauer, D. Gerbig, M. Karni, A. Schäfer, T. Müller, Y. Apeloig, P. R. Schreiner, *Angew. Chem. Int. Ed.* **2015**, *54*, 12404–12409.

[46] Selected examples: a) H. Lavayssiere, J. Barrau, J. Satge, M. Bouchaut, *J. Organomet. Chem.* **1978**, *154*, C9–C12; b) J. Barrau, M. Bouchaut, H. Lavayssiere, G. Dousse, J. Satgé, *Helv. Chim. Acta* **1979**, *62*, 152–154; c) W. Ando, M. Ikeno, Y. Hamada, *J. Chem. Soc. Chem. Commun.* **1981**, 621–622; d) Z. H. Aiube, J. Chojnowski, C. Eaborn, W. A. Stańczyk, *J. Chem. Soc. Chem. Commun*. **1983**, 493–495; e) N. Wiberg, G. Preiner, K. Schurz, *Chem. Ber.* **1988**, *121*, 1407–1412; f) N. Tokitoh, T. Matsumoto, R. Okazaki, *Chem. Lett.* **1995**, *24*, 1087–1088.g) J. Belzner, H. Ihmels, B. O. Kneisel, R. Herbst-Irmer, *Chem. Ber.* **1996**, *129*, 125–130; h) P. Jutzi, H. Schmidt, B. Neumann, H. Stammler, *Organometallics* **1996**, *15*, 741–746; i) T. Matsumoto, N. Tokitoh, R. Okazaki, *Chem. Commun.* **1997**, *418*, 1553–1554; j) N. Takeda, N. Tokitoh, R. Okazaki, *Chem. Lett.* **2000**, *11*, 244–245; k) G. L. Wegner, R. J. F. Berger, A. Schier, H. Schmidbaur, *Organometallics* **2001**, *20*, 418–423.

[47] a) T. Kudo, S. Nagase, *Organometallics* **1986**, *5*, 1207–1215; b) J. Kapp, M. Remko, P. Von Ragué Schleyer, *J. Am. Chem. Soc.* **1996**, *118*, 5745–5751; c) J. Kapp, M. Remko, P. v. R. Schleyer, *Inorg. Chem.* **1997**, *36*, 4241–4246; d) M. Kimura, S. Nagase, *Chem. Lett.* **2001**, *30*, 1098–1099.

[48] L. Li, T. Fukawa, T. Matsuo, D. Hashizume, H. Fueno, K. Tanaka, K. Tamao, *Nat. Chem.* **2012**, *4*, 361–365.

[49] a) S. Yao, Y. Xiong, M. Driess, *Chem. Commun.* **2009**, 6466–6468; b) S. Yao, Y. Xiong, W. Wang, M. Driess, *Chem. Eur. J.* **2011**, *17*, 4890–4895; c) S. Sinhababu, D. Yadav, S. Karwasara, M. K. Sharma, G. Mukherjee, G. Rajaraman, S. Nagendran, *Angew. Chem. Int. Ed.* **2016**, *55*, 7742–7746.

[50] M. Asay, C. Jones, M. Driess, *Chem. Rev.* **2011**, *111*, 354–396.

[51] Recent reviews which concern the role of amidinate and guanidinate ligands in Main Group chemistry: a) F. T. Edelmann, *Adv. Organomet. Chem.* ***2008****, 57, 183–352*; b) C. Jones, *Coord. Chem. Rev.* **2010**, *254*, 1273–1289; c) F. T. Edelmann, *Adv. Organomet. Chem.* **2013**, *61*, 55–374.

[52] a) M. P. Coles, D. C. Swenson, R. F. Jordan, V. G. Young, *Organometallics* **1997**, *16*, 5183–5194; b) A. Xia, H. M. El-Kaderi, M. J. Heeg, C. H. Winter, *J. Organomet. Chem.* **2003**, *682*, 224–232; c) F. Feil, S. Harder, *Eur. J. Inorg. Chem.* **2005**, 4438–4443; d) S. P. Green, C. Jones, G. Jin, A. Stasch, *Inorg. Chem.* **2007**, *46*, 8–10; e) T. Chlupatý, Z. Padělková, F. Deproft, R. Willem, A. Růžička, *Organometallics* **2012**, *31*, 2203–2211.

[53] a) C. Jones, P. C. Junk, J. A. Platts, A. Stasch, *J. Am. Chem. Soc.* **2006**, *128*, 2206–2207; b) C. Jones, P. C. Junk, J. A. Platts, A. Stasch, *Dalton Trans.* **2005**, 2497–2499; c) S. P. Green, C. Jones, P. C. Junk, K. A. Lippert, A. Stasch, *Chem. Commun.* **2006**, 3978–3980; d) C. W. So, H. W. Roesky, J. Magull, R. B. Oswald, *Angew. Chem. Int. Ed.* **2006**, *45*, 3948–3950; e) S. S. Sen, A. Jana, H. W. Roesky, C. Schulzke, *Angew. Chem. Int. Ed.* **2009**, *48*, 8536–8538; f) B. Blom, D. Gallego, M. Driess, *Inorg. Chem. Front.* **2014**, *1*, 134–148; g) S. P. Green, C. Jones, A. Stasch, *Science* **2007**, *318*, 1754–1757; h) C. Jones, S. J. Bonyhady, N. Holzmann, G. Frenking, A. Stasch, *Inorg. Chem.* **2011**, *50*, 12315–12325.

[54] a) M. P. Coles, P. B. Hitchcock, *Chem. Commun.* **2002**, *2*, 2794–2795; b) N. E. Mansfield, M. P. Coles, P. B. Hitchcock, *Dalton Trans.* **2005**, 2833–2841; c) G. Jin, C.

Jones, P. C. Junk, A. Stasch, W. D. Woodul, *New J. Chem.* **2008**, *32*, 835–842; d) G. Jin, C. Jones, P. C. Junk, K. A. Lippert, R. P. Rose, A. Stasch, *New J. Chem.* **2009**, *33*, 64–75.

[55] a) H. tom Dieck, M. Zettlitzer, *Chem. Ber.* **1987**, *120*, 795–801; b) W. A. Herrmann, M. Denk, J. Behm, W. Scherer, F. -R Klingan, H. Bock, B. Solouki, M. Wagner, *Angew. Chem. Int. Ed.* **1992**, *31*, 1485–1488; c) L. Weber, E. Dobbert, H. G. Stammler, B. Neumann, R. Boese, D. Bläser, *Chem. Ber.* **1997**, *130*, 705–710; d) C. J. Carmalt, V. Lomeli, B. G. McBurnett, A. H. Cowley, *Chem. Commun.* **1997**, *810*, 2095–2096; e) E. S. Schmidt, A. Jockisch, H. Schmidbaur, *J. Am. Chem. Soc.* **1999**, *121*, 9758–9759; f) T. Gans-Eichler, D. Gudat, M. Nieger, *Angew. Chem. Int. Ed.* **2002**, *41*, 1888–1891.

[56] D. Bourissou, O. Guerret, F. P. Gabbaï, G. Bertrand, *Chem. Rev.* **2000**, *100*, 39–92.

[57] a) Y. Segawa, M. Yamashita, K. Nozaki, *Science* **2006**, *314*, 113–115; b) Y. Segawa, Y. Suzuki, M. Yamashita, K. Nozaki, *J. Am. Chem. Soc.* **2008**, *130*, 16069–16079.

[58] a) O. Kühl, P. Lönnecke, J. Heinicke, *Polyhedron* **2001**, *20*, 2215–2222; b) I. L. Fedushkin, A. N. Lukoyanov, G. K. Fukin, S. Y. Ketkov, M. Hummert, H. Schumann, *Chem. Eur. J.* **2008**, *14*, 8465–8468.

[59] Selected reviews: a) L. Bourget-Merle, M. F. Lappert, J. R. Severn, *Chem. Rev.* **2002**, *102*, 3031–3065; b) W. E. Piers, D. J. H. Emslie, *Coord. Chem. Rev.* **2002**, 233–234, 131–155; c) S. P. Sarish, S. Nembenna, S. Nagendran, H. W. Roesky, *Acc. Chem. Res.* **2011**, *44*, 157–170; d) Y. C. Tsai, *Coord. Chem. Rev.* **2012**, *256*, 722–758; e) C. Chen, S. M. Bellows, P. L. Holland, *Dalton Trans.* **2015**, *44*, 16654–16670; f) R. L. Webster, *Dalton Trans.* **2017**, *46*, 4483–4498.

[60] a) R. C. Mehrotra, R. Bohra, D. P. Gaur in *Metal β-Diketonates and Allied Derivatives*, Academic Press: New York, **1978**; b) R. H. Holm, G. W. Everett, A. Chakravorty, *Prog. Inorg. Chem.* **1966**, *7*, 83-214; c) G. Wilkinson, R. D. Gillard, J. A. McCleverty in *Comprehensive Coordination Chemistry*, Pergamon: Oxford, U.K., **1987**.

[61] a) Z. Janousek, H. G. Viehe, *Angew. Chem. Int. Ed.* **1971**, *10*, 574–575; b) S. Brenner, H. G. Viehe, *Tetrahedron Lett.* **1976**, *17*, 1617–1620; c) P. T. K. Lee, Master's Thesis, St.Mary's University, Halifax, Canada, **2009**.

[62] Mg^{I}: a) S. J. Bonyhady, S. P. Green, C. Jones, S. Nembenna, A. Stasch, *Angew. Chem. Int. Ed.* **2009**, *48*, 2973–2977; b) S. J. Bonyhady, C. Jones, S. Nembenna, A. Stasch, A. J. Edwards, G. J. McIntyre, *Chem. Eur. J.* **2010**, *16*, 938–955; c) C. Bakewell, A. J. P. White, M. R. Crimmin, *J. Am. Chem. Soc.* **2016**, *138*, 12763–12766; f) C. Jones, *Nat. Rev. Chem.* **2017**, *1*, 59. Additional references can be found in refs 53g and 53h.

[63] Al^{I}: a) C. Cui, H. W. Roesky, H. G. Schmidt, M. Noltemeyer, H. Hao, F. Cimpoesu, *Angew. Chem. Int. Ed.* **2000**, *39*, 4274–4276; b) C. Cui, S. Kopke, R. Herbst-irmer, H. W. Roesky, M. Noltemeyer, H.-G. Schmidt, B. Wrackmeyer, *J. Am. Chem. Soc.* **2001**, *123*, 9091–9098; c) Y. Peng, H. Fan, V. Jancik, H. W. Roesky, R. Herbst-Irmer, *Angew. Chem. Int. Ed.* **2004**, *43*, 6190–6192; d) Y. Peng, H. Fan, H. Zhu, H. W. Roesky, J. Magull, C. E. Hughes, *Angew. Chem. Int. Ed.* **2004**, *43*, 3443–3445; e) H. Zhu, J. Chai, V. Jancik, H. W. Roesky, W. A. Merrill, P. P. Power, *J. Am. Chem. Soc.* **2005**, *127*, 10170–10171; f) T. Chu, I. Korobkov, G. I. Nikonov, *J. Am. Chem. Soc.* **2014**, *136*, 9195–9202; g) T. Chu, Y. Boyko, I. Korobkov, G. I. Nikonov, *Organometallics* **2015**, *34*, 5363–5365; h) M. R. Crimmin, M. J. Butler, A. J. P. White, *Chem. Commun.* **2015**, *51*, 15994–15996.

[64] Ga^{I} and In^{I}: a) N. J. Hardman, B. E. Eichler, P. P. Power, *Chem. Commun.* **2000**, *53*, 1991–1992; b) A. Seifert, D. Scheid, G. Linti, T. Zessin, *Chem. Eur. J.* **2009**, *15*, 12114–12120; c) G. Prabusankar, A. Doddi, C. Gemel, M. Winter, R. A. Fischer, *Inorg. Chem.* **2010**, *49*, 7976–7980; d) C. Helling, C. Wölper, S. Schulz, *J. Am. Chem. Soc.* **2018**, *140*, 5053–5056; e) M. S. Hill, P. B. Hitchcock, *Chem. Commun.* **2004**, *44*, 1818–1819; f) M. S. Hill, P. B. Hitchcock, R. Pongtavornpinyo, *Science* **2006**, *311*, 1904-1907; g) M. S. Hill, P. B. Hitchcock, R. Pongtavornpinyo, *Dalton Trans.* **2007**, *402*, 731–733.

[65] $Ge^{I/II}$ and $Sn^{I/II}$: a) A. Jana, D. Ghoshal, H. W. Roesky, I. Objartel, G. Schwab, D. Stalke, *J. Am. Chem. Soc.* **2009**, 1288–1293; b) A. Jana, H. W. Roesky, C. Schulzke,

A. Döring, *Angew. Chem. Int. Ed.* **2009**, *48*, 1106–1109; c) A. Jana, H. W. Roesky, C. Schulzke, *Dalton Trans.* **2010**, *39*, 132–138; d) W. D. Woodul, E. Carter, R. Müller, A. F. Richards, A. Stasch, M. Kaupp, D. M. Murphy, M. Driess, C. Jones, *J. Am. Chem. Soc.* **2011**, *133*, 10074–10077; e) S. L. Choong, C. Schenk, A. Stasch, D. Dange, C. Jones, *Chem. Commun.* **2012**, *48*, 2504–2506.

[66] C. Camp, J. Arnold, *Dalton Trans.* **2016**, *45*, 14462–14498.

[67] a) C. E. Radzewich, M. P. Coles, R. F. Jordan, *J. Am. Chem. Soc.* **1998**, *120*, 9384–9385; b) A. Ariafard, Z. Lin, R. F. Jordan, *Organometallics* **2005**, *24*, 5140–5146; c) A. J. Boutland, I. Pernik, A. Stasch, C. Jones, *Chem. Eur. J.* **2015**, *21*, 15749–15758.

[68] a) B. Qian, S. W. Baek, M. R. Smith, *Polyhedron* **1999**, *18*, 2405–2414; b) W. D. Woodul, E. Carter, R. Müller, A. F. Richards, A. Stasch, M. Kaupp, D. M. Murphy, M. Driess, C. Jones, *J. Am. Chem. Soc.* **2011**, *133*, 10074–10077.

[69] a) X. Li, X. Cheng, H. Song, C. Cui, *Organometallics* **2007**, *26*, 1039–1043; b) W. Wang, S. Yao, C. Van Wüllen, M. Driess, *J. Am. Chem. Soc.* **2008**, *130*, 9640–9641; c) W. D. Woodul, A. F. Richards, A. Stasch, M. Driess, C. Jones, *Organometallics* **2010**, *29*, 3655–3660; d) J. Li, X. Li, W. Huang, H. Hu, J. Zhang, C. Cui, *Chem. Eur. J.* **2012**, *18*, 15263–15266; e) L. Xie, J. Zhang, H. Hu, C. Cui, *Organometallics* **2013**, *32*, 6875–6878.

[70] Selected examples: a) H. Zhu, J. Chai, A. Stasch, H. W. Roesky, T. Blunck, D. Vidovic, J. Magull, H. G. Schmidt, M. Noltemeyer, *Eur. J. Inorg. Chem.* **2004**, 4046–4051; b) M. Driess, S. Yao, M. Brym, C. van Wüllen, D. Lentz, *J. Am. Chem. Soc.* **2006**, *128*, 9628–9629; c) S. P. Sarish, B. Nekoueishahraki, A. Jana, H. W. Roesky, T. Schulz, D. Stalke, *Chem. Eur. J.* **2011**, *17*, 890–894; d) S. Yao, Y. Xiong, M. Driess, *Organometallics* **2011**, *30*, 1748–1767; e) J. A. B. Abdalla, I. M. Riddlestone, R. Tirfoin, S. Aldridge, *Angew. Chem. Int. Ed.* **2015**, *54*, 5098–5102.

CHAPTER 2

GENERAL EXPERIMENTAL AND COMPUTATIONAL METHODS

2.1 Manipulation of air- and moisture-sensitive materials

The handling of air- and moisture-sensitive materials, which make up the majority of the compounds reported in this thesis, required the use of a dual manifold Schlenk line or a glovebox, which allow for the manipulation and storage of compounds under an inert atmosphere of nitrogen or argon.[1] In most cases, reactions were carried out in the solution phase in a Schlenk vessel, connected to the dual Pyrex manifold *via* PVC tubing.[2] This consists of a manifold (the "gas line") connected to a source of inert gas (nitrogen or argon) at one end, and a mercury bubbler on the other, in order to vent excess pressure. The other manifold (the "vacuum line") is connected to a high vacuum pump *via* a cold trap, immersed in liquid nitrogen, which help to avoid solvents or volatile materials entering the pump. The pressure inside the vacuum line was of the order of 10^{-3} mbar and was monitored by a Pirani pressure gauge. The two manifolds are linked together by PVC tubing (or joined by glass connections), and a series of two-way taps is integrated into the vacuum line, which enables the control over the choice of evacuation or inert gas back-filling of the reaction vessel. Glass joints were lubricated with high vacuum grease to ensure an air-tight seal.

Prior to use, reaction vessels were usually kept in a 110°C oven for at least 12 h to minimise surface moisture. To obtain an air- and moisture-free environment for the reaction, the reaction vessel (fresh from the oven) was connected to the

manifold under dynamic vacuum and evacuated to *ca.* 10^{-2} mbar. The glassware was then heated with a Bunsen burner to remove remaining traces of moisture from the interior walls. The vessel was then subjected to five cycles of "pump and refill", with each involving the vessel being back-filled with inert gas and subsequently evacuated to *ca.* 10^{-1} mbar. Liquid transfer between reaction flasks was carried out with cannulae or syringes to avoid contact with the external atmosphere.

A glovebox under a nitrogen atmosphere was employed primarily for the manipulation of air-sensitive compounds in the solid state. The atmosphere was passed through an activated copper catalyst and 4 Å molecular sieves to remove traces of oxygen and moisture, respectively. Materials were brought into the glovebox *via* an antechamber, which was subjected to three "pump and refill" cycles.

2.2 Analytical techniques

2.2.1 NMR spectroscopy

All NMR spectra were recorded on a Bruker Avance III HD Nanobay 400 MHz NMR spectrometer equipped with a 9.4 T magnet, a Bruker Avance III 500 MHz NMR spectrometer equipped with a 11.75 T magnet or a Bruker Avance 500 MHz NMR spectrometer equipped with a 11.75 T magnet and a ^{13}C detect cryoprobe. Chemical shifts are quoted in ppm and coupling constants in Hz. NMR spectra were measured in $CDCl_3$, CD_2Cl_2, C_6D_6, or C_6D_5Br. ^{1}H and ^{13}C NMR spectra were internally referenced to residual protio-solvent (^{1}H) or solvent (^{13}C) resonances, and reported relative to Me_4Si (δ = 0 ppm). ^{11}B, ^{19}F, ^{27}Al, ^{29}Si, ^{31}P, and ^{119}Sn NMR spectra

were referenced externally to $BF_3{\cdot}OEt_2$, $CFCl_3$, $[Al(H_2O)_6]^{3+}$, Me_4Si, H_3PO_4 (85 % in H_2O), and Me_4Sn (90% in C_6D_6) respectively. NMR samples of air- and moisture-sensitive materials were prepared in 5 mm Wilmad 507-PP tubes fitted with J. Young Teflon valves, under an argon atmosphere (if prepared using the Schlenk manifold) or a nitrogen atmosphere (if prepared in a glovebox).

2.2.2 X-ray crystallography

Crystallographic structure determinations were carried out by Drs Rémi Tirfoin, Arnab Rit, Jesus Campos, Evgeny Kolychev, Jamie Hicks, or Maria Ángeles-Fuentes (Aldridge Group). X-ray quality crystals were selected under Paratone-N oil to avoid contact with air and moisture in the atmosphere, mounted on Micromount loops and cooled rapidly using an Oxford Cryosystems open-flow N_2 cooling device.[3] Data were collected on a Bruker-Nonius KappaCCD or an Agilent SuperNova diffractometer, with either Cu Kα (λ = 1.5418 Å) or Mo Kα (λ = 0.7107 Å) radiation, and reduced using DENZO/SCALEPACK[4] or the CrysAlisPro package, including unit cell parameter refinement and inter-frame scaling (carried out using SCALE3 ABSPACK within CrysAlisPro).[5] Equivalent reflections were merged and diffraction patterns processed with the CrysAlisPro programme. The structures were solved using SIR92,[6] Superflip[7] or SHELXT-2014, and refined with full-matrix least-squares within CRYSTALS[8] or SHELXL 2014 package.[9]

2.2.3 Infrared spectroscopy

IR spectra were measured on a Nicolet 500 FT-IR spectrometer. In a glovebox, samples were prepared as a Nujol mull, loaded between two KBr discs, and sealed

in an airtight cell before measurements were taken. Alternatively, the attenuated total reflectance (ATR) technique was employed, using the iD5 Diamond Crystal ATR accessory. Using this method, the sample was taken out of the glovebox in a sealed vial, quickly loaded onto the ATR crystal and the spectrum measured.

2.2.4 Mass spectrometry

ESI-MS and EI-MS measurements were carried out by Mr. James Wickens, University of Oxford. Air- and moisture-stable samples were prepared as a dilute solution in methanol, while air- and moisture-sensitive solid samples were packed in a sealed glass capillary under vacuum.

2.2.5 Elemental (C,H,N) analyses

Elemental analyses were carried out by Mr. Stephen Boyer (London Metropolitan University). The samples were packed in a sealed glass capillary under vacuum, or in a vial sealed with Parafilm M under a nitrogen atmosphere.

2.3 Preparation and purification of chemicals

2.3.1 Solvents

Generally, solvents were dried by passing through a column of an appropriate drying agent, using the in-house MBRAUN Solvent Purification System (MB-SPS). For the purpose of storage, solvents were kept in glass ampoules fitted with a J. Young's screw tap, over either potassium mirror (for hydrocarbon-based solvents and diethyl ether) or 4 Å molecular sieves (for halogenated solvents), under an argon atmosphere. Prior to use, all solvents were degassed by sparging with argon gas for 15-20 minutes, unless otherwise stated.

Diethyl ether was pre-dried by storage over KOH pellets for a minimum of seven days, prior to distillation with sodium/benzophenone. Chloroform was dried over CaH_2 and distilled under reduced pressure. Deuterated solvents were dried over finely-cut potassium (for C_6D_6) or CaH_2 (for $CDCl_3$, CD_2Cl_2, and C_6D_5Br), distilled under reduced pressure, and subsequently degassed by three "freeze-pump-thaw" cycles. After the last "thawing" step, the ampoule was back-filled with argon gas, ready to be used.

2.3.2 Starting materials

Generally, unless otherwise stated, all starting materials were purchased from commercially available sources, and used without further purification. All reagents that are in the liquid state at ambient conditions were stored in glass ampoules, fitted with a J Young's tap. Information on the supplier and purity of commercially purchased materials are provided in the Appendix. *N,N*-Dimethylacetamide, *N*-butyllithium solution (1.6 M solution in hexanes), trimethylaluminum solution (2.0 M in toluene), and potassium triethylborohydride solution (1.0 M in THF) were transferred from Sure/Seal™ bottles to ampoules *via* cannula for the purpose of long-term storage. *tert*-Butylamine was dried over CaH_2 and distilled under reduced pressure. Due to their high boiling points, aniline derivatives were first distilled under reduced pressure, dried over CaH_2, and subsequently filtered into ampoules containing 4 Å molecular sieves. The following compounds were synthesised according to procedures reported in literature: $Li[Al\{OC(CF_3)_3\}_4]$,[10] IDipp·$SiCl_2$,[11] $NaPCO(dioxane)_x$ (prepared by Drs Alexander Hinz and Frank Tambornino –

Goicoechea Group),[12] K[Si(TMS)$_3$] (Robert Mangan – Aldridge Group),[13] Li[P(TMS)$_2$](dme) (Dr Evgeny Kolychev – Aldridge Group).[14]

2.4 Computational details

For the NacnacH/*N*-nacnacH protio-ligand systems, geometry optimisation was performed using the Amsterdam Density Functional (ADF) 2014 software package by Haoyu Niu (Aldridge Group), using the Vosko–Wilk–Nusair local density approximation with exchange from Becke,[15] correlation correction from Perdew,[16] and 3-dimension dispersion effect (BP86-D3).[17] Slater-type orbitals (STOs) were used for the triple zeta basis set with an additional set of polarization functions (TZP).[18] The full-electron basis set approximation was applied with no molecular symmetry. General numerical quality was good.

DFT calculations which involve systems with Group 14 elements (silylenes/silanones, germylenes, and stannylenes) were undertaken by the author in conjunction with Dr Petra Vasko (Aldridge Group), using the Gaussian09 (Revision D.01) programme package.[19] Geometry optimisations were performed with the PBE1PBE hybrid exchange-correlation functional[20] using Def2-TZVP basis sets for all elements except Sn, for which the Def2-TZVPP basis sets (with relativistic large core ECP) was employed.[21] With respect to the mechanistic investigations of the nucleophilic sila-acyl substitution discussed in chapter 6, calculations were performed in a simulated solvent model (toluene), employing the Polarizable Continuum Model (PCM).[22] Unless otherwise stated, geometry optimisations were carried out for the full ligand systems, and were reported as Gibbs free energies in

the gas phase. To confirm the nature of the stationary points found (minima with no imaginary frequencies or a saddle point for transition states), full frequency calculations were performed for optimised geometries. Analyses of natural bond orbitals (NBO) were carried out using NBO 3.1 as implemented in Gaussian09.[23] Graphics were created with the program GaussView.[24] The xyz-coordinates for each of the optimised geometries are included in the Appendix.

2.5 References

[1] a) R. E. Dodd, P. L. Robinson, *Experimental Inorganic Chemistry. A Guide to Laboratory Practice*; Elsevier, Amsterdam; b) R. J. Errington, *Advanced Practical Inorganic and Metalorganic Chemistry*; Blackie Academic and Professional, London.

[2] D. Shriver, M. Drezdon, *The Manipulation of Air-Sensitive Compounds*; Wiley-Interscience.

[3] B. J. Cosier, A. M. Glazer, *J. Appl. Crystallogr.* **1986**, *19*, 105–107.

[4] Z. Otwinowski, W. Minor, *Processing of X-ray Diffraction Data collected in Oscillation Mode, Methods Enzymol*.

[5] CrysAlisPro v.1.171.35.8 Agilent Technologies. 2011.

[6] A. Altomare, G. Cascarano, C. Giacovazzo, A. Guagliardi, *J. Appl. Crystallogr.* **1993**, *26*, 343–350.

[7] L. Palatinus, G. Chapuis, *J. Appl. Crystallogr.* **2007**, *40*, 786–790.

[8] a) A. L. Thompson, D. J. Watkin, *J. Appl. Crystallogr.* **2011**, *44*, 1017–1022; b) R. I. Cooper, A. L. Thompson, D. J. Watkin, *J. Appl. Crystallogr.* **2010**, *43*, 1100–1107.

[9] a) G. M. Sheldrick, *Acta. Cryst.* **2008**, *64*, 112–122; b) G. M. Sheldrick, *SHELX-2014* **2014**; c) O. V. Dolomanov, L. J. Bourhis, R. J. Gildea, J. A. K Howard, H. Puschmann, *J. Appl. Crystallogr.* **2009**, *42*, 339–341; (d) L. J. Barbour, *J. Supramol. Chem.* **2001**, *1*, 189–191.

[10] I. Krossing, *Chem. Eur. J.* **2001**, *7*, 490-502.

[11] R. Ghadwal, H. Roesky, S. Merkel, J. Henn, D. Stalke, *Angew. Chem. Int. Ed.* **2009**, *48*, 5683-5686.

[12] D. Heift, Z. Benkő, H. Grützmacher, *Dalton Trans.* **2014**, *43*, 831.

[13] a) C. Marschner, *Eur. J. Inorg. Chem.* **1998**, 221-226; b) C. Kayser, R. Fischer, J. Baumgartner, C. Marschner, *Organometallics* **2002**, *21*, 1023–1030.

[14] a) G. Fritz, W. Hölderich, *Z. Anorg. Allg. Chem.* **1976**, *422*, 104–114; b) F. Uhlig, S. Gremler, M. Dargatz, M. Scheer, E. Herrmann, *Z. Anorg. Allg. Chem.* **1991**, *606*, 105–108.

[15] A. D. Becke, *Phys. Rev. A* **1988**, *38*, 3098–3100.

[16] J. P. Perdew, *Phys.Rev. B* **1986**, *33*, 8822–8824.

[17] J. G. Snijders, P. Vernooijs, E. J. Baerends, *At.Data Nucl. Data Tables* **1981**, *26*, 483–509.

[18] E. Lenthe, E. J. Baerends, *J. Comput. Chem.* **2002**, *24*, 1142-1156.

[19] M. J. Frisch, G. W. Trucks, H. B. Schlegel, G. E. Scuseria, M. A. Robb, J. R. Cheeseman, G. Scalmani, V. Barone, B. Mennucci, G. A. Petersson, H. Nakatsuji, M. Caricato, X. Li, H. P. Hratchian, A. F. Izmaylov, J. Bloino, G. Zheng, J. L. Sonnenberg, M. Hada, M. Ehara, K. Toyota, R. Fukuda, J. Hasegawa, M. Ishida, T. Nakajima, Y. Honda, O. Kitao, H. Nakai, T. Vreven, J. A. Montgomery Jr., J. E. Peralta, F. Ogliaro, M. Bearpark, J. J. Heyd, E. Brothers, K. N. Kudin, V. N. Staroverov, R. Kobayashi, J. Normand, K. Raghavachari, A. Rendell, J. C. Burant, S. S. Iyengar, J. Tomasi, M. Cossi, N. Rega, J. M. Millam, M. Klene, J. E. Knox, J. B. Cross, V. Bakken, C. Adamo, J. Jaramillo, R. Gomperts, R. E. Stratmann, O. Yazyev, A. J. Austin, R. Cammi, C. Pomelli, J. W. Ochterski, R. L. Martin, K. Morokuma, V. G. Zakrzewski, G. A. Voth, P. Salvador, J. J. Dannenberg, S. Dapprich, A. D. Daniels, Ö. Farkas, J. B. Foresman, J. V. Ortiz, J. Cioslowski, D. J. Fox, *Gaussian 09*, *Revision D.01*, Gaussian, Inc., Wallingford, CT **2009**.

[20] a) M. Ernzerhof, G. E. Scuseria, *J. Chem. Phys.* **1999**, *110*, 5029–5036; b) C. Adamo, V.Barone, *J. Chem. Phys.* **1999**, *110*, 6158-6170; c) J. P. Perdew, K.Burke, M. Ernzerhof, *Phys. Rev. Lett.* **1997**, *78*, 1396; d) J. P. Perdew, K. Burke, M. Ernzerhof,

Phys. Rev. Lett. **1996**, *77*, 3865-3868; e) J. P. Perdew, M.Ernzerhof, K. Burke, *J. Chem. Phys.* **1996**, *105*, 9982-9985.

[21] F. Weigend, R. Ahlrichs, *Phys. Chem. Chem. Phys.* **2005**, 7, 3297-3305.

[22] J. Tomasi, B. Mennucci, R. Cammi, *Chem. Rev.* **2005**, *105*, 2999-3094.

[23] E. D. Glendening, A. E. Reed, J. E. Carpenter, F. Weinhold, NBO Version 3.1.

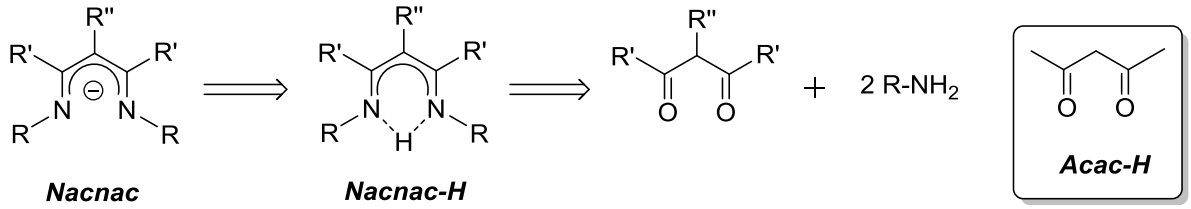
[24] R. D. Dennington, T. A. Keith, J. M. Millam, *GaussView 5.0.8*, Gaussian, **2008.**

CHAPTER 3

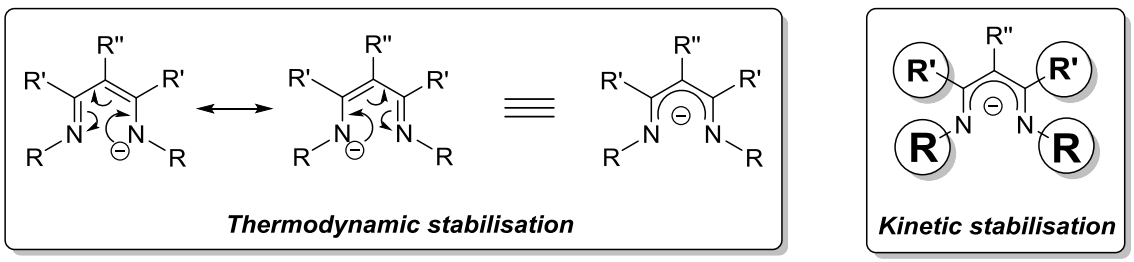
SYNTHESIS AND METALLATION OF AMINO-FUNCTIONALISED NACNAC-LIGANDS

3.1 Introduction

β-diketiminate ligands ($[R''\{C(R')(NR)\}_2]^-$)[1] are monoanionic, *N,N'*-bidentate donor ligands, which have been heavily exploited in the formation of metal complexes featuring a range of elements from the *s*-, *p*-, *d*-, and *f*-blocks of the Periodic Table.[2] They earn their informal (but often used) abbreviated name "Nacnac", by analogy with the closely related O-donor acetylacetonate "Acac" ligands. One of the most common synthetic methodologies for the preparation of "Nacnac-H" protio-ligands is based on the condensation of acetylacetone ("Acac-H") with two equivalents of a primary amine or aniline, typically employing a Lewis acid catalyst (Scheme 3.1).[3]



Scheme 3.1 Retrosynthetic condensation route to Nacnac ligands (R″ = H in most cases)

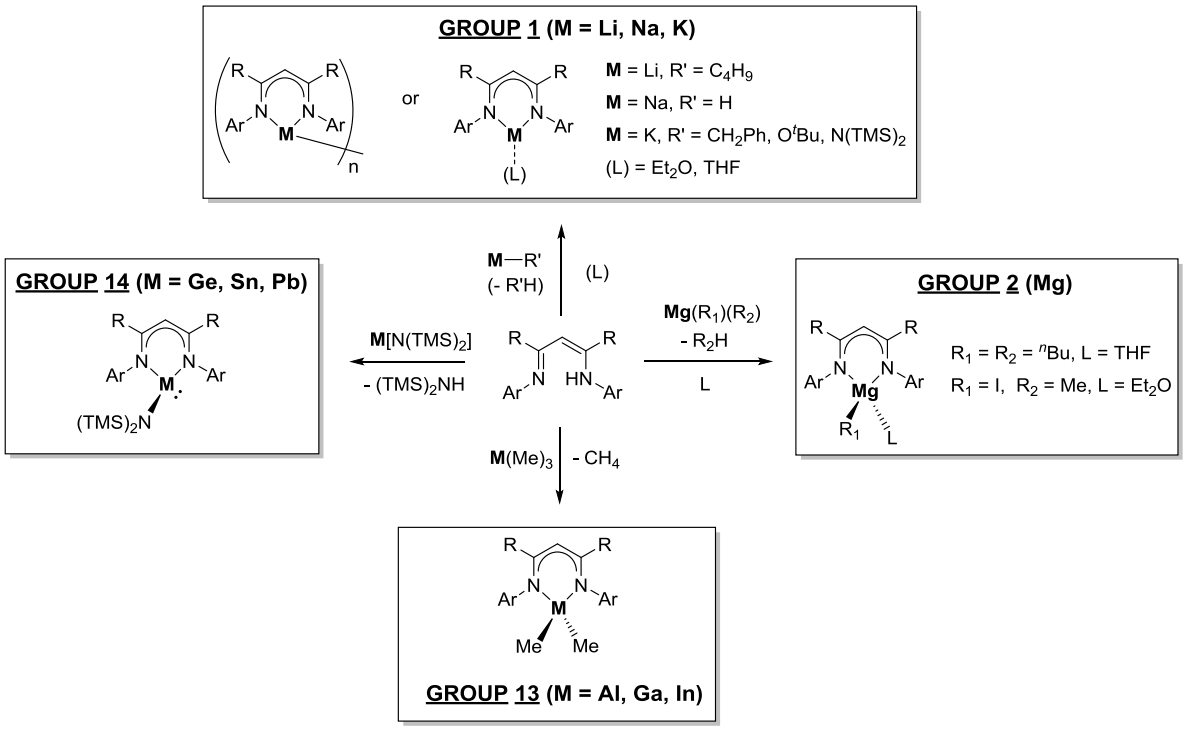


Scheme 3.2 The thermodynamic and kinetic stabilisation effects of Nacnac ligands

There are two main features which render Nacnac donors an attractive, versatile choice of ligand, especially for the stabilisation of reactive sub-valent Main Group complexes. Firstly, the chelating nature of the ligand, coupled with bulky *N*-bound substituents, provides spatial protection for the unsaturated metal centre, thereby inhibiting unwanted oligo-/polymerisation and associative decomposition pathways. Moreover, such structural characteristics can be fine-tuned to tailor the steric demands by altering the *N*-bound groups. Additionally, the electron-rich NC_3N ligand backbone and the chelating *N*-donors help to alleviate the coordinative unsaturation nature of the low-valent metal centre, and thereby stabilise the metal complex electronically (Scheme 3.2). As such, Nacnac-supported low-valent Main Group compounds have been extensively studied in the past 30 years. Prominent examples include the increasingly popular "quasi universal" reducing agent $\{(^{Mes}Nacnac)Mg\}_2$,[4] systems capable of small molecule activation akin to Transition Metals (*e.g.* the Group 13 compounds $\{(^{Dipp}Nacnac)M:\}$, M = Al and Ga),[5-7] the remarkably stable Ge^{I} radical $\{(^{tBu,Dipp}Nacnac)Ge\}^{\bullet}$,[8] and divalent hydrides of the Group 14 elements which have been shown to react with a range of unsaturated substrates *via* insertion into the E─H bond.[9]

In some cases, Nacnac-stabilised Main Group compounds can be accessed *via* direct metallation of the corresponding protio-ligand. Of great synthetic importance are complexes of Group 1 metals (Li, Na, K), which have been widely employed as convenient reagents for the preparation of other metal complexes by transmetallation. These alkali metal complexes can be obtained by treatment of the

protio-ligand with a strong lithium, sodium, or potassium-containing base (*e.g* butyllithium, sodium hydride, potassium bis(trimethylsilyl)amide, *etc.*).[3b,8b,10] Depending on the solvent employed, the resulting metallated species may be isolated as a solvated monomeric compound (*e.g* with O-donor solvents such as diethyl ether/tetrahydrofuran), or as an oligomeric aggregate (typically formed in the absence of a donor solvent). Whatismore, this approach has been extended to Group 2 (Mg),[4c,11] Group 13 (Al, Ga, In),[12] and Group 14 (Ge, Sn, Pb) systems,[13] in each case by employing a metal alkyl or amide as the base (Scheme 3.3). In addition, Nacnac-stabilised iodo-magnesium ((^{Mes}Nacnac)MgI(OEt_2)) and -aluminium compounds ((^{Dipp}Nacnac)AlI_2) have been shown to be useful precursors for highly-reactive sub-valent Mg^I and Al^I complexes.[4c,5a]



Scheme 3.3 Examples of direct metallation of Nacnac ligands with Group 1, 2, 13, and 14 metals

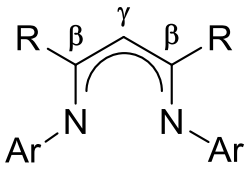


Figure 3.1 Labelling scheme of the ligand backbone carbons (β-C and γ-C) in a generic Nacnac ligand

The commercially availability of a range of diketones ([CH_2{C(O)R}$_2$], R = Me, ^{t}Bu, CF_3) and numerous substituted anilines has allowed for the facile preparation of Nacnac ligands bearing a variety of substituents at nitrogen and at the β-carbons, thereby allowing for different levels of spatial protection (Scheme 3.2, right, and Figure 3.1). Perhaps one of the most common manipulations in this regard is the replacement of the *N*-bound Dipp substituent for a less bulky Mes group. Typically, the Mes-substituted Nacnac derivative is associated with more reactive molecular entities (*cf.* {(^{Dipp}Nacnac)Mg}$_2$ versus {(^{Mes}Nacnac)Mg}$_2$), and a greater degree of aggregation at the metal centre. With this in mind, Dipp-substituted systems have been more widely used to support low-coordinate metal complexes.[4-9] Alternatively, the introduction of ^{t}Bu groups at the β-carbon position of the ligand also helps increase the overall spatial demand of the resulting Nacnac chelate.[8]

While tuning the *steric* profile of Nacnac ligands is common, the systematic modification of *electronic* properties is relatively less well explored. A handful of reports describe the incorporation of electron-withdrawing groups, such as trifluoromethyl substituents at the β-carbon, or (per)fluorinated/perfluoroalkyl-substituted aromatic rings at nitrogen. Such ligands were developed with a view to preparing cationic metal complexes with enhanced Lewis acidity (Figure 3.2).[14] By

contrast, efforts to increase the electron donating capabilities of the Nacnac chelate have been few and far between. This represents a potential shortcoming for the isolation of highly reactive sub-valent Main Group compounds: electron-deficient metal centres might be expected to benefit from the thermodynamic stabilisation provided by more strongly donating ligands.

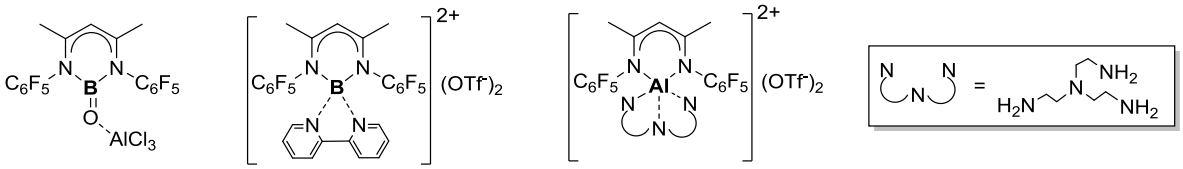
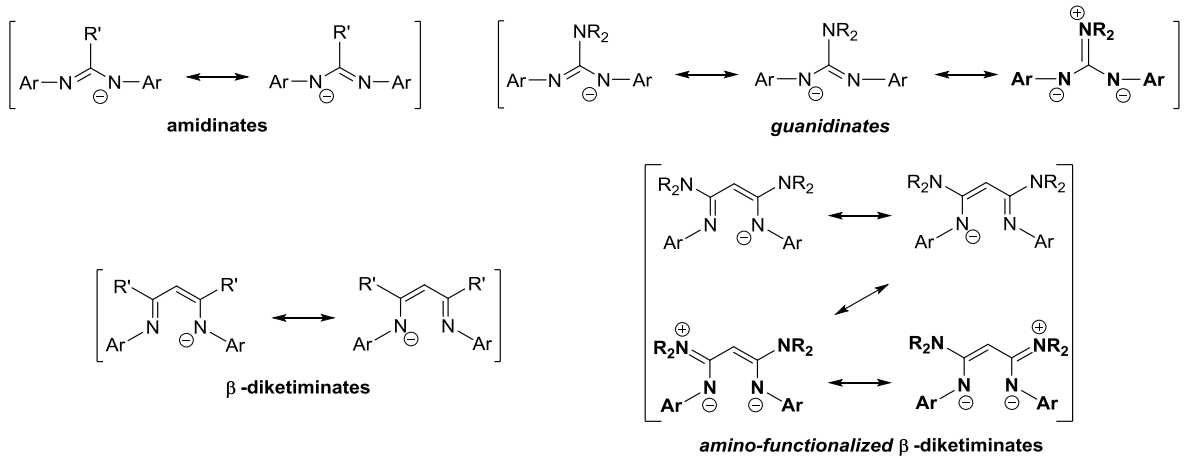


Figure 3.2 Selected examples of the use of electron-deficient Nacnac ligands in Main Group Chemistry

Previously, it has been proposed for amidinates/guanidinates that the inclusion of a backbone amino group renders the system more electron donating, by virtue of an additional dianionic "doubly amido" resonance structure (Scheme 3.4). With this in mind, it was hypothesised that the incorporation of similar π-donating substituents into Nacnac systems might bring about a similar effect, rendering the electronically-modified ligand a better donor (Scheme 3.4).[15] Furthermore, an unpublished study from the group of Clyburne in 2009 appears to support this hypothesis computationally.[16] The use of Nacnac ligands featuring π-donating groups (NMe_2 or OMe) at the β-position is calculated to lead to widened singlet-triplet gaps for the corresponding boron(I) complexes (*borylenes*) compared to the traditional β-methylated version. This extra stabilisation of the singlet state is thought to originate from enhanced π-electron donation into the formally vacant

p-orbital at boron, which destabilises the LUMO and discourages the formation of the triplet state.



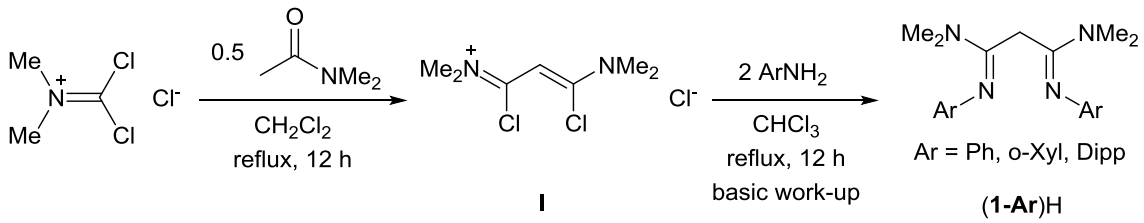
Scheme 3.4 The effect of incorporating amino groups on possible ligand resonance forms – additional "diamido" structures (bold) are introduced

Recognising the dearth of available electronically-modified Nacnac ligands in the complexation chemistry with Main Group elements, we set out to investigate the synthetic viability of a class of amino-functionalised β-diketiminates ("*N*-nacnac"). Our synthetic approach is based on the pioneering experimental work of Viehe *et al.* in the 1970s, and the aforementioned study by the Clyburne group.[16,17] In particular, the target of the work described in this chapter was to establish a versatile route to a range of novel *N*-nacnac ligands offering variation in steric properties by changing the N(imine)-substituted alkyl/aryl groups. The complexation chemistry of these novel ligands with Main Group elements was then to be investigated, focusing on direct metallation reactions.

3.2 Results and Discussion

3.2.1 Protio-ligand synthesis (Ar = Ph, o-Xyl, Dipp)

The synthetic approach utilised for the protio-ligands (^{Ar}N-nacnac)H (Ar = Ph, *o*-Xyl, Dipp) was optimised based on the procedures reported by the groups of Viehe and Clyburne.[16,17] Thus, the reaction between dichloromethylene-dimethyliminium chloride ("Viehe's Salt") and *N,N*-dimethylacetamide was exploited to generate the moisture-sensitive iminium chloride salt **I**, which was subsequently treated *in situ* with the aniline of choice to afford (^{Ph}N-nacnac)H ((**1-Ph**)H), ($^{o\text{-}Xyl}N$-nacnac)H ((**1-Xyl**)H), and (^{Dipp}N-nacnac)H ((**1-Dipp**)H) (Scheme 3.5). While (**1-Ph**)H can be isolated in pure form without further purification (crude yield 50-60 %), additional recrystallisation is required to isolate cleanly the bulkier *o*-Xyl and Dipp analogues (recrystallised yields: 30-40 %).



Scheme 3.5 Synthetic approach for the preparation of *N*-nacnac protio-ligands (^{Ar}N-nacnac)H.

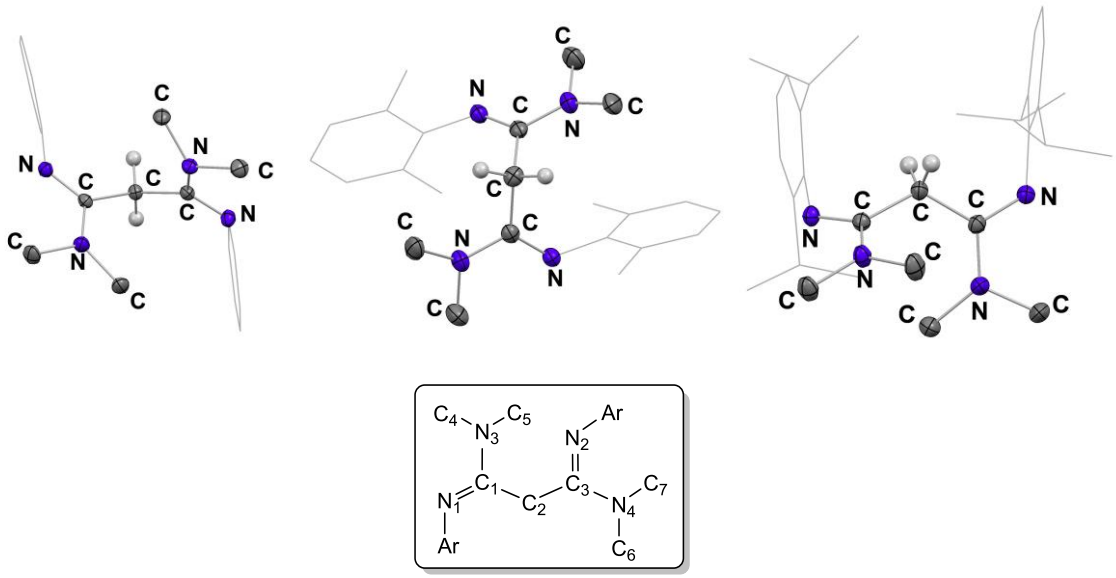


Figure 3.3 *(top, left to right)* Solid-state structures of (**1-Ph**)H**,** (**1-Xyl**)H**,** and (**1-Dipp**)H as determined by X-ray crystallography. Thermal ellipsoids are shown at 35 % probability. *N*-bound aromatic substituents are represented in wireframe format, and all hydrogens apart from those of the methylene linkages have been omitted for clarity. *(below)* Labelling scheme utilised for the structural comparison of the three protio-ligands.

	(**1-Ph**)H	(**1-Xyl**)H[b]	(**1-Dipp**)H
d(C1—N1)[a] / *d*(C3—N2)	1.2923(14) / 1.2879(14)	1.283(3)	1.2868(16) / 1.2861(16)
d(C1—C2) / *d*(C2—C3)	1.5270(13) / 1.5242(13)	1.526(3)	1.5124(17) / 1.5288(17)
d(C1—N3) / *d*(C3—N4)	1.3600(13) / 1.3742(13)	1.369(3)	1.3650(16) / 1.3668(16)
d(N3—C4/5) / *d*(N4—C6/7)	1.4475(15) /1.4547(14) 1.4591(14) / 1.4575(14)	1.453(3) 1.451(4)	1.4506(17) / 1.4516(17) 1.4519(18) / 1.4614(19)

Table 3.1 Selected bond lengths (Å) of the protio-ligands (^{Ar}*N*-nacnac)H (Ar = Ph, *o*-Xyl, Dipp), as determined by X-ray crystallography. Note: [a] Numbering scheme adopted from Figure 3.3; [b] The molecule contains a crystallographically-imposed C_2 axis, hence only one half constitutes the asymmetric unit.

Crystallographic studies of the three amino-functionalised protio-ligands reveal that they all exist as diimines, rather than in the imino-enamine form more frequently observed for NacnacH systems.[3b] A lack of π-delocalisation in the NC_3N five-membered sub-unit is reflected in imine C=N distances (C1—N1 and C3—N2) which are characteristic of isolated C=N double bonds, and C—C distances involving the methylene bridge (C1—C2 and C2—C3) which are typical for C—C single bonds (Table 3.1).[18] On the other hand, the C—NMe_2 bond distances (C1—N3 and C3—N4) fall between the ranges expected for C—N single and double bonds, and are indicative of some degree of electronic delocalisation from the amino groups into the imine functions. These observations fit the description of a diimine configuration, with a backbone γ-CH_2 linkage for *N*-nacnacH protio-ligands ($H_2C\{C(NMe_2)(NAr)\}_2$). In contrast, "traditional" β-methylated NacnacH systems typically adopt the imino-enamine configuration. This features an intramolecular hydrogen bond between the two N(aryl) atoms, and a conjugated, planar structure, featuring a methine CH bridge at the γ-C position (Scheme 3.1). In the absence of hydrogen bonding of this sort, the diimine geometry associated with (^{Ar}*N*-nacnac)H protio-ligands accommodates longer distances between the two N(imine) atoms, thereby allowing the two bulky aromatic groups to project away from each other, relieving the steric congestion. It is also worth mentioning that all three amino-functionalised *N*-nacnacH molecules adopt an *E/E*-configuration relative to the imine functions, with no evidence of alternative *E/Z* or *Z/Z* stereoisomers being detected in the solid state.

As revealed by ^{1}H NMR spectroscopy, the tautomeric configuration of the (**1-Ar**)H systems is retained in solution. Consistent with the results of X-ray crystallography, the (^{Ar}*N*-nacnac)H protio-ligands differ from their (^{Ar}Nacnac)H counterparts through (i) the absence of NH and γ-CH signals in the respective ^{1}H NMR spectra (typically found at 12.0 – 13.5 ppm (NH protons) and 4.5 – 5.0 ppm (γ-CH protons), respectively)[3] and (ii) the existence of a 2H resonance in the more upfield range 3.0 – 3.5 ppm corresponding to the backbone methylene linkage.

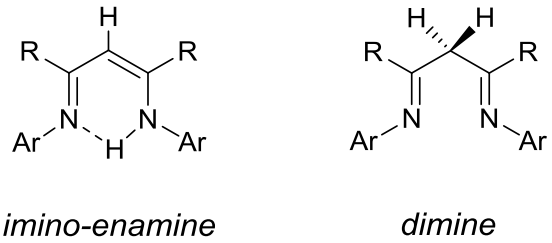


Figure 3.4 The two tautomeric forms of (^{Ar}Nacnac)H/(^{Ar}*N*-nacnac)H, considered in the DFT calculations.

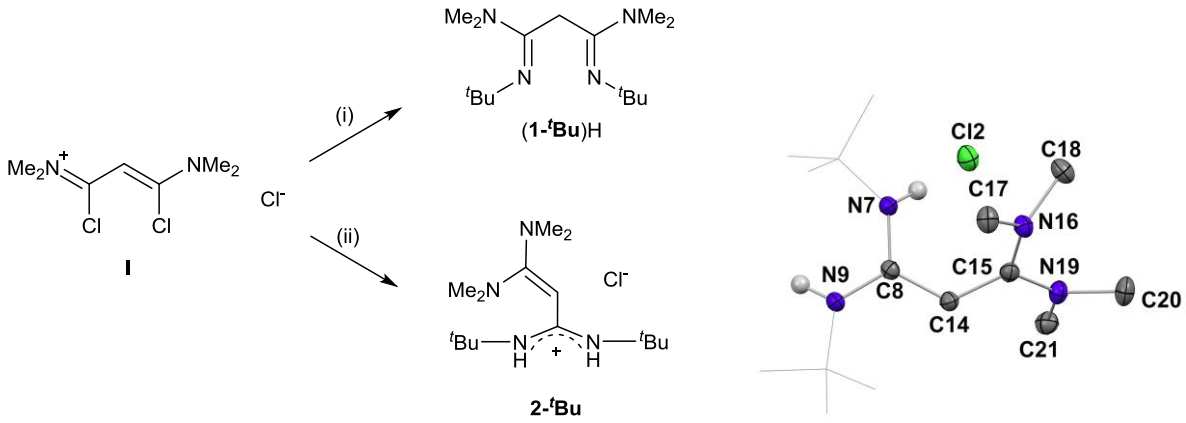
Ligand systems	Ar	ΔE (gas phase)	ΔE (chloroform)	ΔE (benzene)
N-nacnacH	Ph	+6.5	+9.0	+8.3
R = NMe_2	Dipp	-0.6	-0.8	-0.8
NacnacH	Ph	-35.3	-25.6	-28.7
R = Me	Dipp	-60.0	-35.6	-36.1

Table 3.2 Relative energies (kJ mol^{-1}) of the two tautomers shown in Figure 3.4.
ΔE = E(imino-enamine) – E(diimine); thus a negative value reflects a lower energy of the former.

Theoretical insight into the conformational differences between (^{Ar}Nacnac)H and (^{Ar}*N*-nacnac)H protio-ligands (Figure 3.4) is provided by DFT calculations (carried out at the BP86-D3/TZP level) for the Ph- and Dipp-substituted systems. The energetic differences between the imino-enamine and diimine configurations, in

the case of the amino-functionalised variants, are found to be relatively small ($|\Delta E| < 10$ kJ mol^{-1}) in both the gas phase and simulated solvent environments (chloroform or benzene). In the case of Ar = Dipp, ΔE is almost negligible (Table 3.2). On the other hand, parallel calculations carried out on the NacnacH protio-ligands reveal much more substantial energy gaps between the two tautomers; in all cases the imino-enamine conformation is significantly more stable than the diimine form (*cf.* -60 kJ mol^{-1} in the gas phase for Ar = Dipp). Presumably, these DFT-calculated results imply a greater net energy gain upon adopting the conjugated imino-enamine configuration for the commonly employed β-methylated NacnacH systems compared to the novel *N*-nacnacH protio-ligands.

3.2.2 Attempts at protio-ligand synthesis with ^{t}BuNH$_2$



Scheme 3.6 *(left)* The effect of work-up protocol on the outcome of ($^{t\text{Bu}}$*N*-nacnac)H synthesis. General conditions used: ^{t}BuNH$_2$ (2.3 equiv.), EtN^{i}Pr$_2$ (3 equiv.), reflux in CHCl$_3$, 12 h.
Work-up methods: (i) Anhydrous; (ii) Basic aqueous as per ($^{\text{Ar}}$*N*-nacnac)H synthetic protocol.
(right) Solid-state structure of **2-^{t}Bu**, with thermal ellipsoids shown at 35 % probability.
t-butyl substituents are represented in the wireframe format, and all hydrogens apart from those of the NH and central CH protons have been omitted for clarity.

In addition to the widely-employed β-diketiminate scaffolds featuring *N*-aryl substituents, the related system which features *N*-bound *tert*-butyl groups has also

been utilised in the chemistry of Main Group elements.[19] In part, this is due to its facile synthesis *via* the condensation route outlined in Scheme 3.1 using commercially available ^{t}BuNH$_2$.[20] Moreover, various ^{t}Bu-substituted Nacnac complexes have been shown to adopt unusual bonding motifs, with a prominent example featuring two ($^{t\text{Bu}}$Nacnac) ligands which coordinate to a heavier Group 2 metal atom (Ca, Sr, Ba) in an η^5-fashion through the core NC$_3$N ligand scaffold.[19b] Thus, the isolation of the ^{t}Bu-substituted *N*-nacnacH protio-ligand, and the study of its complexation chemistry, would provide a useful direct comparison with that reported for the analogous ($^{t\text{Bu}}$Nacnac)H system.

With this in mind, a synthetic methodology similar to that employed for the preparation of (**1-Ar**)H protio-ligands was explored for the preparation of (**1-^{t}Bu**)H. However, this was found to facilitate the formation of the unexpected product, amidinium chloride salt **2-^{t}Bu**; the identity of which has been unambiguously confirmed by standard spectroscopic techniques and single crystal X-ray crystallography (Scheme 3.6). The solid state structure of **2-^{t}Bu** features a three-membered NCN scaffold in the form of [C(R')(NHR)$_2$]$^+$, with two (protonated) nitrogen-bound ^{t}Bu substituents and a bis(dimethylamino)-ethenyl linkage ({(Me$_2$N)$_2$C=CH}) connected to the central carbon atom *via* the C(H) terminus; the cationic charge is balanced by a chloride counter-anion. Crystallographically, electronic delocalisation across the C8—C14—C15 triatomic unit is evident from the two statistically similar C—C bond distances (1.412(2) Å and 1.407(2) Å for C8—C14 and C14—C15, respectively), which lie between typical reported values for C—C

single and double bonds.[18] Moreover, that the sum of all angles around the C8 atom is 360° and the comparable C8—N(H)(*t*Bu) distances (1.3478(19) Å and 1.3530(19) Å) lie between C—N single and double bonds range, reflects the conjugated nature of the 3-membered N7—C8—N9 fragment, in a fashion akin to that of amidinate/guanidinate ligand systems.[15] The analysis of **2-*t*Bu** by ^{1}H NMR spectroscopy also provides useful insight into the electronic profile of the compound in solution ($CDCl_3$). Extended delocalisation across the backbone is signalled by an unusual upfield shift in the signal associated with the C14 alkenic proton (δ_H = 3.61 ppm), which is characteristic of alkene resonances under the influence of π-donor amino functions.[21]

It has been established that the use of our standard aqueous work-up leads to the formation of the amidinium salt **2-*t*Bu**. Hypothesising that avoiding the aqueous medium might be the key to the generation of (**1-*t*Bu**)H, an anhydrous modification to the work-up strategy was developed. Accordingly, the solid crude material (after the removal of chloroform *in vacuo* during the second reflux step) was extracted into dry diethyl ether, followed by solvent evaporation and sublimation to yield the desired product (**1-*t*Bu**)H, whose identity was confirmed primarily through ^{1}H and ^{13}C{^{1}H} NMR spectroscopy (Scheme 3.6). A characteristic ^{1}H NMR resonance for the backbone methylene bridge is observed at 3.86 ppm, integrating to two protons, and an acidic NH proton resonance is absent, as per the cases of aryl-substituted *N*-nacnac protio-ligands. Unfortunately, efforts to obtain single crystals suitable for X-ray diffraction were thwarted by solvent incompatibility and poor yields

(typically *ca.* 4 %); these problems prevented further exploration of the chemistry of this ligand system.

*3.2.3 Attempted synthesis of (**1-Mes**)H*

Nacnac-stabilised complexes of Main Group elements bearing *N*-bound Mes- substituents have been widely investigated throughout the history of the field.[2,4c,7c,8b] As such, we sought to extend our library of amino-functionalised Nacnac ligands to include (**1-Mes**)H. However, applying the synthetic procedure established for other systems of the type (**1-Ar**)H was found to be more problematic when Ar = Mes. No identifiable amount of the (^{Mes}*N*-nacnac)H protio-ligand could be obtained regardless of the work-up method employed (anhydrous/hydrous as per the ^{t}Bu-substituted case). Instead, X-ray crystallography reveals that the isolated product in all cases is the spiro-cycle **3**, whose formation can be envisaged to have occurred *via* the incorporation of only one equivalent of $MesNH_2$ with a subsequent ring closure process generating a quaternary carbon centre (Figure 3.5).

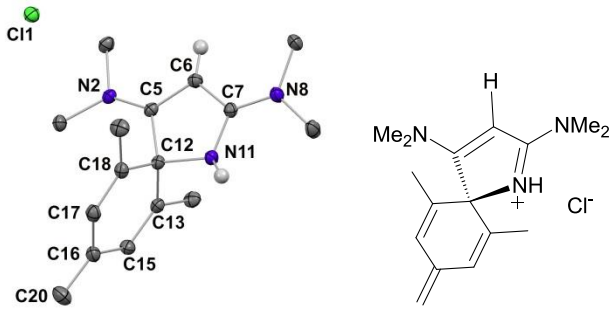


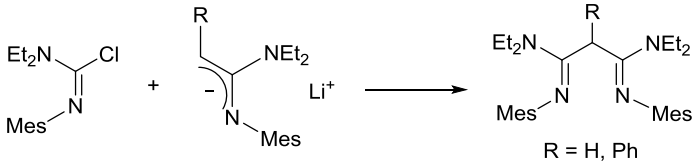
Figure 3.5 Crystallographically determined structure of **3**, with thermal ellipsoids set at 35 % probability, and all hydrogens (apart from C6- and N11- bound protons) have been omitted for clarity.

6-membered ring fragment	C12—C13	C12—C18	C15—C16	C16—C17
	1.529(3)	1.520(3)	1.453(3)	1.459(4)
	C13—C15	C17—C18	C16—C20	
	1.336(3)	1.334(3)	1.351(4)	
5-membered ring fragment	C5—C6	C6—C7	C5—C12	
	1.378(3)	1.418(3)	1.533(3)	
	C7—N11	C12—N11	C5—N2	C7—N8
	1.351(3)	1.484(3)	1.333(3)	1.329(3)

Table 3.3 Selected bond lengths (Å) of **3**, as determined by X-ray crystallography.

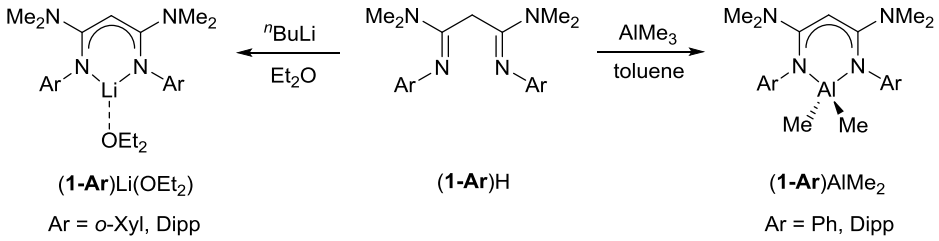
Perhaps the most remarkable feature of this molecule is the activated (deprotonated) *para*-methyl position of the 6-membered ring.[22] This feature results in a loss of aromaticity, as evident from distinct exocyclic (C16—C20) and endocyclic (C13—C15, C17—C18) C=C double bonds (1.33 – 1.36 Å).[18] A considerable degree of extended π-conjugation from the amino substituents to the 5-membered component of the spiro-cycle is also observed. This is reflected by (i) the shortened C—NMe_2 bond distances (1.329(3) Å and 1.333(3) Å), compared to those found in the (**1-Ar**)H protio-ligands (1.3600(13) – 1.3742(13) Å, Table 3.1), and (ii) the small dihedral angles between the mean pyrrollium plane and the two planar amino functions (average 9.9°). Within the 5-membered ring, however, the effect of electronic delocalisation is less pronounced, and is primarily located within the (C5—C6—C7—N21) aza-butadiene unit, which features carbon-carbon and carbon-nitrogen bond lengths falling in the intermediate range between the respective single and double bonds (Table 3.3). [18]

The lack of aromaticity in the 6-membered ring is also consistent with the results of ^{1}H NMR spectroscopy in solution. Alkenic CH_2 (exocyclic) and CH proton signals are observed at 4.96 and 6.25 ppm respectively (with concomitant loss of *p*-CH_3 resonances). Furthermore, the π-donation from both NMe_2 groups increases the electron density at the C6-position, as demonstrated by a slightly more upfield shift of the resonance associated with its CH proton (δ_H = 4.88 ppm). Mechanistically, it is proposed that the ring closure process proceeds *via* the uptake of one equivalent of mesityl-aniline by the iminium salt **I**, followed by mono-deprotonation of the *para*-CH_3 of the mesityl substituent. This generates a carbon-based nucleophile, which, by virtue of resonance, then attacks the electrophilic central carbon of the chloro-iminium function through the *ipso*-position. Deprotonation processes of this nature has been more often associated with the use of strong bases due to the intrinsic weak acidity of aliphatic sp^3 protons; nonetheless, this proposed mechanism is further supported by the fact that the removal of the *p*-CH_3 substituent leads to the facile generation of (**1-Xyl**)H. It is worth mentioning that during the course of this synthetic investigation the group of Jones (at Monash University, Australia) has reported an alternative strategy to access the Mes-substituted protio-ligand. This method is based upon a C—C coupling reaction between two imino-enamine units at the backbone C2 position (Scheme 3.7).[23]



Scheme 3.7 Alternative synthetic route for the preparation of the Mes-substituted protio-ligand, *via* coupling of two imino-enamine units

3.2.4 Direct metallation of N-nacnac ligands with lithium and aluminium alkyls



Scheme 3.8 Direct metalation (Li, Al) of the (^{Ar}*N*-nacnac)H protio-ligands

Having prepared the (^{Ar}*N*-nacnac)H protio-ligands, we sought to explore their coordination chemistry with Group 1 (Li) and Group 13 (Al) elements, as examplars of metal complexes which might be obtained *via* direct metallation. Thus, the reactions of the protio-ligands with ^{n}BuLi in Et_2O can be shown to afford the corresponding lithium derivatives (**1-Ar**)Li(OEt_2) (for Ar = *o*-Xyl, Dipp), in moderate to good yield (60 – 90 %) *via* deprotonation of the backbone CH_2 group (Scheme 3.8). On the other hand, the isolation of an analytically pure sample of the lithium complex with (**1-Ph**) ligand appears to be more problematic (the *in situ*-generated lithiated ligand proved to be sufficiently pure for use in transmetallation chemistry - which is discussed in subsequent chapters).

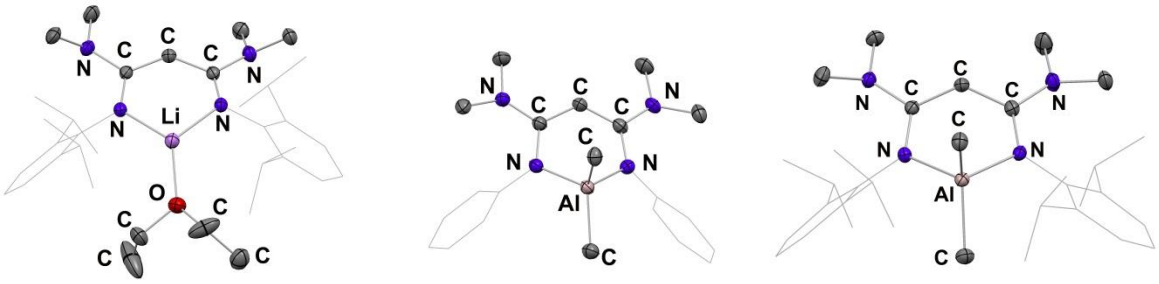


Figure 3.6 *(from left)* Crystallography determined solid-state structures of (**1-Dipp**)Li(OEt_2), (**1-Ph**)$AlMe_2$ (only one molecule from the asymmetric unit is displayed for clarity), and (**1-Dipp**)$AlMe_2$. Thermal ellipsoids are shown at 35 % probability. *N*-bound aromatic substituents are represented in the wireframe format, and all hydrogens have been omitted for clarity.

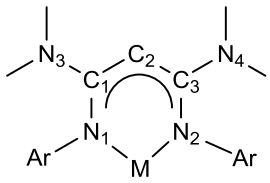
	(**1-Dipp**)Li(OEt_2)	(**1-Ph**)$AlMe_2$ [*]	(**1-Dipp**)$AlMe_2$
d(C1—N1)[a] / *d*(C3—N2)	1.336(2) / 1.321(2)	1.367(6) / 1.353(6) 1.380(6) / 1.367(6)	1.354(3) / 1.345(3)
d(C1—C2) / *d*(C2—C3)	1.408(2) / 1.420(2)	1.396(6) / 1.414(6) 1.394(6) / 1.412(7)	1.404(3) / 1.422(3)
d(C1—N3) / *d*(C3—N4)	1.408(2) / 1.410(2)	1.372(6) / 1.361(6) 1.361(6) / 1.367(6)	1.382(2) / 1.372(3)
d(M—N1) / *d*(M—N2)	1.915(3) / 1.909(3)	1.894(4) / 1.914(4) 1.907(4) / 1.910(4)	1.9234(17) / 1.9233(18)
∠ (N1—M—N2)	101.38(15)	96.00(17) / 95.51(17)	99.45(8)

Table 3.4 Selected bond lengths (Å) and angles (°) of the metallated compounds (M = Li, Al), as determined by X-ray crystallography. Note: [*] There are two individual molecules per asymmetric unit.

Of all the complexes of *N*-nacnac ligands with lithium, single crystals of the Dipp analogue can be obtained from a concentrated solution in diethyl ether, and subsequently studied by X-ray diffraction techniques. The solid-state structure

reveals a near-planar six-membered (NC_3N)Li heterocycle (sum of all endocyclic angles = 718.3°). The metal centre coordinated by two endocyclic nitrogen atoms of the monoanionic NC_3N chelate and a single diethyl ether molecule *via* the oxygen atom, which resides 0.88 Å off the least-squares mean NC_3N plane. The Li—O distance of 1.940(3) Å is very close to the sum of the covalent radii of the two elements (1.94 Å),[24] indicating a strong interaction between the two atoms. In addition, a 6π-electron, delocalised (N1—C1—C2—C3—N2) unit is evident in the solid-state structure: the C—N (1.408(2) Å and 1.410(2) Å) and C—C (1.408(2) and 1.420(2) Å) distances fall in the intermediate ranges between the respective C—N and C—C single and double bonds (Table 3.4).[18] This attribute is reminiscent of the core structural features of the ligand backbone of typical Nacnac complexes. With respect to the least-squares ligand plane, the two flanking *N*-bound Dipp rings are aligned at angles of 68.2° and 80.3°, and their *ipso*-carbons are located 0.20 Å and 0.48 Å away from the plane. Although the short C—NMe_2 distances (1.336(2) Å and 1.321(2) Å) might suggest multiple bond character for this carbon-nitrogen bond, the pendant amino groups are not perfectly co-planar with the mean chelate plane, but instead tilted by 37.3° and 44.8°. Presumably, this hints at a reduced degree of π-donation from the amino functions into the ligand backbone.

In the case of (**1-Xyl**)Li(OEt_2), despite multiple recrystallisation attempts from common organic solvents, the compound could not be obtained as single crystals suitable for X-ray diffraction. Interestingly, an attempt to use hexane as the reaction medium yields the non-donor-stabilised lithiated ligand (**1-Xyl**)Li, whose isolation

as single crystals suitable for X-ray crystallography is not possible much like its etherated analogue, although both compounds are fully characterised by conventional spectroscopic techniques (section 3.4.3).

Spectroscopically, backbone deprotonation of the methylene bridge is reflected by the ^{1}H NMR signals of the γ-CH, which integrates to one proton, for all three lithiated ligands (**1-Xyl**)Li, (**1-Xyl**)Li(OEt$_2$) and (**1-Dipp**)Li(OEt$_2$) (δ_H = 3.8 – 4.1 ppm). These resonances appear at upfield chemical shifts compared to other lithiated Nacnac species (*cf.* 4.98 ppm for (^{Dipp}Nacnac)Li(OEt$_2$)).[25] This effect is in line with a previous report on the π-donating effects of amino groups on alkene resonances, in this case indicated by an increase in electron density at the methine position of the ligand backbone.[21]

Similar metallation chemistry can also be exploited for the preparation of the dimethylaluminium complexes, (^{Ar}*N*-nacnac)AlMe$_2$ (Ar = Ph, Dipp). Thus, treatment of the respective protio-ligands with AlMe$_3$ in toluene generates the corresponding (**1-Ar**)AlMe$_2$ systems in good yields (70 – 90 %, Scheme 3.8). As observed for (**1-Ar**)Li(OEt$_2$), the ^{1}H NMR resonance associated with the γ-CH unit in both compounds is shifted upfield with respect to that in the corresponding Nacnac system, (δ_H = 4.06 and 3.83 ppm for Ar = Ph and Dipp respectively, *cf.* 5.12 ppm for (^{Dipp}Nacnac)AlMe$_2$).[12a] Crystallographically, the solid state structures of the aluminated compounds are based around similar (NC$_3$N)Al six-membered metallocycles as per the lithiated complex (**1-Dipp**)Li(OEt$_2$). However, unlike in the lithium complex, the geometry around the aluminium centre is distorted

tetrahedral, with the metal atom coordinated by the *N,N'*-chelate and two CH_3 groups.

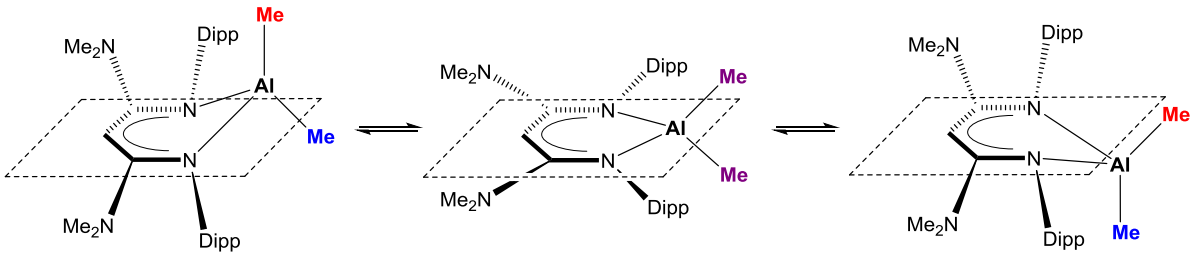


Figure 3.7 The proposed fluxionality of (**1-Dipp**)$AlMe_2$ in solution at ambient conditions.

It is worth noting that the combined spectroscopic and crystallographic profile of (**1-Dipp**)$AlMe_2$ hint at a fluxional behaviour of the compound in solution at ambient conditions (Figure 3.7). Namely, the ^1H NMR spectrum of (**1-Dipp**)$AlMe_2$ exhibits a single resonance for the two magnetically equivalent Al-bound CH_3 groups at -0.28 ppm, and two sets of doublets at 1.24 and 1.40 ppm, each integrating to 12 H, which correspond to the two groups of Dipp-CH_3 protons directed towards/away from the backbone amino functions (section 3.4.4). On the other hand, the solid-state structure of this compound is less symmetrical, as reflected by the two non-equivalent positions occupied by the Al-bound CH_3 groups (*pseudo*-axial and *pseudo*-equatorial) with respect to the least-squares $(NC_3N)Al$ mean plane (Figure 3.6). Thus, the fluxionality of (**1-Dipp**)$AlMe_2$ is likely to be rapid on the NMR timescale, rendering the Al-Me groups equivalent. Put another way, this fluxional process effectively imposes an additional plane of symmetry on the molecule on the NMR timescale.

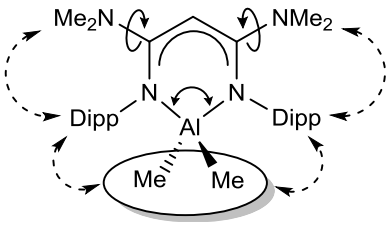


Figure 3.8 Effects of the bulky Dipp groups on the molecular alignment in **(1-Dipp)**$AlMe_2$, through steric repulsion with the backbone amino substituents and the $AlMe_2$ fragment *(in dashed arrows)*, which increases the ligand bite angle and rotates the NMe_2 groups out of the ligand plane.

As expected, the use of Ph and Dipp groups as the *N*-bound aryl substituents leads to subtle differences in the structural properties of the two complexes. These differences are predominantly focused at the metal centre: the more sterically encumbered system, (**1-Dipp**)$AlMe_2$, features a wider N—Al—N angle, elongated Al—N bonds, and shorter C1—N1 / C3—N2 bonds (Table 3.4). Moreover, a shorter distance between the aluminium atom and the least-squares NC_3N plane is observed for (**1-Dipp**)$AlMe_2$ (0.69 Å, compared to 0.75 Å / 0.87 Å for the Ph analogue, which has two molecules in the asymmetric unit). Presumably, this reflects the increased steric bulk surrounding the metal centre for the Dipp-substituted complex, where the N(aryl)—Al distances are lengthened to relieve the spatial congestion within the (N—Al(Me)$_2$—N) unit, and the proximal NMe_2 groups are forced to rotate out of the ligand plane to a greater extent. Consequently, this widens the ligand bite angle, allowing the aluminium atom to sit closer to the least-squares NC_3N chelating plane (Figure 3.8). In a broader sense, these observations are consistent with the renowned ability of Dipp-substituted Nacnac ligands to stabilise monomeric, sub-valent Main Group complexes through enhanced steric protection at the unsaturated metal centre.

3.3 Conclusions

Studies of the synthesis of a new generation of amino-functionalised β-diketiminate protio-ligands ((Ar*N*-nacnac)H) are reported, with a view to examining the effect of incorporating electron-rich amino functions at the ligand backbone on the properties of *N*-nacnac-stabilised lithium and aluminium complexes. As seen with analogous Nacnac systems, the lithiated ligands might serve as attractive synthons for the preparation of other *N*-nacnac-stabilised Main Group complexes *via* transmetallation chemistry. Thus, an optimised synthetic procedure was developed for three *N*-aryl substituted protio-ligands (**1-Ar**)H (Ar = Ph, *o*-Xyl, Dipp), involving a one-pot condensation reaction between the pre-formed bifunctional iminium chloride backbone **I** and the corresponding aniline (Scheme 3.5). This approach, however, was unsuccessful for the ^{t}Bu- and Mes-substituted systems, leading instead to rearrangement products **2-^{t}Bu** and **3**. Although a change to an anhydrous work-up allowed for the successful formation of (**1-^{t}Bu**)H, this system was isolated in an unimpressive yield, preventing further studies of its chemistry. The newly-synthesised protio-ligands were fully characterised by standard analytical methods, including X-ray crystallography, which reveals significant differences compared to their "traditional" β-methylated NacnacH analogues. Both in the solid state and in the solution phase, the diimine tautomer was found to be favoured over the conjugated imino-enamine form commonly seen for their Nacnac counterparts.

Facile backbone deprotonation using either ^{n}BuLi or $AlMe_3$ afforded the corresponding metallated complexes (**1-Ar**)Li(OEt_2) and (**1-Ar**)$AlMe_2$, respectively.

Each of these compounds is characterised by an upfield shift of the resonance associated with the methine (γ-CH) proton, as compared to their Nacnac analogues (where examples were available). This is indicative of a marked degree of π-donation from the pendant amino substituents to the ligand backbone. Analysis of (**1-Dipp**)Li(OEt_2) and (**1-Ar**)$AlMe_2$ (Ar = Ph, Dipp) by single crystal X-ray crystallography shows that all three complexes adopt a near-planar, conjugated, 6-membered (NC_3N)M configuration, consistent with that reported for their Nacnac analogues. Comparison between the two dialkyl-aluminium compounds (which differ in the sizes of the *N*-aryl substituents) reveals a number of differences due to their different steric profiles. Thus, a more "shielded" metal centre was observed in the case of the bulkier Dipp system, which is consistent with the more widespread use of ^{Dipp}Nacnac ligands for the stabilisation of reactive Main Group complexes with unsaturated metal centres.

3.4 Synthesis of Novel Compounds

3.4.1 Synthesis of protio-ligands: To a solution of dichloromethylene-dimethylammonium chloride (15.00 g, 92.3 mmol) in dichloromethane (150 mL) was added dropwise *N*,*N*-dimethylacetamide (4.1 mL, 44.1 mmol) at room temperature, and the reaction mixture refluxed for 14 h. After removal of volatiles *in vacuo*, chloroform was added (150 mL), followed by the amine/aniline of choice (100 mmol) at 0°C. The reaction mixture was then refluxed for a further 15 h. After cooling to room temperature and subsequently to 0°C in an ice bath, *ca.* 400 mL of a 6 M KOH solution was slowly added, followed by water (100 mL). The aqueous layer was

washed twice with chloroform (3 x 100 mL) and the organic layer extracted, washed with brine (100 mL) and dried over $MgSO_4$. The resulting solution was filtered and volatiles removed *in vacuo* to give the crude product.

(^{Ph}*N*-nacnac)H ((**1-Ph**)H): The solid crude product was washed with cold hexane to yield a yellow solid as a spectroscopically pure material. Yield: 7.55 g, 56%. Crystals suitable for X-ray crystallography were grown from a saturated acetone solution at -26˚C. ^{1}H NMR (400 MHz, $CDCl_3$): δ_H 2.84 (s, 12H, (C<u>H</u>$_3$)$_2$N), 3.37 (s, 2H, *N*-nacnac backbone CH_2), 6.57 (d, $^3J_{HH}$ = 7.7 Hz, 4H, *o*-CH of Ph), 6.90 (t, $^3J_{HH}$ = 7.4 Hz, 2H, *p*-CH of Ph), 7.18 (t, $^3J_{HH}$ = 7.6 Hz, 4H, *m*-CH of Ph) ppm. ^{13}C{^{1}H} NMR (101 MHz, $CDCl_3$): δ_C 29.4 (*N*-nacnac backbone CH_2), 38.6 ((<u>C</u>H$_3$)$_2$N), 122.0 (*p*-CH of Ph), 122.7 (*o*-CH of Ph), 129.1 (*m*-CH of Ph), 150.8 (*ipso*-C of Ph), 155.6 (imine quaternary C) ppm. ESI-MS (*m*/*z*, %): 309.2, weak, $[M+H]^+$; accurate mass: calc. for $C_{19}H_{25}N_4$ ($[M+H]^+$) 309.2074, meas. 309.2075. Elemental microanalysis: calc. for $C_{19}H_{24}N_4$: C 73.99, H 7.84, N 18.17%, meas. C 74.13, H 8.01, N 18.00%.

($^{o\text{-}Xyl}$*N*-nacnac)H ((**1-Xyl**)H): (NB. additional base (*N*-ethyl diisopropyl amine, 23.4 mL, 137 mmol) was added prior to the aniline during the second reflux step). The product was recrystallised from minimal acetone/hexane at -26˚C as pale yellow crystals. Yield: 5.67 g (35%). ^{1}H NMR (400 MHz, $CDCl_3$): δ_H 1.98 (s, 12H, CH_3 of Xyl), 2.86 (s, 12H, (C<u>H</u>$_3$)$_2$N), 3.13 (s, 2H, *N*-nacnac backbone CH_2), 6.80 (t, $^3J_{HH}$ = 9.1 Hz, 2H, *p*-CH of Xyl), 6.98 (d, $^3J_{HH}$ = 7.4 Hz, 4H, *m*-CH of Xyl) ppm. ^{13}C{^{1}H} NMR (101 MHz, $CDCl_3$): δ_C 18.6 (CH_3 of Xyl), 31.4 (*N*-nacnac backbone CH_2), 38.6 ((<u>C</u>H$_3$)$_2$N), 121.6 (*p*-CH of Xyl), 128.0 (*m*-CH of Xyl), 128.9 (*o*-C of Xyl), 147.9 (*ipso*-C of xyl), 154.1

(imine quaternary C) ppm. ESI-MS (*m*/*z*, %): 365, weak, $[M+H]^+$; accurate mass: calc. for $C_{23}H_{33}N_4$ 365.2700, meas. 365.2698. Elemental microanalysis: calc. for $C_{23}H_{32}N_4$: C 75.78, H 8.85, N 15.37%, meas. C 75.65, H 9.01, N 15.25.

(^{Dipp}*N*-nacnac)H ((**1-Dipp**)H): (NB. additional base (*N*-ethyl diisopropyl amine, 26.5 mL, 155 mmol) was added prior to the aniline during the second reflux step). The crude product (a dark red oil) was dissolved in an acetone/hexane mixture and stirred vigorously for 10 min. Filtration followed by storage at -26˚C overnight yielded the product as pale yellow crystals. Yield: 6.91 g, 33%. ^{1}H NMR (400 MHz, C_6D_6): δ_H 1.12 (d, $^3J_{HH}$ = 7.1 Hz, 12H, (C$\underline{H}_3$)$_2$CH), 1.18 (d, $^3J_{HH}$ = 7.1 Hz, 12H, (C$\underline{H}_3$)$_2$CH), 2.68 (s, 12H, (C$\underline{H}_3$)$_2$N), 2.95 (br sept, 4H, (CH$_3$)$_2$C$\underline{H}$), 3.21 (s, 2H, *N*-nacnac backbone CH_2), 7.05 (t, $^3J_{HH}$ = 7.5 Hz, 2H, *p*-CH of Dipp), 7.12 (d, $^3J_{HH}$ = 7.5 Hz, 4H, *m*-CH of Dipp) ppm. ^{13}C{^{1}H} NMR (125 MHz, C_6D_6): δ_C 22.5 ((C$\underline{H}_3$)$_2$CH), 24.4 ((C$\underline{H}_3$)$_2$CH), 28.6 ((CH$_3$)$_2$C$\underline{H}$), 32.0 (*N*-nacnac backbone CH_2), 38.5 ((C$\underline{H}_3$)$_2$N), 122.7 (*p*-CH of Dipp), 123.2 (*m*-CH of Dipp), 138.6 (*o*-C of Dipp), 146.0 (*ipso*-C of Dipp), 153.8 (imine quaternary C) ppm. ESI-MS (*m*/*z*, %): 477.4, 100, $[M+H]^+$; accurate mass: calc. for $C_{31}H_{49}N_4$ ($[M + H]^+$) 477.3952, meas. 477.3949. Elemental microanalysis: calc. for $C_{31}H_{48}N_4$: C 78.10, H 10.15, N 11.75%, meas. C 78.27, H 10.06, N 11.85%.

(^{tBu}*N*-nacnac)H ((**1-^{t}Bu**)H): The compound was synthesised in half scale, starting from 7.50 g (46.2 mmol) of dichloromethylene-dimethylammonium chloride. The amount of all other reagents and solvents used in the synthesis were also halved, with respect to that used in the synthetic protocol for (**1-Dipp**)H. (NB. additional

base (*N*-ethyl diisopropyl amine, 11.7 mL, 68 mmol) was added prior to the amine for the second reflux step). After refluxing with chloroform for 12 h, the solvent was removed *in vacuo* to yield an orange rock-like solid as the crude product, which was ground up as fine as possible. Dry diethyl ether (100 mL) was then added and the solution was stirred overnight. After filtration, the solvent was removed *in vacuo* to give a pale yellow spectroscopically pure solid. Yield: 0.24 g, 4% yield. ^{1}H NMR (400 MHz, C_6D_6) δ_H 1.36 (s, 18H, C(C<u>H</u>$_3$)$_3$), 2.43 (s, 12H, (C<u>H</u>$_3$)$_2$N), 3.86 (s, 2H, *N*-nacnac backbone CH_2) ppm. ^{13}C{^{1}H} NMR (101 MHz, C_6D_6) δ_C 29.9 (C(<u>C</u>H$_3$)$_3$), 30.0 (*N*-nacnac backbone CH_2), 35.9 ((<u>C</u>H$_3$)$_2$N), 50.5 (<u>C</u>(CH$_3$)$_3$), 157.4 (imine quaternary C) ppm. ESI-MS (*m*/*z*, %): 269, weak, $[M+H]^+$; accurate mass: calc. for $C_{15}H_{32}N_4$ 269.2700, meas. 269.2686.

3.4.2 Attempted syntheses of (^{tBu}N-nacnac)H and (^{Mes}N-nacnac)H

2-^{t}Bu: The compound was synthesised in half scale, starting from 7.50 g (46.2 mmol) of dichloromethylene-dimethylammonium chloride. The amount of all other reagents and solvents used in the synthesis were also halved, with respect to that used the synthetic protocol for (**1-Dipp**)H. Following the synthetic procedure as per (**1-^{t}Bu**)H, but employing the aqueous work-up by treatment with a 6 M KOH solution, followed by extraction of the organic phase (in chloroform) led to the synthesis of **2-^{t}Bu**. Recrystallisation from acetone/hexane yielded white crystals of (**2-^{t}Bu**)·acetone·H_2O (2.0 g, 29% yield). ^{1}H NMR (400 MHz, $CDCl_3$): δ_H 1.35 (s, 18H, C(C<u>H</u>$_3$)$_3$), 2.85 (s, 12H, (C<u>H</u>$_3$)$_2$N), 3.61 (s, 1H, backbone CH), 6.78 (s, 2H, NH) ppm. ^{13}C{^{1}H} NMR (101 MHz, $CDCl_3$): δ_H 30.3 (C(<u>C</u>H$_3$)$_3$), 41.2 ((<u>C</u>H$_3$)$_2$N), 53.0 (<u>C</u>(CH$_3$)$_3$),

71.2 (CH of backbone), 161.4, 168.1 (backbone quaternary Cs) ppm. ESI-MS (*m*/*z*, %): 269.2, 100, $[M]^+$; accurate mass: calc. for $C_{15}H_{33}N_4$ 269.2700, meas. 269.2706.

3: The compound was synthesised in half scale, starting from 7.50 g (46.2 mmol) of dichloromethylene-dimethylammonium chloride. The amount of all other reagents and solvents used in the synthesis were also halved, with respect to that used the synthetic protocol for (**1-Dipp**)H. The crude product (a dark orange oil) was washed with acetone, which led to the formation of a white solid, and it was subsequently recrystallised from hot acetone/hexane to afford the pure product as white crystals suitable for X-ray crystallography (1.98 g, 31% yield). ^{1}H NMR (400 MHz, $CDCl_3$): δ_H 1.65 (s, 6H, 6-membered ring CH_3), 2.90 (s, 6H, $(C\underline{H}_3)_2N$), 3.09 (s, 3H, $(C\underline{H}_3)_2N$), 3.34 (s, 3H, $(C\underline{H}_3)_2N$), 4.88 (s, 1H, heterocycle CH), 4.96 (s, 2H, alkenic CH_2), 6.25 (s, 2H, alkenic CH), 9.96 (s, 1H, NH) ppm. ^{13}C{^{1}H} NMR (101 MHz, $CDCl_3$): δ_C 17.4 (6-membered ring CH_3), 38.1, 40.5, 40.8, 42.3 ($(\underline{C}H_3)_2N$), 71.7 (C(5)), 83.8 (C(9)), 116.5 (C(1)), 129.0 (C(3/7)), 130.6 (C(4/6), 136.2 (C(2)), 166.2 (C(8/10)), 170.4 (C(8/10)) (see Figure 3.9 below for numbering scheme) ppm. ESI-MS (*m*/*z*, %): 258.2, 100, $[M]^+$; accurate mass: calc. for $C_{16}H_{24}N_3$ 258.1965, meas. 258.1970. Elemental microanalysis: calc. for $C_{16}H_{24}ClN_3$: C 65.40, H 8.23, N 14.30%, meas. C 65.21, 8.35, 14.14%.

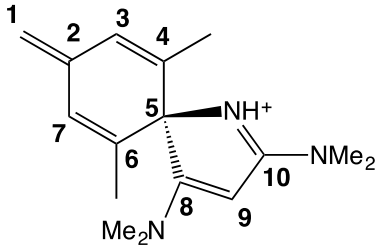


Figure 3.9 Numbering scheme applied to the carbon skeleton of **3**.

3.4.3 Generic procedure for the lithiation of ^{Ar}N-nacnacH: To a solution of (**1-Ar**)H (10 mmol) in Et_2O (100 mL) at -78˚C was added a solution of ^{n}BuLi in hexane (4.4 mL of a 2.5 M solution, 11 mmol); the orange reaction mixture was warmed to room temperature and stirred for 12 h.

(**1-Dipp**)Li(OEt_2): Concentration of the ethereal solution to *ca.* 20 mL and storage at -26˚C overnight yielded colourless crystals of the product as an analytically pure material. Yield 3.45 g, 62%. ^{1}H NMR (400 MHz, C_6D_6): δ_H 0.54 (t, $^3J_{HH}$ = 7.0 Hz, 6H, C$\underline{H}_3$CH$_2$O), 1.20 (d, $^3J_{HH}$ = 7.2 Hz, 12H, (C$\underline{H}_3$)$_2$CH), 1.31 (d, $^3J_{HH}$ = 6.8 Hz, 12H, (C$\underline{H}_3$)$_2$CH), 2.52 (s, 12H, (C$\underline{H}_3$)$_2$N), 2.64 (q, $^3J_{HH}$ = 7.1 Hz, 4H, CH$_3$C$\underline{H}_2$O), 3.51 (sept, $^3J_{HH}$ = 6.8 Hz, 4H, (CH$_3$)$_2$C$\underline{H}$), 4.09 (s, 1H, methine CH), 7.03 (t, $^3J_{HH}$ = 7.4 Hz, 2H, *p*-CH of Dipp), 7.15 (d, $^3J_{HH}$ = 7.6 Hz, 4H, *m*-CH of Dipp) ppm. ^{13}C{^{1}H} NMR (101 MHz, C_6D_6): δ_C 13.6 ($\underline{C}$H$_3$CH$_2$O), 23.7 (($\underline{C}$H$_3$)$_2$CH), 25.4 (($\underline{C}$H$_3$)$_2$CH), 28.1 ((CH$_3$)$_2\underline{C}$H), 41.3 (($\underline{C}$H$_3$)$_2$N), 62.8 (CH$_3\underline{C}$H$_2$O), 72.8 (methine CH), 121.7 (*p*-CH of Dipp), 123.7 (*m*-CH of Dipp), 141.1 (*o*-C of Dipp), 149.5 (*ipso*-C of Dipp), 166.2 (imine quaternary C) ppm.

(**1-Xyl**)Li(OEt_2): Solvent evaporation *in vacuo* afforded the pure product without the need for further purification. All attempts to obtain X-ray quality crystals were unsuccessful. Yield 3.75 g, 84 %. ^{1}H NMR (400 MHz, C_6D_6): δ_H 0.60 (t, $^3J_{HH}$ = 7.1 Hz, 6H, C$\underline{H}_3$CH$_2$O), 2.29 (s, 12H, CH$_3$ of Xyl), 2.53 (s, 12H, (C$\underline{H}_3$)$_2$N), 2.70 (q, $^3J_{HH}$ = 7.1 Hz, 4H, CH$_3$C$\underline{H}_2$O), 3.99 (s, 1H, methine CH), 6.88 (t, $^3J_{HH}$ = 7.4 Hz, 2H, *p*-CH of Xyl), 7.10 (d, $^3J_{HH}$ = 7.4 Hz, 4H, *m*-CH of Xyl) ppm. ^{13}C{^{1}H} NMR (101 MHz, C_6D_6): δ_C 14.1 ($\underline{C}$H$_3$CH$_2$O), 19.8 (CH$_3$ of Xyl), 40.6 (($\underline{C}$H$_3$)$_2$N), 65.5 (CH$_3\underline{C}$H$_2$O), 73.6

(methine CH), 120.1 (*p*-CH of Xyl), 128.5 (*m*-CH of Xyl), 130.6 (*o*-C of Xyl), 152.7 (*ipso*-C of Xyl), 166.8 (imine quaternary C) ppm.

(**1-Xyl**)Li: A similar procedure was applied as for the case of (**1-Xyl**)Li(OEt_2), with hexane as solvent instead of diethyl ether. Yield 2.46 g, 55%. ^{1}H NMR (400 MHz, C_6D_6): δ_H 2.14 (s, 12H, CH_3 of Xyl), 2.40 (s, 12H, $(C\underline{H}_3)_2N$), 3.85 (s, 1H, methine CH), 6.89 (t, $^{3}J_{HH}$ = 7.3 Hz, 2H, *p*-CH of Xyl), 7.07 (d, $^{3}J_{HH}$ = 7.4 Hz, 4H, *m*-CH of Xyl) ppm. $^{13}C\{^{1}H\}$ NMR (101 MHz, C_6D_6): δ_C 19.7 (CH_3 of Xyl), 40.7 ($(\underline{C}H_3)_2N$), 73.9 (methine CH), 120.4 (*p*-CH of Xyl), 128.5 (*m*-CH of Xyl), 131.3 (*o*-C of Xyl), 152.8 (*ipso*-C of Xyl), 166.9 (imine quaternary C) ppm.

3.4.4 Generic procedure for the preparation of N-nacnac-stabilised dimethyl-aluminium complexes ([^{Ar}N-nacnac]AlMe$_2$): To a solution of (**1-Ar**)H (Ar = Ph, Dipp) (2.1 mmol) in toluene (25 mL) at -20˚C was added a solution of $AlMe_3$, also in toluene (1.05 mL of a 2.0 M solution, 2.1 mmol) with rapid stirring. The reaction mixture was slowly warmed to room temperature and volatiles removed *in vacuo* to yield the product as a spectroscopically pure light yellow solid. Slow evaporation of a saturated toluene solution produced crystals suitable for X-ray crystallography.

(**1-Ph**)$AlMe_2$: yield 0.98 g, 75%. ^{1}H NMR (400 MHz, C_6D_6): δ_H -0.28 ($AlC\underline{H}_3$), 2.26 (s, 12H, $(C\underline{H}_3)_2N$), 4.06 (s, 1H, methine CH), 6.82 (t, $^{3}J_{HH}$ = 7.4 Hz, 2H, *p*-CH of Ph), 6.98 (d, $^{3}J_{HH}$ = 7.2 Hz, 4H, *o*-CH of Ph), 7.07 (t, $^{3}J_{HH}$ = 7.8 Hz, 4H, *m*-CH of Ph) ppm. $^{13}C\{^{1}H\}$ NMR (125 MHz, C_6D_6): δ_C -8.9 ($Al\underline{C}H_3$), 40.3 ($(\underline{C}H_3)_2N$), 79.2 (methine CH), 122.4 (*p*-CH of Ph), 125.0 (*o*-CH of Ph), 129.1 (*m*-CH of Ph), 149.1 (*ipso*-C of Ph), 166.4 (imine quaternary C) ppm. ^{27}Al NMR (104 MHz, C_6D_6): δ_{Al} 166 (br) ppm. EI-MS

(*m*/*z*, %): 349.0, 100, $[M\text{-}CH_3]^+$; 304.0, 80 $[M\text{-}2CH_3]^+$; accurate mass: calc. for $C_{20}H_{26}AlN_4$ ($[M - CH_3]^+$) 349.1967, meas. 349.0262. Elemental microanalysis: calc. for $C_{21}H_{29}AlN_4$: C 69.20, H 8.02, N 15.37%, meas. C 69.04, H 7.89, N 15.39%.

(**1-Dipp**)$AlMe_2$: yield 0.94 g, 84%. ^{1}H NMR (500 MHz, C_6D_6): δ_H -0.28 (s, $AlC\underline{H}_3$, 6H), 1.24 (d, $^3J_{HH}$ = 6.7 Hz, 12H, $(C\underline{H}_3)_2CH$), 1.40 (d, $^3J_{HH}$ = 6.7 Hz, 12H, $(C\underline{H}_3)_2CH$), 2.27 (s, 12H, $(C\underline{H}_3)_2N$), 3.57 (sept, $^3J_{HH}$ = 6.7 Hz, 4H, $(CH_3)_2C\underline{H}$), 3.83 (s, 1H, methine CH), 7.16-7.20 (6H, aromatic CH) ppm. $^{13}C\{^1H\}$ NMR (125 MHz, C_6D_6): δ_C -8.1 ($Al\underline{C}H_3$), 24.1 ($(\underline{C}H_3)_2CH$), 26.7 ($(\underline{C}H_3)_2CH$), 28.4 ($(CH_3)_2\underline{C}H$), 41.0 ($(\underline{C}H_3)_2N$), 76.5 (methine CH), 124.7 (*p*-CH of Dipp), 125.5 (*m*-CH of Dipp), 142.8 (*ipso*-C of Dipp), 144.5 (*o*-C of Dipp), 166.8 (imine quaternary C) ppm. ^{27}Al NMR (104 MHz, C_6D_6): δ_{Al} 157 (br) ppm. EI-MS (m/z, %): 517.4, 40 $[M\text{-}CH_3]^+$; accurate mass: calc. for $C_{32}H_{50}AlN_4$ ($[M–CH_3]^+$) 517.3851, meas. 517.3889. Elemental microanalysis: calc. for $C_{33}H_{53}AlN_4$: C 74.39, H 10.03, N 10.52%, meas. C 74.59, H 10.04, N 10.44%.

3.5 References and notes

[1] For the sake of simplicity, only symmetrical Nacnac ligands (bearing identical N(imine)-bound substituents) will be discussed in this thesis.

[2] Selected reviews: a) L. Bourget-Merle, M. F. Lappert, J. R. Severn, *Chem. Rev.* **2002**, *102*, 3031–3065; b) W. E. Piers, D. J. H. Emslie, *Coord. Chem. Rev.* **2002**, 233–234, 131–155; c) M. Asay, C. Jones, M. Driess, *Chem. Rev.* **2011**, *111*, 354–396; d) S. P. Sarish, S. Nembenna, S. Nagendran, H. W. Roesky, *Acc. Chem. Res.* **2011**, *44*, 157–170; e) Y. C. Tsai, *Coord. Chem. Rev.* **2012**, *256*, 722–758; f) C. Chen, S. M. Bellows, P. L. Holland, *Dalton Trans.* **2015**, *44*, 16654–16670; g) R. L. Webster, *Dalton Trans.* **2017**, *46*, 4483–4498; h) T. Chu, G. I. Nikonov, *Chem. Rev.* **2018**, *118*, 3608–3680.

[3] a) J. Feldman, S. J. McLain, A. Parthasarathy, W. J. Marshall, J. C. Calabrese, S. D. Arthur, *Organometallics* **1997**, *16*, 1514–1516; b) M. Stender, R. J. Wright, B. E. Eichler, J. Prust, M. M. Olmstead, H. W. Roesky, P. P. Power, *J. Chem. Soc., Dalton Trans.* **2001**, 3465–3469; c) D. T. Carey, E. K. Cope-Eatough, E. Vilaplana-Mafé, F. S. Mair, R. G. Pritchard, J. E. Warren, R. J. Woods, *Dalton Trans.* **2003**, 1083–1093; d) M. Arrowsmith, B. Maitland, G. Kociok-Köhn, A. Stasch, C. Jones, M. S. Hill, *Inorg. Chem.* **2014**, *53*, 10543–10552.

[4] a) S. P. Green, C. Jones, A. Stasch, *Science* **2007**, *318*, 1754–1757; b) S. J. Bonyhady, S. P. Green, C. Jones, S. Nembenna, A. Stasch, *Angew. Chem. Int. Ed.* **2009**, *48*, 2973–2977; c) S. J. Bonyhady, C. Jones, S. Nembenna, A. Stasch, A. J. Edwards, G. J. McIntyre, *Chem. Eur. J.* **2010**, *16*, 938–955; d) C. Jones, S. J. Bonyhady, N. Holzmann, G. Frenking, A. Stasch, *Inorg. Chem.* **2011**, *50*, 12315–12325; e) C. Bakewell, A. J. P. White, M. R. Crimmin, *J. Am. Chem. Soc.* **2016**, *138*, 12763–12766; f) C. Jones, *Nat. Rev. Chem.* **2017**, *1*, 59.

[5] Al^{I}: a) C. Cui, H. W. Roesky, H. G. Schmidt, M. Noltemeyer, H. Hao, F. Cimpoesu, *Angew. Chem. Int. Ed.* **2000**, *39*, 4274–4276; b) C. Cui, S. Kopke, R. Herbst-irmer, H. W. Roesky, M. Noltemeyer, H.-G. Schmidt, B. Wrackmeyer, *J. Am. Chem. Soc.* **2001**, *123*, 9091–9098; c) Y. Peng, H. Fan, V. Jancik, H. W. Roesky, R. Herbst-Irmer, *Angew. Chem. Int. Ed.* **2004**, *43*, 6190–6192; d) Y. Peng, H. Fan, H. Zhu, H. W. Roesky, J. Magull, C. E. Hughes, *Angew. Chem. Int. Ed.* **2004**, *43*, 3443–3445; e) H. Zhu, J. Chai, V. Jancik, H. W. Roesky, W. A. Merrill, P. P. Power, *J. Am. Chem. Soc.* **2005**, *127*, 10170–10171; f) T. Chu, I. Korobkov, G. I. Nikonov, *J. Am. Chem. Soc.* **2014**, *136*, 9195–9202; g) T. Chu, Y. Boyko, I. Korobkov, G. I. Nikonov, *Organometallics* **2015**, *34*, 5363–5365; h) M. R. Crimmin, M. J. Butler, A. J. P. White, *Chem. Commun.* **2015**, *51*, 15994–15996.

[6] Ga^{I}: a) N. J. Hardman, B. E. Eichler, P. P. Power, *Chem. Commun.* **2000**, *53*, 1991–1992; b) A. Seifert, D. Scheid, G. Linti, T. Zessin, *Chem. Eur. J.* **2009**, *15*, 12114–12120; c) G. Prabusankar, A. Doddi, C. Gemel, M. Winter, R. A. Fischer, *Inorg. Chem.*

2010, *49*, 7976–7980; d) C. Helling, C. Wölper, S. Schulz, *J. Am. Chem. Soc.* **2018**, *140*, 5053–5056.

[7] In^{I}: a) M. S. Hill, P. B. Hitchcock, *Chem. Commun.* **2004**, *44*, 1818–1819; b) M. S. Hill, P. B. Hitchcock, R. Pongtavornpinyo, *Science* **2006**, *311*, 1904-1907; c) M. S. Hill, P. B. Hitchcock, R. Pongtavornpinyo, *Dalton Trans.* **2007**, *402*, 731–733.

[8] Ge^{I}: a) W. D. Woodul, E. Carter, R. Müller, A. F. Richards, A. Stasch, M. Kaupp, D. M. Murphy, M. Driess, C. Jones, *J. Am. Chem. Soc.* **2011**, *133*, 10074–10077; Sn^{I} dimer: b) S. L. Choong, C. Schenk, A. Stasch, D. Dange, C. Jones, *Chem. Commun.* **2012**, *48*, 2504–2506.

[9] Ge^{II}: a) A. Jana, D. Ghoshal, H. W. Roesky, I. Objartel, G. Schwab, D. Stalke, *J. Am. Chem. Soc.* **2009**, 1288–1293; b) A. Jana, H. W. Roesky, C. Schulzke, *Dalton Trans.* **2010**, *39*, 132–138; Sn^{II}: c) A. Jana, H. W. Roesky, C. Schulzke, A. Döring, *Angew. Chem. Int. Ed.* **2009**, *48*, 1106–1109.

[10] a) D. T. Carey, E. K. Cope-Eatough, E. Vilaplana-Mafé, F. S. Mair, R. G. Pritchard, J. E. Warren, R. J. Woods, *Dalton Trans.* **2003**, 1083–1093; b) W. Clegg, E. K. Cope, A. J. Edwards, F. S. Mair, *Inorg. Chem.* **1998**, *37*, 2317–2319; c) A. G. Avent, M. R. Crimmin, M. S. Hill, P. B. Hitchcock, *J. Organomet. Chem.* **2006**, *691*, 1242–1250; d) H. Hamaki, N. Takeda, T. Yamasaki, T. Sasamori, N. Tokitoh, *J. Organomet. Chem.* **2007**, *692*, 44–54; e) P. B. Hitchcock, A. V Khvostov, M. F. Lappert, A. V Protchenko, *Dalton Trans.* **2009**, 2383–2391.

[11] M. H. Chisholm, K. Choojun, J. C. Gallucci, P. M. Wambua, *Chem. Sci.* **2012**, *3*, 3445–3457.

[12] a) B. Qian, D. L. Ward, M. R. Smith, *Organometallics* **1998**, *17*, 3070–3076; b) C. E. Radzewich, I. A. Guzei, R. F. Jordan, *J. Am. Chem. Soc.* **1999**, *121*, 8673–8674; c) D. Vidovic, J. N. Jones, J. A. Moore, A. H. Cowley, *Z. Anorg. Allg. Chem.* **2005**, *631*, 2888–2892; d) Z. Yang, H. Zhu, X. Ma, J. Chai, H. W. Roesky, C. He, J. Magull, H.-G. Schmidt, M. Noltemeyer, *Inorg. Chem.* **2006**, *45*, 1823–1827; e) B. Jana, C. Honaker, W. Uhl, *J. Organomet. Chem.* **2018**, *856*, 78–86.

[13] R. Olejník, Z. Padělková, R. Mundil, J. Merna, A. Růžička, *Appl. Organomet. Chem.* **2014**, *28*, 405–412.

[14] a) D. Vidovic, J. A. Moore, J. N. Jones, A. H. Cowley, *J. Am. Chem. Soc.* **2005**, *127*, 4566–4567; b) D. Vidovic, M. Findlater, A. H. Cowley, *J. Am. Chem. Soc.* **2007**, *129*, 8436–8437; c) D. Vidovic, M. Findlater, G. Reeske, A. H. Cowley, *J. Organomet. Chem.* **2007**, *692*, 5683–5686.

[15] C. Jones, *Coord. Chem. Rev.* **2010**, *254*, 1273–1289.

[16] P. T. K. Lee, Master's Thesis, St.Mary's University, Halifax, Canada, **2009**.

[17] a) Z. Janousek, H. G. Viehe, *Angew. Chem. Int. Ed.* **1971**, *10*, 574–575; b) S. Brenner, H. G. Viehe, *Tetrahedron Lett.* **1976**, *17*, 1617–1620.

[18] J. Emsley in *The Elements* 3rd ed., Clarendon Press, Oxford, **1998**.

[19] a) N. Kuhn, J. Fahl, S. Fuchs, M. Steimann, G. Henkel, A. H. Maulitz, *Z. Anorg. Allg. Chem.* **1999**, *625*, 2108–2114; b) H. M. El-Kaderi, M. J. Heeg, C. H. Winter, *Organometallics* **2004**, *23*, 4995–5002; c) H. M. El-Kaderi, A. Xia, M. J. Heeg, C. H. Winter, *Organometallics* **2004**, *23*, 3488–3495; d) H. M. El-Kaderi, M. J. Heeg, C. H. Winter, *Eur. J. Inorg. Chem.* **2005**, 2081–2088; e) Y. Xiong, S. Yao, M. Driess, *Chem. Asian. J.* **2009**, *4*, 1323–1328; f) D. Li, Y. Peng, C. Geng, K. Liu, D. Kong, *Dalton Trans.* **2013**, *42*, 11295–11303.

[20] N. Kuhn, H. Lanfermann, P. Schmitz, *Liebigs Ann. Chem.* **1987**, 727–728.

[21] E. Pretsch, P. Bühlmann, M. Badertscher in *Structure Determination of Organic Compounds* (eds. M. Badertscher, P. Bühlmann, E. Pretsch), Springer-Verlag, Berlin, **2009**, Chp. 5.

[22] Examples of activated *para*-group for *ipso*-cyclisation in organic chemistry: a) Q. F. Yu, Y. H. Zhang, Q. Yin, B. X. Tang, R. Y. Tang, P. Zhong, J. H. Li, *J. Org. Chem.* **2008**, *73*, 3658–3661; b) X. W. Liang, C. Zheng, S. L. You, *Chem. Eur. J.* **2016**, *22*, 11918–11933.

[23] D. C. H. Do, A. Keyser, A. V Protchenko, B. Maitland, I. Pernik, H. Niu, E. L. Kolychev, A. Rit, D. Vidovic, A. Stasch, C. Jones, *Chem. Eur. J.* **2017**, *23*, 5830–5841.

[24] B. Cordero, V. Gómez, A. E. Platero-Prats, M. Revés, J. Echeverría, E. Cremades, F. Barragán, S. Alvarez, *Dalton Trans.* **2008**, 2832–2838.

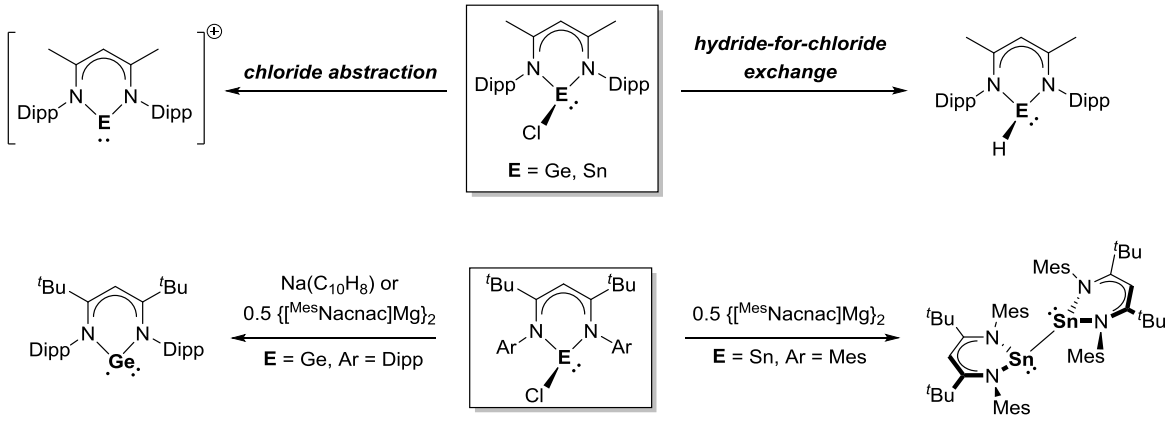
[25] Y. Ding, H. W. Roesky, M. Noltemeyer, H. G. Schmidt, P. P. Power, *Organometallics* **2001**, *20*, 1190–1194.

CHAPTER 4

COMPLEXATION STUDIES OF HEAVIER GROUP 14 ELEMENTS WITH *N*-NACNAC LIGANDS

4.1 Introduction

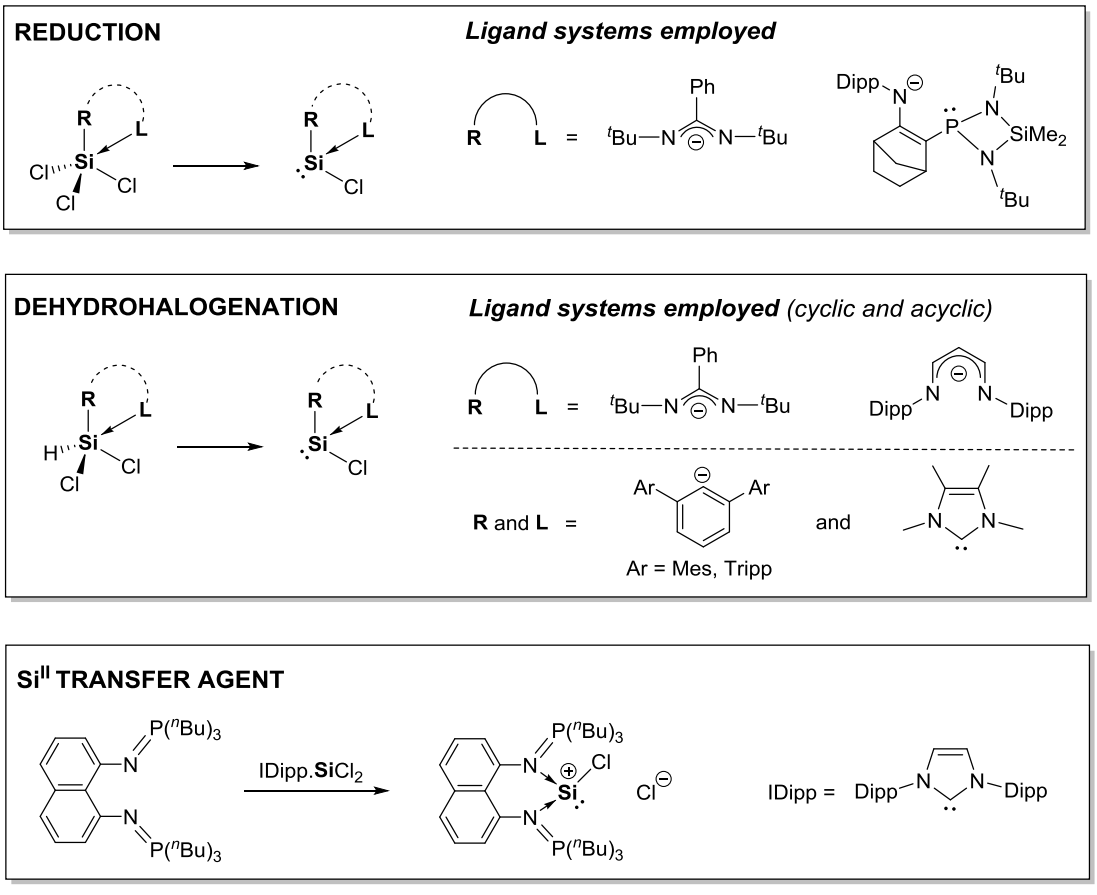
Donor-stabilised monochlorotetrelenes ($R(L)_nE^{II}Cl$, E = Ge, Sn) are potentially valuable reagents in Main Group chemistry, due to the lability of the chloride substituent in a range of chemical transformations.[1,2] Their attractiveness also owes much to their facile preparation; such complexes can potentially be synthesised by transmetallation between a Group 1 complex of the ligand and commercially available MCl_2 sources, such as $SnCl_2$ or the dioxane adduct of $GeCl_2$.[1c,2,3] Both three- ($R(L)E^{II}Cl$) and four-coordinate ($R(L)_2E^{II}Cl$) chlorometallylenes have been extensively studied. Typically, such complexes feature bulky and/or chelating ancillary ligands, which help prevent dimerisation *via* the formation of either chloride-bridges or M=M bonds.[2] With respect to (β-diketiminate)-stabilised chlorogermylenes and stannylenes, a range of interesting chemical transformations involving these compounds as precursors has been reported. These include (i) hydride-for-chloride exchange, forming base-stabilised hydride complexes, which undergo hydrometallation with unsaturated organic substrates,[1d,4] (ii) reduction to monovalent radicals (which may or may not dimerise depending on the metal),[1h,1j] and (iii) chloride abstraction, to yield two-coordinate cationic metallylenes (Scheme 4.1).[1i,5]



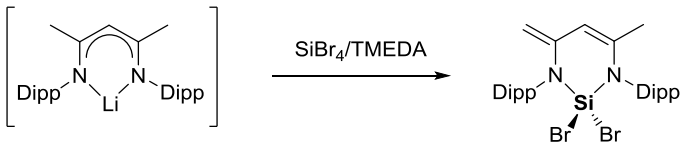
Scheme 4.1 Examples of the reactivity of Nacnac-stabilised chlorogermylenes/stannylenes

Hypothetically, the synthetic methodologies employed for the preparation of monochlorogermylenes/stannylenes can be extended to the corresponding silicon analogues. However, the lack of commercially available Si^{II} precursors reduces the convenience of this method and alternative strategies have been developed.[6] These include (i) reduction of a trichlorosilyl precursor with a Group 1 or Group 2 metal,[6a,6b] (ii) dehydrohalogenation of a $-SiHCl_2$ fragment with a strong base,[6c,6d,6f] and (iii) the reaction of a Group 1 metal complex of the chosen ligand with IDipp·$SiCl_2$ – a versatile Si^{II} source developed by Ghadwal *et al.* in 2009 (Scheme 4.2).[6e] Utilising the reduction approach, Roesky and co-workers isolated and characterised the first example of a chlorosilylene, stabilised by an amidinate ligand ({PhC(N^{t}Bu)$_2$}SiCl).[6a] Moreover, this compound was later found to be accessible from {PhC(N^{t}Bu)$_2$}$SiHCl_2$ *via* dehydrohalogenation pathway (ii) (using Li[N(TMS)$_2$] as the base) with a yield (90 %) significantly increased from that obtained using the reduction methodology.[6c] Very recently, the novel β-diketiminate-ligated chlorosilylene – (^{H,Dipp}Nacnac)SiCl – has been prepared *via* dehydrochlorination of the corresponding Si^{IV} precursor, $LSiHCl_2$, using the *N*-heterocyclic carbene I^{t}Bu.[6f] Attempts to prepare the β-methylated

complex (^{Dipp}Nacnac)$SiBr_3$, from the reaction of the corresponding lithiated ligand with $SiBr_4$, as a potential precursor for the monobromosilylene, were unsuccessful, leading to a mixture of unidentifiable products.[7] When carried out in the presence of TMEDA, however, the same reaction led to the formation of the dibromosilyl species **II**, which can be viewed as the formal dehydrobromination product of the elusive (^{Dipp}Nacnac)$SiBr_3$ (Scheme 4.3). Based on the observed reactivity, the role(s) of TMEDA were proposed to involve (i) complexation of $SiBr_4$, and (ii) deprotonation of a methyl group at the ligand backbone. This propensity for deprotonation underpins the challenge inherent in synthesising monohalosilylenes featuring a β-methylated Nacnac backbone ligand.



Scheme 4.2 Synthetic strategies for the preparation of donor-stabilised monochlorosilylenes



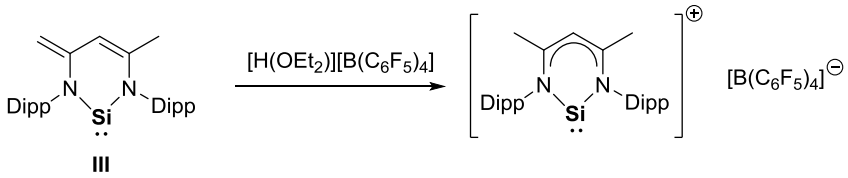
II

Scheme 4.3 Isolation of the dibromosilyl **II**, as part of the attempt to synthesise the elusive Nacnac-stabilised monobromo-silylene (^{Dipp}Nacnac)SiBr

With this existing work in mind and our novel amino-functionalised Nacnac ligands at hand, we therefore sought to explore their coordination chemistry with the Group 14 elements (Si, Ge and Sn). Notably, during the course of this study, the analogous chemistry with carbon as a Group 14 element has been successfully developed by the group of Martin: the isolation of the cationic carbene [(**1-Dipp**)C][PF_6] serves as a rare example of a Nacnac donor stabilising a low-valent electrophilic carbon centre.[8] The synthesis of the monochlorometallylenes (*N*-nacnac)ECl was to be attempted *via* transmetallation reactions between the lithiated *N*-nacnac complexes prepared in chapter 3, and group 14 dihalides (IDipp·$SiCl_2$, $GeCl_2$·dioxane, $SnCl_2$). Utilising three *N*-nacnac ligands with varying degrees of steric encumbrance ((**1-Ar**), Ar = Ph, *o*-Xyl, Dipp), the donor-supported chlorogermylene/stannylene ((**1-Ar**)ECl, E = Ge, Sn) were targeted to provide insight into the effects of the steric bulk of the *N*-substituents on the structures of the resulting complexes. The availability of a wide range of Nacnac-stabilised chlorometallylenes in the existing literature[1g,3b,3d] would also allow for comparison with their electronically modified *N*-nacnac analogues. In addition, the coordination chemistry of these novel ligand systems at silicon was also to be targeted, with a view to isolating and characterising a rare example of a β-diketiminate-stabilised

chlorosilylene.[6f] In a similar fashion to (^{H,Dipp}Nacnac), the use of the *N*-nacnac ligand family is expected to prevent unwanted deprotonation of the backbone during silylene synthesis, a complication which has been observed in the case of the "traditional" beta-methylated (^{Dipp}Nacnac) framework.[7]

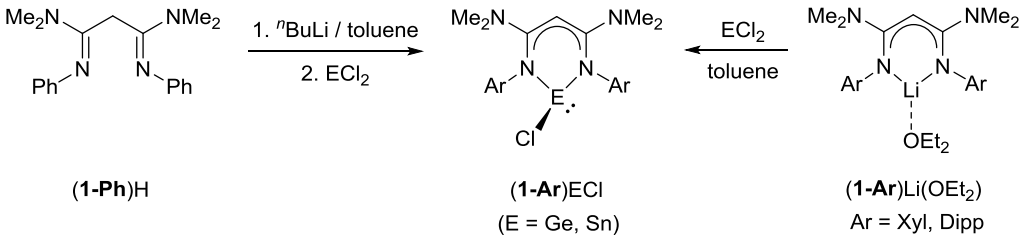
Following successful synthesis of these chloro-substituted systems, the synthetic viability of cationic, two-coordinate Group 14 tetrelenes, ([(^{Dipp}*N*-nacnac)E]$^+$, E = Si, Ge, Sn), was then to be investigated. These compounds are isoelectronic with the neutral monovalent Group 13 complexes ((^{Dipp}Nacnac)M^I, M = Al, Ga, In) and represent heavier congeners of Martin's recently reported carbene.[8,9] By introducing a positive charge, an increase in the electrophilicity of the metal centre would be expected; as such, these cations offer potential as Lewis acids. Cationic complexes of germanium and tin, ligated by the (^{Dipp}Nacnac) ligand, have previously been prepared *via* chloride abstraction from the corresponding chlorotetrelene precursors (Scheme 4.2).[1c,1i] However, in light of the lack of available silicon analogues of the form (Nacnac)SiCl, the cationic species [(^{Dipp}Nacnac)Si][B(C_6F_5)$_4$] was obtained instead by the protonation of neutral diamidosilylene compound **III** using Jutzi's acid (Scheme 4.6).[10] Thus, the isolation of a series of compounds of the form (**1-Dipp**)ECl (E = Si, Ge, Sn) might allow for a systematic approach for the synthesis of the corresponding cationic complexes *via* chloride abstraction.



Scheme 4.6 Synthesis of the Nacnac-stabilised cationic silylene *via* protonation of **III**

4.2 Results and Discussion

4.2.1 Synthesis and characterisation of N-nacnac-ligated chlorotetrelenes (^{Ar}N-nacnac)ECl (E = Ge, Sn)



Scheme 4.4 Preparation of *N*-nacnac-stabilised monochlorogermylenes/stannylenes *via* transmetallation reactions.

The *N*-nacnac-stabilised chlorogermylenes and stannylenes ((**1-Ar**)ECl**,** E = Ge or Sn, Ar = Ph/*o*-Xyl/Dipp) can be prepared in a facile manner, *via* transmetallation reactions between the lithiated ligand and the corresponding metal dichloride (Scheme 4.4). In the case of (**1-Ph**) the lithiated ligand is generated and used *in situ*, while for (**1-Xyl**) and (**1-Dipp**) the isolated ether adduct of the corresponding lithium derivatives are employed. All six Ge^{II}/Sn^{II} compounds have been unambiguously characterised by conventional spectroscopic techniques and X-ray diffraction. A collective solid state feature common to all the chlorotetrelenes is the six-membered (NC_3N)E metallacycle, in which the metal centre adopts a distorted trigonal-pyramidal geometry. Within the metal coordination sphere, the chloride substituent resides in the *pseudo*-axial position, leaving the lone pair of electrons to

occupy the remaining (*pseudo*-equatorial) coordination site. Other molecular features of the core HC[(C(NMe$_2$)N]$_2$ skeleton of the chlorotetrelenes largely resemble those of the lithiated and aluminated ligand precursors reported in chapter 3.

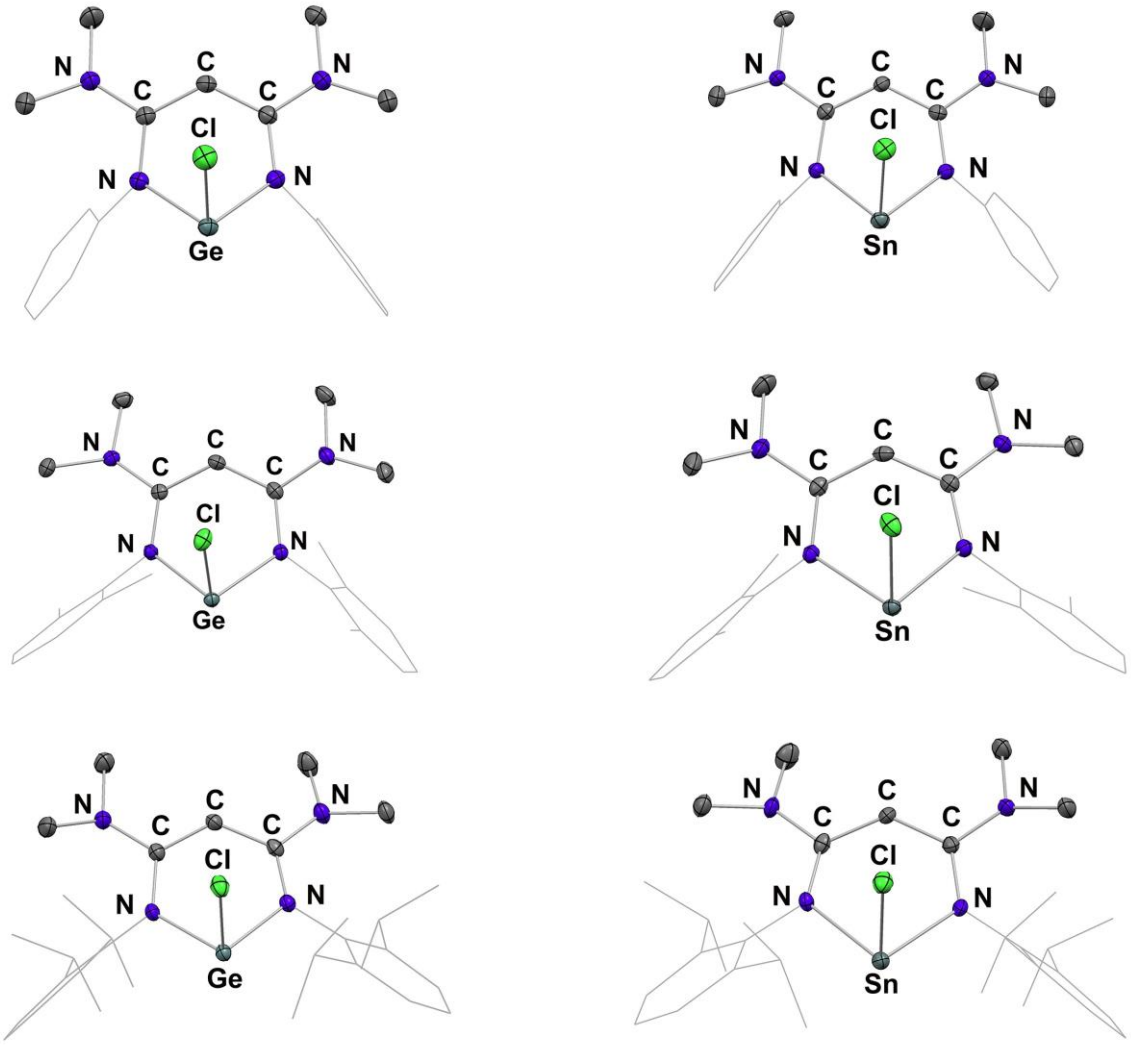


Figure 4.1 Solid-state structures of (**1-Ar**)ECl (Ar = Ph, *o*-Xyl, Dipp (*from top to bottom*); E = Ge (*left column*), Sn (*right column*)), as determined by X-ray crystallography. Thermal ellipsoids are shown at 35 % probability level. *N*-bound aromatic substituents are shown in the wireframe format, and all hydrogens have been omitted for clarity.

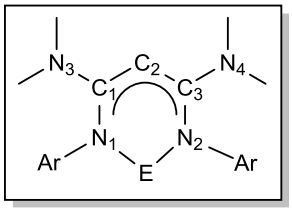


Figure 4.2 General labelling scheme employed for the structural comparison of the novel monochlorotetrelenes

	(**1-Ph**)GeCl	(**1-Xyl**)GeCl	(**1-Dipp**)GeCl
d(C1—N1) / d(C3—N2)	1.369(2) / 1.367(2)	1.3523(16) / 1.3584(17)	1.358(2) / 1.347(2)
d(C1—N3) / d(C3—N4)	1.356(2) / 1.357(2)	1.3644(17) / 1.3620(17)	1.368(2) / 1.367(2)
d(E—N1) / d(E—N2)	1.9646(15) / 1.9683(15)	1.9588(11) / 1.9685(11)	1.9680(13) / 1.9733(14)
d(E—Cl)	2.3023(5)	2.3221(4)	2.3490(4)
d(N1—N2)	2.781	2.817	2.890
d(N_{imine}—C_{ipso})	1.422(2) / 1.423(2)	1.4413(16) / 1.4372(17)	1.448(2) / 1.457(2)
d(E—least-squares [NC_3N] chelate plane)	0.82	0.74	0.55
∠(N1—E—N2)	89.99(6)	91.65(5)	94.31(6)
Sum of all endocyclic (NC_3N)E angles	702.6	706.0	711.7
∠(NMe_2 planes and least-squares [NC_3N] chelate plane)	17.2 / 15.5	23.9 / 20.2	29.2 / 25.1

Table 4.1 Selected bond lengths (Å) and angles (°) of the *N*-nacnac-stabilised monochlorogermylenes (**1-Ar**)GeCl, as determined by X-ray crystallography

	(1-Ph) SnCl	**(1-Xyl)**SnCl	**(1-Dipp)**SnCl
d(C1—N1) / *d*(C3—N2)	1.368(5) / 1.362(5)	1.353(3) / 1.351(3)	1.342(6) / 1.355(6)
d(C1—N3) / *d*(C3—N4)	1.364(5) / 1.364(5)	1.368(3) / 1.376(3)	1.384(6) / 1.371(6)
d(E—N1) / *d*(E—N2)	2.156(3) / 2.157(3)	2.156(2) / 2.148(2)	2.167(4) / 2.156(4)
d(E—Cl)	2.4672(12)	2.4795(6)	2.4920(14)
d(N1—N2)	2.896	2.945	3.052
d(N_{imine}—C_{ipso})	1.419(5) / 1.419(5)	1.438(3) / 1.437(3)	1.453(6) / 1.449(6)
d(E—least-squares [NC_3N] chelate plane)	0.99	0.86	0.56
∠(N1—E—N2)	84.35(13)	86.35(8)	89.80(16)
Sum of all endocyclic (NC_3N)E angles	699.6	704.3	713.0
∠(NMe_2 planes and least-squares [NC_3N] chelate plane)	16.3 / 19.3	22.2 / 24.9	25.3 / 30.8

Table 4.2 Selected bond lengths (Å) and angles (°) of the *N*-nacnac-stabilised monochlorostannylenes (**1-Ar**)SnCl, as determined by X-ray crystallography

Determination of the solid state structures of the *N*-nacnac-ligated tetrelene complexes allows for a systematic comparison of their molecular metrics. Thus, it is observed that the metal centre drops closer to the least-squares NC_3N chelate plane (that is, the E—NC_3N mean-plane distances become shorter) as the *N*-bound aryl substituents become more bulky (0.82, 0.74 and 0.55 Å for Ar = Ph, *o*-Xyl, Dipp, respectively, for the Ge^{II} systems). This is in line with the observation of longer E—Cl

bonds, which presumably helps to relieve unfavourable steric interactions between the chloride ligand and the flanking aryl groups. Moreover, an increase in the distance between the chelating nitrogen atoms (N1—N2) is observed as the *N*-bound substituents become bulkier, which leads to a widening of the N—E—N bite angles (89.99(6), 91.65(5) and 94.31(6)° for Ar = Ph, *o*-Xyl, Dipp, respectively, for the Ge^{II} systems).

At the ligand backbone, the structural impact of varying the N(imine)-substituents complements the trends observed at the metal site. Thus, larger *N*-bound aromatic groups are associated with shorter distances from the ECl unit to the least-squares five-membered ligand plane. To accommodate this unit within the coordination sphere, the flanking aromatic groups are forced to rotate towards the backbone NMe_2 substituents, leading to an increasing steric repulsion between these two bulky functions. This is corroborated by (i) the increasing N(imine)—C(*ipso*) distances as the aryl group becomes bulkier, (ii) a shortening of the imine C—N bonds, and (iii) the reduced π-conjugation from the pendant amino groups into the ligand scaffold. In particular, the last effect is exemplified by an increase in torsion angles between the planes containing the amino groups and the mean ligand plane (*cf.* average values of 16.3° and 27.1° for (**1-Ph**)GeCl and (**1-Dipp**)GeCl, respectively). Thus, it has been demonstrated that bulkier *N*-aryl substituents (Ph < *o*-Xyl < Dipp) exert increasing steric repulsion on the backbone amino groups, forcing them to rotate out of plane (with respect to the mean ligand

plane). This in turn leads to less steric hindrance (*i.e.* less "puckered" environment) around the metal centre (Figure 4.3).

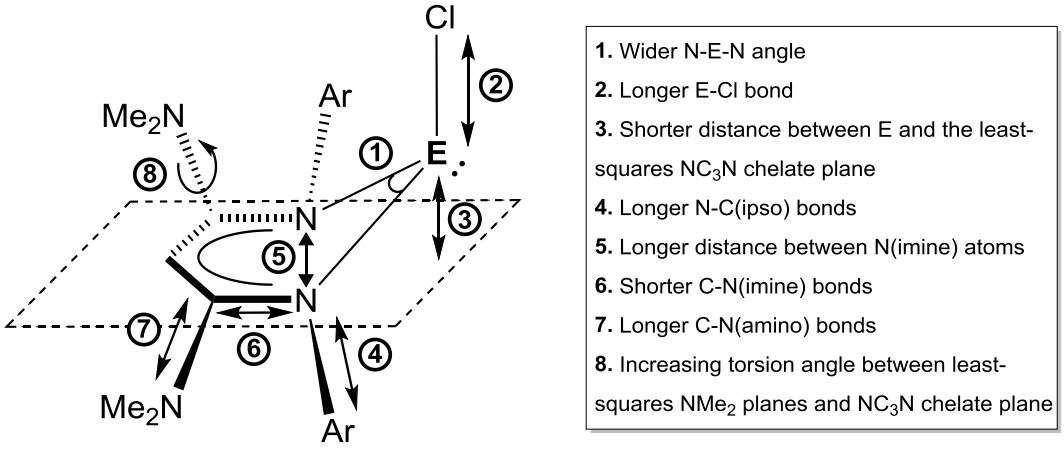


Figure 4.3 An overview of the structural realignments caused by an increase in steric bulk of the Ar substituents.

The fact that a number of chlorogermylenes and stannylenes stabilised by Dipp-substituted Nacnac ligands have been reported in the literature[1g,3b,3d] allows for comparison with the novel *N*-nacnac-supported tetrelene systems (**1-Dipp**)ECl. In terms of molecular metrics, complexes with *N*-nacnac ligands are generally associated with a more "shielded" metal atom within the vicinity of the *N*,*N*'-chelate, as shown by the shorter distances observed between the metal centre and the mean NC_3N chelate plane. Consistent with the trend observed in the *N*-nacnac series, this effect is complemented by longer E─Cl and N(imine)─ N(imine) distances, and wider bite angles (Tables 4.2 and 4.3).

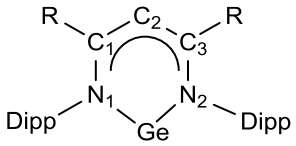
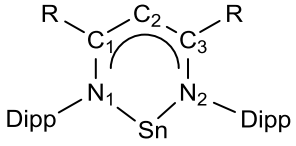
	([Dipp]Nacnac)GeCl	([tBu,Dipp]Nacnac)GeCl	(**1-Dipp**)GeCl
d(Ge—N1) / *d*(Ge—N2)	1.988(2) / 1.997(3)	1.9394(19) / 2.036(2)	**1.9680(13) / 1.9733(14)**
d(Ge—Cl)	2.295(12)	2.2942(8)	**2.3490(4)**
d(N1—N2)	2.840	2.860	**2.890**
d(Ge—least-squares [NC_3N] chelate plane)	0.56	0.60	**0.55**
∠(N1—Ge—N2)	90.89(10)	91.99(8)	**94.31(6)**
	([Dipp]Nacnac)SnCl	([tBu,Dipp]Nacnac)SnCl	(**1-Dipp**)SnCl
d(Sn—N1) / *d*(Sn—N2)	2.185(2) / 2.180(2)	2.223(3) / 2.136(3)	**2.167(4) / 2.156(4)**
d(Sn—Cl)	2.473(9)	2.4466(13)	**2.4920(14)**
d(N1—N2)	2.955	3.017	**3.052**
d(Sn—least-squares [NC_3N] chelate plane)	0.66	0.69	**0.56**
∠(N1—Sn—N2)	85.21(8)	87.60(12)	**89.80(16)**

Table 4.3 A comparison of the structural features of Dipp-substituted Nacnac-stabilised monochlorogermylenes/stannylenes, which differ only in the β-carbon substituents (bond lengths and angles are expressed in angstroms and degrees, respectively)

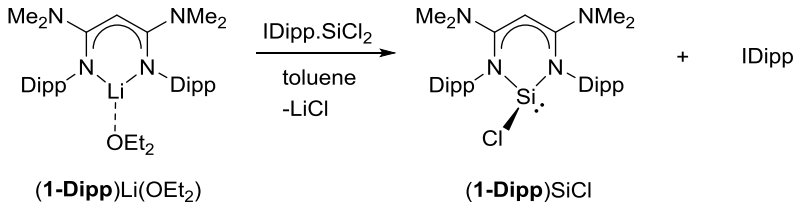
While structural features are similar in both Nacnac and *N*-nacnac series, more pronounced differences are observed in the spectroscopic parameters of the chlorometallylenes (Table 4.4). Thus, the ^{1}H NMR resonances associated with the backbone γ-CH protons of the (**1-Dipp**)ECl complexes are found at significantly more upfield chemical shifts, compared to those of their Nacnac analogues (Table 4.4).[1g,3b,3d] This effect is in line with the well-studied influence of π-donors

on the CH resonances of alkenes, and is thus indicative of a more electron-rich *N*-nacnac ligand backbone.[11] By contrast, the ^{119}Sn resonance associated with (**1-Dipp**)SnCl (δ_{Sn} = -192 ppm) is more downfield than those of the other Dipp-substituted (Nacnac)SnCl (δ_{Sn} = -224 and -252 ppm, Table 4.4).[3b,3d] This might be indicative of a more positively-charged, and therefore deshielded, tin atom in (**1-Dipp**)SnCl. Such a phenomenon suggests that at the tin centre (which is both coordinatively saturated and projected out of the ligand plane), the σ-withdrawing effect of the backbone amino groups *via* the electronegative nitrogen atoms outweighs the π-donor ability of these substituents, leading to a net reduction in electron density at the tin centre.

	(^{Dipp}Nacnac)GeCl	($^{tBu, Dipp}$Nacnac)GeCl	(**1-Dipp**)GeCl
δ_H (γ-CH)	5.14	6.41	**4.26**
	(^{Dipp}Nacnac)SnCl	($^{tBu, Dipp}$Nacnac)SnCl	(**1-Dipp**)SnCl
δ_H (γ-CH)	5.05	6.14	**4.03**
δ_{Sn}	-224	-252	**-192**

Table 4.4 Selected ^{1}H and ^{119}Sn resonances (ppm) of the Dipp-substituted β-diketiminate-stabilised monochlorogermylenes/stannylenes

4.2.2 Synthesis and characterisation of the chlorosilylene (^{Dipp}N-nacnac)SiCl



(**1-Dipp**)Li(OEt$_2$) (**1-Dipp**)SiCl

Scheme 4.5 Synthesis of a *N*-nacnac-stabilised chlorosilylene

Previously, IDipp·$SiCl_2$ has been shown to function as an effective Si^{II} source for the syntheses of an acyclic silylene, $[(Me_3Si)\{(DippNCH)_2B\}N]_2Si$, from the corresponding lithiated borylamide ligand, and a bis(iminophosphorane)-stabilised chlorosilyliumylidene chloride complex from the neutral bis(iminophosphorane) ligand.[6e,12] Inspired by this result, the transmetallation reaction between the lithiated complex (**1-Dipp**)Li(OEt_2) and IDipp·$SiCl_2$ was attempted, leading to the formation of (**1-Dipp**)SiCl, and an equimolar amount of IDipp carbene as the co-product (Scheme 4.5). Fractional recrystallisation at -26°C allows for the removal of the NHC, and the pure chlorosilylene can be obtained in moderate yield (41 %), and characterised by standard analytical methods. The $^{29}Si\{^1H\}$ NMR spectrum of (**1-Dipp**)SiCl features a singlet at 1.8 ppm, which is shifted downfield compared to the Nacnac analogue (^{H,Dipp}Nacnac)SiCl (δ_{Si} = -10.7 ppm),[6f] and thus is indicative of a higher partial positive charge on the silicon atom in (**1-Dipp**)SiCl. In a similar fashion to the stannylenes discussed above, this implies that the net electronic influence of the *N*-nacnac ligand on the group 14 element centre is dominated by the σ-withdrawing effects of the NMe_2 substituents, rather than π-donation. Nonetheless, the $^{29}Si\{^1H\}$ chemical shift of (**1-Dipp**)SiCl is more upfield than that of the amidinate-stabilised chlorosilylene $\{PhC(N^tBu)_2\}SiCl$ (δ_{Si} = 14.6 ppm),[6a] which presumably highlights the superior donor capability of *N*-nacnac systems compared to three-membered amidinates, within the class of *N,N'*-chelating ligands.

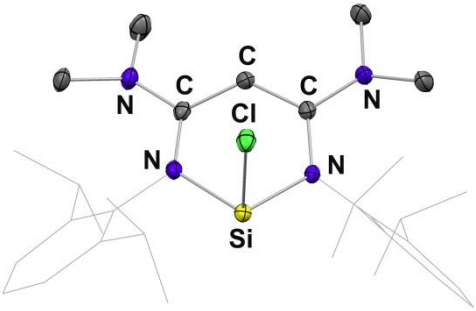


Figure 4.4 Solid-state structure of (**1-Dipp**)SiCl, as determined by X-ray crystallography. Thermal ellipsoids are shown at 35 % probability level. *N*-bound aromatic substituents are represented in the wireframe format, and all hydrogens have been omitted for clarity.

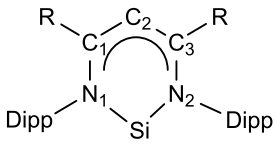
	(**1-Dipp**)SiCl	(^{H,Dipp}Nacnac)SiCl
d(C1—N1) / *d*(C3—N2)	**1.3683(15) / 1.3527(15)**	1.341(6) / 1.312(4)
d(Si—N1) / *d*(Si—N2)	**1.8461(10) / 1.8591(10)**	1.865(2) / 1.860(3)
d(Si—Cl)	**2.2533(8)**	2.195(1)
d(N1—N2)	**2.771**	2.670
∠ (N1—Si—N2)	**96.82(5)**	91.6(1)

Table 4.5 Selected bond lengths (Å) and angles (°) of (**1-Dipp**)SiCl and the Nacnac counterpart (^{H,Dipp}Nacnac)SiCl, as determined by X-ray crystallography.

From a solid state perspective, (**1-Dipp**)SiCl features broadly similar geometric characteristics to the germylene and stannylene analogues, *i.e.* a near-planar six-membered (NC_3N)E heterocycle (sum of all endocyclic angles = 710.4°) with a three-coordinate Si^{II} centre and a chloride substituent lying in the *pseudo*-axial position. Moreover, the endocyclic C—C and C—N bond distances, as well as the C—NMe_2 distances, are largely comparable to those of the heavier chlorotetrelenes

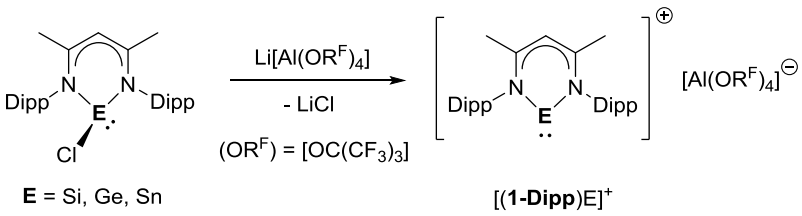
(Tables 4.2, 4.3 and 4.5). On the other hand, the differences in molecular metrics around the metal centre reflect the intrinsic differences in covalent radii of the three elements Si, Ge, and Sn (1.17 Å, 1.22 Å, and 1.40 Å, respectively).[13] Thus, a bigger group 14 atom (Sn > Ge > Si) is associated with longer E—Cl and E—N(imine) bonds, and the N—E—N angle consequently becomes more acute. The latter structural characteristic implies a higher contribution of *s*-character to the lone pair at the group 14 centre with increasing atomic number (Si – 73.0 %, Ge – 82.3 %, Sn – 86.9 %, as derived from NBO calculations), and is consistent with the well-documented decrease in *s*-*p* mixing for heavier Main Group elements.[14]

Comparison of (**1-Dipp**)SiCl and the only other reported Nacnac-supported chlorosilylene, (^{H,Dipp}Nacnac)SiCl,[6f] reflects the differences in the steric bulk of the β-carbon bound substituents (H and NMe_2). Namely, there is an increase in the imine C—N distances in the *N*-nacnac complex (*cf*. 1.3683(15) Å/1.3527(15) Å *vs* 1.341(6) Å/1.312(4) Å for the Nacnac counterpart), presumably to accommodate the two sterically encumbered C(imine)-bound amino and N(imine)-bound Dipp groups. This allows the N(imine) atoms to be further apart from each other, which relieves the spatial clash between the bulky *N*-bound aryl substituents, and thus yields a wider ligand bite angle (96.82(5)° compared to 91.6(1)° for the Nacnac complex). A secondary steric influence of the bulky amino functions is also observed at the flanking aryl groups, which are projected away from the —NMe_2 groups, and simultaneously towards the silicon atom. Consequently, a longer Si—Cl bond is observed (2.2533(8) Å, compared to 2.195(1) Å for (^{H,Dipp}Nacnac)SiCl), which

presumably occurs in order to relieve the mutual steric repulsion between the chloride ligand and the neighbouring Dipp substituents.

4.2.3 Formation of cationic tetrelenes via chloride abstraction

The chloride abstraction chemistry of the bulky Dipp-substituted chlorotetrelenes (**1-Dipp**)ECl (E = Si, Ge, Sn) was subsequently explored, with a view to synthesising the corresponding cationic tetrelene systems, [(**1-Dipp**)E]$^+$. The increasingly-popular weakly-coordinating anion [Al(OR^F)$_4$]$^-$ (R^F = OC(CF$_3$)$_3$), largely developed by Krossing and co-workers, was chosen based on its advantageous crystallising properties, and its facile synthesis as the lithium salt, Li[Al(OR^F)$_4$].[15] Accordingly, treatment of the chlorotetrelenes with Li[Al(OR^F)$_4$] at room temperature leads to the formation of the corresponding cationic tetrelene derivatives [(**1-Dipp**)E][Al(OR^F)$_4$] (E = Si, Ge, Sn) in moderate isolated yields (Scheme 4.6).



Scheme 4.6 Synthesis of the *N*-nacnac-stabilised cationic tetrelenes [(**1-Dipp**)E]$^+$

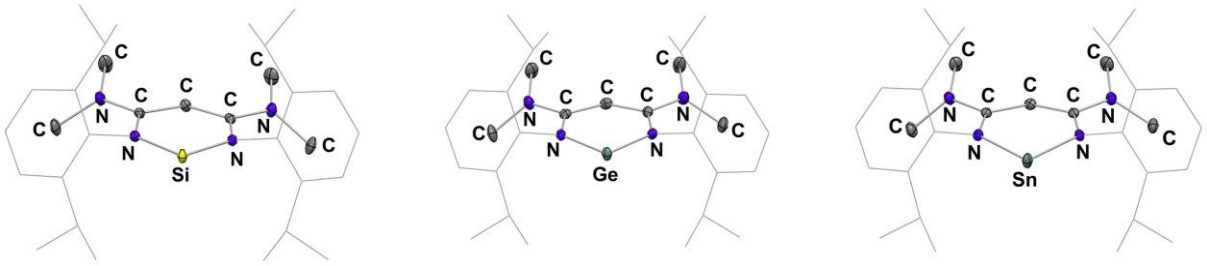


Figure 4.5 Crystallographically determined solid-state structures of [(**1-Dipp**)E][Al(OR^F)$_4$] (E = Si, Ge, Sn). Thermal ellipsoids are shown at 35 % probability. *N*-bound aromatic substituents are represented in the wireframe format. All hydrogens and anions have been omitted for clarity.

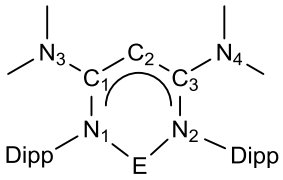
	[(**1-Dipp**)Si]$^+$	[(**1-Dipp**)Ge]$^+$	[(**1-Dipp**)Sn]$^+$
d(C1—N1) / *d*(C3—N2)	1.378(4) / 1.378(3)	1.374(4) / 1.372(4)	1.363(3) / 1.360(3)
d(C1—N3) / *d*(C3—N4)	1.350(4) / 1.349(4)	1.358(4) / 1.361(4)	1.374(3) / 1.367(3)
d(E—N1) / *d*(E—N2)	1.768(2) / 1.765(2)	1.881(2) / 1.882(2)	2.089(2) / 2.095(2)
d(E—least-squares [N1—C1—C2—C3—N2] plane)	0.03	0.01	0.06
∠ (N1—E—N2)	99.07(11)	96.00(12)	90.14(9)
Sum of all endocyclic (NC_3N)E angles	719.8	719.9	719.9

Table 4.6 Selected bond lengths (Å) and angles (°) of [(**1-Dipp**)E][$Al(OR^F)_4$], as determined by X-ray crystallography

Crystallographic studies (Figure 4.5 and Table 4.6) reveal feature common to all three cations, which include a six-membered (NC_3N)E heterocycle incorporating a two-coordinate, *N,N'*-chelated tetrel centre, partnered with a weakly-coordinating $[Al(OR^F)_4]^-$ anion which interacts minimally with the cation. Notably, the heterocycles closely approach planarity (sum of all internal angles ≈ 720°), with the group 14 element centre in each case lying significantly closer to the least-squares NC_3N mean plane than in the chlorotetrelene precursor (Tables 4.2, 4.3 and 4.5). In terms of frontier orbitals, this supports a description of the tetrel-based lone pair located coplanar with the NC_3N chelate, with the corresponding (formally) vacant *p*-type orbital lying approximately perpendicular to the plane. Indeed, DFT studies reveal that the LUMOs of these cationic species are predominantly the vacant *np*

orbital, while the lone pair of the respective tetrel contributes to relatively low-energy occupied orbitals (HOMO-4 and HOMO-5 for the silylene, HOMO-6 and HOMO-7 for the germylene, HOMO-7 for the stannylene). This is consistent with the stabilising effect of the cationic charge (localised at the tetrel atom) on the energies of the tetrel-centred molecular orbitals (Figure 4.6). These frontier orbital energies also suggest that these cationic tetrelenes might show interesting reactivity as potent Lewis acids. Additionally, the introduction of the formal positive charge on the metal centre also leads to contraction of the E—N bonds, and widening of the N—E—N angle (1.768(2)/1.765(2) Å and 99.07(11)° for [(**1-Dipp**)Si][Al(OR^F)$_4$], *cf.* 1.8461(10)/1.8591(10) Å and 96.82(5)° for (**1-Dipp**)SiCl). A secondary influence of this charge is manifested in the elongation of the imine C—N bonds (1.378(4) / 1.378(3) Å, *cf.* 1.3683(15) / 1.3527(15) Å for (**1-Dipp**)SiCl). Alternatively, this may be accredited to the less sterically crowded two-coordinate environment around the metal centre, allowing for more spatial separation between the C(imine)-bound amino substituents and the N(imine)-bound aryl groups.

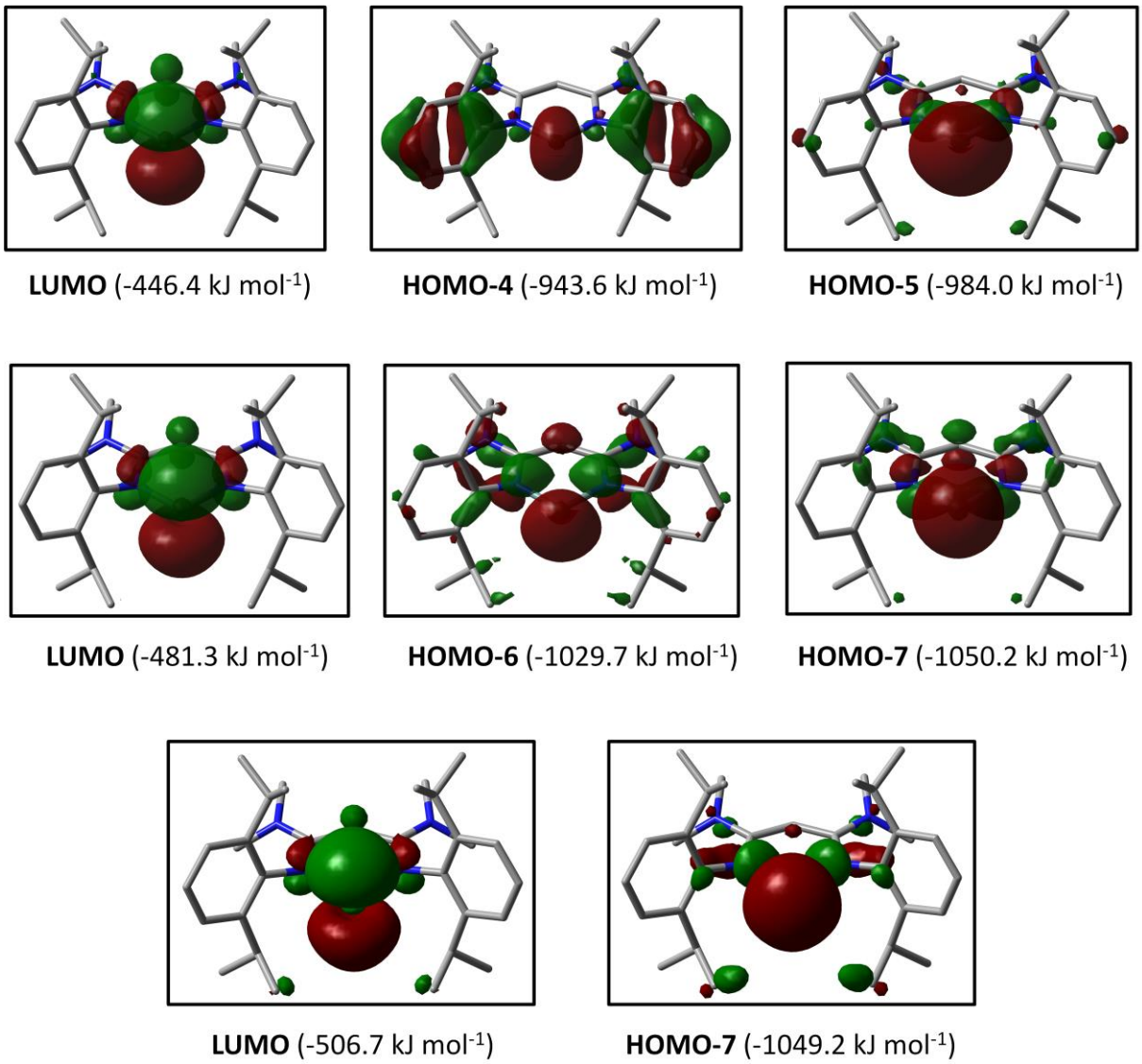


Figure 4.6 Tetrel-centred frontier orbitals of [(**1-Dipp**)Si]$^+$ (*top row*), [(**1-Dipp**)Ge]$^+$ (*middle row*), and [(**1-Dipp**)Sn]$^+$ (*bottom row*), set at the iso-surface value of 0.04.

Spectroscopically, the higher degree of symmetry in these cationic complexes, compared to their (**1-Dipp**)ECl precursors, is manifested by the pattern of ^{1}H NMR resonances assigned to the Dipp ^{i}Pr protons. Thus, the ^{1}H NMR spectrum of each cation features two doublets (each integrating to 12 H), and a single septet signal integrating to 4 H, consistent with the presence of two planes of symmetry. By contrast, the ^{1}H NMR spectra of the chlorotetrelene precursors feature four sets of

(6 H) doublets corresponding to the ^{i}Pr-methyl protons, and two septet signals (each 2H) associated with the ^{i}Pr-methine protons. In the ^{29}Si NMR spectrum, the resonance associated with the silicon centre of [(**1-Dipp**)Si][Al(OR^{F})$_4$] (δ_{Si} = 80.0 ppm) is significantly more downfield than that of its chloro precursor (δ_{Si} = 1.8 ppm), which is consistent with decreased shielding of the silicon centre. By contrast, an unexpected upfield shift in ^{119}Sn NMR is detected for the cationic stannylene (δ_{Sn} = -313 ppm) as compared to the chloro starting material (δ_{Sn} = -192 ppm). This phenomenon, although counter-intuitive, is not without precedent: a similar effect has been observed previously for stannylene systems stabilised by bulky amide ligands, such as [{(Ar*)(Me$_3$Si)N}Sn][Al(OR^{F})$_4$].[1k] In that case, chloride abstraction leads to an upfield shift of the ^{119}Sn NMR signal associated with the tin centre, from 173.7 ppm to 46.3 ppm, which was attributed to weak interactions between the tin atom and a proximal arene ring, as demonstrated by X-ray crystallography. Although a similar effect is not apparent in the *solid-state* structure of [(**1-Dipp**)Sn][Al(OR^{F})$_4$], it is conceivable that in solution, a secondary interaction between the electrophilic tin centre and the NMR solvent (CD_2Cl_2) might account for the upfield shift of the cationic species compared to its chloro precursor.

4.3 Conclusions

The synthesis and characterisation of a range of *N*-nacnac-ligated Group 14 chlorotetrelenes, of the form (**1-Ar**)ECl, has been described. For E = Ge/Sn, variation of the steric profile of the *N*-aryl substituents is shown to subtly affect the geometry of the resulting complexes. Thus, more sterically demanding aromatic substituents

(Dipp > *o*-Xyl > Ph) are associated with a less puckered chelate ring, and less electronic delocalisation from the NMe_2 substituents to the NC_3N backbone. The latter reflects torsional rotation away from the least-squares plane of the β-diketiminate ligand caused by steric repulsion between the C(imine)-bound amino and N(imine)-bound aryl substituents. Nonetheless, some degree of π-conjugation into the ligand backbone is evident from the marked upfield shift of the resonances associated with the γ-CH protons of the *N*-nacnac backbone, as compared to those observed for β-alkylated Nacnac analogues. Interestingly, ^{119}Sn NMR studies of the stannylene series, stabilised by Dipp-substituted Nacnac ligands, reveal the opposite trend, in which the most downfield signal is observed for the *N*-nacnac systems. In light of the coordinatively-saturated nature of the tin atom, it is proposed that the σ-withdrawing ability of the NMe_2 groups outweighs the π-donating capability, yielding a tin centre with a greater partial positive charge.

The analogous chemistry has also been explored with silicon, leading to the isolation of a novel *N*-nacnac-stabilised chlorosilylene (**1-Dipp**)SiCl. Structural comparison of this compound with the only other Nacnac-supported chlorosilylene, (^{H,Dipp}Nacnac)SiCl, reflects the differences in steric bulk of the substituents at the ligand β-position: (**1-Dipp**)SiCl is associated with a longer Si—Cl bond, a wider N—Si—N angle, and a silicon centre deviating away from the mean ligand plane. Spectroscopically (as with its germanium and tin analogues), an upfield shift of the γ-CH proton resonance in (**1-Dipp**)SiCl is observed compared to Nacnac analogues.

Preliminary reactivity studies of these novel chlorotetrelenes have been undertaken, focusing on the synthesis of the corresponding two-coordinate cationic tetrelene analogues [(**1-Dipp**)E]$^+$. These compounds are readily accessible from their monochloro precursors *via* a common method (chloride abstraction), employing the lithium salt of the weakly-coordinating anion $[Al(OR^F)_4]^-$. Characterisation of these compounds by X-ray diffraction reveals in each case a near-planar (NC_3N)E six-membered ring as the most prominent feature of the three cationic species. DFT studies reveal their carbenoid character, with a lone pair corresponding to a low-lying occupied orbital (typically HOMO-4 to HOMO-7) and a vacant *p*-type orbital corresponding to the LUMO. Further investigations of the reactivity of the chlorotetrelenes are discussed in the subsequent chapters.

4.4 Synthesis of novel compounds

4.4.1 General procedure for the preparation of (^{Dipp}N-nacnac)ECl (Ar = Ph, Xyl, Dipp, E = Ge, Sn): All six compounds were prepared *via* a common method. A solution of ((**1-Ar**))H (1 mmol) in toluene (30 mL) was treated with ^{n}BuLi (1.1 equiv.) at -78°C, and the reaction mixture warmed slowly to room temperature and stirred for 2 h (Alternatively, in the case of R = Xyl and Dipp, the isolated lithium salts of the ligands can be used instead). The resulting solution was added to a suspension of $GeCl_2$·dioxane or $SnCl_2$ (1.1 equiv.) in toluene (10 mL) at -78°C, and the resulting mixture warmed to room temperature with stirring. After 12 h, volatiles were removed *in vacuo*, and the resulting residue washed with cold hexane (0°C) to yield (in all cases) the product as near-white, spectroscopically pure solid. X-ray quality

crystals were obtained from a concentrated toluene solution, layered with hexane, and stored at -26°C for several days.

(**1-Ph**)GeCl: Yield 0.21 g, 50 %. ^{1}H NMR (400 MHz, C_6D_6): δ_H 2.40 (s, 12H, (C$\underline{H}_3$)$_2$N), 4.52 (s, 1H, methine CH), 6.90-7.35 (10H, aromatic protons) ppm. ^{13}C{^{1}H} NMR (101 MHz, C_6D_6): δ_C 40.4 ((C$\underline{H}_3$)$_2$N), 82.3 (methine CH), 123.2, 124.3, 129.7, 147.4 (aromatic carbons), 163.6 (imine quaternary C) ppm. EI-MS (*m*/*z*, %): 416.1, weak, [M]$^+$; accurate mass: calc. for $C_{19}H_{23}ClGeN_4$ ([M]$^+$) 416.0823, found 416.0824.

(**1-Xyl**)GeCl: Yield 0.30 g, 63 %. ^{1}H NMR (400 MHz, C_6D_6): δ_H 1.96 (s, 6H, CH_3 of Xyl), 2.19 (s, 12H, (C$\underline{H}_3$)$_2$N), 2.89 (s, 6H, CH_3 of Xyl), 4.20 (s, 1H, methine CH), 6.84 – 7.02 (6H, aromatic protons) ppm. ^{13}C{^{1}H} NMR (101 MHz, C_6D_6): δ_C 19.3 (CH_3 of Xyl), 22.3 (CH_3 of Xyl), 40.0 ((C$\underline{H}_3$)$_2$N), 79.8 (methine CH), 124.8, 129.1, 130.2, 134.0, 135.1, 144.7 (aromatic carbons), 164.2 (imine quaternary C) ppm. EI-MS (*m*/*z*, %): 468, 100, [M]$^+$; accurate mass: calc. 468.1474, meas. 468.1471.

(**1-Dipp**)GeCl: Yield 0.38 g, 66 %. ^{1}H NMR (400 MHz, C_6D_6): δ_H 1.08 (d, $^{3}J_{HH}$ = 6.8 Hz, 6H, (C$\underline{H}_3$)$_2$CH), 1.11 (d, $^{3}J_{HH}$ = 6.4 Hz, 6H, (C$\underline{H}_3$)$_2$CH), 1.29 (d, $^{3}J_{HH}$ = 6.8 Hz, 6H, (C$\underline{H}_3$)$_2$CH), 1.65 (d, $^{3}J_{HH}$ = 6.8 Hz, 6H, (C$\underline{H}_3$)$_2$CH), 2.25 (s, 12H, (C$\underline{H}_3$)$_2$N), 2.99 (virtual sept, $^{3}J_{HH}$ = 6.7 Hz, 2H, (CH_3)$_2$C$\underline{H}$), 4.26 (s, 1H, methine CH), 4.53 (virtual sept, $^{3}J_{HH}$ = 6.7 Hz, 2H, (CH_3)$_2$C$\underline{H}$), 7.04-7.18 (6H, aromatic CH) ppm. ^{13}C{^{1}H} NMR (101 MHz, C_6D_6): δ_C 24.1, 24.2, 26.7, 27.9 ((C$\underline{H}_3$)$_2$CH), 28.3, 28.9 ((CH_3)$_2$C$\underline{H}$), 41.0 (C$\underline{H}_3$)$_2$N), 80.0 (methine CH), 124.4, 125.7 (*m*-CH of Dipp), 126.5 (*p*-CH of Dipp), 140.9, 145.0, 146.5 (aromatic carbons), 164.8 (imine quaternary C) ppm. EI-MS (*m*/*z*, %): 584.3, weak, [M]$^+$; accurate mass: calc. for $C_{19}H_{23}ClGeN_4$

([M]$^+$) 584.2701, found 584.2720. Elemental microanalysis: calc. for $C_{31}H_{47}ClGeN_4$: C 63.78, H 8.11, N 9.60%, meas. C 63.84, H 8.16, N 9.46 %.

(**1-Ph**)SnCl: Yield 0.32 g, 69%. ^{1}H NMR (400 MHz, C_6D_6): δ_H 2.29 (s, 12H, (C$\underline{H}_3$)$_2$N), 4.25 (s, 1H, methine CH), 6.77 (t, $^3J_{HH}$ = 7.0 Hz, 2H, *p*-CH of Ph), 6.84 (d, $^3J_{HH}$ = 8.0 Hz, 4H, *o*-CH of Ph), 7.01 (t, $^3J_{HH}$ = 7.6 Hz, 4H, *m*-CH of Ph) ppm. ^{13}C{^{1}H} NMR (101 MHz, C_6D_6): δ_C 40.6 ((C$\underline{H}_3$)$_2$N), 82.9 (methine CH), 122.3 (*p*-CH of Ph), 123.6 (*o*-CH of Ph), 129.9 (*m*-CH of Ph), 148.9 (*ipso*-C of Ph), 165.1 (imine quaternary C) ppm. ^{119}Sn{^{1}H} NMR (186 MHz, C_6D_6): δ_{Sn} -169 ppm. EI-MS (*m/z*, %): 462.1, 6, [M]$^+$; 426.1, 2 [M-Cl]$^+$; accurate mass: calc. for $C_{19}H_{23}ClN_4Sn$ ([M]$^+$) 462.0633, meas. 462.0678.

(**1-Xyl**)SnCl: Yield: 0.31 g, 59%. ^{1}H NMR (400 MHz, C_6D_6): δ_H 2.02 (s, 6H, CH_3 of Xyl), 2.21 (s, 12H, (C$\underline{H}_3$)$_2$N), 2.77 (s, 6H, CH_3 of Xyl), 4.01 (s, 1H, methine CH), 7.01 – 6.84 (overlapping m, 6H, *p*- and *m*-CH of Xyl) ppm. ^{13}C{^{1}H} NMR (101 MHz, C_6D_6): δ_C 19.4, 21.9 (CH_3 of Xyl), 40.2 ((C$\underline{H}_3$)$_2$N), 79.6 (methine CH), 124.2 (*p*-CH of Xyl), 129.2, 130.1 (*m*-CH of Xyl), 133.5, 133.6 (*o*-C of Xyl), 146.2 (*ipso*-C of Xyl), 165.5 (imine quaternary C) ppm. ^{119}Sn{^{1}H} NMR (186 MHz, THF-d_8): δ_{Sn} -199 ppm. EI-MS (*m/z*, %): 510, 100, [M]$^+$; accurate mass: calc. for $C_{23}H_{31}ClN_4{}^{112}Sn$ 510.1285, meas. 510.1264.

((**1-Dipp**))SnCl: Yield 0.49 g, 78%. ^{1}H NMR (400 MHz, C_6D_6): δ_H 1.11 (d, $^3J_{HH}$ = 6.8 Hz, 6H, (C$\underline{H}_3$)$_2$CH), 1.13 (d, $^3J_{HH}$ = 6.4 Hz, 6H, (C$\underline{H}_3$)$_2$CH), 1.28 (d, $^3J_{HH}$ = 6.4 Hz, 6H, (C$\underline{H}_3$)$_2$CH), 1.59 (d, $^3J_{HH}$ = 6.8 Hz, 6H, (C$\underline{H}_3$)$_2$CH), 2.24 (s, 12H, (C$\underline{H}_3$)$_2$N), 3.02 (virtual sept, $^3J_{HH}$ = 6.7 Hz, 2H, (CH$_3$)$_2$C$\underline{H}$), 4.03 (s, 1H, methine CH),

4.47 (virtual sept, $^{3}J_{HH}$ = 6.7 Hz, 2H, $(CH_3)_2C\underline{H}$), 7.05-7.15 (6H, aromatic CH) ppm. $^{13}C\{^{1}H\}$ NMR (101 MHz, C_6D_6): δ_C 24.0 ($(\underline{C}H_3)_2CH$), 24.2 ($(\underline{C}H_3)_2CH$), 27.0 ($(\underline{C}H_3)_2CH$), 28.3 ($(\underline{C}H_3)_2CH$), 28.3 ($(CH_3)_2\underline{C}H$), 28.4 ($(CH_3)_2\underline{C}H$), 41.3 ($\underline{C}H_3)_2N$), 79.9 (methine CH), 124.5, 125.5, 126.3, 142.1, 144.5, 145.5 (aromatic C), 165.9 (imine quaternary C) ppm. $^{119}Sn\{^{1}H\}$ NMR (186 MHz, C_6D_6): δ_{Sn} -192 ppm. EI-MS: (*m/z*, %): 630.3, 3 $[M]^+$; 587.2, 30 $[M\text{-}NMe_2]^+$; accurate mass: calc. for $C_{31}H_{47}ClN_4{}^{116}Sn$ (M^+) 626.2507, meas. 626.2506.

4.4.2 Synthesis of the chlorosilylene (^{Dipp}N-nacnac)SiCl: A cooled (0˚C) toluene solution of (**1-Dipp**)Li(OEt)$_2$ (3.80 g, 6.82 mmol) was added slowly to a solution of IDipp·$SiCl_2$ (3.33 g, 6.83 mmol), also in toluene, at -78˚C. The reaction mixture was allowed to warm to room temperature and stirred for 15 h. The resulting dark red suspension was filtered, yielding a solution which was partially concentrated (*ca.* 15 mL) and stored at -26˚C overnight, producing an off-white precipitate. This solid was isolated by filtration, washed with hot hexane and dried *in vacuo* to afford a spectroscopically pure product. X-ray quality crystals were grown from a saturated hexane solution at 4˚C. Yield 1.5 g, 41 %. ^{1}H NMR (C_6D_6, 400 MHz): δ_H 1.05 (d, 6H, $(C\underline{H}_3)_2CH$, $^{3}J_{HH}$ = 6.8 Hz), 1.14 (d, 6H, $(C\underline{H}_3)_2CH$, $^{3}J_{HH}$ = 6.6 Hz), 1.29 (d, 6H, $(C\underline{H}_3)_2CH$, $^{3}J_{HH}$ = 6.8 Hz), 1.75 (d, 6H, $(C\underline{H}_3)_2CH$, $^{3}J_{HH}$ = 6.4 Hz), 2.22 (s, 12H, $(C\underline{H}_3)_2N$), 2.99 (virtual sept, 2H, $(CH_3)_2C\underline{H}$, $^{3}J_{HH}$ = 6.8 Hz), 4.40 (s, 1H, methine H), 4.51 (virtual sept, 2H, $(CH_3)_2C\underline{H}$-, $^{3}J_{HH}$ = 6.5 Hz), 7.03-7.20 (6H, aromatic protons) ppm. $^{13}C\{^{1}H\}$ NMR (C_6D_6, 101 MHz): δ_C 24.1, 24.2, 26.3, 27.4 ($(\underline{C}H_3)_2CH$), 28.4, 29.5 ($(CH_3)_2\underline{C}H$), 40.9 ($(\underline{C}H_3)_2N$), 80.8 (methine C), 124.4, 125.9, 126.9, 141.1, 145.1, 147.1

(aromatic carbons), 164.4 (imine quaternary C) ppm. $^{29}Si\{^{1}H\}$ NMR (C_6D_6, 99 MHz): δ_{Si} 1.8 ppm. Elemental analysis: calc. for $C_{31}H_{47}ClN_4Si$: C 69.04 %, H 8.79 %, N 10.39 %; meas. C 68.85 %, H 8.84 %, N 10.25 %.

4.4.3 General synthetic scheme for the N-nacnac-stabilised cationic tetrelenes [(^{Dipp}N-nacnac)E]$^+$[Al(OR^F)$_4$]$^-$ (E = Si, Ge, Sn): A fluorobenzene solution (10 mL) of (**1-Dipp**)ECl (0.2 mmol) was slowly added to a solution of Li[Al(OR^F)$_4$] (1.1 equiv.), also in fluorobenzene (5 mL), at room temperature. The reaction mixture was stirred for an additional 15 h, filtered and concentrated to *ca.* 2 mL. Layering with hexane and storage for several days produced crystals which were suitable for X-ray crystallography.

[(**1-Dipp**)Si][Al(OR^F)$_4$]: Yield 0.182 g (as light yellow crystals), 62 %. ^{1}H NMR (C_6D_5Br, 500 MHz): δ_H 0.96 (d, 12H, (C$\underline{H}_3$)$_2$CH, $^3J_{HH}$ = 6.9 Hz), 1.03 (d, 12H, (C$\underline{H}_3$)$_2$CH, $^3J_{HH}$ = 6.8 Hz), 2.29 (s, 12H, (C$\underline{H}_3$)$_2$N), 2.63 (sept, 4H, (CH$_3$)$_2$C$\underline{H}$, $^3J_{HH}$ = 6.8 Hz), 4.61 (s, 1H, methine H), 6.99 (d, 4H, *m*-H of Dipp, J = 7.8 Hz), 7.18 (t, 2H, *p*-H of Dipp, J = 7.8 Hz). $^{13}C\{^{1}H\}$ NMR (C_6D_5Br, 101 MHz): δ_C 22.7, 25.3 ((C$\underline{H}_3$)$_2$CH), 29.2 ((CH$_3$)$_2$C$\underline{H}$), 41.4 ((C$\underline{H}_3$)$_2$N), 79.6 ((CF$_3$)$_3$C$\underline{C}$), 83.7 (methine C), 121.9 (q, (C$\underline{F}_3$)$_3$C, $^1J_{C\text{-}F}$ = 293 Hz), 125.6, 133.0, 145.7 (aromatic carbons), 161.7 (imine quaternary C). $^{29}Si\{^{1}H\}$ NMR (C_6D_5Br, 99 MHz): δ_{Si} 80.5 ppm. $^{19}F\{^{1}H\}$ NMR (C_6D_5Br, 470.6 MHz): δ_F -74 ppm. $^{27}Al\{^{1}H\}$ NMR (C_6D_5Br, 130 MHz): δ_{Al} 36 ppm.

[(**1-Dipp**)Ge][Al(OR^F)$_4$]: Yield 0.069 g (as light yellow crystals), 23 %. ^{1}H NMR (400 MHz, CD_2Cl_2): δ_H 1.16 (d, $^3J_{HH}$ = 6.9 Hz, 12H, (C$\underline{H}_3$)$_2$CH), 1.30 (d, $^3J_{HH}$ = 6.8 Hz, 12H, (C$\underline{H}_3$)$_2$CH), 2.73 (s, 12H, (C$\underline{H}_3$)$_2$N), 2.86 (sept, $^3J_{HH}$ = 6.8 Hz, 4H, (CH$_3$)$_2$C$\underline{H}$), 5.01

(s, 1H, methine CH), 7.35 (d, $^{3}J_{HH}$ = 7.7 Hz, 4H, *m*-H of Dipp), 7.47 (t, $^{3}J_{HH}$ = 7.7 Hz, 2H, *p*-H of Dipp) ppm. $^{13}C\{^{1}H\}$ NMR (125 MHz, CD_2Cl_2): δ_C 23.2, 26.4 (($\underline{C}H_3)_2CH$), 29.4 (($CH_3)_2\underline{C}H$), 42.4 (($\underline{C}H_3)_2N$), 85.0 (methine CH), 121.8 (q, $^{1}J_{CF}$ = 291 Hz, C($\underline{C}F_3)_3$), 126.0 (*m*-C of Dipp), 130.5 (*p*-C of Dipp), 134.9 (*o*-C of Dipp), 145.4 (*ipso*-C of Dipp), 163.6 (imine quaternary C) ppm. $^{19}F\{^{1}H\}$ NMR (376 MHz, CD_2Cl_2): δ_F -76 ppm. $^{27}Al\{^{1}H\}$ NMR (104 MHz, CD_2Cl_2): δ_{Al} 35 ppm. Elemental microanalysis: calc. for $C_{47}H_{47}AlF_{36}GeN_4O_4$: C 37.25, H 3.13, N 3.70 %, meas. C 37.15, H 3.01, N 3.64%.

[(**1-Dipp**)Sn][Al(OR^F)$_4$]: Yield 0.151 g (as orange crystals), 48%. ^{1}H NMR (500 MHz, CD_2Cl_2): δ_H 1.14 (d, $^{3}J_{HH}$ = 6.8 Hz, 12H, ($C\underline{H}_3)_2CH$), 1.21 (d, $^{3}J_{HH}$ = 6.8 Hz, 12H, ($C\underline{H}_3)_2CH$), 2.88 (sept, $^{3}J_{HH}$ = 6.8 Hz, 4H, ($CH_3)_2C\underline{H}$), 2.93 (s, 12H, ($C\underline{H}_3)_2N$), 3.83 (s, 1H, methine CH), 7.20-7.25 (m, 6H, aromatic protons) ppm.$^{13}C\{^{1}H\}$ NMR (125 MHz, CD_2Cl_2): δ_C 23.3, 26.5 (($\underline{C}H_3)_2CH$), 29.5 (($CH_3)_2\underline{C}H$), 41.2 (($\underline{C}H_3)_2N$), 49.8 (methine CH), 121.8 (q, $^{1}J_{CF}$ = 292 Hz, C($\underline{C}F_3)_3$), 125.0, 127.5, 139.0, 141.6 (aromatic carbons), 163.8 (imine quaternary C) ppm. $^{19}F\{^{1}H\}$ NMR (376 MHz, CD_2Cl_2): δ_F -76 ppm. $^{27}Al\{^{1}H\}$ NMR (104 MHz, CD_2Cl_2): δ_{Al} 35 ppm. $^{119}Sn\{^{1}H\}$ NMR (186 MHz, CD_2Cl_2): δ_{Sn} -313 ppm. Elemental microanalysis: calc. for $C_{47}H_{47}AlF_{36}N_4O_4Sn$: C 36.15, H 3.03, N 3.59 %, meas. C 36.22, H 2.88, N 3.64%.

4.5 References

[1] Some examples: a) H. V. R. Dias, Z. Wang, *J. Am. Chem. Soc.* **1997**, *119*, 4650–4655; b) M. M. Olmstead, L. Pu, R. S. Simons, P. P. Power, *Chem. Commun.* **1997**, 1595–1596; c) M. Stender, A. D. Phillips, P. P. Power, *Inorg. Chem.* **2001**, *40*, 5314–5315; d) L. W. Pineda, V. Jancik, K. Starke, R. B. Oswald, H. W. Roesky, *Angew. Chem. Int. Ed.* **2006**, *45*, 2602–2605; e) C. Jones, R. P. Rose, A. Stasch, *Dalton Trans.* **2008**, 2871–2878; f) J. Li, C. Schenk, C. Goedecke, G. Frenking, C. Jones, *J. Am. Chem.*

Soc. **2011**, *133*, 18622–18625; g) W. D. Woodul, A. F. Richards, A. Stasch, M. Driess, C. Jones, *Organometallics* **2010**, *29*, 3655–3660; h) W. D. Woodul, E. Carter, R. Müller, A. F. Richards, A. Stasch, M. Kaupp, D. M. Murphy, M. Driess, C. Jones, *J. Am. Chem. Soc.* **2011**, *133*, 10074–10077; i) M. J. Taylor, A. J. Saunders, M. P. Coles, J. R. Fulton, *Organometallics* **2011**, *30*, 1334–1339; j) S. L. Choong, C. Schenk, A. Stasch, D. Dange, C. Jones, *Chem. Commun.* **2012**, *48*, 2504–2506; k) J. Li, C. Schenk, F. Winter, H. Scherer, N. Trapp, A. Higelin, S. Keller, R. Pöttgen , I. Krossing, C. Jones, *Angew. Chem. Int. Ed.* **2012**, *51*, 9557–9561; l) T. J. Hadlington, B. Schwarze, E. I. Izgorodina, C. Jones, *Chem. Commun.* **2015**, *51*, 6854–6857.

[2] Y. Mizuhata, T. Sasamori, N. Tokitoh, *Chem. Rev.* **2009**, *109*, 3479–3511.

[3] Some examples: a) L. Pu, M. M. Olmstead, P. P. Power, B. Schiemenz, *Organometallics* **1998**, *17*, 5602–5606; b) Y. Ding, H. W. Roesky, M. Noltemeyer, H. G. Schmidt, P. P. Power, *Organometallics* **2001**, *20*, 1190–1194; c) S. P. Green, C. Jones, P. C. Junk, K. A. Lippert, A. Stasch, *Chem. Commun.* **2006**, 3978–3980; d) A. P. Dove, V. C. Gibson, E. L. Marshall, H. S. Rzepa, A. J. P. White, D. J. Williams, *J. Am. Chem. Soc.* **2006**, *128*, 9834–9843; e) J. Li, A. Stasch, C. Schenk, C. Jones, *Dalton Trans.* **2011**, *40*, 10448–10456.

[4] a) Y. Ding, H. Hao, H. W. Roesky, M. Noltemeyer, H. G. Schmidt, *Organometallics* **2001**, *20*, 4806–4811; b) A. Jana, D. Ghoshal, H. W. Roesky, I. Objartel, G. Schwab, D. Stalke, *J. Am. Chem. Soc.* **2009**, 1288–1293; c) A. Jana, H. W. Roesky, C. Schulzke, A. Döring, *Angew. Chem. Int. Ed.* **2009**, *48*, 1106–1109; d) A. Jana, H. W. Roesky, C. Schulzke, *Dalton Trans.* **2010**, *39*, 132–138. A comprehensive review can be found at: e) S. K. Mandal, H. W. Roesky, *Acc. Chem. Res.* **2012**, *45*, 298–307.

[5] a) A. Akkari, J. J. Byrne, I. Saur, G. Rima, H. Gornitzka, J. Barrau, *J. Organomet. Chem.* **2001**, *622*, 190–198; b) S. L. Choong, W. D. Woodul, A. Stasch, C. Schenk, C. Jones, *Aust. J. Chem.* **2011**, *64*, 1173–1176.

[6] a) C. W. So, H. W. Roesky, J. Magull, R. B. Oswald, *Angew. Chem. Int. Ed.* **2006**, *45*, 3948–3950; b) D. Gau, T. Kato, N. Saffon-Merceron, A. De Cózar, F. P. Cossío, A. Baceiredo, *Angew. Chem. Int. Ed.* **2010**, *49*, 6585–6588; c) S. S. Sen, H. W. Roesky, D.

Stern, J. Henn, D. Stalke, *J. Am. Chem. Soc.* **2010**, *132*, 1123–1126; d) A. C. Filippou, O. Chernov, B. Blom, K. W. Stumpf, G. Schnakenburg, *Chem. Eur. J.* **2010**, *16*, 2866–2872; e) Y. Xiong, S. Yao, S. Inoue, E. Irran, M. Driess, *Angew. Chem. Int. Ed.* **2012**, *51*, 10074–10077; f) M. Driess, S. Yao, Y. Xiong, A. Kostenko, *Dalton Trans.* **2018**, 2152–2155.

[7] M. Driess, S. Yao, M. Brym, C. van Wüllen, D. Lentz, *J. Am. Chem. Soc.* **2006**, *128*, 9628–9629.

[8] V. Regnier, Y. Planet, C. E. Moore, J. Pecaut, C. Philouze, D. Martin, *Angew. Chem. Int. Ed.* **2017**, *56*, 1031–1035.

[9] a) C. Cui, H. W. Roesky, H. G. Schmidt, M. Noltemeyer, H. Hao, F. Cimpoesu, *Angew. Chem. Int. Ed.* **2000**, *39*, 4274–4276; b) N. J. Hardman, B. E. Eichler, P. P. Power, *Chem. Commun.* **2000**, *53*, 1991–1992; c) M. S. Hill, P. B. Hitchcock, *Chem. Commun.* **2004**, *44*, 1818–1819.

[10] M. Driess, S. Yao, M. Brym, C. Van Wüllen, *Angew. Chem. Int. Ed.* **2006**, *45*, 6730–6733.

[11] E. Pretsch, P. Bühlmann, M. Badertscher in *Structure Determination of Organic Compounds* (eds. M. Badertscher, P. Bühlmann, E. Pretsch), Springer-Verlag, Berlin, **2009**, Chp. 5.

[12] T. J. Hadlington, J. A. B. Abdalla, R. Tirfoin, S. Aldridge, C. Jones, *Chem. Commun.* **2016**, *52*, 1717–1720.

[13] J. Emsley in *The Elements* 3rd ed., Clarendon Press, Oxford, **1998**.

[14] P. W. Atkins, D. F. Shriver, in *Shriver & Atkins' Inorganic Chemistry*, Oxford University Press, Oxford, **2010**, Chp. 2.

[15] a) I. Krossing, *Chem. Eur. J.* **2001**, *7*, 490–502. For a comprehensive review of the use of the anion in stabilising *p*-block cations see: b) T. A. Engesser, M. R. Lichtenthaler, M. Schleep, I. Krossing, *Chem. Soc. Rev.* **2016**, *45*, 789–799.

CHAPTER 5

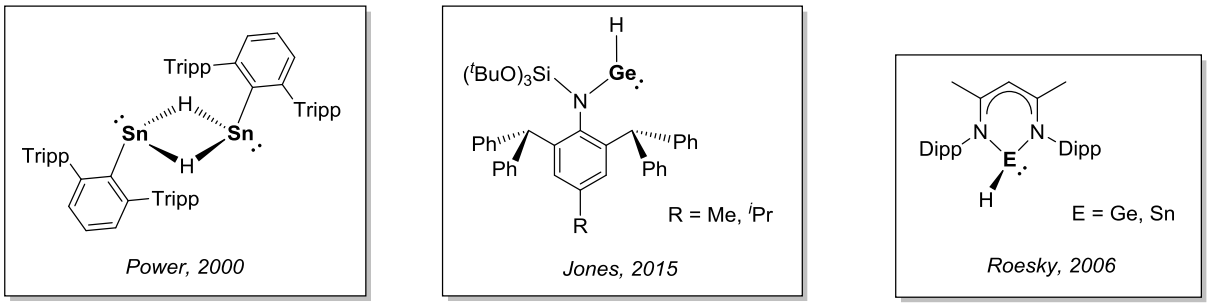
SYNTHESIS AND REACTIVITY STUDIES OF *N*-NACNAC-STABILISED HYDRIDO- AND PHOSPHAKETENYL-TETRELENES

5.1 Introduction

Within the realm of the chemistry of low-coordinate divalent Group 14 tetrelenes, $(R_1)(R_2)E$, there is growing interest in hydride complexes of the form (R)(H)E.[1] In part, this is due to analogies drawn with Group 13 elemental hydrides (such as $NaBH_4$, $LiAlH_4$, etc.), which are well known as widely-employed and versatile stoichiometric reducing agents in both organic and inorganic chemistry.[2] Compared to their tetravalent Group 14 counterparts (*i.e.* systems of the form R_3EH), examples of divalent hydridotetrelenes are generally more scarce; such compounds are also more reactive due to the presence of an additional lone pair and an empty *p*-type orbital at the metal centre. As a result, a number of hydridotetrelenes have been synthesised which participate in the hydrometallation of unsaturated organic substrates, even reversibly in some cases.[1b,1c,3] However, this increased reactivity is often associated with a reduced stability, as evidenced by the facile decomposition pathways often associated with hydridotetrelenes - *e.g.* reductive elimination to yield the protio-ligand RH and E(0). In part, this can be attributed to a reduced degree of kinetic stabilisation in the hydride complex, compared to compounds of the form $(R_1)(R_2)E$, due to a reduction in steric protection brought about by changing a bulky R substituent with a significantly smaller H atom. Thus, a major challenge in the field of Main Group chemistry is the

stabilisation of low-valent hydride compounds under ambient conditions. This challenge applies in particular to systems that are monomeric, which are desirable due to the presence of an open reactive site at the metal centre, namely both a vacant *p*-type orbital and a lone pair of electrons on the tetrel atom.

In 2000, employing the sterically encumbered 2,6-Trip$_2$-C$_6$H$_3$ terphenyl ligand, the group of Power isolated and characterised the first example of an ambient-temperature stable hydridotetrelene complex {(2,6-Trip$_2$-C$_6$H$_3$)Sn(μ-H)}$_2$, which exists as a dimer in the solid state (Figure 5.1).[4] This finding represented a milestone in the quest for two-coordinate heavier Group 14 elemental hydrides, representing as it did a first demonstration of the use of large organic substituents in the isolation of low-valent hydride derivatives. More recently, carefully tailored ligand design has enabled the preparation of the first *bona fide* two-coordinate hydridogermylenes, stabilised by the extremely bulky amide ligand [(Ar*)(^{t}Bu$_3$SiO)N]$^-$ developed by the group of Jones.[5] These hugely bulky *N*-donors are proposed to help inhibit germylene dimerisation, and thus stabilise the monomeric form.



MONODENTATE LIGAND THREE-COORDINATE

MONODENTATE LIGAND TWO-COORDINATE

BIDENTATE LIGAND THREE-COORDINATE

Figure 5.1 Landmark examples of hydridogermylene and stannylene complexes

In addition to the use of sterically encumbered monodentate ligands, an alternative strategy employed for the stabilisation of monomeric divalent Group 14 elemental hydrides is the coordination of additional neutral ligand/multidentate donor at the metal centre (*i.e.* in systems of the form (R)(H)$(L)_n$E). From a structural point of view, this of course quenches the vacant coordination site of the putative two-coordinate complex, and provides additional kinetic stabilisation through the spatial protection provided by the L group(s). In this respect, Nacnac ligands (effectively a chelating (R)(L) system) have been successfully utilised in the isolation and characterisation of monomeric, donor-supported hydridogermylene and stannylene complexes (^{Dipp}Nacnac)EH (Figure 5.1).[6] Interestingly, the two complexes possess contrasting thermal stabilities: while the tin species slowly decomposes over the course of four days under inert conditions, the germanium analogue is more persistent under the same conditions. Presumably, this is in line with the effect of weaker E—H bonds descending group 14, as manifested by the calculated average bond energies of 289 kJ mol^{-1} for Ge—H bonds, and 253 kJ mol^{-1} for Sn—H bonds.[7]

Another family of highly reactive molecules of interest from a fundamental perspective are monomeric pnictides/pnictinidenes containing a terminal E═Pn function (E = Main Group element), particularly when heavier pnictogens (Pn = P, As, Sb) are involved, due to the potential exotic reactivities originated from the heteroelement-pnictogen multiple bond character in these species.[8] Compared to a handful of stable monomeric pnicta-alkynes which possess a terminal C≡P or C≡As

moiety,[9] as well as pnicta-diazonium salts (having a terminal N≡P or N≡As moiety, Figure 5.2),[10] analogous examples featuring heavier Main Group element-pnictogen bonding are much less prevalent. In 2016, the group of Bertrand reported the synthesis of a landmark monomeric (phosphino)phosphinidene containing a terminal P─P fragment, which is kinetically protected by bulky flanking aromatic substituents.[11] This compound was later found to be a potent electrophile, as demonstrated by reactions with carbon monoxide and Lewis bases such as NHCs and phosphines.[12]

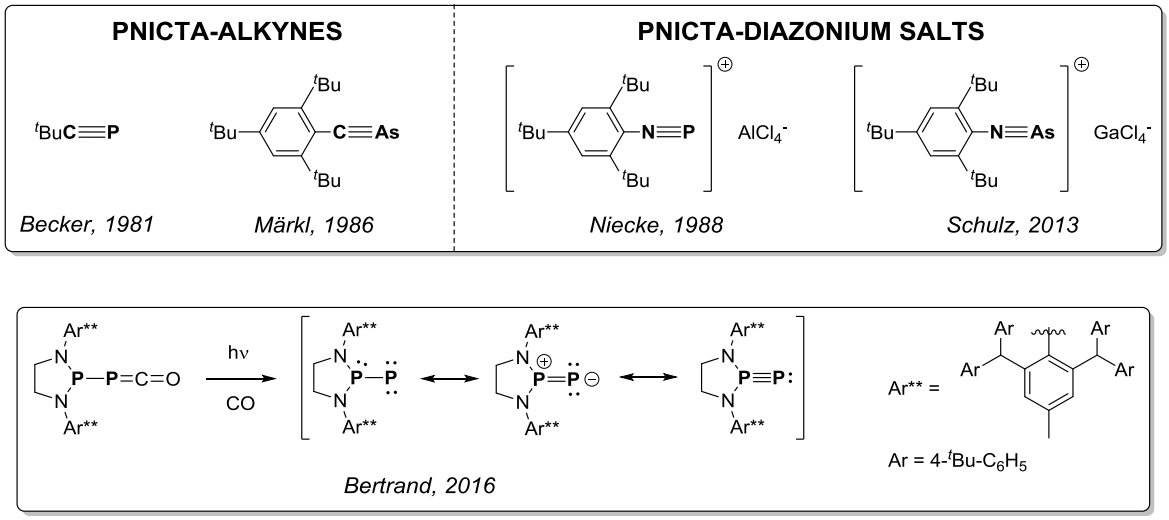


Figure 5.2 Early reports of compounds featuring terminal carbon- and nitrogen-heavy pnictogen bonds (*top*); the synthesis of a stable phosphinidene containing a terminal P─P fragment (*bottom*)

With respect to terminal pnictides/pnictinidenes of heavier Group 14 elements, although such species have not been isolated to-date, they have been predicted to exist as fleeting intermediates in the desilylation of a bis(trimethylsilyl)phosphidosilylene,[13] or more commonly in the decarbonylation of pnictaketenyl complexes of the form E─(PnCO) (Pn = P, As, Figure 5.3).[14] This speculation is largely based on the solid-state structures of the isolated products

from these reactions, the majority of which are suggestive of dimerisation of the putative terminal pnictides/pnictinidenes. Most importantly, from a synthetic viewpoint, these examples have demonstrated the potential of heavier Group 14 pnicta-ketenyl complexes as precursors to the elusive terminal pnictides.

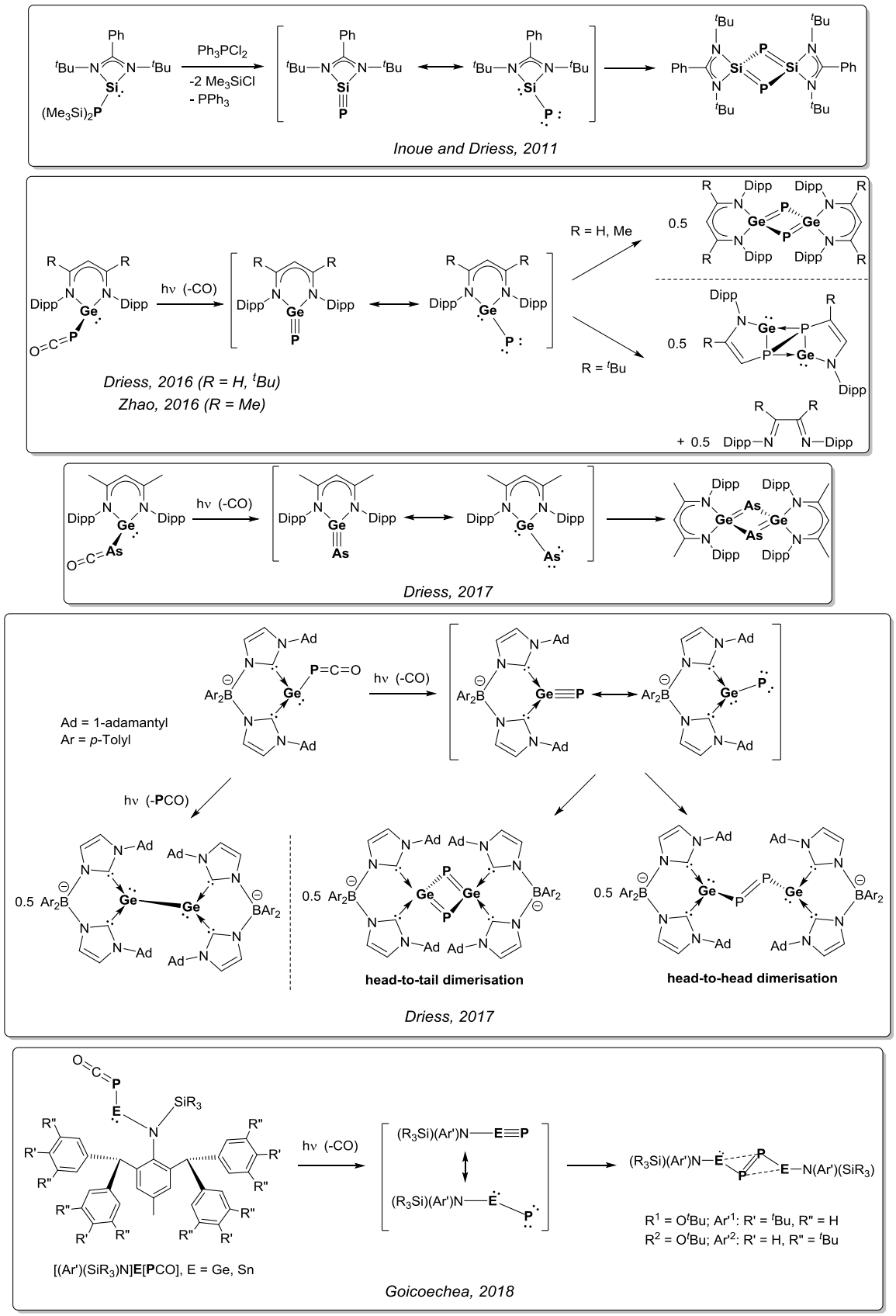


Figure 5.3 Notable attempts to isolate terminal pnictides/pnictinidenes of heavier Group 14 elements

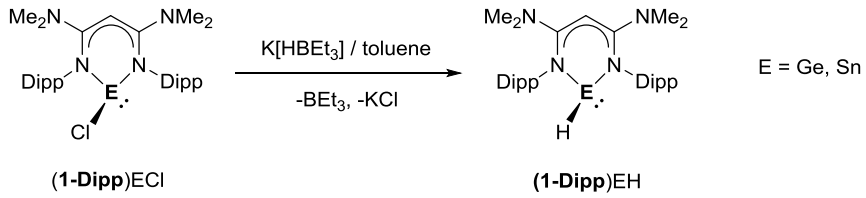
Besides dimerisation processes, putative terminal pnictide/pnictinidenes have also been found to undergo insertion into the ligand backbone.[14a,c,f] This was observed in the attempted synthesis of a ^{t}Bu-substituted Nacnac-stabilised phosphagermyne ((${}^{t\text{Bu,Dipp}}$Nacnac)GeP); the intermediate generated immediately post-decarbonylation was proposed to engage in multiple molecular rearrangements, resulting eventually in the formation of the *N,P*-heterocyclic bis-germylene and the diimine {(DippN)C(^{t}Bu)}$_2$ (Figure 5.3).[14a] Given that head-to-tail dimerisation was observed in the cases of the less bulky (${}^{\text{R,Dipp}}$Nacnac)GeP intermediates (R = H and Me),[14a,b] it is plausible that the steric and/or electronic nature of the β-carbon substituents of the Nacnac ligands might have influenced the ultimate outcome of the decarbonylation processes. Indeed, computational studies (B97-D/6-31G(d), cc-pVTZ(-PP) for Ge and P) suggested a higher activation energy for (${}^{t\text{Bu,Dipp}}$Nacnac)GeP to dimerise (51.0 kJ mol^{-1}, *cf.* 13.0 kJ mol^{-1} for (${}^{\text{H,Dipp}}$Nacnac)GeP), which was credited to the difference in steric bulk of the ^{t}Bu functions compared to the H atoms.[14a] Thus, one might argue that another variant of β-carbon substituents on electronic grounds – for example, the π-donating, σ-withdrawing amino groups – might induce a different mode of reactivity altogether, which would be particularly beneficial to the understanding of the chemistry of heavier Group 14 pnictides/pnictinidenes.

Having prepared *N*-nacnac-stabilised chlorogermylene and stannylene complexes featuring the bulky *N*-Dipp framework (Chapter 4), their transformations to the corresponding hydrido- and phosphaketenyltetrelenes are described in this

chapter. Investigations on the impact of incorporating the amino groups into the ligand backbone on the photochemical behaviour of the phosphaketenyl complexes were also targeted, both experimentally and computationally.

5.2 Results and Discussion

5.2.1 Synthesis and characterisation of the hydridogermylenes and stannylenes



Scheme 5.1 General synthetic scheme for the preparation of (**1-Dipp**)EH (E = Ge, Sn)

Utilising potassium (triethyl)borohydride as the hydride source, the hydridotetrelenes (**1-Dipp**)EH (E = Ge, Sn) were prepared *via* a facile hydride-for-chloride exchange from their chloride precursors (Scheme 5.1). Consistent with the degree of stability observed for its Nacnac analogue,[6b] the hydridostannylene is thermally fragile and shows significant decomposition *via* deposition of tin metal, even in an inert atmosphere, over the course of several days at ambient temperature. By contrast, the germylene analogue can be stored under the same conditions effectively indefinitely without degradation. Spectroscopically, the presence of the metal-bound hydride is confirmed in each case by a characteristic M—H signal in the downfield region in ^{1}H NMR spectrum (δ_H = 8.14 ppm and 13.42 ppm, respectively for the germylene and stannylene). These parameters, together with the ^{119}Sn NMR signal of the hydridostannylene (δ_{Sn} = -18 ppm), are comparable to those observed for the (^{Dipp}Nacnac)EH analogues (δ_H = 8.08 ppm and 13.96 ppm for

E = Ge, Sn, respectively; δ_{Sn} = -4.5 ppm for the latter).[6b,c] IR spectroscopy further confirms the presence of the metal-bound hydride in (**1-Dipp**)GeH: an absorption which corresponds to the Ge—H stretch is observed at 1755 cm^{-1} (*cf.* ν_{Ge-H} = 1733 cm^{-1} for (^{Dipp}Nacnac)GeH).[6b] Due to the instability of the stannylene analogue (**1-Dipp**)SnH even in an inert glovebox atmosphere, reliable IR data of this compound could not be obtained.

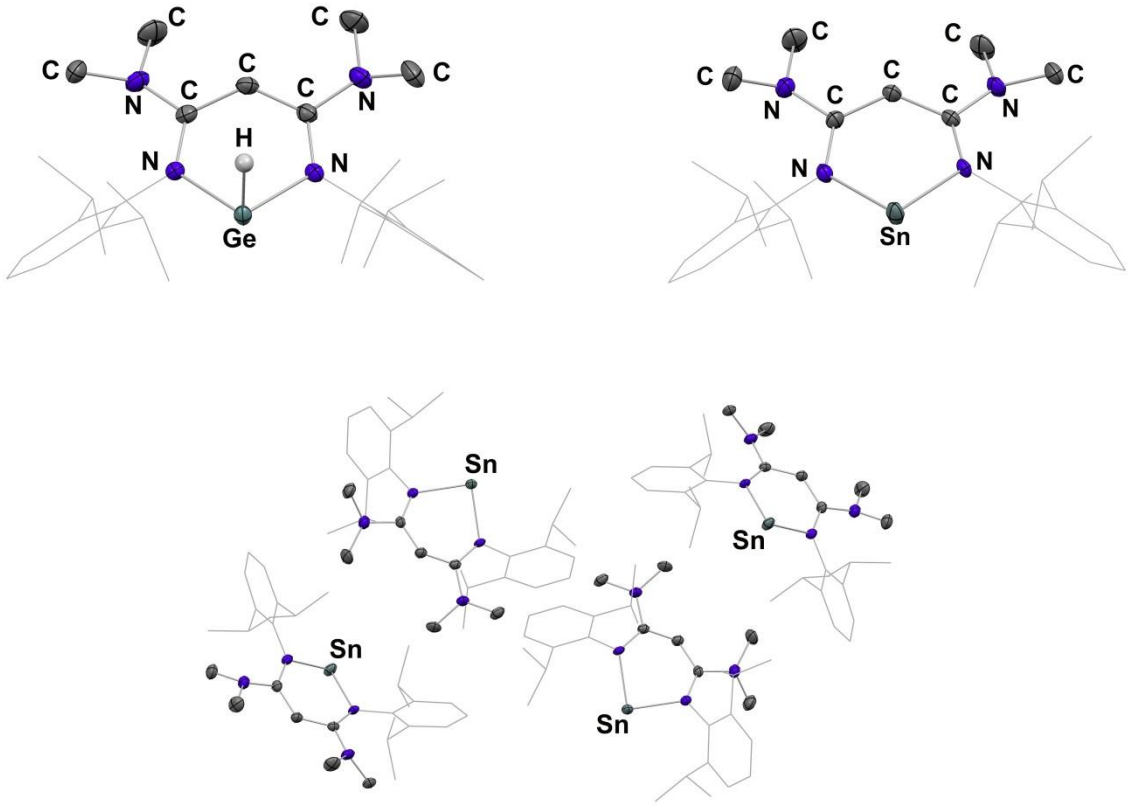


Figure 5.4 Molecular structures of (**1-Dipp**)EH (E = Ge, Sn) (*top*) and the solid-state packing motif of (**1-Dipp**)SnH (*bottom*), as determined by single crystal X-ray diffraction. Thermal ellipsoids are shown at 35 % probability level. *N*-bound aromatic substituents are represented in the wireframe format, and all hydrogens with the exception of the metal-bound hydride (for (**1-Dipp**)GeH) have been omitted for clarity.

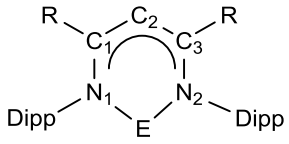
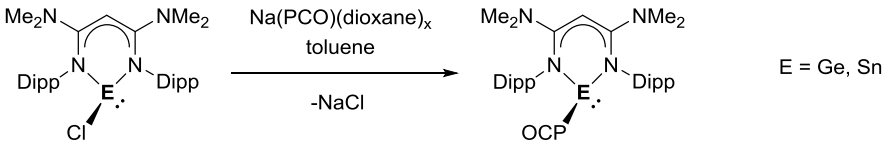
	(**1-Dipp**)GeH	([Dipp]Nacnac)GeH	(**1-Dipp**)SnH	([Dipp]Nacnac)SnH
d(C1—N1) / *d*(C3—N2)	**1.3414(16) / 1.3447(16)**	1.326(3) / 1.328(3)	**1.337(6) / 1.339(6)**	1.326(3) / 1.326(3)
d(E—N1) / *d*(E—N2)	**2.0111(12) / 1.9922(12)**	1.989(2) / 1.989(2)	**2.190(4) / 2.194(3)**	2.1944(18) / 2.1984(17)
d(E—least-squares [N1—C1—C2—C3—N2] plane)	**0.65**	0.74	**0.68**	0.73
∠ (N1—E—N2)	**93.45(5)**	90.33(9)	**89.40(13)**	85.10(7)

Table 5.1 Selected bond lengths (Å) and angles (°) of the *N*-nacnac-stabilised hydridotetrelenes (**1-Dipp**)EH, as determined by X-ray crystallography

While the traditional β-methylated and amino-functionalised Nacnac-stabilised hydridotetrelenes exhibit comparable spectroscopic parameters, studies of their molecular structures by X-ray crystallography are suggestive of divergence in the ligand properties, particularly for the stannylene complexes. As such, weak Sn···Sn interactions (*d*(Sn—Sn) = 3.71 Å) and bridging Sn···H contacts (*d*(Sn—H) = 4.01(3) Å) are observed in the solid-state packing of Roesky's ([Dipp]Nacnac)SnH;[6b] these result from a head-to-head orientation of the molecular units in the solid state. Although the location of the Sn-bound hydrogen atom cannot be reliably located by single crystal X-ray diffraction, it is evident that (**1-Dipp**)SnH features an alternative *head-to-tail* molecular alignment in the solid state (shortest Sn···Sn distance = 8.68 Å), which precludes any Sn—H···Sn interactions (Figure 5.4). This discrepancy can be related to the difference in the steric profiles of the β-carbon methyl and amino substituents; the intrinsic steric

repulsion between these substituents and the N(imine)-bound Dipp groups influences the geometry around the metal centre. Thus, the use of the *N*-nacnac ligand yields a more "shielded" tin atom in the hydridostannylene complex, as reflected by a shorter distance from the tin atom to the least-squares mean NC_3N chelate plane (0.68 Å, *cf*. 0.73 Å for (^{Dipp}Nacnac)SnH).

5.2.2 Synthesis and reactivity studies of the phosphaketenylgermylenes and stannylenes



(**1-Dipp**)ECl (**1-Dipp**)E(PCO)

Scheme 5.2 Synthetic approach for the preparation of phosphaketenyltetrelenes (**1-Dipp**)E(PCO) (E = Ge, Sn)

Phosphaketenyltetrelene complexes (**1-Dipp**)E(PCO) (E = Ge, Sn) can also be prepared by metathesis processes, in this case involving the reactions of the chlorotetrelene precursors and the dioxane adduct of the Na(PCO) salt (Scheme 5.2).[15] Notably, (**1-Dipp**)Sn(PCO) represents one of the first examples of a donor-supported phosphaketenylstannylene. It gives rise to a resonance at -332 ppm in $^{31}P\{^1H\}$ NMR spectrum, which displays coupling to both ^{117}Sn and ^{119}Sn nuclei ($^1J_{SnP}$ = 731 Hz and 765 Hz, respectively). Consistently, the ^{119}Sn NMR spectrum features a doublet resonance at -120 ppm ($^1J_{SnP}$ = 765 Hz). Studies of the molecular structure of (**1-Dipp**)Sn(PCO) by single crystal X-ray diffraction reveal a near-linear PCO unit (∠ [P—C—O] = 177.75(10)°), with the phosphorus atom occupying the *pseudo*-axial position within the coordination sphere of the tin centre (Figure 5.5).

The remaining solid-state features of (**1-Dipp**)Sn(PCO) closely resemble those of the chlorostannylene precursor and the hydridostannylene (**1-Dipp**)SnH, with a six-membered metallacycle, in which the metal centre adopts a distorted trigonal-pyramidal geometry, and is slightly displaced from the least-squares NC_3N chelate plane by 0.85 Å. In a similar fashion to (**1-Dipp**)SnH, (**1-Dipp**)Sn(PCO) slowly decomposes over the course of several days at ambient temperature in both the solid and solution phases, as evidenced by the deposition of metallic tin; this hampered efforts to obtain accurate IR data for this compound. Preliminary photochemical studies of (**1-Dipp**)Sn(PCO) indicate the complete consumption of the starting material, together with the formation of a new tin-containing species after 3 h of broadband UV irradiation, as evident from the emergence of one sharp new singlet at -157 ppm in the $^{119}Sn\{^1H\}$ NMR spectrum. However, the $^{31}P\{^1H\}$ NMR spectrum of the reaction mixture at that stage is more complicated, featuring a singlet at 156 ppm as the major resonance, and multiple minor peaks in the -180 ppm to -130 ppm range. In addition, during the photochemical experiment, rapid deposition of tin metal was observed, which was detrimental to the attempts to isolate the product(s) for identification and characterisation purposes.

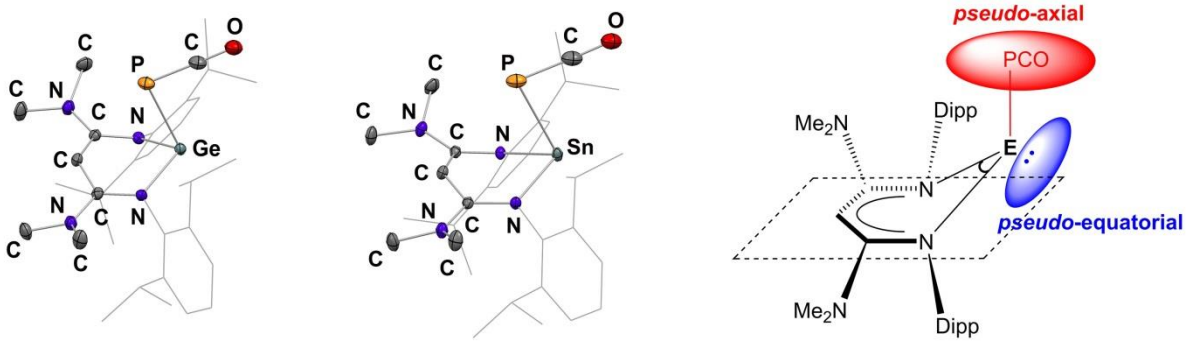


Figure 5.5 Solid-state structures of (**1-Dipp**)E(PCO) (E = Ge, Sn), as determined by X-ray crystallography, and the naming convention of the *pseudo*-axial and equatorial positions. Thermal ellipsoids are shown at 35 % probability level. *N*-bound aromatic substituents are shown in the wireframe format, and all hydrogens have been omitted for clarity.

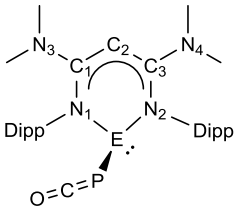
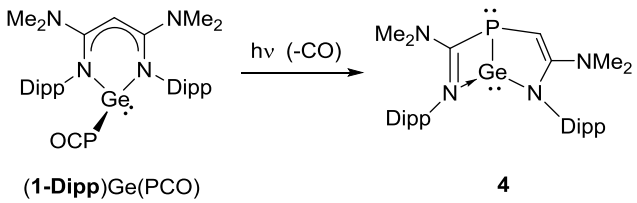
	(**1-Dipp**)Ge(PCO)	(**1-Dipp**)Sn(PCO)
d(C1—N1) / *d*(C3—N2)	1.344(3) / 1.363(2)	1.348(3) / 1.369(3)
d(C1—N3) / *d*(C3—N4)	1.359(3) / 1.365(2)	1.361(4) / 1.368(3)
d(E—N1) / *d*(E—N2)	1.9872(15) / 1.9652(15)	2.175(2) / 2.1540(19)
d(E—P)	2.5470(6)	2.6955(8)
d(P—C)	1.684(5)	1.696(6)
d(C—O)	1.187(6)	1.210(7)
∠ (N1—E—N2)	93.04(7)	88.64(8)
∠ (N—E—P)	91.62(5) / 90.35(5)	89.27(6) / 88.66(6)
∠ (E—P—C)	87.29(16)	82.98(15)
∠ (P—C—O)	179.11(10)	177.75(10)

Table 5.2 Selected bond lengths (Å) and angles (°) of the *N*-nacnac-stabilised phosphaketenyltetrelenes (**1-Dipp**)E(PCO), as determined by X-ray crystallography

By contrast, the germanium analogue (**1-Dipp**)Ge(PCO) is significantly more thermally stable and can be stored indefinitely in an inert atmosphere, without signs

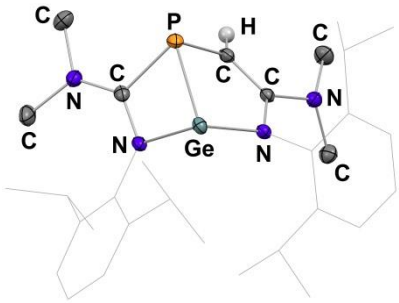
of decomposition. It displays a signal at -317 ppm in $^{31}P\{^{1}H\}$ NMR spectrum, which is marginally more downfield than that of its tin counterpart, and is close to the range (-299 to -302 ppm) observed for the series of (^{R,Dipp}Nacnac)Ge(PCO) analogues (R = H, Me, ^{t}Bu).[14a,b] Furthermore, IR spectroscopy corroborates the presence of the —PCO moiety, showing a characteristic C=O stretching frequency at 1876 cm^{-1} (*cf.* $\nu_{C=O}$ = 1879 – 1895 cm^{-1} for Nacnac-stabilised phosphaketenylgermylenes).[14a,b] The solid-state molecular structure of (**1-Dipp**)Ge(PCO) resembles closely those of related Nacnac systems, and comprises a near-linear PCO moiety (∠ [P—C—O] = 179.11(10)°), of which the phosphorus atom resides in the *pseudo*-axial site within the coordination sphere of germanium (Figure 5.5). As previously observed for the monochlorotetrelene series, however, the $^{13}C\{^{1}H\}$ NMR spectrum of (**1-Dipp**)Ge(PCO) exhibits a resonance for the γ-CH carbon which is markedly upfield shifted (δ_C = 81.3 ppm), compared to the range of 95.0 – 106.5 ppm reported for phosphaketenylgermylenes stabilised by "regular" Nacnac ligands.[14a,b] Hypothetically, this difference in the electronic properties of the γ-carbons might give rise to differences in reactivity of photolytically-induced P—C bond cleavage, as the interaction between the phosphorus atom and the γ-carbon has previously been proposed be involved in the decarbonylation mechanism.[14a]



(**1-Dipp**)Ge(PCO) **4**

Scheme 5.3 Photolytically-induced P—C bond cleavage of (**1-Dipp**)Ge(PCO)

When (**1-Dipp**)Ge(PCO) is subjected to broadband UV irradiation under ambient conditions for 6 h, the colour of the solution changes from light-yellow to dark-red; subsequent recrystallisation of the product from pentane at -26°C yields dark-red crystals. Definitive structural characterisation of this species is made possible by X-ray crystallography, which reveals it to be the bicyclic system **4** (Scheme 5.3 and Figure 5.6). This compound can be described as an *N,P*-heterocyclic germylene, stabilised by an imine tether. Consistent with the solid-state structure, the singlet resonance observed in the $^{31}P\{^{1}H\}$ NMR spectrum (δ_P = -50 ppm) is split into a doublet in the proton-coupled ^{31}P NMR ($^{2}J_{PH}$ = 33 Hz), reflecting two-bond coupling between the phosphorus nucleus and the proximal alkenic proton.



Bond lengths:

Ge1—P2 2.4323(9), Ge1—N5 1.938(3), Ge1—N22 2.038(3),
P2—C3 1.803(3), P2—C21 1.883(3), C3—C4 1.383(4),
C4—N18 1.394(4), C4—N5 1.387(4), C21—N35 1.335(4), C21—N22 1.328(4).

Angles:

Ge1—P2—C3 90.27(10), Ge1—P2—C21 74.75(10),
C3—P2—C21 98.85(14), P2—Ge1—N5 88.14(8),
P2—Ge1—N22 71.44(8), N5—Ge1—N22 99.30(10).

Figure 5.6 Solid-state structure of **4**, as determined by X-ray crystallography. Thermal ellipsoids are shown at 35 % probability level. *N*-bound aryl groups are represented in the wireframe format, and all hydrogens (apart from the alkenic proton) have been omitted for clarity (*left*); selected bond lengths (Å) and angles (°) (*right*).

Crystallographically, the mean planes containing two cyclic components are hinged about the Ge—P linkage (inter-plane angle = 80.0°). The Ge—P distance of 2.4323(9) Å is *ca.* 5 % shorter than that measured for the phosphaketenyl precursor (*d*(Ge—P(CO)) = 2.5470(6) Å), but significantly longer than the Ge=P double bonds reported for phosphagermenes (2.138(3) – 2.175(1) Å),[16] which confirms the single

bond nature of the germanium-phosphorus linkage in **4**. A significant degree of pyramidalisation at both the germanium and the phosphorus centres is in evidence; the sum of the angles being 259° (for Ge) and 264° (for P). The Ge1—N5 and Ge1—N22 distances (1.938(3) and 2.038(3) Å) are consistent with single and dative bonds, respectively.[17]

The extent of the electronic influence of the NMe_2 substituents on the molecular metrics of the two heterocycles is found to be strongly dependent on the degree of co-planarity between the planes containing the amino groups and the respective rings. Thus, in the five-membered ring unit (Ge1—P2—C3—C4—N5), the dihedral angle between these planes is 37.5°, which is significantly larger than the corresponding value for the four-membered (Ge1—P2—C21—N22) unit (18.1°). Accordingly, a longer $C—N(Me)_2$ distance is observed in the five-membered component (*d*(C4—N18) = 1.394(4) Å) as a result of the diminished π-conjugation from the pendant amino groups into the ring (*cf.* *d*(C21—N35) = 1.335(4) Å for the four-membered moiety). Moreover, extensive π-delocalisation throughout the $(C)_2N35—C21—N22$ triatomic unit is corroborated by (i) the two statistically identical C21—N35 and C21—N22 bond distances (1.335(4) Å and 1.328(4) Å, respectively), (ii) the small dihedral angle between the mean planes of the $(C)_2N35$ and N22—C21—N35 units (3.3°), and (iii) the negligible degree of pyramidalisation of the nitrogen atoms (respective sums of the angles around N22 and N35: 358.9° and 360.0°).

DFT calculations have been undertaken in order to provide insight into plausible reaction pathways for the formation of **4**. At the outset, the mechanism suggested by the group of Driess for the formation of the *N,P*-heterocyclic bis-germylene {DippNC(*t*Bu)C(H)PGe}$_2$ (Figure 5.3) was inspected, which involves initial photo-induced loss of CO to generate a transient phosphagermyne intermediate followed by insertion into a C—C bond in the Nacnac-ligand backbone (Scheme 5.4).[14a] This hypothesis was considered first due to the structural similarities between **4** and one of the proposed intermediates in the reaction scheme for the backbone *t*Bu-substituted Nacnac counterpart. Both systems feature a core (C_2NGeP) five-membered heterocycle and a pendant imine function (Figure 5.7). Moreover, these mechanistic investigations were extended to include all four (^{Dipp}Nacnac) ligand systems with different β-carbon-bound R groups ((^{R}**L**); R = H, Me, *t*Bu, NMe_2) which have previously been utilised in the chemistry of phosphaketenylgermylenes. This approach was pursued with a view to understanding the differences between the observed photochemical behaviour of these complexes, namely the dimerisation of the phosphagermyne intermediate in the case of (^{H}**L**) and (^{Me}**L**) ligand systems, and the formation of the bis-germylene (with the concomitant extrusion of a diaza-butadiene molecule) from the decarbonylation of the more bulky (^{tBu}**L**)Ge(PCO) (Figure 5.3).[14a,b]

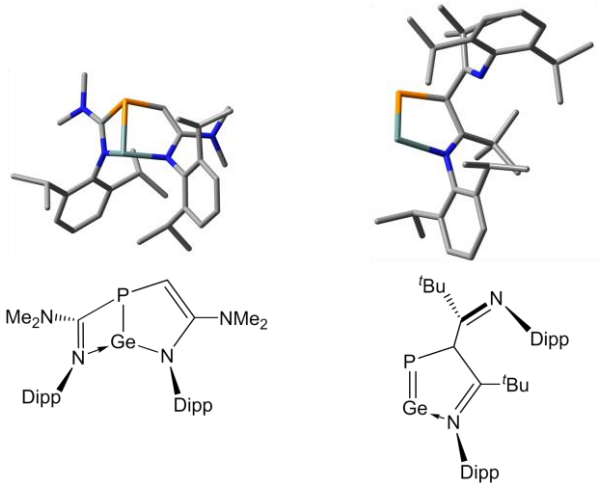
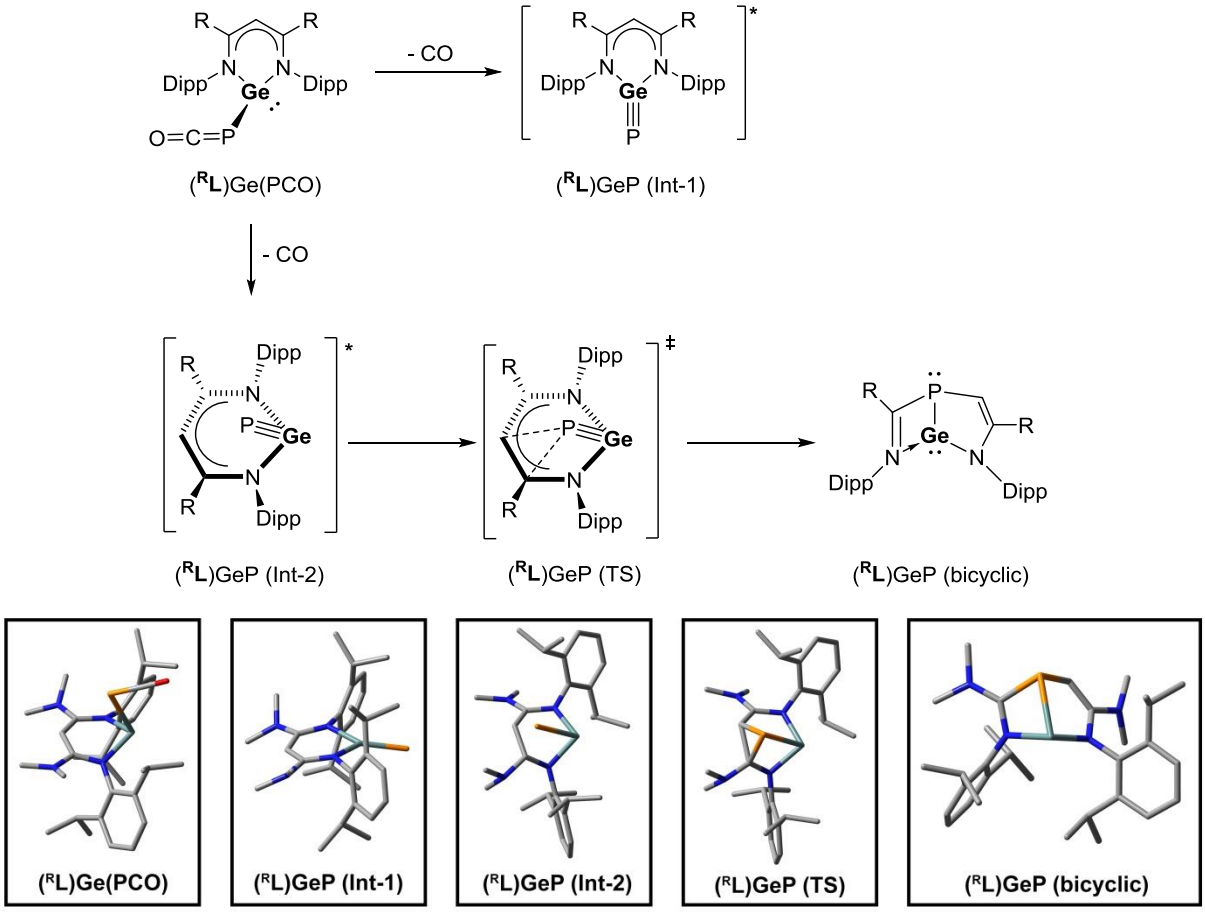


Figure 5.7 Comparison between the optimised structures of **4** and one of the proposed intermediates for the decarbonylation of the ($^{t\text{Bu,Dipp}}$Nacnac)Ge(PCO) system (graphics generated by GaussView)



Scheme 5.4 Stepwise mechanism proposed for the photolytically-initiated decarbonylation of phosphaketenylgermylenes, stabilised by various β-diketiminate ligands (**RL**) (R: substituents at the β-carbon position of the ligand backbone) (*top*); graphical representations (generated by GaussView) of the involved species in the mechanism, with the *N*-nacnac ligand system as an example (*bottom*)

Thus, two geometries were proposed for the (^{R}**L**)GeP intermediates, which differ only in the relative orientations of the Ge—P unit and the five-membered Nacnac backbone (Scheme 5.4). The geometry of the intermediate (^{R}**L**)GeP (Int-1) was chosen based on the identical {(NC_3N)GeP} core conformation to one of the (^{R,Dipp}Nacnac)GeP intermediates (R = H, ^{t}Bu) proposed by the group of Driess.[14a] In this species, the Ge—P unit lies co-planar with the least-squares NC_3N chelate plane, with the phosphorus atom projected away from the ligand backbone. The geometry of the other intermediate (^{R}**L**)GeP (Int-2) was optimised based on the structure associated with the local minimum in the energetic profile of the "reverse" potential energy surface (PES) scan, carried out by continuous shortening of the distance between the two carbon atoms directly bonded to phosphorus in compound **4** (C3 and C21, Figure 5.6). This features the phosphorus atom projected away from the (NacnacGe) plane, approaching ever-closer to the C—C bond of the ligand scaffold. For all four Nacnac systems this alternative intermediate was found to be more thermodynamically stable than the other intermediate (^{R}**L**)GeP (Int-1) by 10 – 40 kJ mol^{-1}; for example, the Gibbs' free energies associated with the (^{NMe2}**L**)GeP (Int-1) and (^{NMe2}**L**)GeP (Int-2) are 149.9 and 135.2 kJ mol^{-1}, respectively (Figures 5.8 and 5.9). These results reflect the close geometric resemblance of the intermediate species (^{R}**L**)GeP (Int-2) to the phosphaketenylgermylene precursors, and perhaps indicate that the plausible stepwise mechanism needs not involve the intermediates (^{R}**L**)GeP (Int-1) proposed by Driess and co-workers.

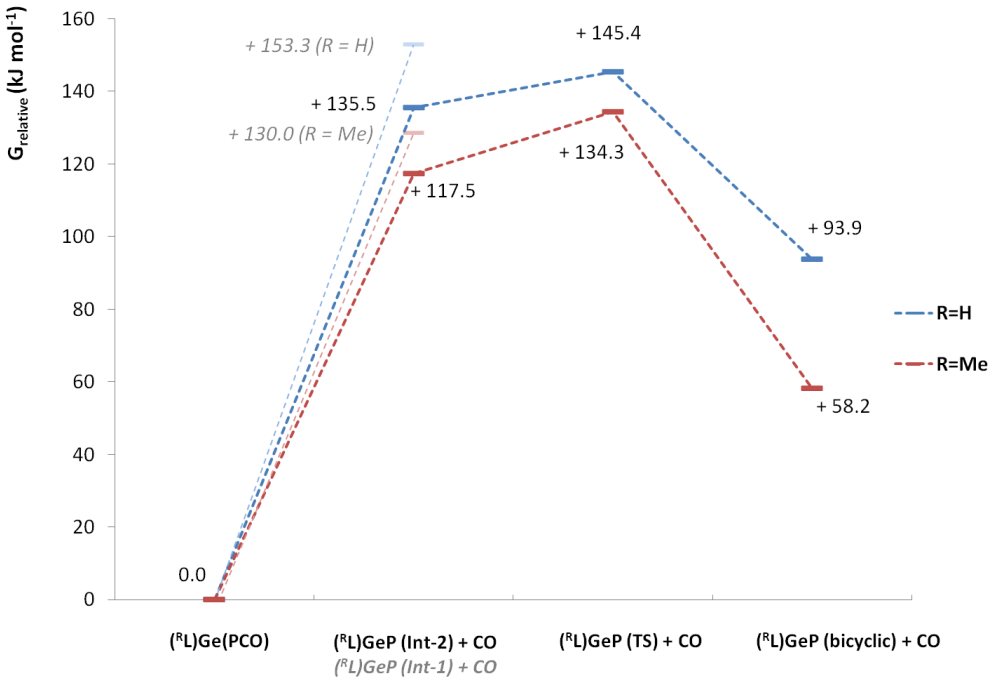


Figure 5.8 Energy profiles of the stepwise mechanism for the formation of (^{R}**L**)GeP (R = H and Me).

Note: The energy levels in grey correspond to the combined energies of [(^{R}L)GeP (Int-1) + CO]

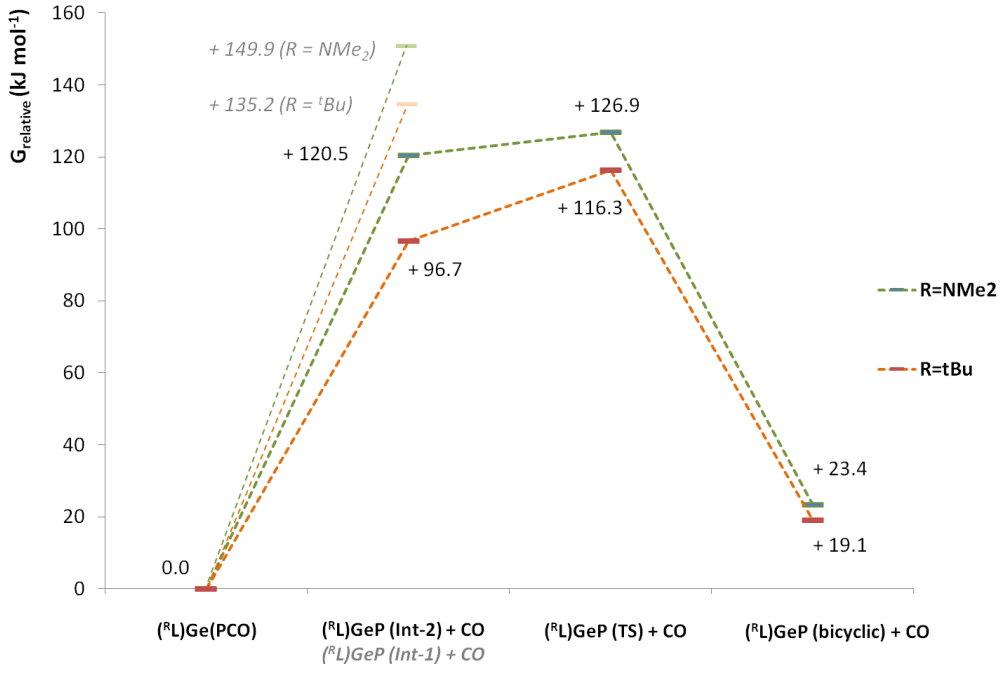
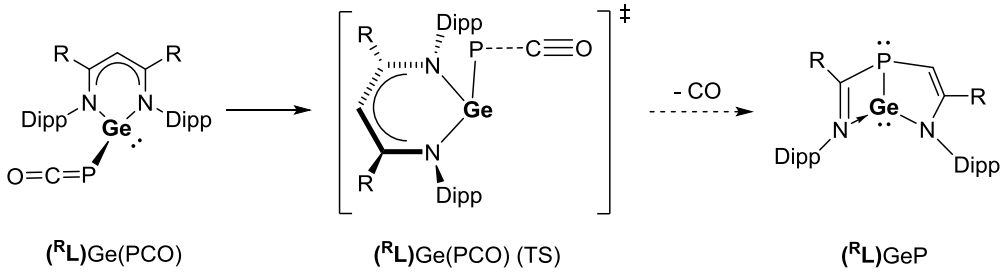


Figure 5.9 Energy profiles of the stepwise formation mechanism of (^{R}**L**)GeP (R = ^{t}Bu and NMe_2).

Note: The energy levels in grey correspond to the combined energies of [(^{R}L)GeP (Int-1) + CO]

The subsequent conversion to the final bicyclic product is proposed to proceed *via* a transition state (**RL**)GeP (TS), in which insertion into the C—C bond by the phosphide fragment takes place. Access to this transition state from Int-2 (Scheme 5.4) was found to be the least energetically expensive in the *N*-nacnac system (+6.4 kJ mol^{-1}, compared to +19.6 kJ mol^{-1} for the ^{t}Bu counterpart, for example). Whilst ultimately the overall decarbonylation process is found to be endoergic for all of the considered ligand series, the driving force for the reaction can be attributed to the liberation of CO gas.



Scheme 5.5 The concerted mechanism proposed for the formation of the bicyclic species, which involves a single transition state (**RL**)Ge(PCO) (TS) in the pathway

The close proximity of the phosphorus atom to the ligand backbone in both the experimental and calculated structures of (**1-Dipp**)Ge(PCO), and the fact that the interaction between the P centre and the Nacnac backbone constitutes a key step in the above mechanism, suggested to us the possibility of an alternative "concerted" reaction pathway. In this process, the formation of the final product **4** can be proposed to occur *via* elongation of the P—C(O) bond, with accompanying shortening of the distance between the phosphorus centre and the backbone γ-carbon atom (Scheme 5.5). This mechanism therefore avoids the necessity to invoke a transient phosphagermyne/germaphosphinidene intermediate. A single

transition state (^{NMe2}**L**)Ge(PCO) (TS) corresponding to this process has been located (by a potential energy surface scan, carried out by sequentially increasing the P—C(O) distance), at a Gibbs' energy *ca.* +165.6 kJ mol^{-1} higher than that of the starting material (**1-Dipp**)Ge(PCO) (Figures 5.10 and 5.11). While this is more energetically expensive than the generally-accepted barrier for spontaneous *thermal* reactions at room temperature (*ca.* 70 kJ mol^{-1}), this process is likely to be viable through a photolytically-induced mode of activation – in fact, the UV quanta utilised ($\lambda \approx 365$ nm) provide an amount of energy in excess of 300 kJ mol^{-1}.

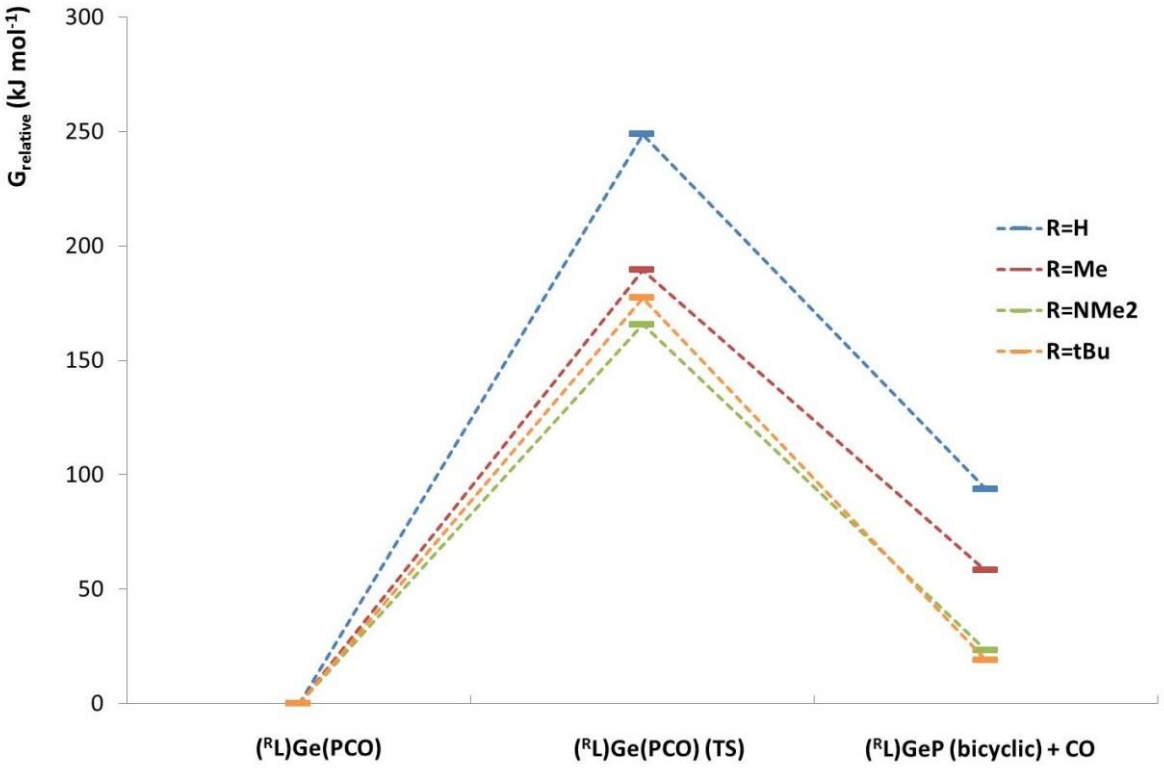


Figure 5.10 Free energy profiles of the concerted mechanism for the formation of the bicyclic species

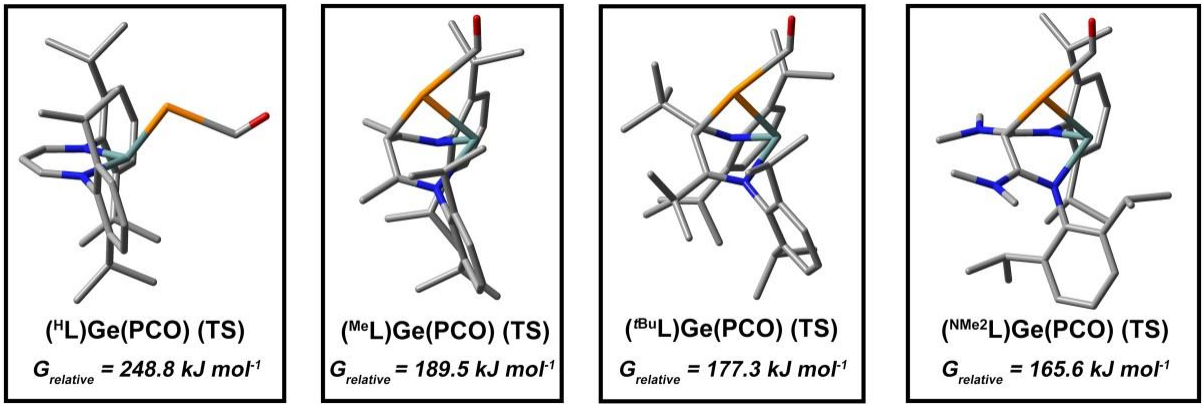


Figure 5.11 Graphical representations (generated by GaussView) of the transition states in the concerted mechanism; their associated relative Gibbs' energies are calculated with respect to those of the phosphaketenyl-complex starting materials.

Similar mechanistic investigations for related Nacnac-ligated phosphaketenyl systems featuring H, Me and ^{t}Bu-substituted backbones were undertaken, which in all cases, yield higher Gibbs energies for the transition states compared to the *N*-nacnac analogue (Figure 5.10). Moreover, the energy barriers associated with the systems (^{NMe2}**L**)Ge(PCO) and (^{tBu}**L**)Ge(PCO) are lower compared to those of the less bulky backbone versions (^{H}**L**)Ge(PCO) and (^{Me}**L**)Ge(PCO). Presumably, this is in line with the experimental findings that the interaction between the phosphorus centre and the backbone γ-carbon atom has the possibility to influence the outcomes of the decarbonylation processes of (^{NMe2}**L**)Ge(PCO) and (^{tBu}**L**)Ge(PCO). In particular, (and in contrast to the other Nacnac systems), elongation of the P—C(O) bond in (^{H}**L**)Ge(PCO) leads to a more protruded Ge—P unit from the five-membered NC_3N chelate. This is corroborated by the optimised geometry of the transition state (^{H}**L**)Ge(PCO) (TS), which lacks any interaction between the phosphorus and the backbone γ-carbon atom, and is associated with the highest relative Gibbs' free energy (248.8 kJ mol^{-1}). Such observations are fully consistent

with the tendency of the (^{H}**L**)Ge(PCO) system to partake in the head-to-tail dimerisation pathway upon photo-induced decarbonylation instead of backbone C—C bond insertion.

5.3 Conclusions

In this chapter, studies of the complexation chemistry of *N*-nacnac ligands with the heavier Group 14 elements has been extended to include the hydrido- and phosphaketenyl-tetrelenes, the syntheses of which involve facile salt metathesis reactions from the corresponding chloro precursors. As with the analogous Nacnac-ligated complexes, the resulting stannylene complexes were found to be significantly less thermally stable than their germanium counterparts. Notably, (**1-Dipp**)Sn(PCO) represents one of the first examples of a structurally-characterised, donor-supported phosphaketenylstannylene. As compared to their Nacnac analogues, the *N*-nacnac-based complexes exhibit broadly comparable spectroscopic properties and solid-state parameters. However, in the case of (**1-Dipp**)SnH, the absence of weak Sn—H···Sn intra-molecular interactions (as observed for (^{Dipp}Nacnac)SnH in the solid state), might be construed as indicative of greater steric repulsion exerted by the backbone amino functions on the coordination environment at the metal centre.

While the thermal sensitivity of (**1-Dipp**)Sn(PCO) hampered any meaningful photochemical studies of this system, the corresponding reactivity of (**1-Dipp**)Ge(PCO) could conveniently be examined, both experimentally and computationally. The use of broadband UV irradiation results in cleavage of the

P—C bond, with accompanying liberation of CO gas, leading to the formation of **4** – an *N,P*-heterocyclic germylene, stabilised by an imine tether. Mechanistic investigations of the formation of the bicyclic product were performed for four Nacnac ligand variants which differ only in the β-carbon-bound substituents ((**^{R}L**); R = H, Me, ^{t}Bu, NMe_2), thus allowing for energetic comparison between the systems. Two possible reaction pathways were proposed, which involve either (i) phosphagermyne/germaphosphinidene intermediates, generated by the loss of CO, followed by their insertion into the backbone C—C bond in a step-wise manner, or (ii) a concerted CO ejection/(P—C) bond formation process. With regards to the latter mechanism, access to the transition state – which simultaneously features lengthening of the P—CO bond and attack of the phosphorus atom on the γ-carbon – was found to be the least energetically expensive in the case of the (**^{NMe2}L**)Ge(PCO) system. Presumably, this can be linked to the exceptionally electron-rich nature of the γ-carbon in the *N*-nacnac ligand backbone, compared to those in other Nacnac systems, which might have rendered the interaction with the phosphorus centre more thermodynamically favourable.

5.4 Synthesis of novel compounds

5.4.1 General synthetic procedure for the preparation of N-nacnac-stabilised hydridogermylenes/stannylenes: To a toluene solution (30 mL) of (**1-Dipp**)ECl (0.5 mmol) was added a 1.0 M solution of K[$HBEt_3$] in THF (1.1 equiv.) at -78˚C, over a period of 5 min. The reaction mixture was slowly warmed to room temperature and

stirred for an additional 2 h, before volatiles were removed *in vacuo*. The residual solid was extracted into cold hexane (4˚C); storage at -26˚C produced light yellow crystals suitable for X-ray crystallography.

(**1-Dipp**)GeH**:** Yield 0.159 g, 58 %. ^{1}H NMR (400 MHz, C_6D_6): δ_H 1.19 (d, $^{3}J_{HH}$ = 6.8 Hz, 6H, (C$\underline{H}_3$)$_2$CH), 1.20 (d, $^{3}J_{HH}$ = 6.7 Hz, 6H, (C$\underline{H}_3$)$_2$CH), 1.27 (d, $^{3}J_{HH}$ = 6.8 Hz, 6H, (C$\underline{H}_3$)$_2$CH), 1.60 (d, $^{3}J_{HH}$ = 6.7 Hz, 6H, (C$\underline{H}_3$)$_2$CH), 2.27 (s, 12H, (C$\underline{H}_3$)$_2$N), 3.29 (virtual sept, $^{3}J_{HH}$ = 6.8 Hz, 2H, (CH$_3$)$_2$C$\underline{H}$), 3.66 (virtual sept, $^{3}J_{HH}$ = 6.7 Hz, 2H, (CH$_3$)$_2$C$\underline{H}$), 4.17 (s, 1H, methine CH), 7.11-7.16 (6H, aromatic CH), 8.14 (s, 1H, GeH) ppm.^{13}C{^{1}H} NMR (100 MHz, C_6D_6): δ_C 23.9, 24.1, 26.6, 27.7 ((C$\underline{H}_3$)$_2$CH), 28.4, 29.1 ((CH$_3$)$_2$C$\underline{H}$), 41.2 ((C$\underline{H}_3$)$_2$N), 78.2 (methine CH), 124.3, 124.8, 125.8, 143.5, 144.2, 146.2 (aromatic carbons), 165.5 (imine quaternary C) ppm. IR (Nujol, $\nu_{Ge\text{-}H}$/cm^{-1}): 1755. EI-MS: (*m/z*, %): 549.3, 3 [M]$^+$; 506.3, 36 [M-NMe$_2$]$^+$; accurate mass: *m/z* calc. for $C_{31}H_{47}GeN_4$ ([M-H]$^+$) 549.3007, found 549.3029. Elemental microanalysis: calc. for $C_{31}H_{48}GeN_4$: C 67.77, H 8.81, N 10.20%, meas. C 67.58, H 8.74, N 9.98%.

(**1-Dipp**)SnH: Yield 0.042 g, 14%. ^{1}H NMR (400 MHz, C_6D_6): δ_H 1.19 (d, $^{3}J_{HH}$ = 6.3 Hz, 6H, (C$\underline{H}_3$)$_2$CH), 1.21 (d, $^{3}J_{HH}$ = 6.8 Hz, 6H, (C$\underline{H}_3$)$_2$CH), 1.27 (d, $^{3}J_{HH}$ = 6.8 Hz, 6H, (C$\underline{H}_3$)$_2$CH), 1.54 (d, $^{3}J_{HH}$ = 6.8 Hz, 6H, (C$\underline{H}_3$)$_2$CH), 2.28 (s, 12H, (C$\underline{H}_3$)$_2$N), 3.30 (virtual sept, $^{3}J_{HH}$ = 6.8 Hz, 2H, (CH$_3$)$_2$C$\underline{H}$), 3.72 (virtual sept, $^{3}J_{HH}$ = 6.7 Hz, 2H, (CH$_3$)$_2$C$\underline{H}$), 4.02 (s, 1H, methine CH), 7.08-7.16 (6H, aromatic CH), 13.42 (s, 1H, SnH, ^{119}Sn satellite with $^{1}J_{SnH}$ = 52 Hz) ppm. ^{13}C{^{1}H} NMR (100 MHz, C_6D_6): δ_C 23.9, 24.1, 26.7, 27.8 ((C$\underline{H}_3$)$_2$CH), 28.3, 28.4 ((CH$_3$)$_2$C$\underline{H}$), 41.5 ((C$\underline{H}_3$)$_2$N), 78.8 (methine CH), 124.4, 124.7, 125.5, 143.8, 144.3, 145.3 (aromatic C), 167.0 (imine

quaternary C) ppm. ^{119}Sn{^{1}H} NMR (186 MHz, C_6D_6): δ_{Sn} -18 ppm. EI-MS: (m/z, %): 595.0, weak $[M-H]^+$. Note: *The crystalline product decomposes rapidly even in an inert glovebox atmosphere, hence reliable IR data and micro-analysis results could not be obtained.*

5.4.2 General synthetic procedure for the preparation of N-nacnac-stabilised phosphaketenylgermylenes/stannylenes: To a suspension of Na(PCO)(dioxane)$_x$ (1.3 equiv.) in toluene (20 mL) at -78˚C, was added a solution of (**1-Ar**)ECl (0.2 mmol), also in toluene (20 mL), over a period of 5 min. The reaction mixture was slowly warmed to room temperature and stirred for 15 h (in the germylene case) or for 1 h (in the stannylene case). Volatiles were subsequently removed *in vacuo*, and the residual solid extracted into hexane (*ca.* 10 mL). Storage at -26˚C over several days produced light yellow crystals suitable for X-ray crystallography.

(**1-Dipp**)Ge(PCO): Yield 0.062 g, 51 %. ^{1}H NMR (400 MHz, C_6D_6): δ_H 1.04 (d, $^{3}J_{HH}$ = 6.7 Hz, 6H, (C$\underline{H}_3$)$_2$CH), 1.09 (d, $^{3}J_{HH}$ = 6.8 Hz, 6H, (C$\underline{H}_3$)$_2$CH), 1.33 (d, $^{3}J_{HH}$ = 6.6 Hz, 6H, (C$\underline{H}_3$)$_2$CH), 1.71 (d, $^{3}J_{HH}$ = 6.7 Hz, 6H, (C$\underline{H}_3$)$_2$CH), 2.21 (s, 12H, (C$\underline{H}_3$)$_2$N), 2.93 (virtual sept, $^{3}J_{HH}$ = 6.7 Hz, 2H, (CH$_3$)$_2$C$\underline{H}$), 4.16 (s, 1H, methine CH), 4.47 (virtual sept, $^{3}J_{HH}$ = 6.8 Hz, 2H, (CH$_3$)$_2$C$\underline{H}$), 7.02 (d, $^{3}J_{HH}$ = 7.6 Hz, 2H, *m*-H of Dipp), 7.07 (t, $^{3}J_{HH}$ = 7.6 Hz, 2H, *p*-H of Dipp), 7.13 (d, $^{3}J_{HH}$ = 7.6 Hz, 4H, *m*-H of Dipp) ppm. ^{13}C{^{1}H} NMR (100 MHz, C_6D_6): δ_C 24.1 (overlapping signals), 26.7, 28.3 ((C$\underline{H}_3$)$_2$CH), 30.5 (overlapping signals) ((CH$_3$)$_2$C$\underline{H}$), 41.0 ((C$\underline{H}_3$)$_2$N), 81.3 (d, methine CH, $^{4}J_{CP}$ = 9.2 Hz), 124.5, 125.7 (*m*-C of Dipp), 126.3 (*p*-C of Dipp), 143.5, 144.2, 146.2 (*o*-C and *ipso*-C of Dipp), 165.5 (imine quaternary C), 191.4 (d, $^{1}J_{CP}$ = 88 Hz, P$\underline{C}$O)

ppm. $^{31}P\{^{1}H\}$ NMR (162 MHz, C_6D_6): δ_P -317 ppm. IR (ATR, $\nu_{C\text{-}O}/cm^{-1}$): 1876. ESI-MS (*m*/*z*, %): 549.3, weak, $[M - PCO]^+$; accurate mass: calc. for $C_{31}H_{47}GeN_4$ ($[M - PCO]^+$) 549.3013, meas. 549.3028. Elemental microanalysis: calc. for $C_{32}H_{47}GeN_4OP$: C 63.28, H 7.80, N 9.22%, meas. C 63.42, H 7.96, N 9.18%.

(**1-Dipp**)Sn(PCO): Yield 0.024 g, 19 %. ^{1}H NMR (400 MHz, C_6D_6): δ_H 1.09 (d, $^{3}J_{HH}$ = 6.8 Hz, 6H, $(C\underline{H}_3)_2CH$), 1.12 (d, $^{3}J_{HH}$ = 6.8 Hz, 6H, $(C\underline{H}_3)_2CH$), 1.31 (d, $^{3}J_{HH}$ = 6.6 Hz, 6H, $(C\underline{H}_3)_2CH$), 1.63 (d, $^{3}J_{HH}$ = 6.8 Hz, 6H, $(C\underline{H}_3)_2CH$), 2.22 (s, 12H, $(C\underline{H}_3)_2N$), 2.99 (virtual sept, $^{3}J_{HH}$ = 6.8 Hz, 2H, $(CH_3)_2C\underline{H}$), 3.97 (s, 1H, methine CH), 4.38 (virtual sept, $^{3}J_{HH}$ = 6.6 Hz, 2H, $(CH_3)_2C\underline{H}$), 7.05-7.11 (m, 6H, aromatic protons) ppm. $^{13}C\{^{1}H\}$ NMR (100 MHz, C_6D_6): δ_C 24.0, 24.1, 27.0, 28.3, 28.5 ($(\underline{C}H_3)_2CH$), 29.7 (overlapping signals) ($(CH_3)_2\underline{C}H$), 41.3 ($(\underline{C}H_3)_2N$), 81.1 (methine CH), 124.6, 125.4, 125.9, 142.2, 144.2, 145.2 (aromatic carbons), 166.4 (imine quaternary C), 187.8 (P$\underline{C}$O, $^{1}J_{CP}$ = 90.4 Hz) ppm. $^{31}P\{^{1}H\}$ NMR (162 MHz, C_6D_6): δ_P -332 ppm (s, ^{117}Sn satellite with $^{1}J_{SnP}$ = 731 Hz, ^{119}Sn satellite with $^{1}J_{SnP}$ = 765 Hz). $^{119}Sn\{^{1}H\}$ NMR (186 MHz, C_6D_6): δ_{Sn} -120 ppm (d, $^{1}J_{SnP}$ = 765 Hz). Note: *The crystalline product decomposes rapidly even in an inert glovebox atmosphere, hence reliable IR data and micro-analysis results could not be obtained.*

5.4.3 Synthesis of the N,P-heterocyclic germylene ***4***: A sample of (**1-Dipp**)Ge(PCO) (100 mg, 0.165 mmol) in toluene (10 mL) was subjected to broadband UV irradiation for 6 h under ambient conditions, whereafter the solvent was removed under reduced pressure to yield a dark-red residue. This was re-dissolved in pentane, and recrystallization *via* storage at -26°C over the course of several days yielded the pure

product in crystalline form. ^{1}H NMR (400 MHz, C_6D_6): δ_H 1.02 (d, $^{3}J_{HH}$ = 6.9 Hz, 3H, $(C\underline{H}_3)_2CH$), 1.05 (d, $^{3}J_{HH}$ = 6.8 Hz, 3H, $(C\underline{H}_3)_2CH$), 1.09 (d, $^{3}J_{HH}$ = 6.9 Hz, 3H, $(C\underline{H}_3)_2CH$), 1.20 (d, $^{3}J_{HH}$ = 6.8 Hz, 3H, $(C\underline{H}_3)_2CH$), 1.22 (d, $^{3}J_{HH}$ = 6.8 Hz, 3H, $(C\underline{H}_3)_2CH$), 1.27 (d, $^{3}J_{HH}$ = 6.8 Hz, 3H, $(C\underline{H}_3)_2CH$), 1.30 (d, $^{3}J_{HH}$ = 7.0 Hz, 3H, $(C\underline{H}_3)_2CH$), 1.44 (d, $^{3}J_{HH}$ = 6.8 Hz, 3H, $(C\underline{H}_3)_2CH$), 2.09 (s, 3H, $(C\underline{H}_3)_2N$), 2.27 (s, 3H, $(C\underline{H}_3)_2N$), 2.46 (s, 3H, $(C\underline{H}_3)_2N$), 2.63 (s, 3H, $(C\underline{H}_3)_2N$), 3.90 (m, 1H, $(CH_3)_2C\underline{H}$), 4.19 (sept, $^{3}J_{HH}$ = 6.4 Hz, 1H, $(CH_3)_2C\underline{H}$), 6.94-7.22 (6H, aromatic CH) ppm. ^{31}P NMR (162 MHz, C_6D_6): δ_P -50 (d, $^{2}J_{PH}$ = 33 Hz) ppm.

5.5 References

[1] Selected reviews: a) S. Aldridge, A. J. Downs, *Chem. Rev.* **2001**, *101*, 3305–3365; b) S. K. Mandal, H. W. Roesky, *Acc. Chem. Res.* **2012**, *45*, 298–307; c) T. J. Hadlington, M. Driess, C. Jones, *Chem. Soc. Rev.* **2018**, *47*, 4176–4197.

[2] H. C. Brown, P. V. Ramachandran, *Reductions in Organic Synthesis*, American Chemical Society, **1996**, 1-30.

[3] Selected examples of reversible activation of organic substrates: a) R. Rodriguez, D. Gau, T. Kato, N. Saffon-Merceron, A. De Cõzar, F. P. Cossío, A. Baceiredo, *Angew. Chem. Int. Ed.* **2011**, *50*, 10414–10416; b) R. Rodriguez, D. Gau, Y. Contie, T. Kato, N. Saffon-Merceron, A. Baceiredo, *Angew. Chem. Int. Ed.* **2011**, *50*, 11492–11495; c) F. Lips, J. C. Fettinger, A. Mansikkamäki, H. M. Tuononen, P. P. Power, *J. Am. Chem. Soc.* **2014**, *136*, 634–637; d) T. J. Hadlington, M. Hermann, G. Frenking, C. Jones, *Chem. Sci.* **2015**, *6*, 7249–7257; e) R. Rodriguez, Y. Contie, R. Nouguï, A. Baceiredo, N. Saffon-Merceron, J. M. Sotiropoulos, T. Kato, *Angew. Chem. Int. Ed.* **2016**, *55*, 14355–14358; f) S. Wang, M. L. McCrea-Hendrick, C. M. Weinstein, C. A. Caputo, E. Hoppe, J. C. Fettinger, M. M. Olmstead, P. P. Power, *J. Am. Chem. Soc.* **2017**, *139*, 6596–6604.

[4] B. E. Eichler, P. P. Power, *J. Am. Chem. Soc.* **2000**, *122*, 8785–8786.

[5] T. J. Hadlington, B. Schwarze, E. I. Izgorodina, C. Jones, *Chem. Commun.* **2015**, *51*, 6854–6857.

[6] a) Y. Ding, H. Hao, H. W. Roesky, M. Noltemeyer, H. G. Schmidt, *Organometallics* **2001**, *20*, 4806–4811; b) L. W. Pineda, V. Jancik, K. Starke, R. B. Oswald, H. W. Roesky, *Angew. Chem. Int. Ed.* **2006**, *45*, 2602–2605; c) A. Jana, H. W. Roesky, C. Schulzke, A. Döring, *Angew. Chem. Int. Ed.* **2009**, *48*, 1106–1109.

[7] N.N. Greenwood, A. Earnshaw, *Chemistry of the Elements (2nd ed.)*, Butterworth-Heinemann , **1997**.

[8] L. Dostál, *Coord. Chem. Rev.* **2017**, *353*, 142–158.

[9] Selected examples: a) G. Becker, G. Gresser, W. Uhl, *Z. Naturforsch., B: Chem. Sci.* **1981**, *36*, 16–19; b) G. Märkl, H. Sejpka, *Angew. Chem. Int. Ed.* **1986**, *25*, 264–264; c) A. M. Arif, A. R. Barron, A. H. Cowley, S. W. Hall, *J. Chem. Soc., Chem. Commun.* **1988**, 171-172; d) P. B. Hitchcock, C. Jones, J. F. Nixon, *J. Chem. Soc., Chem. Commun.* **1994**, 2061-2062; e) J.-C. Guillemin, L. Lassalle, P. Dréan, G. Wlodarczak, J. J. Demaison, *J. Am. Chem. Soc.* **1994**, *116*, 8930-8936; f) M. Finze; E. Bernhardt; H. Willner, C. W. Lehmann, *Angew. Chem. Int. Ed.* **2004**, *43*, 4160-4163.

[10] a) E. Niecke, M. Nieger, F. Reichert, *Angew. Chem. Int. Ed.* **1988**, *27*, 1715–1716; b) M. Kuprat, A. Schulz, A. Villinger, *Angew. Chem. Int. Ed.* **2013**, *52*, 7126–7130.

[11] L. Liu, D. A. Ruiz, D. Munz, G. Bertrand, *Chem* **2016**, *1*, 147–153.

[12] M. M. Hansmann, R. Jazzar, G. Bertrand, *J. Am. Chem. Soc.* **2016**, *138*, 8356–8359.

[13] S. Inoue, W. Wang, C. Präsang, M. Asay, E. Irran, M. Driess, *J. Am. Chem. Soc.* **2011**, *133*, 2868–2871.

[14] a) S. Yao, Y. Xiong, T. Szilvási, H. Grützmacher, M. Driess, *Angew. Chem. Int. Ed.* **2016**, *55*, 4781–4785; b) Y. Wu, L. Liu, J. Su, J. Zhu, Z. Ji, Y. Zhao, *Organometallics* **2016**, *35*, 1593–1596; c) N. Del Rio, A. Baceiredo, N. Saffon-Merceron, D. Hashizume, D. Lutters, T. Müller, T. Kato, *Angew. Chem. Int. Ed.* **2016**, *55*, 4753–4758; d) Y. Xiong,

S. Yao, T. Szilvási, E. Ballestero-Martínez, H. Grützmacher, M. Driess, *Angew. Chem. Int. Ed.* **2017**, *56*, 4333–4336; e) S. Yao, Y. Grossheim, A. Kostenko, E. Ballestero-Martínez, S. Schutte, M. Bispinghoff, H. Grützmacher, M. Driess, *Angew. Chem. Int. Ed.* **2017**, *56*, 7465–7469; f) A. Hinz, J. M. Goicoechea, *Chem. Eur. J.* **2018**, *24*, 7358–7363.

[15] D. Heift, Z. Benkő, H. Grützmacher, *Dalton Trans.* **2014**, *43*, 831.

[16] a) M. Dräger, J. Escudié, C. Couret, H. Ranaivonjatovo, J. Satge, *Organometallics* **1988**, *7*, 1010–1013; b) V. Y. Lee, M. Kawai, A. Sekiguchi, H. Ranaivonjatovo, J. Escudié, *Organometallics* **2009**, *28*, 4262–4265.

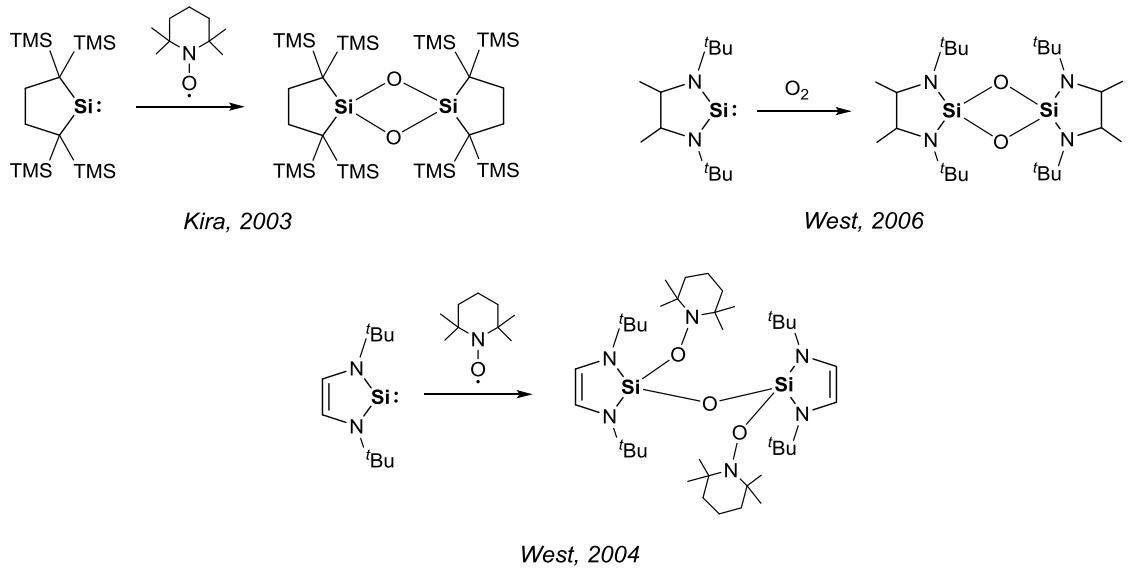
[17] a) I. L. Fedushkin, M. Hummert, H. Schumann, *Eur. J. Inorg. Chem.* **2006**, 3266–3273; b) A. Mcheik, N. Katir, A. Castel, H. Gornitzka, S. Massou, P. Rivière, T. Hamieh, *Eur. J. Inorg. Chem.* **2008**, 5397–5403; c) S. P. Chia, Y. Li, R. Ganguly, C. W. So, *Eur. J. Inorg. Chem.* **2014**, 526–532.

CHAPTER 6

THE OXIDATION AND SUBSTITUTION CHEMISTRY OF A *N*-NACNAC STABILISED CHLOROSILYLENE

6.1 Introduction

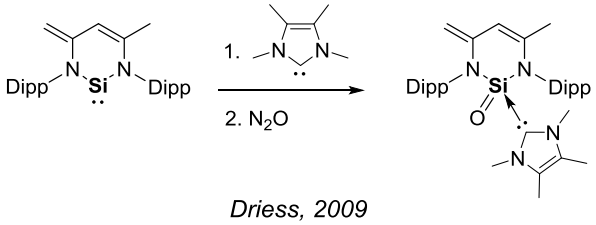
Ketones, $(R_1)(R_2)C{=}O$, are molecules which belong to the family of carbonyl compounds, and are widely employed in organic synthesis as one of the most important building-block molecules, thanks in part to their versatility and robustness under ambient conditions.[1] On the other hand, their silicon counterparts, $(R_1)(R_2)Si{=}O$ (herein referred to as *sila*-ketones/*silanones*), are known to be transient in nature, rendering their synthesis and characterisation more challenging. Generally, the instability of silanones is attributed to the poor π-overlap between the silicon-3*p*/oxygen-2*p* orbitals, and the marked difference in the electronegativities (Si – 1.90, O – 3.44, Pauling scale),[2] which lead to a significant degree of polarisation across the silicon-oxygen bond. Such zwitterionic character ($Si{=}O \leftrightarrow Si^{\delta+}{-}O^{\delta-}$) provides the impetus for oligo/polymerisation, leading to the generation of polysiloxanes, the formation of which is thermodynamically favourable.[3] This is reflected in the overwhelming prevalence of Si—O *single* bonds in Main Group chemistry, and the small number of reports on silicon-oxygen multiple bonding.[4]



Scheme 6.1 Early attempts at silylene oxidation, resulting in compounds featuring Si—O bridges

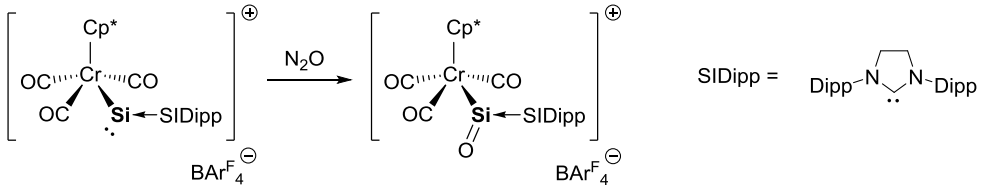
The earliest records of research on compounds potentially bearing a Si=O unit date back to the 1860s with the pioneering work of Friedel and Crafts,[5] which was followed by further synthetic investigations by Kipping three decades later.[6] Although lacking definitive structural elucidation, the results obtained from ebullioscopic experiments and boiling point measurements of these "silanones" (as referred to at that time) suggested that they were, in fact, Si_3O_3 trimers.[6b] Subsequent experiments utilising cryogenic techniques, such as matrix trapping at liquid N_2 temperature (-196°C), enabled the isolation of transient silanone species, which could be characterised by IR spectroscopy – typically *via* a signature Si=O stretching band at 1150 – 1300 cm^{-1}.[7] Alternatively, evidence for the metastable *sila*-formaldehyde molecule ($H_2Si=O$) could be obtained from mass spectrometry and millimetre-wave rotational spectroscopy in the gas phase.[8] Thereafter, the successful isolation of several stable silylenes [3f,9] has offered the potential for systematic access to silanones, *via* direct oxidation of the corresponding Si^{II}

precursor. At the outset, this strategy was often found to generate (undesired) compounds containing siloxo-bridges, including four-membered cyclic siloxanes, which can be considered as the formal head-to-tail dimer of the elusive sila-ketone (Scheme 6.1).[9c,10] In part, this reflects the perennial challenges of taming the polarisation of the silicon-oxygen bond, and preventing the monomeric silanone form from undergoing intermolecular association. To overcome these problems, strongly electron-donating and sterically encumbered Si-substituents have been extensively explored, which quench the electronic deficiency of the silicon centre and discourage polymerisation. As a result, recent years have witnessed a surge in the number of structurally-characterised (base-stabilised) silanones (Scheme 6.2).[11]



Driess, 2009

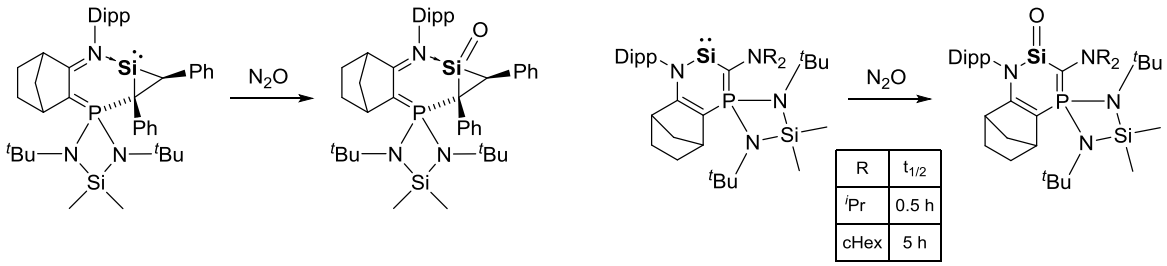
DIAMIDO and NHC



Filippou, 2014

ELECTRON-RICH TRANSITION METAL FRAGMENT

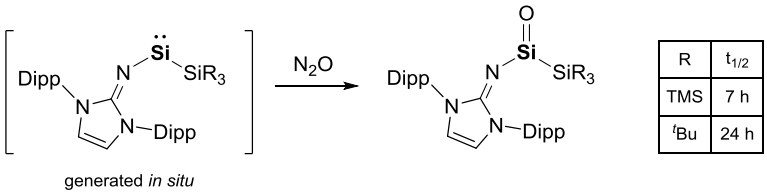
and NHC



Baceiredo and Kato

2013 **DIALKYL and IMINE**

2017 **AMINO and YLIDE**



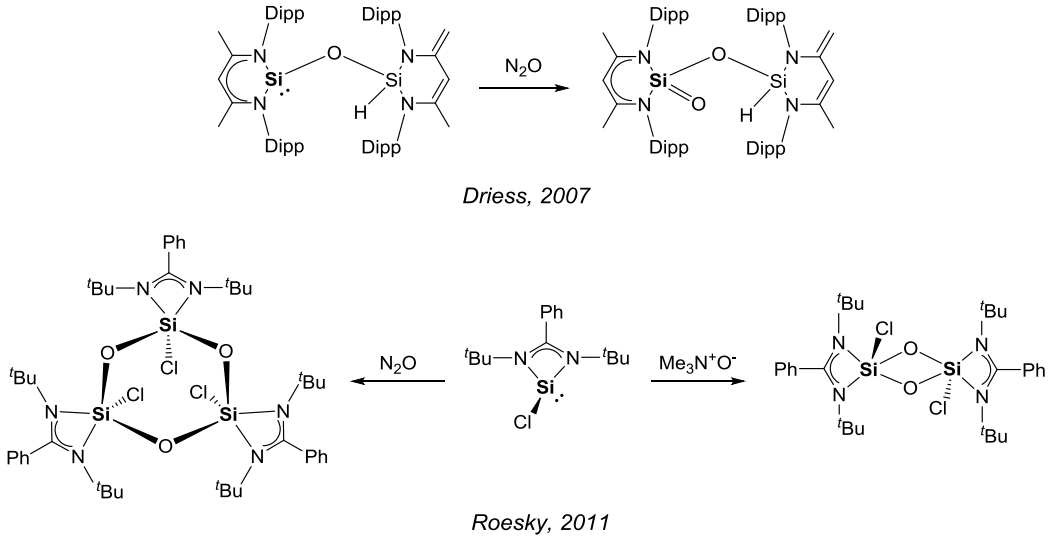
Inoue, 2017

N-HETEROCYCLIC IMINO and SILYL

Scheme 6.2 Prominent examples of (base-stabilised) silanones, synthesised *via* oxidation of the corresponding silylene precursors

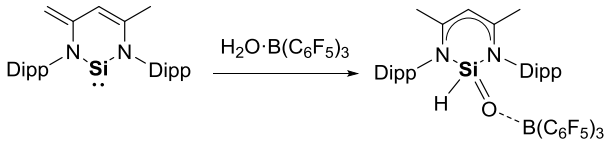
Compared to sila-ketones, silicon analogues of other fundamental members of the carbonyl family (acyl chlorides, aldehydes, esters etc.) remain rather under-investigated.[11e,12] Drawing analogies from the oxidative synthetic route

utilised for the silanones outlined above, this can be attributed to the paucity of silylene species bearing hydride, chloride, or alkoxide substituents, even in a base-stabilised form, (R)(L)Si(X) (X = H, Cl, OR').[12a,13] Moreover, the target *sila*-carbonyl complexes, in particular the *sila*-aldehyde and *sila*-acyl chloride, can be expected to possess a lower degree of steric protection, due to the smaller sizes of the X groups, compared to bulkier R substituents. With respect to the chloride function, its intrinsic electron-withdrawing capability would also be expected to increase the electrophilicity of the silicon centre, and further polarise the Si=O bond in the sila-acyl chloride molecule. This in turn would be expected to destabilise the monomeric form with respect to aggregation. Such factors are illustrated by two previous attempts to oxidise a monochlorosilylene complex reported by Roesky and co-workers. Reactions of the amidinate stabilised system {PhC(N^{t}Bu)$_2$}SiCl with O-atom sources resulted in either dimerisation or trimerisation of the putative sila-acyl chloride intermediate (Scheme 6.3).[14]

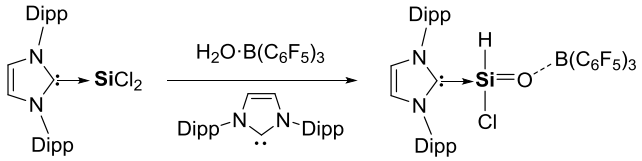


Scheme 6.3 Oxidation attempts of base-stabilised alkoxo- and chlorosilylene

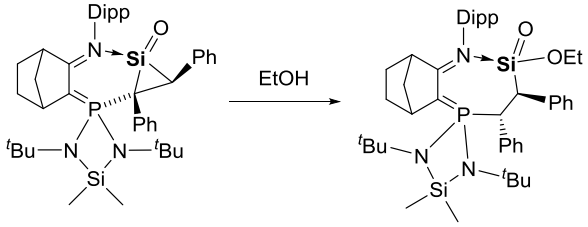
In fact, while there is an existing example of a *sila*-ester synthesised *via* direct oxidation of the corresponding siloxo-silylene (Scheme 6.3),[12a] the majority of reports of other sila-carbonyl analogues bearing a —Si(O)(X) unit have exploited alternative synthetic methodologies. One approach which has been employed with silylene systems stabilised by either a Nacnac-derived *N*,*N*′-dianionic chelate or an NHC donor, is the reaction with a Lewis acid-water adduct (*e.g* $H_2O{\cdot}B(C_6F_5)_3$, Scheme 6.4), which facilitates the formation of the —Si[O{$B(C_6F_5)_3$}](X) containing product.[12b,12d,12e] The additional coordination of $B(C_6F_5)_3$ reflects the partial negative charge on the oxygen atom in the polar $Si^{\delta+}—O^{\delta-}$ bond, which readily takes up the electrophilic Lewis acidic borane from the reaction mixture. Ligand-heteroelement cooperative reactivity is another strategy utilised by the groups of Baceiredo and Kato, and involves treatment of a pre-formed —$Si(=O)_n$ containing system with either EtOH (n = 1) or a silane source (n = 2) to afford the corresponding sila-esters (Scheme 6.4).[11e,12f]



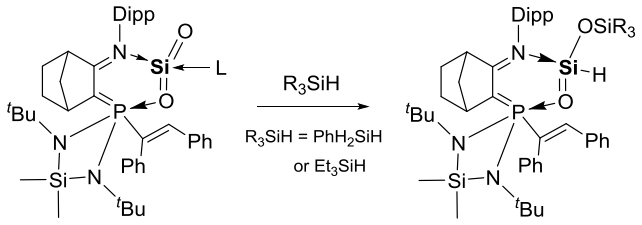
Driess, 2007



Roesky, 2012



Baceiredo and Kato, 2013



Baceiredo and Kato, 2017

Scheme 6.4 Alternative synthetic approaches for compounds bearing an −Si(O)(X) unit

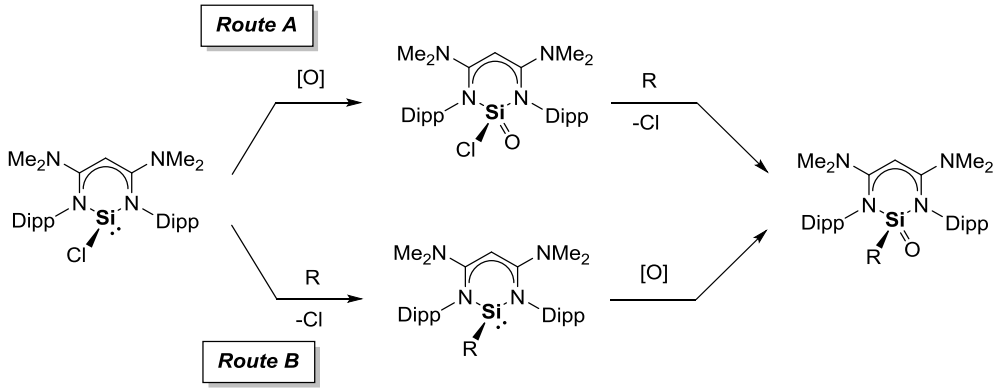
It has been shown that access to systems containing a Lewis acid-free −Si(O)(X) function *via* the direct oxidation route is thus far only viable with X being an electron-donating OR group.[12a] As a result, the challenge remains to generate other sila-carbonyl compounds, utilising a facile oxidation process from the corresponding silylene starting materials. In particular, with analogies to classical organic chemistry, sila-acyl chlorides would serve as powerful synthons in the chemistry of heavier Group 14 carbonyl analogues, thanks to the lability of the

chloride substituent in a range of functional group transformations.[15] Thus, having synthesised the chlorosilylene (**1-Dipp**)SiCl, its oxidation-substitution chemistry was targeted, with a view to isolating a series of sila-carbonyl species featuring a common ligand scaffold. Most importantly, the propensity of the sila-acyl chloride to undergo functional group exchange was to be investigated, in order to provide a direct comparison with the analogous chemistry of classical carbonyl systems.

6.2 Results and Discussion

6.2.1 Syntheses of sila-carbonyl species by oxidation-substitution

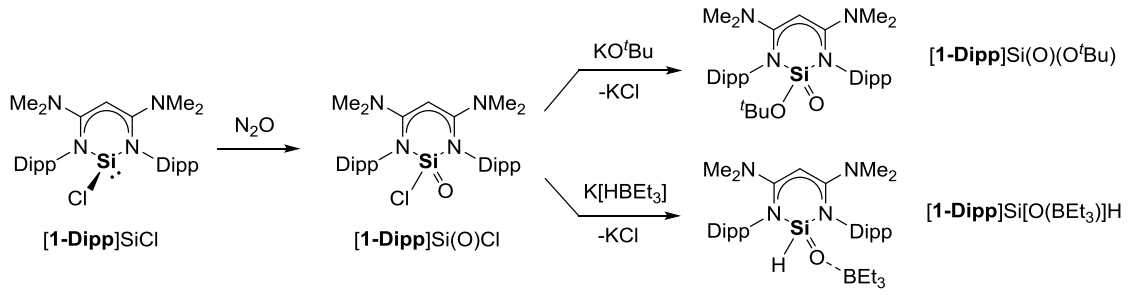
With the chlorosilylene (**1-Dipp**)SiCl in hand, two synthetic strategies were proposed for the target sila-carbonyl systems (**1-Dipp**)Si(O)R, which comprise the same combination of salt metathesis and oxidation reactions, but carried out in a different order (Routes A and B, Scheme 6.5).



Scheme 6.5 Proposed synthetic strategies towards *N*-nacnac-stabilised sila-carbonyl complexes

At the outset, Route A (oxidation-substitution) was first considered. Accordingly, (**1-Dipp**)SiCl was subjected to mild oxidation by N_2O under ambient conditions, after which crystallographic studies reveal the identity of the isolated product to be the monomeric sila-acyl chloride (**1-Dipp**)Si(O)Cl (Scheme 6.5). Unlike

a previously reported (borane-coordinated) sila-formyl chloride [(IDipp)Si{O(BC_6F_5)$_3$(H)(Cl)}] (Scheme 6.4),[12e] extra stabilisation from a Lewis acid is not observed at the −Si(O)Cl unit, and the compound shows no signs of decomposition upon prolonged storage in an inert atmosphere. Not only does this underline the advantage of the synthetic protocol employed for the preparation of (**1-Dipp**)Si(O)Cl, which is both straightforward and avoids the unwanted inclusion of Lewis acids, but in a practical sense it also enables further chemistry to be explored with this system. Accordingly, the versatility of (**1-Dipp**)Si(O)Cl towards functional group exchange can be demonstrated by its facile conversion into the corresponding (borane-stabilised) sila-aldehyde (**1-Dipp**)Si[O(BEt_3)]H and sila-ester (**1-Dipp**)Si(O)(O^{t}Bu), through treatment with K[$HBEt_3$] or KO^{t}Bu, respectively (Scheme 6.6). These transformations represent the first demonstration of systematic access from a sila-acyl chloride to other sila-carbonyl analogues featuring a common ligand platform *via* Si-centred nucleophilic substitution.



Scheme 6.6 Oxidation-substitution route employed for the synthesis of the sila-carbonyl species

Spectroscopically, the ^{29}Si{^{1}H} NMR signals associated with all three *N*-nacnac-stabilised sila-carbonyls are found in the range -60 to -80 ppm, which is consistent with those reported previously for four-coordinate sila-carbonyl species (typically -50 to -90 ppm).[11a-e,12a-e] Whatismore, these signals are shifted upfield

from that of the chlorosilylene precursor (δ_{Si} = 2 ppm), a finding which is consistent with the conversion of a Si^{II} system to a related sila-carbonyl complex (*cf.* 88 ppm for the "backbone-deprotonated" Nacnac-supported diamidosilylene, and -85 ppm for the derived silanoic ester, Scheme 6.3).[12a] Evidence for the Si-bound hydride in the sila-aldehyde compound (**1-Dipp**)Si[O(BEt_3)]H can be obtained from ^{1}H NMR (δ_{SiH} = 4.88 ppm, silicon satellites with $^1J_{SiH}$ = 289 Hz) and IR spectroscopy (ν_{Si-H} = 2219 cm^{-1}). These values are comparable with the spectroscopic parameters associated with the Si-bound hydride in a closely-related (borane-capped) ^{Dipp}Nacnac-stabilised sila-aldehyde (δ_{SiH} = 5.64 ppm, ν_{Si-H} = 2223 cm^{-1}, Scheme 6.4).[12b] Perhaps of greater spectroscopic interest for comparative purposes are the IR stretching frequencies of the Si=O bonds in the newly-synthesised sila-carbonyl complexes. These fall in the range 1120 – 1160 cm^{-1}, and are thus broadly in line with the handful of reported values for systems bearing a Si=O unit.[11b,11c,12b] The lower stretching frequency in the case of (**1-Dipp**)Si[O(BEt_3)]H (1129 cm^{-1}) can be attributed to the additional coordination of the O-bound borane function, which intrinsically weakens the Si=O bond. Consistently, the Lewis acid-free sila-acyl chloride and sila-ester are characterized by Si=O stretches at higher wavenumbers (1157 and 1145 cm^{-1}, respectively).

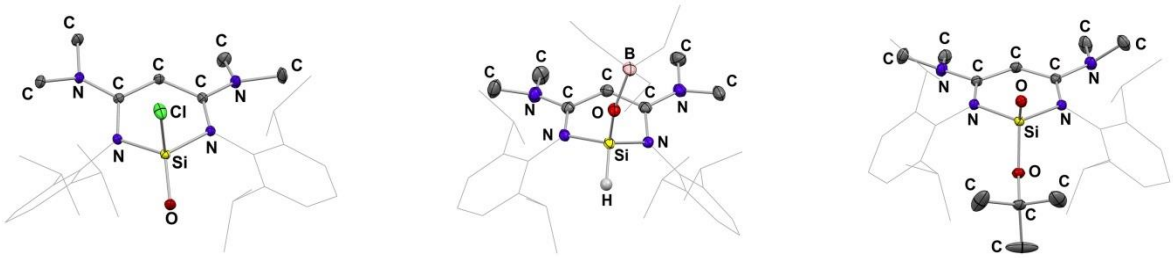


Figure 6.1 (*from left*) Solid-state structures of(**1-Dipp**)Si(O)Cl, (**1-Dipp**)Si[O(BEt$_3$)]H, and (**1-Dipp**)Si(O)(O^{t}Bu) as determined by X-ray crystallography. Thermal ellipsoids are shown at 35 % probability level. *N*-bound aromatic substituents are represented in the wireframe format, and all hydrogens have been omitted for clarity, with the exception of the Si-bound hydride.

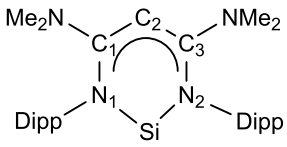
	(**1-Dipp**)Si(O)Cl [a,b]	(**1-Dipp**)Si[O(BEt$_3$)]H [c]	(**1-Dipp**)Si(O)(O^{t}Bu) [d]
d(Si=O)	1.5280(14) / 1.5329(14)	1.5514(10)	1.5367(12)
d(Si—N1) / *d*(Si—N2)	1.7626(15) /1.7880(15), 1.7619(15) / 1.7906(16)	1.7815(12) / 1.7711(12)	1.8028(13) / 1.8155(13)
∠ (N1—Si—N2)	103.41(7) / 103.61(7)	101.44(6)	100.39(6)

Table 6.1 Selected bond lengths (Å) and angles (°) of *N*-nacnac-stabilised sila-carbonyl compounds, as determined by X-ray crystallography. Note: [a] There are two molecules in an asymmetric unit; [b] *d*(Si—Cl) = 2.0976(6)/2.0891(6) Å ; [c] *d*(B—O) = 1.5639(19) Å; [d] *d*(Si—O(^{t}Bu)) = 1.6431(11) Å

Definitive characterisation by X-ray crystallography allows for a systematic structural comparison between the three newly-synthesised sila-carbonyl complexes, each of which features the (*N*-nacnac)Si(O) fragment. The silicon-oxygen (formal) double bond distances are of particular interest (Figure 6.1 and Table 6.1). Thus, the shorter Si=O bond lengths are associated with the Lewis acid-free sila-acyl chloride and sila-ester (1.5280(14)/1.5329(14) Å and 1.5367(12) Å respectively). Moreover, these values are remarkably close to those measured for more reactive

three-coordinate silanone systems, as reported by the groups of Baceiredo (1.527(3) /1.533(1) Å)[11i] and Inoue (1.537(3) Å, Figure 6.2).[11j] Notably, the Si=O distance in (**1-Dipp**)Si(O)(O^{t}Bu) is markedly shorter than the corresponding distance in the analogous Nacnac-derived silanoic ester (^{Dipp}Nacnac)Si[OB(C_6F_5)$_3$]H (1.579(3) Å), first isolated by Driess and co-workers in 2007.[12a] On the other hand, there is a *ca.* 2% elongation of the Si=O distance in the complex (**1-Dipp**)Si[O(BEt$_3$)]H (1.5514(10) Å) compared to the sila-acyl chloride and sila-ester. Consistent with the IR-derived $\nu_{Si=O}$ stretching frequencies, the weaker/longer silicon-oxygen bond in the sila-aldehyde can be accredited to the additional coordination of the borane function. That said, the relatively long B—O separation of 1.5639(19) Å (*cf.* 1.503(3) Å in the sila-ester (^{Dipp}Nacnac)Si[OB(C_6F_5)$_3$]H) implies that the perturbation of the Si=O unit is not huge.[12a,12b,16] Structurally, the three sila-carbonyl species all feature shorter Si—N bonds and more acute N—Si—N bite angles compared to (**1-Dipp**)SiCl, which is in line with the change in oxidation state of silicon from Si^{II} to Si^{IV}. Among the two Lewis acid-free complexes, the slightly stronger electron-donating capability of ^{t}BuO$^-$ (over Cl$^-$) is thought to result in a slightly less electrophilic Si^{IV} centre in the sila-ester, compared to the sila-acyl chloride. This is accordingly reflected by longer Si—N bonds (1.8028(13) / 1.8155(13) Å, *cf.* 1.7626(15) /1.7880(15) and 1.7619(15) / 1.7906(16) Å in (**1-Dipp**)Si(O)Cl), longer Si=O bond (1.5367(12)Å, *cf.* 1.5280(14) / 1.5329(14) Å in (**1-Dipp**)Si(O)Cl), and a narrower N—Si—N angle (100.39(6)°, *cf.* 103.41(7)° / 103.61(7)° in (**1-Dipp**)Si(O)Cl).

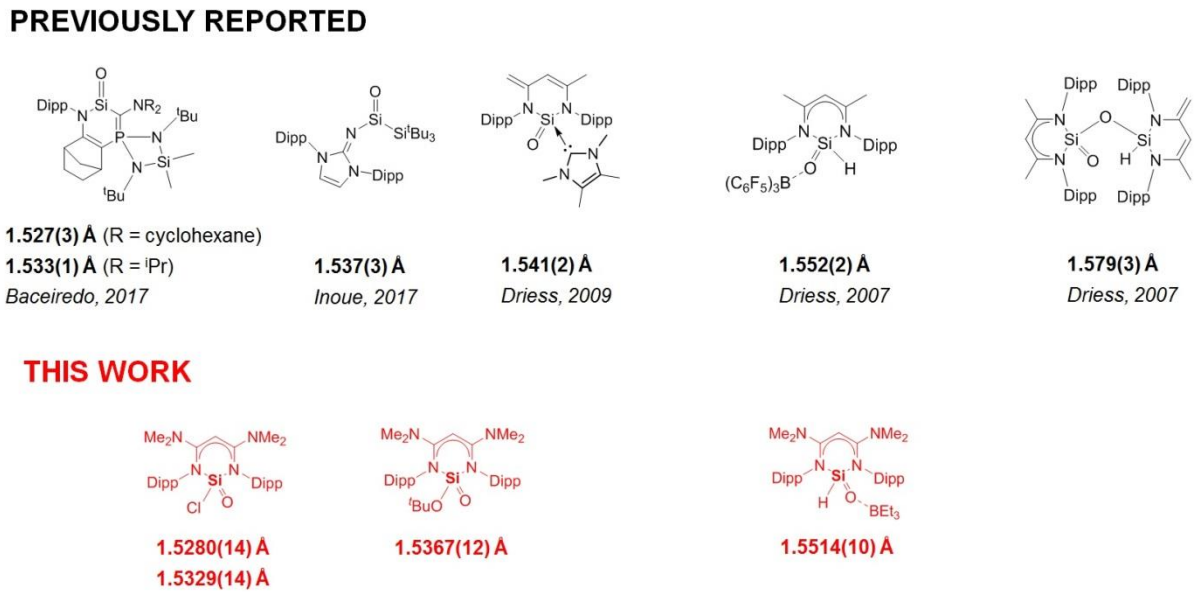


Figure 6.2 A summary of Si=O bond distances in the *N*-nacnac-stabilised sila-carbonyl complexes and selected reported examples

In order to shed further light on the nature of the silicon-oxygen bonds in these new compounds, and postulate plausible mechanism(s) for nucleophilic substitution at the Si^{IV} centre, DFT calculations were carried out at PBE1PBE/Def2-TZVP level of theory. Frontier orbital studies of the optimised sila-acyl chloride and sila-ester species reveal limited contribution from the silicon-based orbitals to the four highest occupied orbitals (HOMO, HOMO-1, HOMO-2, HOMO-3) within the Si=O fragment (Figure 6.3). By contrast, the contribution from the oxygen to these occupied orbitals is very significant, in keeping with the predicted polarity of the Si=O bond. Additionally, the Wiberg bond indices of these species, obtained from NBO analyses, are considerably less than 2 (sila-acyl chloride: 1.0993; (borane-coordinated) sila-aldehyde: 0.7955; sila-ester: 1.0441). These observations presumably reflect the major contribution of the zwitterionic resonance structure ($Si^{\delta+}—O^{\delta-}$), compared to the carbonyl-like Si=O form, in donor-supported silanones and related complexes.[18]

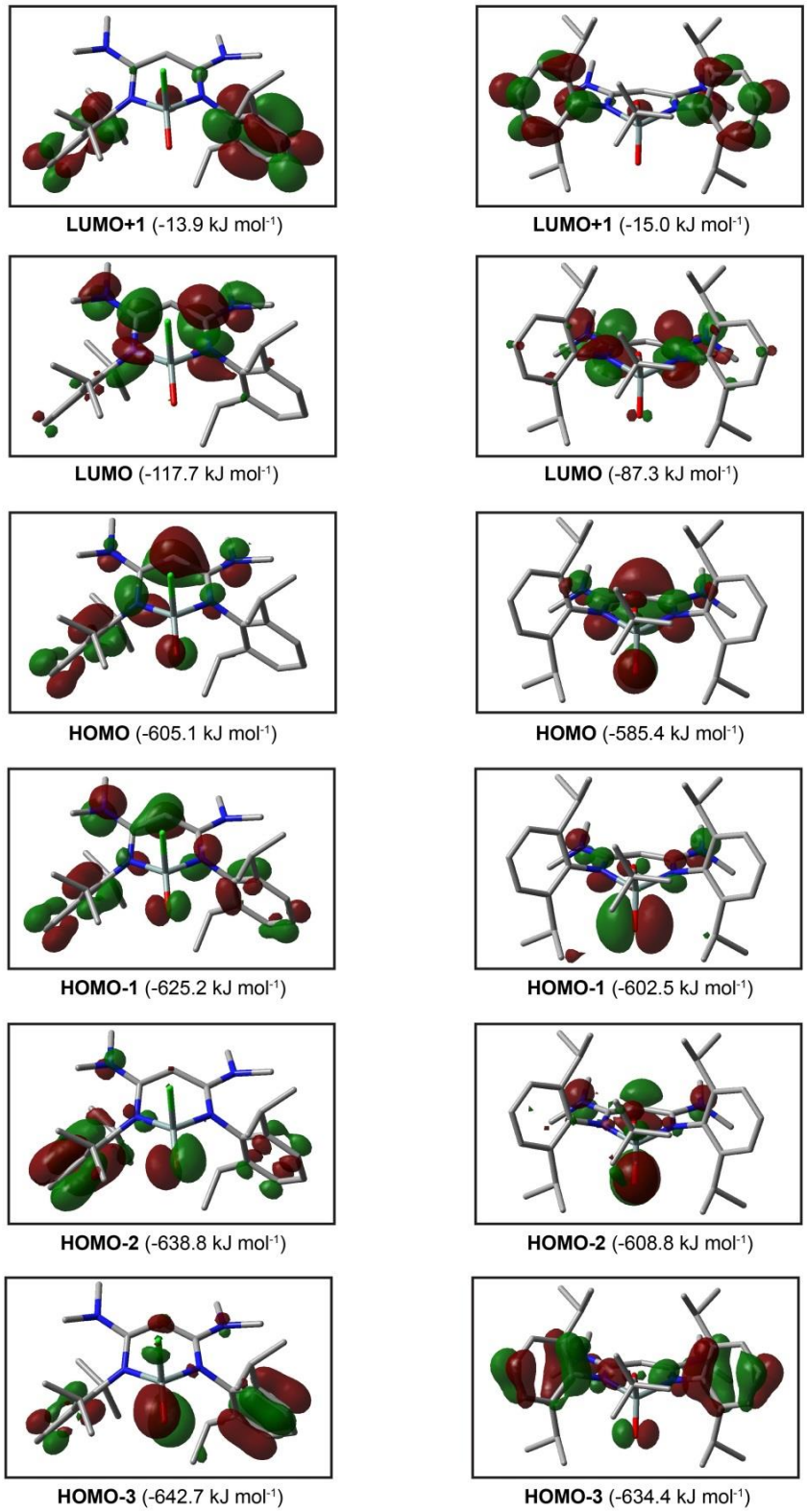


Figure 6.3 Frontier orbitals of the (**1-Dipp**)Si(O)Cl (*left*) and (**1-Dipp**)Si(O)(O^{t}Bu) (*right*), set at the iso-surface value of 0.04 (generated by the GaussView programme)

Notably, while the LUMO is predominantly located at the NC_3N ligand backbone, the LUMO+1 has a contribution from a vacant orbital of silicon. This is particularly important for the sila-acyl chloride, as it hints at a plausible nucleophilic substitution mechanism for the transformation to the sila-ester, involving an attack of an electron-rich fragment (^{t}BuO$^-$) on this empty orbital. To test this hypothesis, mechanistic investigations on the Si-centred substitution process (and in particular, the transformation from the sila-acyl chloride to the sila-ester) were carried out using a simplified ligand-substrate model (MeO^- anion and the (^{Ph}N-nacnac)-substituted sila-acyl chloride (**1-Ph**)Si(O)Cl in place of the ^{t}BuO$^-$/(**1-Dipp**)Si(O)Cl combination) for computational efficiency. The solvent environment was modelled after toluene using the SCRF (PCM) method. The reaction is proposed to occur *via* an S_N2-like pathway, in which nucleophilic attack of the methoxide anion on the electrophilic Si^{IV}-centre proceeds *via* a penta-coordinate, quasi-trigonal bipyramidal silicon transition state (Figure 6.5). That this transition state is only *ca.* 55 kJ mol^{-1} higher in (free) energy compared to the starting materials (and the overall process is substantially exoergic to the tune of -192.5 kJ mol^{-1}) is consistent with the facile nature of this transformation, which proceeds readily under ambient conditions. For further comparison, an S_N1-like mechanism was also considered, which involves the formation of a putative *sila*-acylium intermediate [(**1-Ph**)SiO]$^+$. However, the excessive energy barrier associated with the generation of such species (+368.5 kJ mol^{-1}) suggests that this pathway is unlikely to be feasible in practice.

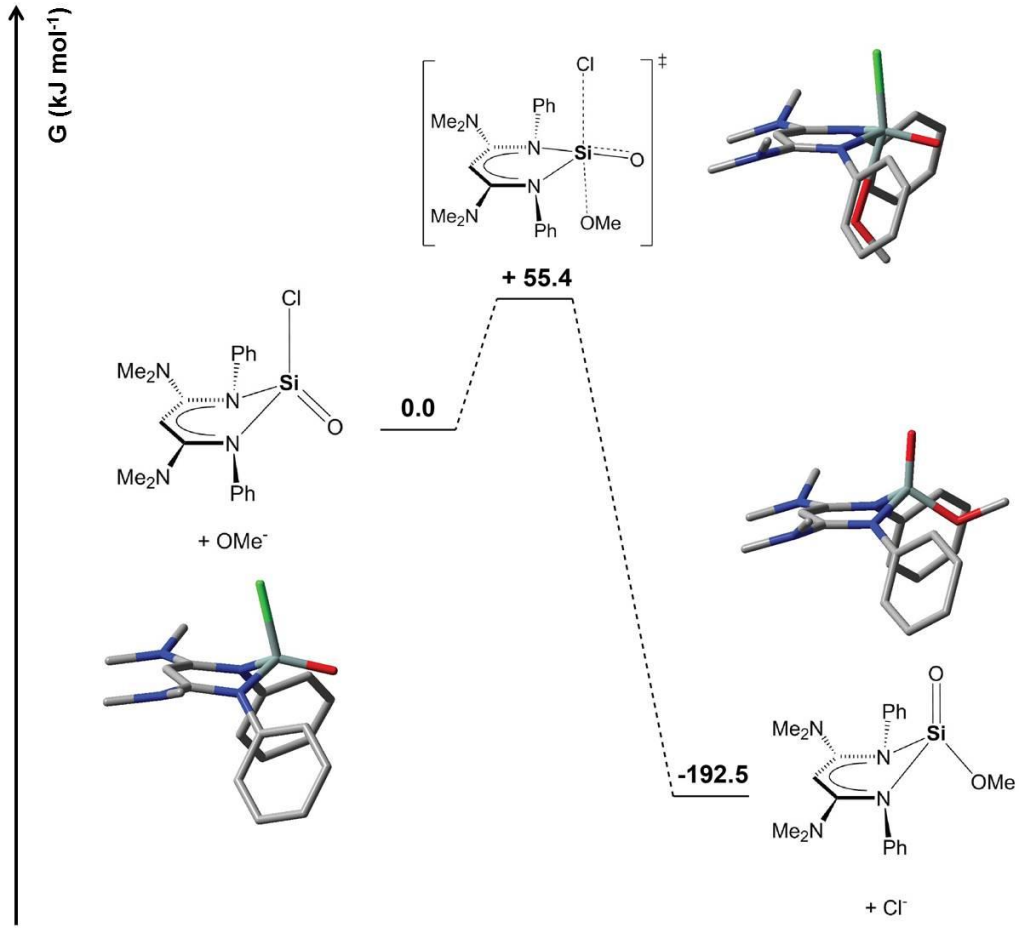
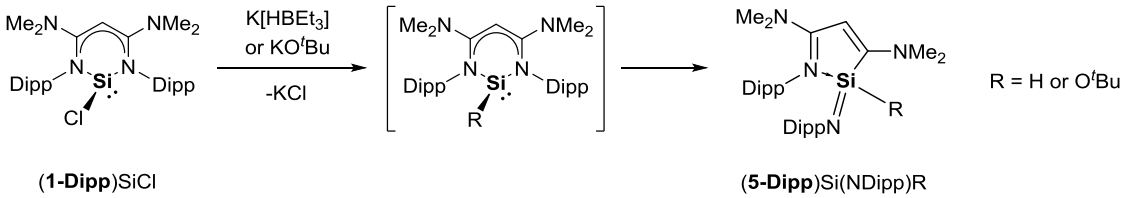


Figure 6.4 The proposed S_N2-like mechanism of the nucleophilic sila-acyl substitution process

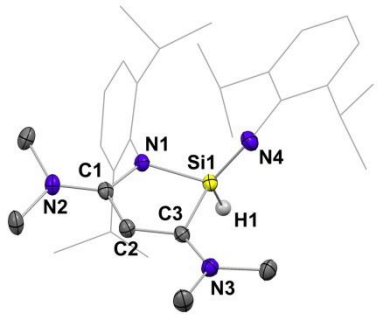
6.2.2 Ring-contraction chemistry initiated by ligand exchange with the chlorosilylene

Having established the viability of the oxidation-substitution route for the synthesis of *N*-nacnac-stabilised sila-carbonyl compounds, the viability of the reverse methodology (Route B - substitution-oxidation, Scheme 6.5) was subsequently examined – with differing results. Unexpectedly, salt metathesis between (**1-Dipp**)SiCl and sources of hydride (K[HBEt$_3$]) or alkoxide (KO^{t}Bu) are shown to afford the five-membered Si^{IV} complexes (**5-Dipp**)Si(NDipp)R (R = H, O^{t}Bu) instead of the simple substitution products (**1-Dipp**)SiR.



Scheme 6.7 Salt metathesis reactions of (**1-Dipp**)SiCl with sources of hydride and *tert*-butoxide

The change in the oxidation state is signaled by a marked shift in $^{29}Si\{^{1}H\}$ resonance, from the positive region (*ca.* 2 ppm) for the chlorosilylene to an upfield range of -70 to -90 ppm for the hydrido-/alkoxo-silane complexes, which is characteristic of tetravalent silicon species.[4] Moreover, a common spectroscopic pattern is evident in the ^{1}H NMR spectrum of both five-membered heterocycles (apart from the signals associated with the Si-bound R groups), which reflects a lowering of molecular symmetry with respect to the chloro precursor. As such, there are six Dipp methyl (integrating in the ratio 1:1:1:1:2:2) and three amino methyl resonances (1:1:2) observed for the (**5-Dipp**)Si(NDipp)R compounds (R = H, O^{t}Bu), compared to four equally intense Dipp methyl resonances, and a single NMe_2 signal in the case of (**1-Dipp**)SiCl. Additionally, the identity of the Si^{IV}-bound hydride in (**5-Dipp**)Si(NDipp)H is confirmed by both ^{1}H NMR (δ_{SiH} = 6.14 ppm, silicon satellites with $^{1}J_{SiH}$ = 234 Hz) and IR spectroscopy (ν_{Si-H} = 2050 cm^{-1}).



Bond lengths:

Si1—N4: 1.5764(14); Si1—N1: 1.8184(12); Si1—C3: 1.9011(15); N1—C1: 1.3597(18); C1—C2: 1.431(2); C2—C3: 1.380(2); C1—N2: 1.3431(19); C3—N3: 1.3341(19)

Angles:

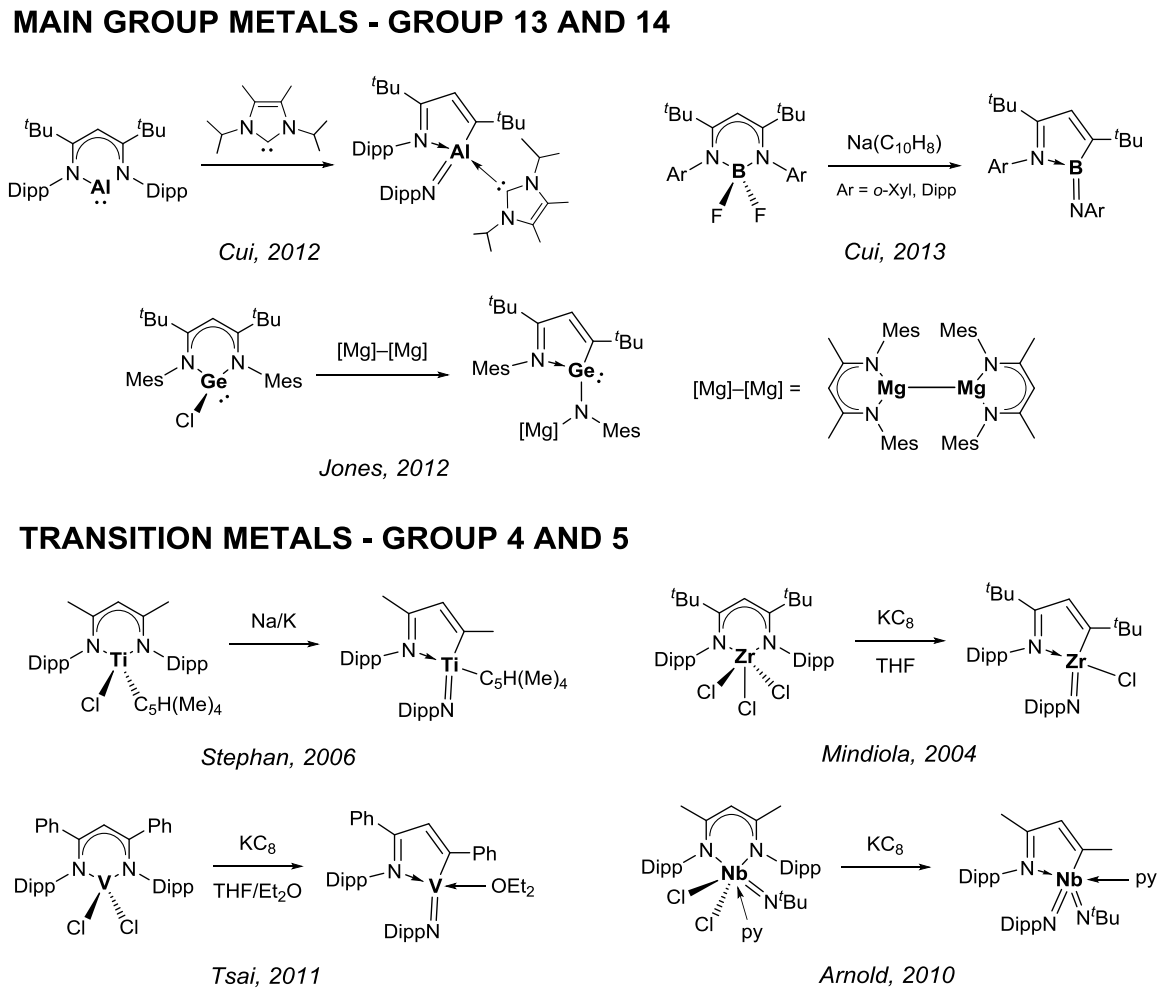
Si1—N1—C1: 111.59(9); N1—C1—C2: 115.91(12); C1—C2—C3: 114.60(13); C2—C3—Si1: 108.79(11); C3—Si1—N1: 88.79(6); Si1—N4—C_{ipso}: 172.37(14)

Figure 6.5 (*left*) Solid-state structures of (**5-Dipp**)Si(NDipp)H, as determined by X-ray crystallography. Thermal ellipsoids are shown at 35 % probability level. *N*-bound aromatic substituents are represented in the wireframe format, and all hydrogens have been omitted for clarity, with the exception of the Si-bound hydride; (*right*) selected bond lengths (Å) and angles (°)

While obtaining single crystals of the silyl-alkoxide proves to be problematic, (**5-Dipp**)Si(NDipp)H can readily be recrystallised from methylcyclohexane, and subsequently analysed by X-ray crystallography (Figure 6.5). The solid-state structure of the hydride species features a near-planar five-membered $SiNC_3$ heterocycle (sum of all angles = 539.7°), which subtends relatively small torsion angles with the least-squares planes of the two NMe_2 functions (5.0° and 13.9°). Within the heterocycle, the imine C=N and C—NMe_2 distances fall in the range 1.3341(19) – 1.3597(18) Å, and the C—C bond lengths (1.380(2) Å and 1.431(2) Å) fall between the domains of isolated C—C single and double (1.34 – 1.54 Å) bonds.[2] These observations hint at extended π-delocalisation across the amino functions and the five-membered ring. Crystallographic studies also reveal an almost-linear exocyclic Si=N—C(*ipso*) unit (172.37(14)°) and a very short Si=N distance of 1.5765(14) Å, which is typical of known silicon-nitrogen double bonds (1.568 – 1.714 Å).[17] Overall, the solid-state structure of (**5-Dipp**)Si(NDipp)H reflects

its description as an imidohydrido-silane, stabilised by a monoanionic *N,C*-azabutadiene ligand.

The formation of the rearranged species (**5-Dipp**)Si(NDipp)R (as determined by NMR spectroscopy and/or X-ray crystallography) necessitates a form of insertion chemistry involving the silicon centre and the *N*-nacnac ligand backbone, whereby the heteroatom inserts into one of the imine C=N bonds, resulting in a ring contraction process and the formal oxidation of silicon from Si^{II} to Si^{IV}. This phenomenon has been previously observed in other Nacnac-ligated Main Group complexes, and is usually initiated by an increase in the electron density at the metal centre, and intramolecular attack at the backbone by the resulting low-valent complex.[19] Beyond the realm of Main Group chemistry, such C=N bond insertion processes have also been observed in Nacnac-stabilised Group 4 and 5 metal complexes, presumably driven thermodynamically by favourable M=N bond formation (Scheme 6.8).[20]



Scheme 6.8 Examples of reductive C=N cleavage in metal complexes with Nacnac ligands

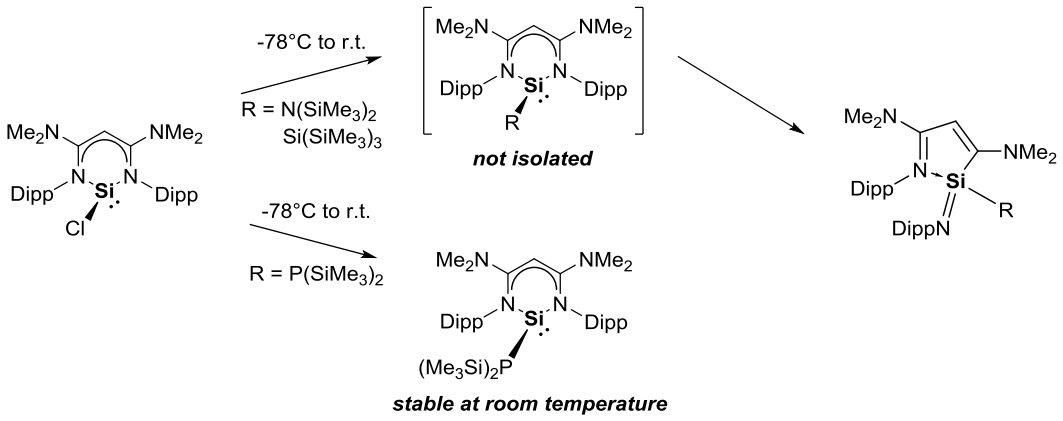
These aza-butadienyl complexes are typically accessed *via* reduction of the corresponding Nacnac system with a Group 1/Group 2 metal (or their derivatives),[19b,19c,19e,19f,20] or by the additional coordination of a strong σ-donor.[19a, 19d] Mechanistically, the interaction between the electron-rich elemental centre and the electrophilic carbon at the β-position of the Nacnac ligand has been advanced as the key intramolecular step in this rearrangement.[19f,20b-d] However, the effect(s) of varying the electron density at the central atom on the tendency of the corresponding complex to undergo backbone reductive cleavage has not yet been systematically assessed. Presumably, this is due to the synthetic challenges

associated with fine-tuning the electronic properties of the elemental centre. In the previous section, substituting the chloride ligand in (**1-Dipp**)SiCl with a more electron-donating group was shown to induce a similar ring contraction effect, as shown by ^{1}H NMR in the cases of the *tert*-butoxide and hydride complexes, and by X-ray crystallography for the latter. These results hint at the prospect of a systematic variation of the silicon-bound substituent, with a view to probing the factors underpinning reductive C=N cleavage in *N*-nacnac-silylene systems. Moreover, appraisal of the steric effect(s) of these substituents should also be possible, a factor which is often overlooked in comparison with electronic factors. Combined with computational investigations, the second part of the studies reported in this chapter aim to offer a better understanding of the nature of the ring contraction process in *N*-nacnac chemistry, which is a formally the reductive cleavage of one of the imine C=N bond in the ligand backbone and oxidation of the silicon centre from Si^{II} to Si^{IV}. Ultimately, the results from this study would hopefully help explain the relevant observations in previously-reported Main Group systems.

6.2.3 The rearrangement of N-nacnac ligands: Effects of silicon-bound substituents

With the idea of variation in Si-bound substituent in mind, a series of trimethylsilyl-substituted ligands of the form $[E(SiMe_3)_n]^-$ ($N(SiMe_3)_2$, $P(SiMe_3)_2$, $Si(SiMe_3)_3$) were selected for metathesis with the *N*-nacnac-stabilised chlorosilylene, (**1-Dipp**)SiCl, based on the differences in their donor capabilities and steric bulk compared to H and O^{t}Bu. Amongst them, $N(SiMe_3)_2$ and $P(SiMe_3)_2$ are marginally less bulky than $Si(SiMe_3)_3$, and both Group 15 element-based substituents possess an

additional lone pair capable of π-donation. Moreover, between them, the phosphide anion is a stronger σ-donor than the amide anion, which is due to the higher electronegativity of nitrogen compared to phosphorus.



Scheme 6.9 Salt metathesis of (**1-Dipp**)SiCl with sources of per(trimethylsilyl) anions

At the outset, a common synthetic methodology was utilised for the salt metathesis reactions of (**1-Dipp**)SiCl with Na[N(SiMe$_3$)$_2$], K[Si(SiMe$_3$)$_3$], and Li[P(SiMe$_3$)$_2$](dme)). The chlorosilylene was added to the inorganic salt at -78°C, and the reaction mixture slowly warmed to room temperature over a period of *ca.* 12 h. The identities of the products, isolated after work-up *via* recrystallisation, reveal that (under these conditions) ring contraction results in the formation of the aza-butadienyl-supported Si^{IV} complexes (**5-Dipp**)Si(NDipp){N(SiMe$_3$)$_2$} and (**5-Dipp**)Si(NDipp){Si(SiMe$_3$)$_3$} in the cases of the amide and silyl reagents, while a straightforward metathesis process with the phosphide reagent affords the phosphidosilylene (**1-Dipp**)Si{P(SiMe$_3$)$_2$} (Scheme 6.9). Remarkably, this species represents one of the few examples of stable phosphidosilylenes reported to date.[21] Spectroscopically, the ^{29}Si{^{1}H} NMR signals associated with the *N,C*-chelated Si^{IV} centres in (**5-Dipp**)Si(NDipp){N(SiMe$_3$)$_2$} and (**5-Dipp**)Si(NDipp){Si(SiMe$_3$)$_3$} are

located in the upfield region (δ_{Si} = -81.1 and -62.2 ppm, respectively, for the amido- and silyl-silane), being comparable to those measured for (**5-Dipp**)Si(NDipp)H and (**5-Dipp**)Si(NDipp)(O^{t}Bu) (δ_{Si} = -74.2 and -85.4 ppm respectively). Moreover, (**5-Dipp**)Si(NDipp){Si(SiMe$_3$)$_3$} shares a broadly similar spectroscopic pattern in its ^{1}H NMR spectrum with the analogous hydrido and butoxide systems (six Dipp methyl and three NMe$_2$ methyl resonances), while the ^{1}H NMR spectrum of (**5-Dipp**)Si(NDipp){N(SiMe$_3$)$_2$} comprises eight Dipp methyl and four NMe$_2$ methyl signals. By contrast, the ^{29}Si NMR spectrum of (**1-Dipp**)Si{P(SiMe$_3$)$_2$} features a signal at a relatively more downfield chemical shift (δ_{Si} = 18.6 ppm; $^1J_{SiP}$ = 213 Hz), which reflects the presence of a Si^{II} centre (*cf.* 1.8 ppm for (**1-Dipp**)SiCl). This chemical shift is upfield compared to phosphidosilylenes stabilised by the amidinate ligand [PhC(N^{t}Bu)$_2$]$^-$ (30 to 60 ppm),[21b-d] which (as with the chlorosilylene systems discussed in chapter 4), hints at the stronger donor capability of *N*-nacnac ligand family. In addition, the ^{31}P{^{1}H} resonance for (**1-Dipp**)Si{P(SiMe$_3$)$_2$} is observed at -230.2 ppm; the two satellite signals (frequency separation = 46 and 213 Hz) are indicative of the coupling between the silicon atoms in the SiMe$_3$ groups and the central Si^{II} atom, respectively. Overall, the spectroscopic parameters of (**1-Dipp**)Si{P(SiMe$_3$)$_2$} are comparable to the closely-related amidinate-based system {PhC(N^{t}Bu)$_2$}Si{P(SiMe$_3$)$_2$} (δ_{Si} = 44.0 ppm, δ_P = -211.0 ppm, frequency separation = 23 Hz and 194 Hz).[21c]

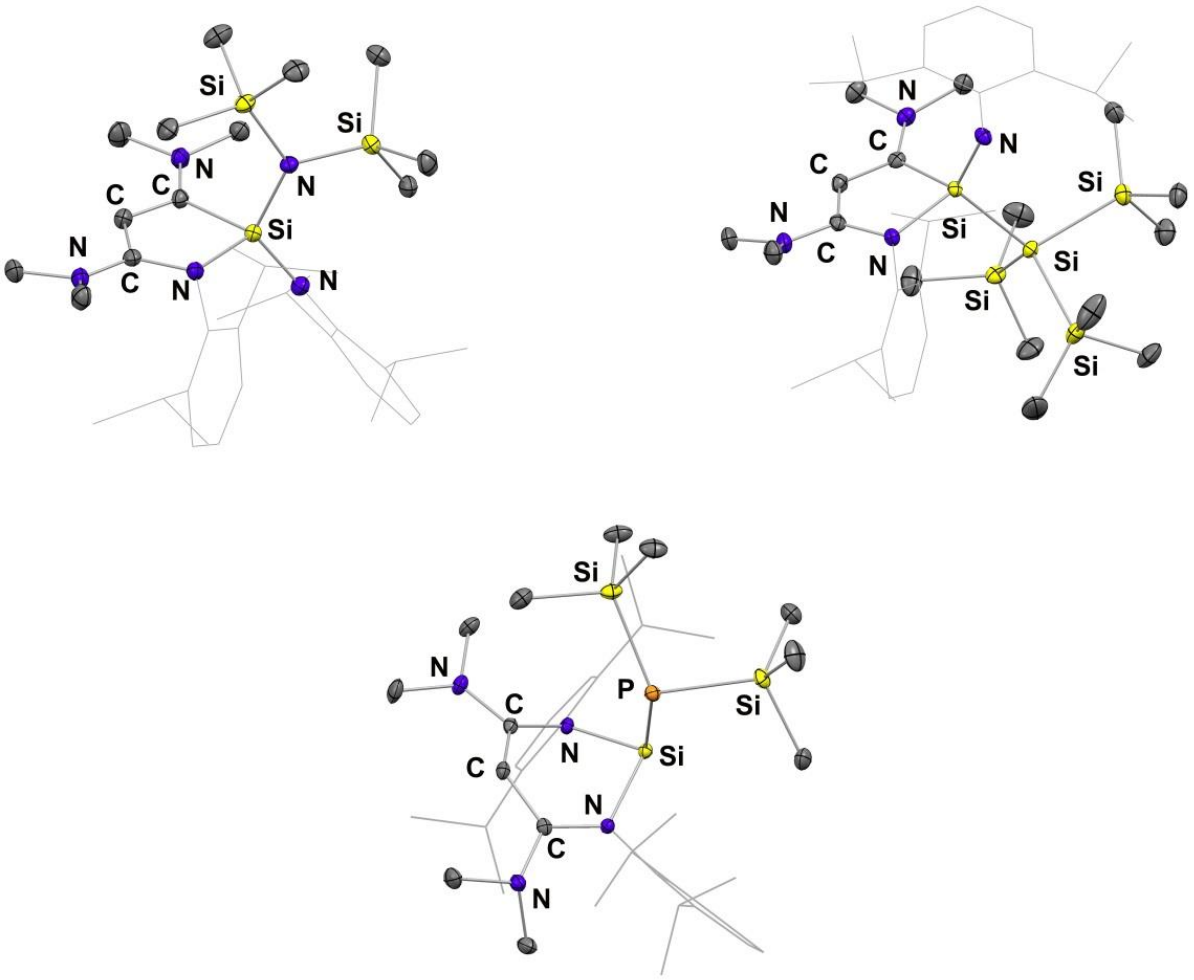


Figure 6.6 Solid-state structures of (**5-Dipp**)Si(NDipp){N(SiMe$_3$)$_2$} (*top left*), (**5-Dipp**)Si(NDipp){Si(SiMe$_3$)$_3$} (*top right*), and (**1-Dipp**)Si{P(SiMe$_3$)$_2$} (*bottom*), as determined by X-ray crystallography. Thermal ellipsoids are shown at 35 % probability level. *N*-bound aromatic substituents are shown in the wireframe format, and all hydrogens have been omitted for clarity.

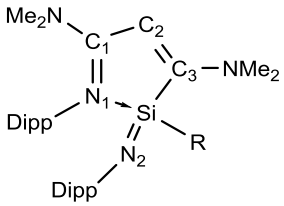
	(**5-Dipp**)Si(NDipp)R R = $Si(SiMe_3)_3$	(**5-Dipp**)Si(NDipp)R R = $N(SiMe_3)_2$	*(**5-Dipp**)Si(NDipp)R* *R = H*
d(Si—N1)	1.8694(12)	1.8418(18)	*1.8184(12)*
d(Si—C3)	1.9346(13)	1.926(2)	*1.9011(15)*
d(Si—N2)	1.6126(11)	1.5899(19)	*1.5764(14)*
d(N1—C1)	1.3657(18)	1.372(3)	*1.3597(18)*
d(C1—C2)	1.415(2)	1.424(3)	*1.431(2)*
d(C2—C3)	1.384(2)	1.382(3)	*1.380(2)*
d(C1—N[Me_2])	1.3516(19)	1.342(3)	*1.3431(19)*
d(C3—N[Me_2])	1.3299(18)	1.336(3)	*1.3341(19)*
∠ (N1—Si—C3)	86.63(6)	88.61(9)	*88.79(6)*
∠ (Si1—N2—C_{ipso})	153.00(11)	173.46(18)	*172.37(14)*
∠(NMe_2 planes and least-squares [NC_3Si] plane)	32.5[a] and 14.0[b]	19.1[a] and 7.8[b]	*13.9*[a] *and 5.0*[b]
Sum of all endocyclic angles	539.2	540.0	*539.7*

Table 6.2 Selected bond lengths (Å) and angles (°) of (**5-Dipp**)Si(NDipp){$Si(SiMe_3)_3$} and (**5-Dipp**)Si(NDipp){$N(SiMe_3)_2$}, as determined by X-ray crystallography, with the corresponding parameters of (**5-Dipp**)Si(NDipp)H provided for comparison.
Note: [a] C1-bound NMe_2 plane; [b] C3-bound NMe_2 plane

For the five-membered ring species, crystallographic studies reveal the influence of the steric profile of the pendant substituents on the geometry at the central silicon atom (Figure 6.6). The more sterically encumbered groups ($Si(SiMe_3)_3$ > $N(SiMe_3)_2$ >> H) are associated with (i) longer endocyclic Si—N and

Si—C bonds, as well as a narrower (N1—Si1—C3) angle within the five-membered ring, and (ii) a longer exocyclic Si—N bond, and a narrower (Si1—N2— C(*ipso*)) angle within the Si=NDipp moiety (Table 6.2). In addition, at the aza-butadienyl backbone, the torsion angles between the planes containing the NMe_2 pendants and the mean (NC_3Si) plane increase for larger R groups. Nevertheless, the sums of all endocyclic angles in the extended aza-butadienyl NC_3Si ring appear to be unaffected by the varying sizes of R, which are virtually identical (at *ca.* 540°) for all three compounds, indicating an essentially planar heterocycle in each case. With regards to the exocyclic Si—R bonds, the Si—$N(SiMe_3)_2$ distance (1.7441(18) Å) falls in the middle of the range of reported bond lengths between four-coordinate silicon and three-coordinate nitrogen (1.65 – 1.85 Å), while the Si—$Si(SiMe_3)_3$ distance of 2.4055(5) Å is towards the longer end in the range of structurally-characterised silicon-silicon single bonds (2.30 – 2.45 Å).[17] Notably, the Si—$Si(SiMe_3)_3$ bond in (**5-Dipp**)Si(NDipp){$Si(SiMe_3)_3$} is longer than the corresponding distance in the two-coordinate acyclic silylene complex [(Dipp)(Me_3Si)N][($Me_3Si)_3$Si]Si (*d*(Si—Si) = 2.386(1) Å),[22] despite the contracted covalent radius of Si^{IV} compared to that of Si^{II}.

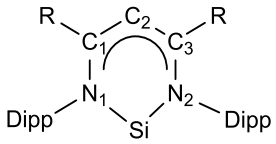
	(**1-Dipp**)Si{P(SiMe$_3$)$_2$}	*(**1-Dipp**)SiCl*
d(C1—N1) / *d*(C3—N2)	1.3422(15) / 1.3782(15)	*1.3683(15) / 1.3527(15)*
d(Si—N1) / *d*(Si—N2)	1.9014(10) / 1.8313(10)	*1.8461(10) / 1.8591(10)*
d(Si—least-squares [N1—C1—C2—C3—N2] plane)	0.78	*0.55*
∠ (N1—Si—N2)	93.07(5)	*96.82(5)*

Table 6.3 Selected bond lengths (Å) and angles (°) of (**1-Dipp**)Si{P(SiMe$_3$)$_2$}, as determined by X-ray crystallography, with the corresponding parameters of (**1-Dipp**)SiCl provided for comparison

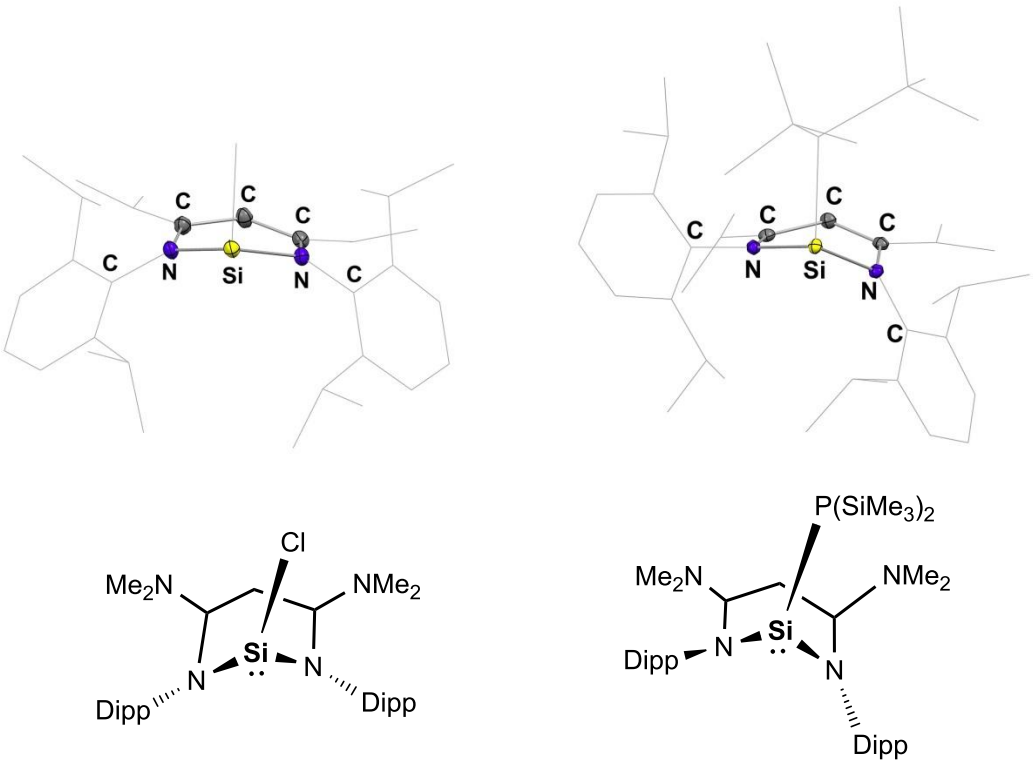


Figure 6.7 A comparison of the solid-state structures of (**1-Dipp**)SiCl (*left*) and (**1-Dipp**)Si{P(SiMe$_3$)$_2$}, as determined by X-ray crystallography. All atoms apart from the six-membered (NC$_3$N)Si ring are shown in the wireframe format, and all hydrogens have been omitted for clarity. Thermal ellipsoids are shown at 35 % probability level.

For the six-membered ring compounds, the contrasting steric bulk between the Cl and $P(SiMe_3)_2$ substituents is reflected in differences in the molecular metrics of the two silylene complexes (**1-Dipp**)SiCl and (**1-Dipp**)Si{$P(SiMe_3)_2$} in the solid state (Table 6.3). Thus, the more sterically congested phosphidosilylene is associated with a lower degree of molecular symmetry, as manifested by larger differences (i) between the two imine C—N distances (0.0360(15) Å, *cf.* 0.0156(15) Å in (**1-Dipp**)SiCl), and (ii) in the two Si—N bond lengths (0.070(1) Å, *cf.* 0.013(1) Å in (**1-Dipp**)SiCl). Moreover, a pronounced steric clash between the —$P(SiMe_3)_2$ moiety and one of the Dipp groups in (**1-Dipp**)Si{$P(SiMe_3)_2$} forces the latter to rotate out from the least-squares mean NC_3N plane; this in turn drives the other Dipp group to rotate in the opposite direction. This results in the two *ipso*-carbons of the aryl functions lying on opposite sides of the mean ligand plane (Figure 6.7). The distance between the NC_3N plane to the *ipso*-carbon that is *syn* to the silicon-bound function $P(SiMe_3)_2$ ("above the plane") is 0.19 Å, while the corresponding parameter for the *ipso*-carbon lying below the plane is 1.05 Å. By contrast, in (**1-Dipp**)SiCl, both *ipso*-carbons of the aryl pendants reside below the least-squares NC_3N plane ($d(C_{ipso}$—(NC_3N) plane) = 0.39 Å and 0.62 Å), with the Cl atom being projected out of the plane in the opposite sense. In addition, to accommodate the bulky phosphide group, the silicon atom in (**1-Dipp**)Si{$P(SiMe_3)_2$} is displaced further away from the mean ligand plane (d(Si—(NC_3N) plane) = 0.78 Å, *cf.* 0.55 Å in (**1-Dipp**)SiCl). This in turn results in a slightly narrower bite angle in the phosphidosilylene compound, compared to its chloride analogue (93.07(5)° and 96.82(5)° respectively). The central

Si—P distance of 2.3674(4) Å in (**1-Dipp**)Si{P(SiMe$_3$)$_2$} is longer than the corresponding value in the amidinate-based system {PhC(N^{t}Bu)$_2$}Si{P(SiMe$_3$)$_2$} (2.2838(12) Å),[21c] which is consistent with the more sterically hindered nature of the divalent silicon centre in the *N*-nacnac-ligated complex.

6.2.4 Computational investigation of the rearrangement process

DFT calculations have been performed in order to identify factors which influence the propensity for *N*-nacnac ligated silylene complexes to undergo ring contraction. At the outset, analyses of the frontier orbitals obtained from the optimised structures of the isolated silylene species (**1-Dipp**)SiR (R = Cl, P(SiMe$_3$)$_2$) reveal a major contribution from the lone pair on the silicon centre to the HOMO, while the LUMO is best described as a ligand-based anti-bonding π*-orbital (Figure 6.8). These features are also common to the (hypothetical) silylene complexes (**1-Dipp**)SiR (R = H, N(SiMe$_3$)$_2$, Si(SiMe$_3$)$_3$), the geometries of which have also been optimised with no restraints. In all cases, it is evident that the energy of the LUMO is relatively unperturbed by a change in the silicon-bound substituent R, with most of these falling in the range -90 to -105 kJ mol^{-1}, with the exception of (**1-Dipp**)SiH (-79.3 kJ mol^{-1}). On the other hand, varying the R group is found to significantly affect the energy of the HOMO (Figure 6.9). This can be attributed to the direct linkage of R to the silicon centre – the lone pair of which contributes substantially to the HOMO. Thus, the HOMO with the highest energy (-432.8 kJ mol^{-1}) is associated with (**1-Dipp**)Si{Si(SiMe$_3$)$_3$}, reflecting the strongly σ-donating nature of the Si(SiMe$_3$)$_3$ function. At the other end of the spectrum, the σ-withdrawing effect of Cl

presumably explains the much lower HOMO energy in (**1-Dipp**)SiCl (-508.3 kJ mol^{-1}). Overall, a plausible trend can be established based on the σ-donating capability of the R substituent in the silylene complexes (**1-Dipp**)SiR: the stronger σ-donor is associated with a HOMO of higher energy (*i.e.* a more electron-rich silicon centre), and consequently a smaller HOMO-LUMO gap (Figure 6.9 and Table 6.4).

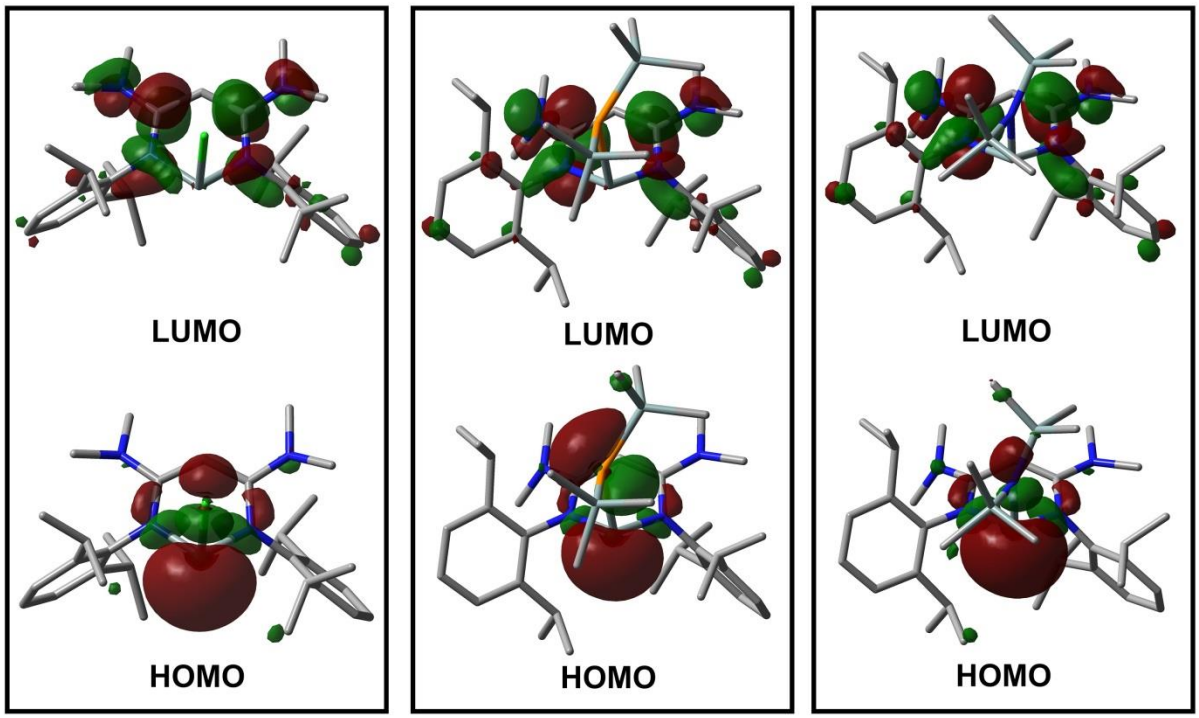


Figure 6.8 Graphical representations of the frontier orbitals (HOMO and LUMO), associated with the optimised structures of the *N*-nacnac-stablised silylene complexes (**1-Dipp**)SiR (*from left*: R = Cl, $P(SiMe_3)_2$, and $N(SiMe_3)_2$). All figures have been generated by GaussView (iso-value = 0.04).

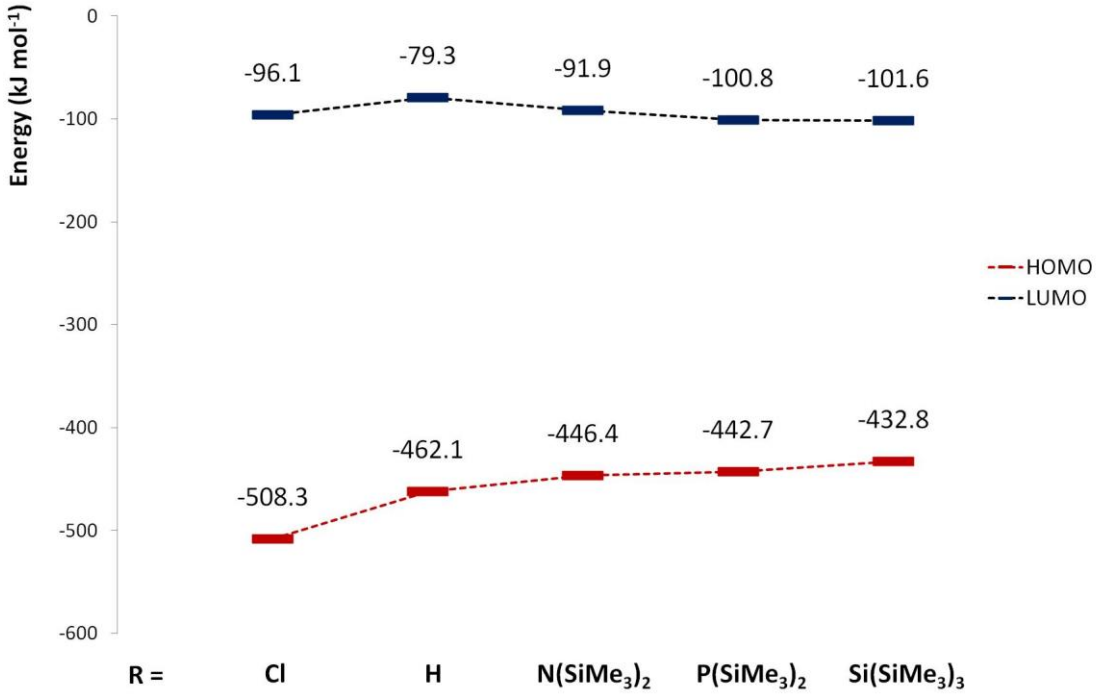


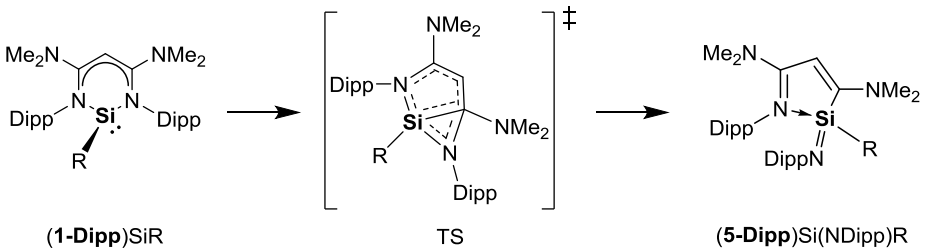
Figure 6.9 Energies of the frontier orbitals (HOMO and LUMO), associated with the optimised structures of (**1-Dipp**)SiR (R = Cl, H, $N(SiMe_3)_2$, $P(SiMe_3)_2$, $Si(SiMe_3)_3$)

R	Cl	H	$N(SiMe_3)_2$	$P(SiMe_3)_2$	$Si(SiMe_3)_3$
HOMO-LUMO gap (kJ mol^{-1})	412.2	382.8	354.6	341.8	331.2

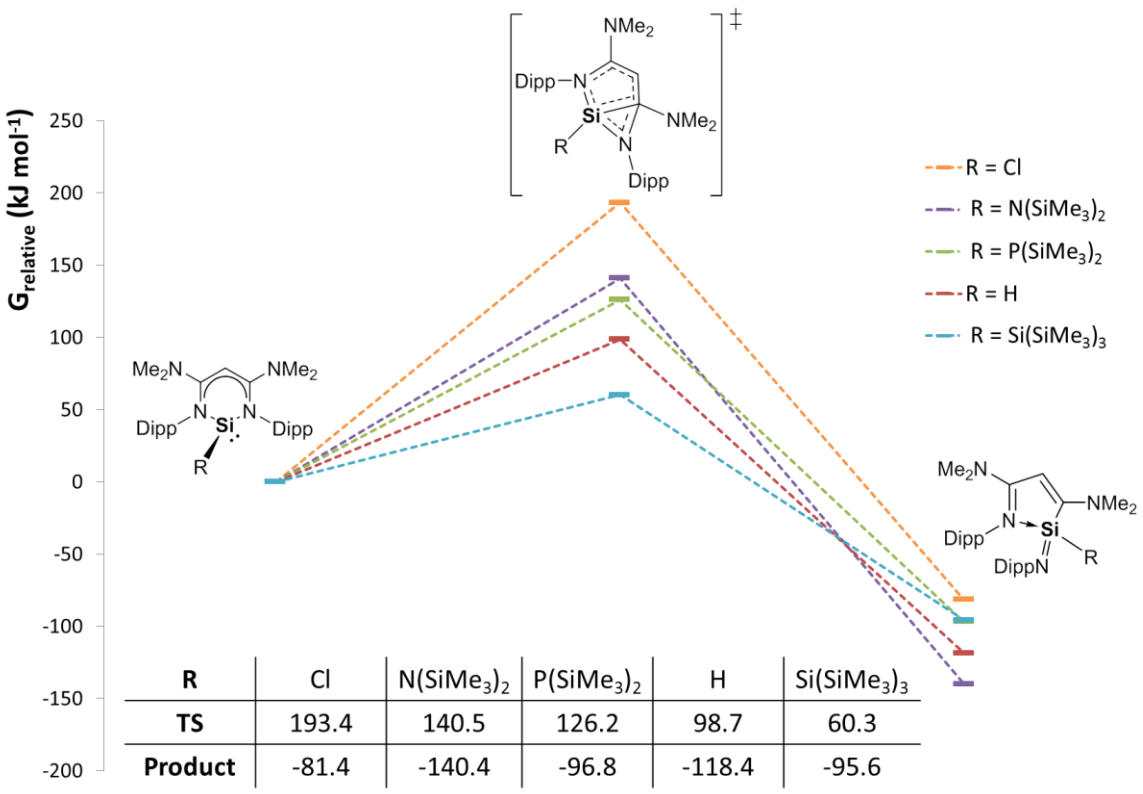
Table 6.4 HOMO-LUMO gaps of the silylene species (**1-Dipp**)SiR

The frontier orbital compositions of (**1-Dipp**)SiR species, outlined in Figure 6.9, appear to be consistent with the ring contraction mechanism previously suggested for Nacnac-ligated boron, niobium, and titanium complexes, which is initiated by the nucleophilic attack on the β-carbon by the electron rich metal centre. [19f,20b-d] From an elementary molecular orbital point of view, this step can be described as involving interaction between the HOMO (effectively the lone pair on the Si centre) and the LUMO, of which the imine π*-orbital (polarised towards the carbon atom) is a component. Based on these observations, a plausible mechanism is

proposed for the conversion of the six-membered Si^{II} species (**1-Dipp**)SiR to their five-membered Si^{IV} counterparts (**5-Dipp**)Si(NDipp)R, which proceeds *via* a single transition state, involving the formation of the Si—(β-carbon) bond, and accompanying C=N bond cleavage (Scheme 6.10).



Scheme 6.10 Proposed mechanism for the ring contraction process



R	Cl	$N(SiMe_3)_2$	$P(SiMe_3)_2$	H	$Si(SiMe_3)_3$
TS	193.4	140.5	126.2	98.7	60.3
Product	-81.4	-140.4	-96.8	-118.4	-95.6

Figure 6.10 Free energy profiles for the ring contraction mechanism outlined in Scheme 6.10, and the corresponding free energies for the transition state (TS) and the product (relative in each case to the (**1-Dipp**)-ligated starting complex)

Interestingly, the free energy profile shown in Scheme 6.11 implies that the formation of the aza-butadienyl complexes (**5-Dipp**)Si(NDipp)R is exoergic for *all* silicon-bound R groups (ranging from -80 to -150 kJ mol^{-1}). This presumably reflects the higher thermodynamic stability of the tetravalent silicon species (**5-Dipp**)Si(NDipp)R compared to their isomeric silylenes (**1-Dipp**)SiR (Figure 6.10), consistent with the greater stability of the +4 oxidation state for silicon. Nonetheless, the substantial activation energy associated with the ring contraction process in the case of R = Cl (+193.4 kJ mol^{-1}) reflects the *kinetic* stability of (**1-Dipp**)SiCl, which is experimentally demonstrated by the robustness of the compound at ambient temperature. In a broader sense, this relative inertness correlates with the largest HOMO-LUMO gap observed for all silylene species in (**1-Dipp**)SiCl (412.2 kJ mol^{-1}, Table 6.4), implying that the interaction between the key frontier orbitals is the least accessible in this case. Consistently, access to the transition state in the case of (**1-Dipp**)Si{$Si(SiMe_3)_3$} – which has the smallest HOMO-LUMO gap – is significantly more facile at only 60.3 kJ mol^{-1}; this activation barrier is found to be the lowest for all systems under consideration (Figure 6.10). Interestingly, the activation energy in the case of R = H (98.7 kJ mol^{-1}) is lower than those of the $P(SiMe_3)_2$ and $N(SiMe_3)_2$-substituted systems (126.2 and 140.5 kJ mol^{-1}), despite the hypothetical silylene species (**1-Dipp**)SiH having a wider HOMO-LUMO gap (382.8 kJ mol^{-1}, Table 6.4). Presumably, steric factors are also important in accessing the key transition state - the bulkier amide and phosphide functions can be envisaged to exert a greater steric clash with the neighbouring Dipp groups, compared to H. All

in all, the DFT-calculated free energy profiles for the ring contraction mechanism (outlined in Scheme 6.10 and Figure 6.10) are in good agreement with the experimental findings. One exception to this involves the activation energy for the (**1-Dipp**)Si{P(SiMe$_3$)$_2$}-to-(**5-Dipp**)Si(NDipp){P(SiMe$_3$)$_2$} conversion, which is calculated to be slightly lower than that of the N(SiMe$_3$)$_2$-substituted system (Figure 6.10), despite the fact that the former can be experimentally isolated as the six-membered ring silylene system at ambient temperatures, while the latter readily rearranges under the similar conditions.

*6.2.5 Investigation of the thermal stabilities of (**1-Dipp**)Si{P(SiMe$_3$)$_2$} and (**1-Dipp**)SiCl*

The above DFT studies suggest that the aza-butadienyl complexes (**5-Dipp**)Si(NDipp)R (R = Cl, P(SiMe$_3$)$_2$) are more thermodynamically stable than the corresponding silylenes, (**1-Dipp**)SiR. Thus, it was envisaged that by providing sufficient thermal energy, it might be possible to overcome the activation barrier associated with the ring contraction process in (**1-Dipp**)SiCl and (**1-Dipp**)Si{P(SiMe$_3$)$_2$}, and form the respective five-membered ring species. To examine the viability of this hypothesis, a C_6D_6 solution of (**1-Dipp**)Si{P(SiMe$_3$)$_2$} was heated at 100°C in a sealed J. Young's NMR tube. Daily monitoring by $^{31}P\{^1H\}$ NMR spectroscopy revealed the emergence of a new resonance at *ca.* -246 ppm after 1 d, which subsequently grows in intensity at the expense of the signal due to (**1-Dipp**)Si{P(SiMe$_3$)$_2$} (δ_P = -230.2 ppm; Figure 6.11). Near-complete consumption of the phosphidosilylene starting material was evident after 3 d, at which point the $^{31}P\{^1H\}$ NMR spectrum exhibited only one peak at -246.3 ppm. Subsequently, the

identity of the product associated with this resonance was unambiguously confirmed by X-ray crystallography to be the aza-butadienyl complex (**5-Dipp**)Si(NDipp){P(SiMe$_3$)$_2$}, thereby confirming that the expected ring contraction has indeed occurred (Figure 6.12).

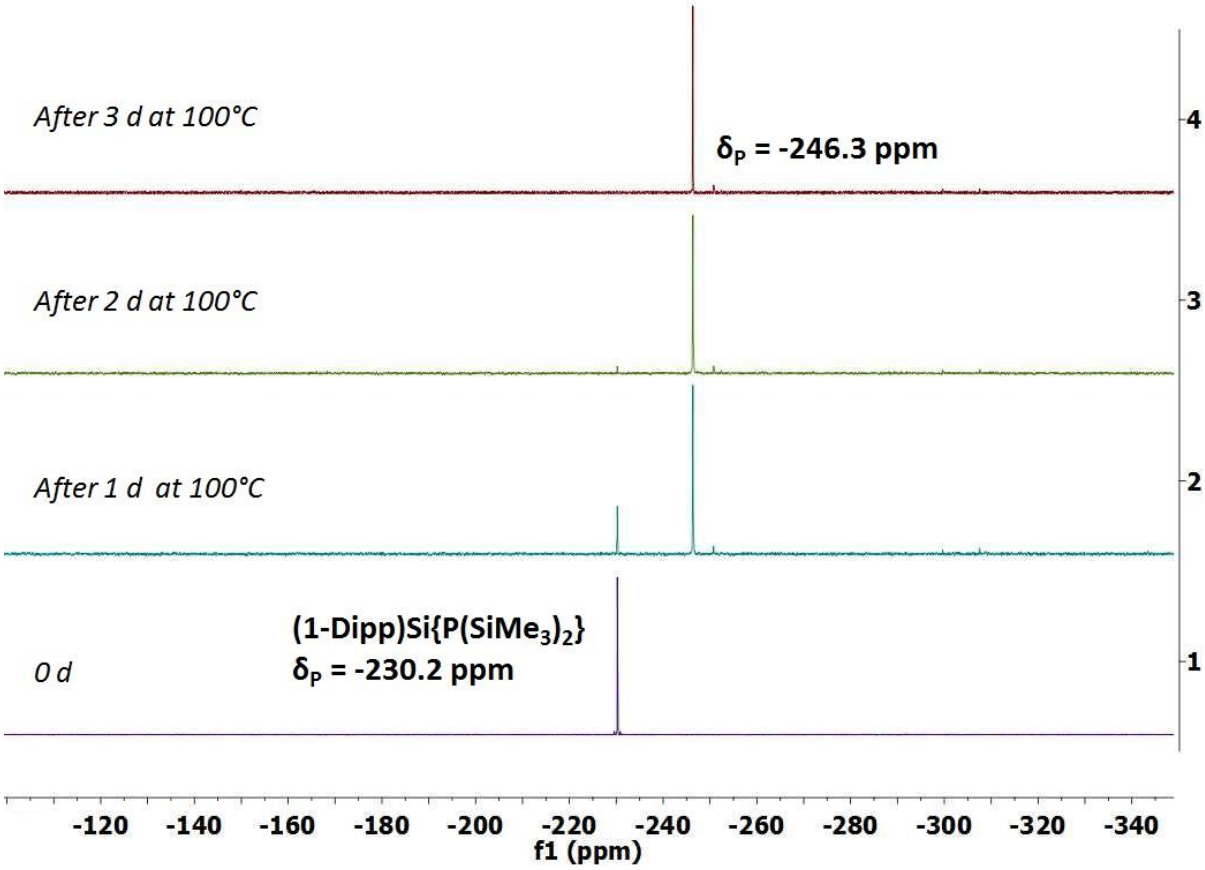
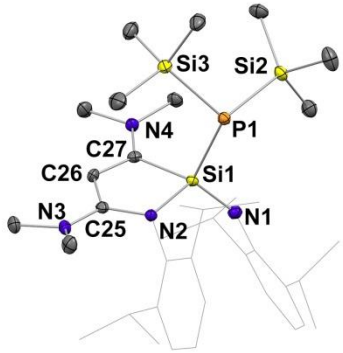


Figure 6.11 $^{31}P\{^1H\}$ NMR spectra of a sample of (**1-Dipp**)Si{P(SiMe$_3$)$_2$} in C_6D_6, showing the reaction progress at 100°C, over the course of 3 d

The molecular metrics of (**5-Dipp**)Si(NDipp){P(SiMe$_3$)$_2$} (apart from those associated with the silicon-bound P(SiMe$_3$)$_2$ group) closely resemble those of the related system (**5-Dipp**)Si(NDipp){N(SiMe$_3$)$_2$} (Table 6.2). The Si─P(SiMe$_3$)$_2$ distance of 2.2456(10) Å is markedly shorter than the corresponding value in (**1-Dipp**)Si{P(SiMe$_3$)$_2$} (2.3674(4) Å), presumably reflecting the smaller covalent

radius of Si^{IV} compared to that of Si^{II} (Figure 6.12). Spectroscopically, (**5-Dipp**)Si(NDipp){P($SiMe_3$)$_2$} displays a diagnostic $^{29}Si\{^1H\}$ NMR doublet signal for the central silicon atom at -75.8 ppm ($^1J_{SiP}$ = 25 Hz), which is consistent with other (**5-Dipp**)Si(NDipp)R complexes (typically -60 to -90 ppm). Such a coupling constant is also indicative of a Si^{IV}—P^{III} bond, compared to those reported for Si^{II}—P^{III} bonds, which are all in excess of 150 Hz.[21b-d]



Bond lengths :

Si1—N1: 1.587(2); Si1—N2: 1.836(2); Si1—C27: 1.922(2);
N2—C25: 1.365(3); C25—C26: 1.422(3); C26—C27: 1.373(3);
C25—N3: 1.342(3); C27—N4: 1.341(3); Si1—P1: 2.2456(10)

Angles:

Si1—N2—C25: 111.55(16); N2—C25—C26: 116.0(2);
C25—C26—C27: 115.6(2); C26—C27—Si1: 108.66(18);
C27—Si1—N1: 88.13(10)

Figure 6.12 Solid-state structures of (**5-Dipp**)Si(NDipp){P($SiMe_3$)$_2$} (*left*), and selected bond lengths (Å) and angles (°), as determined by X-ray crystallography. Thermal ellipsoids are shown at 35 % probability. *N*-bound aromatic substituents are shown in the wireframe format, and all hydrogens have been omitted for clarity.

Having successfully established the synthetic protocol for the thermally-induced ring contraction of (**1-Dipp**)SiP{($SiMe_3$)$_2$}, the corresponding process for the chloride analogue was also investigated. Thus, under similar conditions, a sample of (**1-Dipp**)SiCl in C_6D_6 was heated at 100°C, with daily monitoring by ^1H NMR spectroscopy. After 36 d at this temperature nearly all of the starting material had been consumed (Figure 6.14). The pattern of the ^1H NMR resonances at that point features six Dipp-methyl signals (in integrated ratio 1:1:1:1:2:2) and three NMe_2-methyl signals (1:1:2), and is characteristic of the (**5-Dipp**)Si(NDipp)R series

of compounds. Furthermore, a new singlet appears at -90.0 ppm in the $^{29}Si\{^{1}H\}$ NMR spectrum, which is significantly upfield compared to that of (**1-Dipp**)SiCl (δ_{Si} = 1.8 ppm), and similar to those observed for other (**5-Dipp**)Si(NDipp)R systems. Thus, although the solid-state structure of the product remains elusive, spectroscopic evidence suggests that the product is the aza-butadienyl complex (**5-Dipp**)Si(NDipp)Cl.

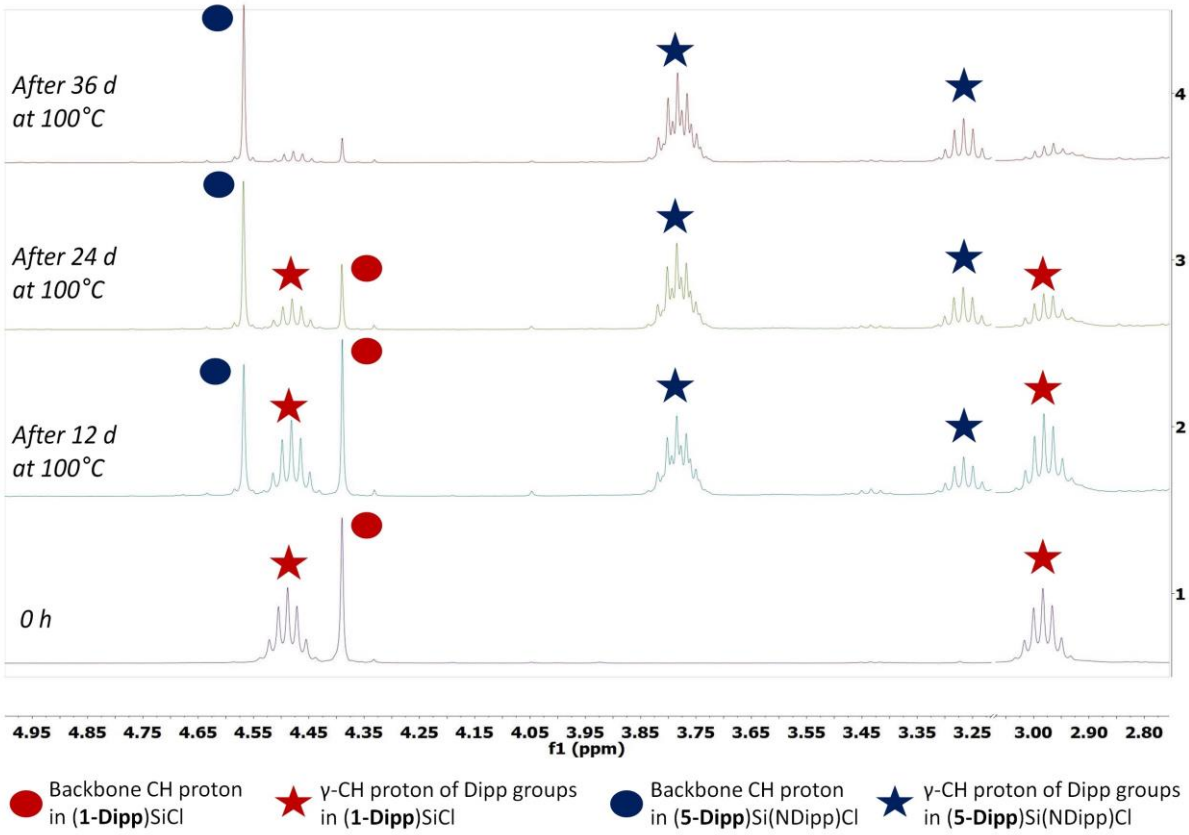


Figure 6.13 Thermally-induced ring contraction in (**1-Dipp**)SiCl, as demonstrated by selected ^{1}H NMR spectra, recorded after 0, 12, 24, and 36 d at 100°C.

Of mechanistic interest is the kinetic profile for this six-to-five-membered ring transformation which (given the timeframe) is conveniently monitored by *in situ* NMR for the Cl-substituted system. Firstly, the concentration of the silylene species ($C_{1\text{-Dipp}}$) at any time is calculated from the (**1-Dipp**)SiCl : (**5-Dipp**)SiCl concentration

ratio, which in turn is derived from the ratio of the methine CH protons at the *N*-nacnac/aza-butadienyl ligand backbones. A plot of the natural logarithm of the concentration of (**1-Dipp**)SiCl against time yields a straight line, indicating that the reaction follows the 1st-order rate law (Figure 6.14). The rate constant is calculated to be 6.93 (±0.03) × 10^{-7} s^{-1}, corresponding to a half-life of *ca.* 12 days, which is fully consistent with the very high activation energy associated with the process (+193.4 kJ mol^{-1}).

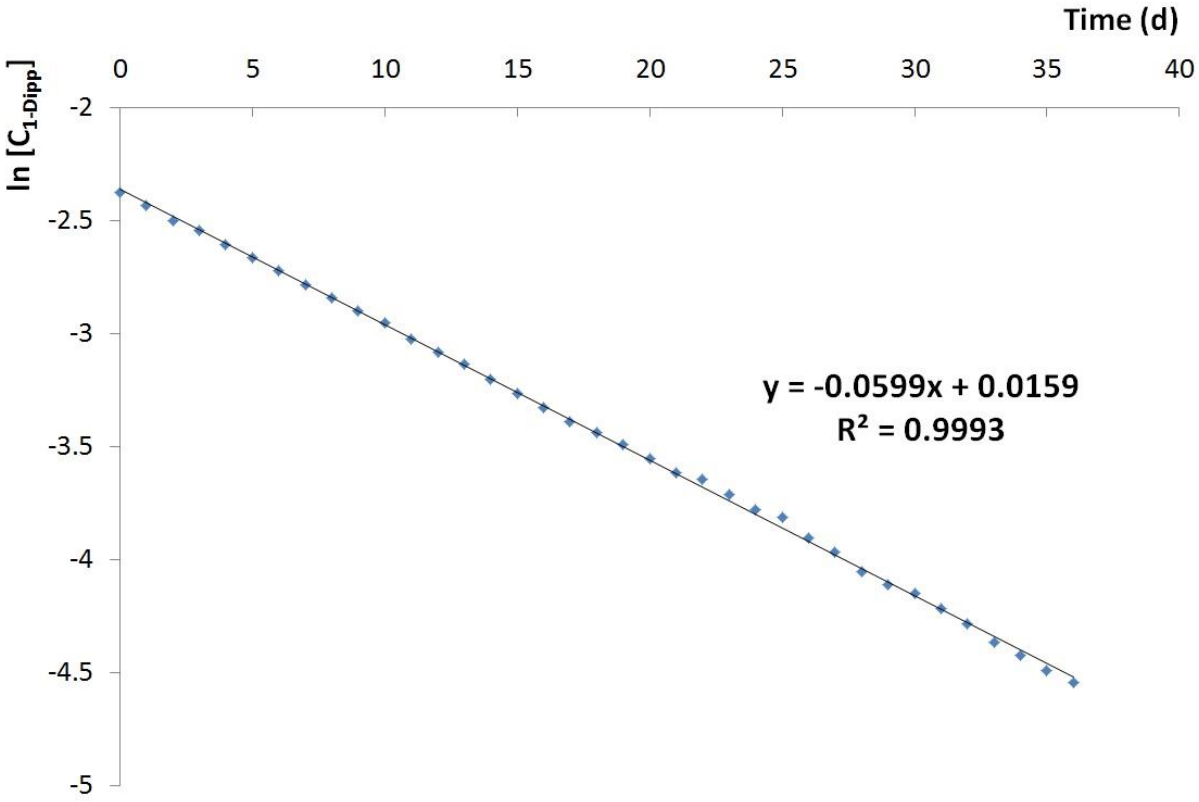


Figure 6.14 Plot of the natural logarithm of the concentration of (**1-Dipp**)SiCl versus time

6.5 Conclusions

Hitherto unknown in the chemistry of Si=O containing species, a *N*-nacnac-supported sila-acyl chloride (**1-Dipp**)Si(O)Cl has been synthesised by the direct oxidation of the monochlorosilylene precursor (**1-Dipp**)SiCl with N_2O. The

stability of this complex even in the absence of a Lewis acid is largely credited to the superior donor capability and/or steric encumbrance of the *N*-nacnac ligand. Importantly, (**1-Dipp**)Si(O)Cl can be shown to undergo facile functional group exchange, affording the corresponding (borane-coordinated) sila-aldehyde (**1-Dipp**)Si[O(BEt_3)]H and sila-ester (**1-Dipp**)Si(O)(O^tBu). While such transformations – formally a nucleophilic substitution process – are well-documented for carbonyls, they are without precedent in the analogous chemistry of silicon. Mechanistic investigations with a simplified model complex suggest an S_N2-like reaction pathway; a low energy barrier (*ca.* 55 kJ mol^{-1}) associated with a penta-coordinate transition state is consistent with the experimentally-observed spontaneous transformation under ambient conditions.

The isolation of the sila-carbonyl species bearing a common *N*-nacnac ligand platform has allowed for a systematic comparison of these species, based on their spectroscopic and crystallographic properties. Thus, while the ^{29}Si NMR signals of all compounds are broadly in the range of known four-coordinate sila-carbonyls, the Lewis acid-free systems (sila-acyl chloride and sila-ester) are associated with higher Si=O IR stretching frequencies and shorter Si=O distances compared to the sila-aldehyde. This reflects the weaker Si=O bond in the latter, presumably due to the coordination of the borane function at oxygen, a hypothesis which is further corroborated computationally by the Wiberg bond indices of the three sila-carbonyl species. Remarkably, the Si=O bond distances in the sila-acyl chloride and sila-ester compounds are comparable to those found in three-coordinate silanones, and are

thus among the shortest formal silicon-oxygen double bonds known for structurally-characterised silanones.

Unexpected reactivity has been observed when the order of steps in the oxidation-substitution methodology was reversed: attempts to substitute the chloride substituent in (**1-Dipp**)SiCl with either hydride or *tert*-butoxide (prior to oxidation at silicon) result in ring-contraction processes, *via* formal reductive C=N cleavage of the ligand backbone, with accompanying oxidation of the silicon centre from Si^{II} to Si^{IV}. This provided the impetus for an investigation, by both experimental and quantum chemical means, of the effect(s) of the silicon-bound substituent on the tendency for the *N*-nacnac ligand to rearrange. Thus, when (**1-Dipp**)SiCl was subjected to salt metathesis with sources of $[N(SiMe_3)_2]^-$, $[P(SiMe_3)_2]^-$, and $[Si(SiMe_3)_3]^-$ anions at ambient temperature, simple anionic exchange facilitated the formation of corresponding silylene only in the case of the phosphide reagent; by contrast, ring contraction leads to the isolation of (**5-Dipp**)Si(NDipp){$N(SiMe_3)_2$} and (**5-Dipp**)Si(NDipp){$Si(SiMe_3)_3$} in the case of the amide/silyl reagents.

Frontier orbital studies of the optimised structures of the silylene complexes (**1-Dipp**)SiR yield energies for the HOMO (effectively a lone pair at silicon), which hint at an increase in σ-donor capability of the R substituent in the order $Cl < H < N(SiMe_3)_2 < P(SiMe_3)_2 < Si(SiMe_3)_3$. Based on the arrangements of the frontier orbitals, ring contraction is proposed to proceed *via* a single transition state, which involves the interaction between the putative HOMO and LUMO of the

silylene species. The free energy profiles associated with such a mechanism were found to agree well with the trends established from experimental studies.

The propensity for ring contraction at higher temperatures (100°C) was probed for the isolated silylenes (**1-Dipp**)SiCl and (**1-Dipp**)Si{P($SiMe_3$)$_2$}. While the conversion of the P($SiMe_3$)$_2$-substituted system was effectively complete after 72 h, the chloride analogue reacts at a much slower rate, consistent with the calculated activation barriers. X-ray diffraction studies confirmed the identity of the rearranged product in the phosphide case as (**5-Dipp**)Si(NDipp){P($SiMe_3$)$_2$}, while evidence from the ^{1}H and ^{29}Si{^{1}H} NMR have been used to confirm the formation of (**5-Dipp**)Si(NDipp)Cl in solution.

6.6 Syntheses of novel compounds

6.6.1 Syntheses of the sila-carbonyl compounds

Synthesis of (1-Dipp)Si(O)Cl: A toluene solution of (**1-Dipp**)SiCl (100 mg, 0.18 mmol) in an ampoule was degassed (freeze-pump-thaw), prior to treatment with excess N_2O at room temperature. The reaction mixture was stirred overnight at room temperature, during which time the colour changed from yellow to off-white, with the accompanying formation of a white precipitate. The solution was then filtered, and the precipitate washed with hot hexane. Drying the powder *in vacuo* afforded the spectroscopically pure product (66 mg, 43 % yield). X-ray quality crystals were grown from a concentrated toluene solution at -26˚C. ^{1}H NMR (C_6D_6, 400 MHz): δ_H 1.12 (d, 6H, (C$\underline{H}_3$)$_2$CH, $^{3}J_{HH}$ = 6.7 Hz), 1.16 (d, 6H, (C$\underline{H}_3$)$_2$CH, $^{3}J_{HH}$ = 6.8 Hz), 1.53 (d, 6H, (C$\underline{H}_3$)$_2$CH, $^{3}J_{HH}$ = 6.6 Hz), 1.58 (d, 6H, (C$\underline{H}_3$)$_2$CH, $^{3}J_{HH}$ = 6.5 Hz), 2.12

(s, 12H, (C<u>H</u>$_3$)$_2$N), 3.46 (virtual sept, 2H, (CH$_3$)$_2$C<u>H</u>, $^3J_{HH}$ = 6.7 Hz), 3.95 (s, 1H, methine H), 4.26 (virtual sept, 2H, (CH$_3$)$_2$C<u>H</u>, $^3J_{HH}$ = 6.6 Hz), 7.06-7.16 (aromatic protons, 6H) ppm. ^{13}C{^{1}H} NMR (C_6D_6, 125 MHz): δ_C 24.1, 24.4, 26.9, 27.2 ((<u>C</u>H$_3$)$_2$CH), 28.8, 29.2 ((CH$_3$)$_2$<u>C</u>H), 41.0 ((<u>C</u>H$_3$)$_2$N), 78.0 (methine C), 125.1, 125.5, 137.9, 146.3, 147.3 (aromatic carbons), 164.8 (imine quaternary C) ppm. ^{29}Si{^{1}H} NMR (C_6D_6, 99 MHz): δ_{Si} -69.9 ppm. IR (Nujol, $\nu_{Si=O}$/cm^{-1}): 1157. Elemental analysis: calc. for $C_{31}H_{47}ClN_4OSi$: C 69.04 %, H 8.79 %, N 10.39 %; meas. C 68.94 %, H 8.62 %, N 10.26 %.

Synthesis of (1-Dipp)Si[O(BEt$_3$)]H: A 1.0 M THF solution of K[HBEt$_3$] (0.2 mL, 1.1 equiv.) was added to the *in-situ* generated (**1-Dipp**)Si(O)Cl (103 mg, 0.18 mmol, assumed 100 % yield), and the reaction mixture was stirred for 2 d at ambient conditions. The solution was collected by filtration, and susbsequently concentrated under reduced pressure to *ca.* 5 mL. Layering with hexane at -26˚C yielded the pure product as colourless crystals (26 mg, 23 % yield) over several days. ^{1}H NMR (C_6D_6, 400 MHz): δ_H 0.89 (br q, 6H, B(C<u>H</u>$_2$CH$_3$)$_3$), 0.90 (d, 6H, (C<u>H</u>$_3$)$_2$CH, $^3J_{HH}$ = 6.6 Hz), 0.99 (d, 6H, (C<u>H</u>$_3$)$_2$CH, $^3J_{HH}$ = 6.7 Hz), 1.42 (d, 6H, (C<u>H</u>$_3$)$_2$CH, $^3J_{HH}$ = 6.5 Hz), 1.49 (br t, 9H, B(CH$_2$C<u>H</u>$_3$)$_3$), 1.56 (d, 6H, (C<u>H</u>$_3$)$_2$CH, $^3J_{HH}$ = 6.5 Hz), 2.20 (s, 12H, (C<u>H</u>$_3$)$_2$N), 2.63 (virtual sept, 2H, (CH$_3$)$_2$C<u>H</u>, $^3J_{HH}$ = 6.6 Hz), 4.14 (s, 1H, methine H), 4.64 (virtual sept, 2H, (CH$_3$)$_2$C<u>H</u>, $^3J_{HH}$ = 6.6 Hz), 4.88 (s, 1H, Si-H, silicon satellites with $^1J_{SiH}$ = 289 Hz), 6.92-7.16 (aromatic protons, 6H) ppm. ^{13}C{^{1}H} NMR (C_6D_6, 101 MHz): δ_C 12.2 (B(CH$_2$<u>C</u>H$_3$)$_3$), 17.8 (B(<u>C</u>H$_2$CH$_3$)$_3$), 24.0, 24.8, 26.5, 27.3 ((<u>C</u>H$_3$)$_2$CH), 28.1, 28.2 ((CH$_3$)$_2$<u>C</u>H), 40.6 ((<u>C</u>H$_3$)$_2$N), 79.1 (methine C), 124.9, 127.0, 127.3, 136.9, 144.1, 146.4

(aromatic carbons), 164.0 (imine quaternary C) ppm. $^{29}Si\{^1H\}$ NMR (C_6D_6, 80 MHz): δ_{Si} -64.4 ppm. $^{11}B\{^1H\}$ NMR (C_6D_6, 128 MHz): δ_B 4.4 ppm. IR (Nujol, cm^{-1}): 1129 ($\nu_{Si=O}$), 2219 (ν_{Si-H}). Elemental analysis: calc. for $C_{37}H_{63}BN_4OSi$: C 71.81 %, H 10.26 %, N 9.05 %; meas. C 66.96 %, H 9.90 %, N 8.85 %.

Synthesis of (1-Dipp)Si(O)(O^{t}Bu): An identical procedure to the sila-aldehyde was applied, replacing the superhydride THF solution with a suspension of KO^{t}Bu (22 mg, 1.1 equiv.) in toluene (5 mL). The pure product was isolated as off-white to yellow crystals (48 mg, 44 % yield). ^1H NMR (C_6D_6, 500 MHz): δ_H 0.90 (s, 9H, (C$\underline{H}_3$)$_3$C), 1.07 (d, 6H, (C$\underline{H}_3$)$_2$CH, $^3J_{HH}$ = 6.8 Hz), 1.25 (d, 6H, (C$\underline{H}_3$)$_2$CH, $^3J_{HH}$ = 6.8 Hz), 1.44 (d, 6H, (C$\underline{H}_3$)$_2$CH, $^3J_{HH}$ = 6.8 Hz), 1.99 (d, 6H, (C$\underline{H}_3$)$_2$CH, $^3J_{HH}$ = 6.4 Hz), 2.14 (s, 12H, (C$\underline{H}_3$)$_2$N), 3.08 (virtual sept, 2H, (CH$_3$)$_2$C$\underline{H}$, $^3J_{HH}$ = 6.8 Hz), 3.77 (s, 1H, methine H), 4.85 (virtual sept, 2H, (CH$_3$)$_2$C$\underline{H}$, $^3J_{HH}$ = 6.6 Hz), 7.09-7.29 (aromatic protons, 6H) ppm . $^{13}C\{^1H\}$ NMR (C_6D_6, 125 MHz): δ_C 24.6, 25.3, 25.8, 27.3 ((C$\underline{H}_3$)$_2$CH), 28.6, 29.5 ((CH$_3$)$_2$C$\underline{H}$), 31.8 ((C$\underline{H}_3$)$_3$C), 41.6 ((C$\underline{H}_3$)$_2$N), 73.4 ((CH$_3$)$_3$C), 75.9 (methine C), 124.1, 126.2, 127.6, 138.7, 145.9, 149.0 (aromatic carbons), 164.5 (imine quaternary C) ppm. $^{29}Si\{^1H\}$ NMR (C_6D_6, 80 MHz): δ_{Si} -80.9 ppm. IR (Nujol, cm^{-1}): 992 (ν_{Si-O}), 1145 ($\nu_{Si=O}$). Elemental analysis: calc. for $C_{35}H_{56}N_4O_2Si$: C 70.90 %, H 9.52 %, N 9.45 %; meas. C 70.69 %, H 9.42 %, N 9.31 %.

6.6.2 Syntheses of the rearranged aza-butadienyl complexes

Synthesis of (5-Dipp)Si(NDipp)H: To a solution of (**1-Dipp**)SiCl (108 mg, 0.2 mmol) in toluene (10 mL), a 1.0 M THF solution of K[HBEt$_3$] (0.22 mL, 1.1 equiv.) was added at -78°C, and the reaction mixture was slowly warmed to room

temperature over 15 h with stirring. The solution was subsequently collected by filtration, and toluene was removed *in vacuo* to yield a red oil, which was recrystallised in hexane at -26˚C to afford the pure product as light orange crystals. X-ray quality crystals were grown by slow-evaporation of a saturated solution in methylcyclohexane at room temperature. Yield 0.032 g, 32 %. ^{1}H NMR (C_6D_6, 400 MHz): δ_H 1.01 (d, 3H, (C$\underline{H}_3$)$_2$CH, $^{3}J_{HH}$ = 6.9 Hz), 1.07 (d, 3H, (C$\underline{H}_3$)$_2$CH, $^{3}J_{HH}$ = 6.6 Hz), 1.08 (d, 3H, (C$\underline{H}_3$)$_2$CH, $^{3}J_{HH}$ = 6.9 Hz), 1.28 (d, 6H, (C$\underline{H}_3$)$_2$CH, $^{3}J_{HH}$ = 6.9 Hz), 1.32 (d, 3H, (C$\underline{H}_3$)$_2$CH, $^{3}J_{HH}$ = 6.7 Hz), 1.49 (d, 6H, (C$\underline{H}_3$)$_2$CH, $^{3}J_{HH}$ = 6.9 Hz), 2.03 (s, 6H, (C$\underline{H}_3$)$_2$N), 2.19 (s, 3H, (C$\underline{H}_3$)$_2$N), 3.05 (sept, 1H, (CH$_3$)$_2$C$\underline{H}$, $^{3}J_{HH}$ = 6.8 Hz), 3.09 (s, 3H, (C$\underline{H}_3$)$_2$N), 3.76 (sept, 2H, (CH$_3$)$_2$C$\underline{H}$, $^{3}J_{HH}$ = 6.9 Hz), 3.88 (sept, 1H, (CH$_3$)$_2$C$\underline{H}$, $^{3}J_{HH}$ = 6.8 Hz), 4.58 (1H, methine H), 6.14 (s, 1H, SiH, silicon satellites with $^{1}J_{SiH}$ = 234 Hz), 6.93-7.31 (aromatic protons, 6H) ppm. ^{13}C{^{1}H} NMR (C_6D_6, 101 MHz): δ_C 23.7, 24.1, 24.1, 24.2, 24.8, 25.9 ((C$\underline{H}_3$)$_2$CH), 28.6, 28.8, 28.9 ((CH$_3$)$_2$C$\underline{H}$), 38.2, 40.3, 44.6 ((C$\underline{H}_3$)$_2$N), 87.9 (methine C), 114.2, 122.2, 124.4, 125.3, 137.2, 139.8, 145.9, 147.6, 149.5 (aromatic C), 168.6, 174.5 (imine quaternary C and silyl-dimethylamino C) ppm. ^{29}Si{^{1}H} NMR (C_6D_6, 80 MHz): δ_{Si} -74.2 ppm. IR (nujol, ν_{Si-H}/cm^{-1}): 2050. *Due to the sensitive nature of the compound, a reliable elemental analysis result could not be obtained.*

Synthesis of (5-Dipp)Si(NDipp)(O^{t}Bu): The procedure is identical to that of (**5-Dipp**)SiH, replacing the superhydride with KO^{t}Bu (25 mg, 1.1 equiv.), and recrystallisation was done in hexane at -26˚C, affording light-yellow crystals. Yield 0.060 g, 52 %. ^{1}H NMR (C_6D_6, 400 MHz): δ_H 0.96 (d, 3H, (C$\underline{H}_3$)$_2$CH, $^{3}J_{HH}$ = 6.8 Hz), 1.00 (d, 3H, (C$\underline{H}_3$)$_2$CH, $^{3}J_{HH}$ = 6.8 Hz), 1.23 (d, 3H, (C$\underline{H}_3$)$_2$CH, $^{3}J_{HH}$ = 6.5 Hz), 1.30 (d,

6H, (C<u>H</u>$_3$)$_2$CH, $^3J_{HH}$ = 6.9 Hz), 1.38 (d, 3H, (C<u>H</u>$_3$)$_2$CH, $^3J_{HH}$ = 6.7 Hz), 1.42 (d, 6H, (C<u>H</u>$_3$)$_2$CH, $^3J_{HH}$ = 6.9 Hz), 1.44 (s, 9H, (C<u>H</u>$_3$)$_3$C), 2.14 and 2.15 (overlapping singlets, 9H, (C<u>H</u>$_3$)$_2$N), 3.02 (sept, 1H, (CH$_3$)$_2$C<u>H</u>, $^3J_{HH}$ = 6.7 Hz), 3.13 (s, 3H, (C<u>H</u>$_3$)$_2$N), 3.70 (sept, 1H, (CH$_3$)$_2$C<u>H</u>, $^3J_{HH}$ = 6.7 Hz), 4.04 (sept, 2H, (CH$_3$)$_2$C<u>H</u>, $^3J_{HH}$ = 6.7 Hz), 4.65 (1H, methine H), 6.98-7.36 (6H, aromatic protons) ppm. ^{13}C{^{1}H} NMR (C_6D_6, 125 MHz): δ_C 24.7, 24.8, 25.0, 25.1, 25.3, 25.9 ((<u>C</u>H$_3$)$_2$CH), 28.0, 28.3, 28.4 ((CH$_3$)$_2$<u>C</u>H), 32.7 (<u>C</u>H$_3$)$_3$C), 38.2, 39.8, 44.4 ((<u>C</u>H$_3$)$_2$N), 73.3 (CH$_3$)$_3$<u>C</u>), 87.2 (methine C), 114.0, 122.5, 124.4, 125.6, 138.5, 140.5, 145.8, 146.9, 149.5 (aromatic C), 169.0, 174.8 (imine quaternary C and silyl-dimethylamino C) ppm. ^{29}Si{^{1}H} NMR (C_6D_6, 99 MHz): δ_{Si} -85.4 ppm. Elemental analysis: calc. for $C_{35}H_{56}N_4OSi$: C 72.86 %, H 9.78 %, N 9.71 %; meas. C 72.72 %, H 9.86 %, N 9.59 %.

Synthesis of (5-Dipp)Si(NDipp){N(SiMe$_3$)$_2$}: To a solution of Na[N(SiMe$_3$)$_2$] (40 mg, 1.1 equiv.) in toluene at -78˚C, was added a solution of (**1-Dipp**)SiCl (108 mg, 0.2 mmol) also in toluene. The reaction mixture was warmed slowly to room temperature and stirred for an additional 15 h. After filtration, volatiles were removed *in vacuo* to yield a red oil. This was re-dissolved in a combination of toluene:hexane (1:4 ratio), and storage at -26˚C afforded the product as pale orange crystals. Yield 0.039 g, 29 %. ^{1}H NMR (C_6D_6, 400 MHz): δ_H 0.33 (s, 9H, (C<u>H</u>$_3$)$_3$Si), 0.51 (d, 3H, (C<u>H</u>$_3$)$_2$CH, $^3J_{HH}$ = 7.1 Hz), 0.53 (s, 9H, (C<u>H</u>$_3$)$_3$Si), 0.58 (d, 3H, (C<u>H</u>$_3$)$_2$CH, $^3J_{HH}$ = 6.6 Hz), 0.77 (d, 3H, (C<u>H</u>$_3$)$_2$CH, $^3J_{HH}$ = 6.8 Hz), 1.24 (d, 3H, (C<u>H</u>$_3$)$_2$CH, $^3J_{HH}$ = 6.9 Hz), 1.27 (d, 3H, (C<u>H</u>$_3$)$_2$CH, $^3J_{HH}$ = 6.6 Hz), 1.34 (d, 3H, (C<u>H</u>$_3$)$_2$CH, $^3J_{HH}$ = 7.0 Hz), 1.40 (d, 3H, (C<u>H</u>$_3$)$_2$CH, $^3J_{HH}$ = 7.1 Hz), 1.59 (d, 3H, (C<u>H</u>$_3$)$_2$CH, $^3J_{HH}$ = 6.8 Hz), 1.72 (s,

3H, (C<u>H</u>$_3$)$_2$N), 2.09 (s, 3H, (C<u>H</u>$_3$)$_2$N), 2.39 (s, 3H, (C<u>H</u>$_3$)$_2$N), 2.76 (sept, 1H, (CH$_3$)$_2$C<u>H</u>, $^3J_{HH}$ = 6.5 Hz), 3.28 (s, 3H, (C<u>H</u>$_3$)$_2$N), 3.63 (sept, 2H, (CH$_3$)$_2$C<u>H</u>, $^3J_{HH}$ = 6.6 Hz), 3.96 (sept, 1H, (CH$_3$)$_2$C<u>H</u>, $^3J_{HH}$ = 6.9 Hz), 4.63 (s, 1H, methine H), 6.82-7.20 (6H, aromatic protons) ppm. ^{13}C{^{1}H} NMR (C_6D_6, 125 MHz): δ_C 5.3, 7.2 ((<u>C</u>H$_3$)$_3$Si), 23.8, 24.1, 24.9, 25.4, 26.4, 26.6, 26,6, 26.7 ((<u>C</u>H$_3$)$_2$CH), 27.3, 27.8, 28.5 ((CH$_3$)$_2$<u>C</u>H), 38.9, 39.7, 40.5, 45.1 ((<u>C</u>H$_3$)$_2$N), 90.4 (methine C), 113.7, 122.6, 123.2, 125.1, 125.7, 127.1, 137.6, 139.9, 140.1, 145.8, 147.6, 147.9 (aromatic C), 170.2, 176.4 (imine quaternary C and silyl-dimethylamino C) ppm. ^{29}Si{^{1}H} NMR (C_6D_6, 99 MHz): δ_{Si} -81.1 (N(imine)-coordinated Si), -1.7, 2.3 (Me$_3$<u>Si</u>) ppm. EI/MS (*m*/*z*, %): 663.4, 8, [M]$^+$; 620.4, 67, [M – NMe$_2$]$^+$; accurate mass: calc. for $C_{37}H_{65}N_5Si_3$ ([M]$^+$) 663.4548, found 663.4523. Elemental analysis: calc. for $C_{37}H_{65}N_5Si_3$: C 66.91 %, H 9.86 %, N 10.54 %; meas. C 66.85 %, H 9.98 %, N 10.42 %.

Synthesis of (1-Dipp)Si{P(SiMe$_3$)$_2$}: The procedure used was identical to that for (**5-Dipp**)Si(NDipp){N(SiMe$_3$)$_2$}, replacing Na[N(SiMe$_3$)$_2$] with Li[P(SiMe$_3$)$_2$](dme) (60 mg, 1.1 equiv.). After the removal of the LiCl salt by filtration, the toluene solution was concentrated to the point of incipient crystallisation, and subsequently stored at -26˚C. After 2 d, the pure product precipitated out of the solution as a red solid. Yield 0.075 g, 55 %. Single crystals suitable for X-ray diffraction were grown from a concentrated solution in toluene at room temperature. ^{1}H NMR (C_6D_6, 400 MHz): δ_H 0.48 (d, 9H, (C<u>H</u>$_3$)$_3$Si, $^3J_{PH}$ = 3.8 Hz), 0.50 (d, 9H, (C<u>H</u>$_3$)$_2$CH, $^3J_{PH}$ = 4.2 Hz), 1.03 (d, 6H, (C<u>H</u>$_3$)$_2$CH, $^3J_{HH}$ = 6.7 Hz), 1.26 (d, 6H, (C<u>H</u>$_3$)$_2$CH, $^3J_{HH}$ = 7.0 Hz), 1.28 (d, 6H, (C<u>H</u>$_3$)$_2$CH, $^3J_{HH}$ = 7.0 Hz), 1.71 (d, 6H, (C<u>H</u>$_3$)$_2$CH, $^3J_{HH}$ = 6.5 Hz), 2.24 (s, 12H,

($C\underline{H}_3)_2N$), 3.21 (virtual sept, 2H, $(CH_3)_2C\underline{H}$, $^3J_{HH}$ = 6.7 Hz), 3.67 (virtual sept, 2H, $(CH_3)_2C\underline{H}$, $^3J_{HH}$ = 6.6 Hz), 4.59 (s, 1H, methine H), 7.05 (dd, 2H, $^3J_{HH}$ = 7.7 Hz, $^4J_{HH}$ = 1.8 Hz, *m*-H of Dipp), 7.12 (t, 2H, $^3J_{HH}$ = 7.6 Hz, *p*-H of Dipp), 7.20 (dd, 2H, $^3J_{HH}$ = 7.6 Hz, $^4J_{HH}$ = 1.8 Hz, *m*-H of Dipp) ppm. $^{13}C\{^1H\}$ NMR (C_6D_6, 101 MHz): δ_C 5.4 (d, $(\underline{C}H_3)_3Si$, $^2J_{CP}$ = 8.8 Hz), 5.9 (d, $(\underline{C}H_3)_3Si$, $^2J_{CP}$ = 10.7 Hz), 24.6 (d, $(\underline{C}H_3)_2CH$, J_{CP} = 3.7 Hz), 26.1 ($(\underline{C}H_3)_2CH$), 28.2, 28.3 (overlapping multiplets, $(\underline{C}H_3)_2CH$ and $(CH_3)_2\underline{C}H$), 29.8 (d, $(CH_3)_2\underline{C}H$, J_{CP} = 4.7 Hz), 40.7 ($(\underline{C}H_3)_2N$), 79.6 (methine C), 124.8, 125.4 (*m*-C of Dipp), 126.3 (*p*-C of Dipp), 142.2 (d, *ipso*-C of Dipp, , J_{CP} = 3.2 Hz), 144.7, 146.2 (*o*-C of Dipp), 166.1 (d, imine quaternary C, J_{CP} = 7.1 Hz) ppm. $^{29}Si\{^1H\}$ NMR (C_6D_6, 80 MHz): δ_{Si} -1.3 (d, $Me_3\underline{Si}$, $^1J_{SiP}$ = 58 Hz), 2.6 (s, $Me_3\underline{Si}$) 18.6 (d, $N\underline{Si}N$, $^1J_{SiP}$ = 213 Hz) ppm. $^{31}P\{^1H\}$ NMR (C_6D_6, 162 MHz): δ_P -230.2 (s, $^1J_{SiP}$ = 46 and 213 Hz) ppm. Elemental analysis: calc. for $C_{37}H_{65}N_4PSi_3$: C 65.24 %, H 9.62 %, N 8.23 %; meas. C 65.16 %, H 9.74 %, N 8.08%.

Synthesis of (5-Dipp)Si(NDipp){P(SiMe$_3$)$_2$}: A solution of (**1-Dipp**)Si{P($SiMe_3$)$_2$} (25 mg, 0.033 mmol) in C_6D_6 (0.5 mL) was heated at 100˚C for 84 h, after which time slow evaporation at room temperature afforded the pure product as dark orange crystals, which were suitable for X-ray crystallography (18 mg, 72 % isolated yield). ^1H NMR (C_6D_6, 400 MHz): δ_H 0.28 (d, 9H, $(C\underline{H}_3)_3Si$, $^3J_{PH}$ = 4.4 Hz), 0.41 (d, 9H, $(C\underline{H}_3)_3Si$, $^3J_{PH}$ = 5.0 Hz), 0.61 (d, 3H, $(C\underline{H}_3)_2CH$, $^3J_{HH}$ = 6.8 Hz), 0.83 (d, 3H, $(C\underline{H}_3)_2CH$, $^3J_{HH}$ = 6.6 Hz), 0.84 (d, 3H, $(C\underline{H}_3)_2CH$, $^3J_{HH}$ = 6.3 Hz), 1.25 (d, 3H, $(C\underline{H}_3)_2CH$, $^3J_{HH}$ = 6.8 Hz), 1.36 (d, 3H, $(C\underline{H}_3)_2CH$, $^3J_{HH}$ = 6.9 Hz), 1.40 (d, 3H, $(C\underline{H}_3)_2CH$, $^3J_{HH}$ = 6.9 Hz), 1.44 (d, 3H, $(C\underline{H}_3)_2CH$, $^3J_{HH}$ = 7.0 Hz), 1.76 (d, 3H,

($C\underline{H}_3)_2CH$, $^3J_{HH}$ = 6.6 Hz), 2.10 (br s, 6H, ($C\underline{H}_3)_2N$), 2.37 (s, 3H, ($C\underline{H}_3)_2N$), 3.05 (sept, 1H, $(CH_3)_2C\underline{H}$, $^3J_{HH}$ = 6.7 Hz), 3.14 (sept, 1H, $(CH_3)_2C\underline{H}$, $^3J_{HH}$ = 6.8 Hz), 3.49 (s, 3H, ($C\underline{H}_3)_2N$), 3.94 (sept, 1H, $(CH_3)_2C\underline{H}$, $^3J_{HH}$ = 6.9 Hz), 4.31 (doublet of septets, 1H, $(CH_3)_2C\underline{H}$, $^3J_{HH}$ = 6.9 Hz, J_{HP} = 2.1 Hz), 4.61 (s, 1H, methine H), 6.81-7.22 (6H, aromatic protons) ppm. $^{13}C\{^1H\}$ NMR (C_6D_6, 101 MHz): δ_C 3.6 (d, ($\underline{C}H_3)_3Si$, $^2J_{CP}$ = 11.6 Hz), 4.8 (d, ($\underline{C}H_3)_3Si$, $^2J_{CP}$ = 12.9 Hz), 24.2, 24.3, 24.6, 25.3, 25.5, 26.2 (($\underline{C}H_3)_2CH$), 27.5 ($(CH_3)_2\underline{C}H$, J_{CP} = 13.9 Hz), 27.9 (d, ($\underline{C}H_3)_2CH$), J_{CP} = 11.5 Hz), 28.3 (d, $(CH_3)_2\underline{C}H$, J_{CP} = 12.5 Hz), 29.1 (($CH_3)_2\underline{C}H$), 38.9, 40.4, 45.4 (($\underline{C}H_3)_2N$), 87.1 (methine C), 114.5, 122.2, 122.8, 125.2, 125.5, 138.1, 138.4, 140.0, 147.2, 147.5, 148.3 (aromatic carbons), 168.5 (d, imine quaternary C, J_{CP} = 3.4 Hz), 174.3 (d, silyl-dimethylamino C, J_{CP} = 13.5 Hz), ppm. $^{29}Si\{^1H\}$ NMR (C_6D_6, 80 MHz): δ_{Si} -75.8 (d, N(imine)-coordinated Si, $^1J_{SiP}$ = 25 Hz), -0.3 (d, $Me_3\underline{Si}$, $^1J_{SiP}$ = 29 Hz), 3.3 (d, $Me_3\underline{Si}$, $^1J_{SiP}$ = 17 Hz) ppm. $^{31}P\{^1H\}$ NMR (C_6D_6, 162 MHz): δ_P -246.3 (s) ppm.

Synthesis of (5-Dipp)Si(NDipp){Si(SiMe$_3$)$_3$}: The procedure used is identical to that for (**5-Dipp**)Si(NDipp){$N(SiMe_3)_2$}, replacing Na[$N(SiMe_3)_2$] with K[$Si(SiMe_3)_3$] (63 mg, 1.1 equiv.). Recrystallisation was achieved by slow-evaporation of a concentrated toluene solution at ambient temperature, affording the product as dark-red crystals. Yield 71 mg, 51 %. (N.B.: X-ray quality crystals were obtained from storage of a concentrated hexane solution at 4˚C for several days). ^1H NMR (C_6D_6, 400 MHz): δ_H 0.37 (s, 27H, ($C\underline{H}_3)_3Si$), 0.81 (d, 3H, ($C\underline{H}_3)_2CH$, $^3J_{HH}$ = 6.8 Hz), 0.88 (d, 3H, ($C\underline{H}_3)_2CH$, $^3J_{HH}$ = 6.6 Hz), 1.23 and 1.24 (overlapping doublets, 9H, ($C\underline{H}_3)_2CH$, $^3J_{HH}$ = 6.8 and 6.6 Hz), 1.30 (d, 6H, ($C\underline{H}_3)_2CH$, $^3J_{HH}$ = 6.9

Hz), 1.33 (d, 3H, (C<u>H</u>$_3$)$_2$CH, $^3J_{HH}$ = 6.7 Hz), 2.01 (br s, 6H, (C<u>H</u>$_3$)$_2$N), 2.31 (s, 3H, (C<u>H</u>$_3$)$_2$N), 2.80 (sept, 1H, (CH$_3$)$_2$C<u>H</u>, $^3J_{HH}$ = 6.6 Hz), 3.40 (s, 3H, (C<u>H</u>$_3$)$_2$N), 3.55 (sept, 1H, (CH$_3$)$_2$C<u>H</u>, $^3J_{HH}$ = 6.6 Hz), 3.89 (sept, 2H, (CH$_3$)$_2$C<u>H</u>, $^3J_{HH}$ = 6.6 Hz), 4.74 (s, 1H, methine H), 6.99 – 7.05 (m, 4H, aromatic protons), 7.29 (d, 2H, aromatic protons) ppm. ^{13}C{^{1}H} NMR (C_6D_6, 101 MHz): δ_C 5.4 ((<u>C</u>H$_3$)$_3$Si), 25.1, 25.3, 25.5, 25.8, 26.5 ((<u>C</u>H$_3$)$_2$CH), 27.5 ((CH$_3$)$_2$<u>C</u>H), 28.3 ((<u>C</u>H$_3$)$_2$CH), 28.9, 29.2 ((CH$_3$)$_2$<u>C</u>H), 38.4, 40.7, 46.3 ((<u>C</u>H$_3$)$_2$N), 90.0 (methine C), 115.1, 122.7, 125.9, 126.7, 126.9, 140.2, 140.9, 143.9, 146.9, 149.3 (aromatic C), 170.8, 176.1 (imine quaternary C and silyl-dimethylamino C) ppm. ^{29}Si{^{1}H} NMR (C_6D_6, 80 MHz): δ_{Si} -127.6 ([SiMe$_3$]$_3$<u>Si</u>), -62.2 (N(imine)-coordinated Si), -10.2 (Me$_3$<u>Si</u>) ppm.

Conversion of (1-Dipp)SiCl to (5-Dipp)Si(NDipp)Cl at 100°C: A solution of (**1-Dipp**)SiCl (25 mg, 0.046 mmol) in C_6D_6 (0.5 mL) was heated at 100˚C for 36 d, with daily spectroscopic monitoring by ^{1}H NMR spectroscopy. The colour of the solution gradually changed from light yellow to dark red. The following spectroscopic data were recorded after 36 d. ^{1}H NMR (C_6D_6, 400 MHz): δ_H 0.98 (d, 3H, (C<u>H</u>$_3$)$_2$CH, $^3J_{HH}$ = 6.8 Hz), 1.02 (d, 3H, (C<u>H</u>$_3$)$_2$CH, $^3J_{HH}$ = 6.8 Hz), 1.06 (d, 3H, (C<u>H</u>$_3$)$_2$CH, $^3J_{HH}$ = 6.6 Hz), 1.25 (d, 6H, (C<u>H</u>$_3$)$_2$CH, $^3J_{HH}$ = 6.9 Hz), 1.46 (d, 3H, (C<u>H</u>$_3$)$_2$CH, $^3J_{HH}$ = 6.5 Hz), 1.48 (d, 6H, (C<u>H</u>$_3$)$_2$CH, $^3J_{HH}$ = 6.9 Hz), 1.98 (br s, 6H, (C<u>H</u>$_3$)$_2$N), 2.17 (s, 3H, (C<u>H</u>$_3$)$_2$N), 3.14 (s, 3H, (C<u>H</u>$_3$)$_2$N), 3.27 (sept, 1H, (CH$_3$)$_2$C<u>H</u>, $^3J_{HH}$ = 6.7 Hz), 3.73 – 3.83 (overlapping multiplets, 3H, (CH$_3$)$_2$C<u>H</u>), 4.57 (s, 1H, methine H), 6.94 – 7.29 (6H, aromatic protons) ppm. ^{13}C{^{1}H} NMR (C_6D_6, 101 MHz): δ_C 24.1, 24.2, 24.5, 25.3, 26.1 ((<u>C</u>H$_3$)$_2$CH), 28.6, 28.7, 29.0 ((CH$_3$)$_2$<u>C</u>H), 38.4, 40.2, 44.6

(($\underline{C}H_3)_2N$), 86.6 (methine C), 115.5, 122.3, 125.1, 125.4, 136.3, 139.8, 146.6, 147.0, 147.6 (aromatic C), 168.4, 171.4 (imine quaternary C and silyl-dimethylamino C) ppm. $^{29}Si\{^1H\}$ NMR (C_6D_6, 80 MHz): δ_{Si} -90.0 ppm.

6.7 References

[1] J. Clayden, S. G. Warren, N. Greeves in *Organic Chemistry*, OUP Oxford, Oxford, **2012**.

[2] J. Emsley in *The Elements* 3rd ed., Clarendon Press, Oxford, **1998**.

[3] a) M. W. Schmidt, P. N. Truong, M. S. Gordon, *J. Am. Chem. Soc.* **1987**, *109*, 5217–5227; b) P. von Rague Schleyer, D. Kost, *J. Am. Chem. Soc.* **1988**, *110*, 2105–2109; c) J. Küpp, M. Remko, P. von R. Schleyer, *J. Am. Chem. Soc.* **1996**, *1118*, 5745–5751; d) V. G. Avakyan, V. F. Sidorkin, E. F. Belogolova, S. L. Guselnikov, L. E. Gusel'nikov, *Organometallics* **2006**, *25*, 6007–6013. Selected reviews discussing the topic of tetrelones: e) G. Raabe, J. Michl, *Chem. Rev.* **1985**, *85*, 419-509; f) Y. Mizuhata, T. Sasamori, N. Tokitoh, *Chem. Rev.* **2009**, *109*, 3479–3511; g) R. C. Fischer, P. P. Power, *Chem. Rev.* **2010**, *110*, 3877–3923.

[4] S. Patai, Z. Rappoport, Y. Apeloig, in *The Chemistry of Organic Silicon Compounds*, *Vol.* 2, Wiley, Chichester, **1998**.

[5] C. Friedel, J. Crafts, *Ann. Chim. Phys.* **1866**, *9*, 5.

[6] a) F. S. Kipping, L. L. Lloyd, *J. Chem. Soc. Trans.* **1901**, *79*, 449–459; b) R. Robison, F. S. Kipping, *J. Chem. Soc., Trans.* **1908**, *93*, 439-456.

[7] a) J. W. Hastie, R. H. Hauge, J. L. Margrave, *Inorganica Chim. Acta* **1969**, *3*, 601–606; b) C. A. Arrington, J. Michl, R. West, *J. Am. Chem. Soc.* **1983**, *105*, 6176–6177; c) R. Withnall, L. Andrews, *J. Am. Chem. Soc.* **1985**, *107*, 2567–2568; d) D. A. Dixon, J. L. Gole, *Chem. Phys. Lett.* **1986**, *125*, 179–183; e) R. Withnall, L. Andrews, *J. Phys. Chem.* **1988**, *92*, 594–602.

[8] a) R. J. Glinski, J. L. Gole, D. A. Dixon, *J. Am. Chem. Soc.* **1985**, *107*, 5891–5894; b) S. Bailleux, M. Bogey, C. Demuynck, J. L. Destombes, A. Walters, *J. Chem. Phys.* **1994**, *101*, 2729–2733.

[9] a) B. Gehrhus, M. F. Lappert, J. Heinicke, R. Boese, D. Bläser, *J. Chem. Soc. Chem. Commun.* **1995**, 1931–1932; b) R. West, M. Denk, *Pure Appl. Chem.* **1996**, *68*, 785–788; c) W. Li, N. J. Hill, A. C. Tomasik, G. Bikzhanova, R. West, *Organometallics* **2006**, *25*, 3802–3805; d) A. C. Tomasik, A. Mitra, R. West, *Organometallics* **2009**, *28*, 378–381; e) P. Zark, A. Schäfer, A. Mitra, D. Haase, W. Saak, R. West, T. Müller, *J. Organomet. Chem.* **2010**, *695*, 398–408; f) M. Asay, S. Inoue, M. Driess, *Angew. Chem. Int. Ed.* **2011**, *50*, 9589–9592; g) T. Abe, R. Tanaka, S. Ishida, M. Kira, T. Iwamoto, *J. Am. Chem. Soc.* **2012**, *134*, 20029–20032; h) T. Kosai, S. Ishida, T. Iwamoto, *Angew. Chem. Int. Ed.* **2016**, *55*, 15554–15558; i) H. Wang, T. L. Chan, Z. Xie, *Chem. Commun.* **2018**, *54*, 385–388. Selected reviews on silylenes: j) M. Haaf, T. A. Schmedake, R. West, *Acc. Chem. Res.* **2000**, *33*, 704–714; k) N. J. Hill, R. West, *J. Organomet. Chem.* **2004**, *689*, 4165–4183.

[10] a) T. Iwamoto, H. Masuda, S. Ishida, C. Kabuto, M. Kira, *J. Am. Chem. Soc.* **2003**, *125*, 9300–9301; b) A. Naka, N. J. Hill, R. West, *Organometallics* **2004**, *23*, 6330–6332.

[11] a) Y. Xiong, S. Yao, M. Driess, *J. Am. Chem. Soc.* **2009**, *131*, 7562–7563; b) Y. Xiong, S. Yao, R. Müller, M. Kaupp, M. Driess, *Nat. Chem.* **2010**, *2*, 577–580; c) S. Yao, Y. Xiong, M. Driess, *Chem. Eur. J.* **2010**, *16*, 1281–1288. d) R. Rodriguez, D. Gau, T. Troadec, N. Saffon-Merceron, V. Branchadell, A. Baceiredo, T. Kato, *Angew. Chem. Int. Ed.* **2013**, *52*, 8980–8983; e) R. Rodriguez, T. Troadec, D. Gau, N. Saffon-Merceron, D. Hashizume, K. Miqueu, J. M. Sotiropoulos, A. Baceiredo, T. Kato, *Angew. Chem. Int. Ed.* **2013**, *52*, 4426–4430; f) A. C. Filippou, B. Baars, O. Chernov, Y. N. Lebedev, G. Schnakenburg, *Angew. Chem. Int. Ed.* **2014**, *53*, 565–570; g) T. Muraoka, K. Abe, H. Kimura, Y. Haga, K. Ueno, Y. Sunada, *Dalton Trans.* **2014**, *43*, 16610–16613; h) M. M. Linden, H. P. Reisenauer, D. Gerbig, M. Karni, A. Schäfer, T. Müller, Y. Apeloig, P. R. Schreiner, *Angew. Chem. Int. Ed.* **2015**, *54*, 12404–12409; i) I.

Alvarado-Beltran, A. Rosas-Sánchez, A. Baceiredo, N. Saffon-Merceron, V. Branchadell, T. Kato, *Angew. Chem. Int. Ed.* **2017**, *56*, 10481–10485; j) D. Wendel, D. Reiter, A. Porzelt, P. J. Altmann, S. Inoue, B. Rieger, *J. Am. Chem. Soc.* **2017**, *139*, 17193–17198. A comprehensive review on stable silanones can be found at: k) Y. Xiong, S. Yao, M. Driess, *Angew. Chem. Int. Ed.* **2013**, *52*, 4302–4311.

[12] a) S. Yao, Y. Xiong, M. Brym, M. Driess, *J. Am. Chem. Soc.* **2007**, *129*, 7268–7269; b) S. Yao, M. Brym, C. Van Wüllen, M. Driess, *Angew. Chem. Int. Ed.* **2007**, *46*, 4159–4162; c) Y. Xiong, S. Yao, M. Driess, *Angew. Chem. Int. Ed.* **2010**, *49*, 6642–6645; d) R. S. Ghadwal, R. Azhakar, H. W. Roesky, K. Pröpper, B. Dittrich, S. Klein, G. Frenking, *J. Am. Chem. Soc.* **2011**, *133*, 17552–17555; e) R. S. Ghadwal, R. Azhakar, H. W. Roesky, K. Pröpper, B. Dittrich, C. Goedecke, G. Frenking, *Chem. Commun.* **2012**, *48*, 8186; f) R. Rodriguez, D. Gau, J. Saouli, A. Baceiredo, N. Saffon-Merceron, V. Branchadell, T. Kato, *Angew. Chem. Int. Ed.* **2017**, *56*, 3935–3939.

[13] a) C. W. So, H. W. Roesky, J. Magull, R. B. Oswald, *Angew. Chem. Int. Ed.* **2006**, *45*, 3948–3950; b) D. Gau, T. Kato, N. Saffon-Merceron, A. De Cózar, F. P. Cossío, A. Baceiredo, *Angew. Chem. Int. Ed.* **2010**, *49*, 6585–6588; c) S. S. Sen, H. W. Roesky, D. Stern, J. Henn, D. Stalke, *J. Am. Chem. Soc.* **2010**, *132*, 1123–1126; d) A. C. Filippou, O. Chernov, B. Blom, K. W. Stumpf, G. Schnakenburg, *Chem. Eur. J.* **2010**, *16*, 2866–2872; e) R. Azhakar, R. S. Ghadwal, H. W. Roesky, H. Wolf, D. Stalke, *Organometallics* **2012**, *31*, 4588–4592; f) Y. Xiong, S. Yao, S. Inoue, E. Irran, M. Driess, *Angew. Chem. Int. Ed.* **2012**, *51*, 10074–10077; g) M. Driess, S. Yao, Y. Xiong, A. Kostenko, *Dalton Trans.* **2018**, 2152–2155.

[14] a) A. Jana, R. Azhakar, S. P. Sarish, P. P. Samuel, H. W. Roesky, C. Schulzke, D. Koley, *Eur. J. Inorg. Chem.* **2011**, 5006–5013; b) S. Khan, S. S. Sen, D. Kratzert, G. Tavčar, H. W. Roesky, D. Stalke, *Chem. Eur. J.* **2011**, *17*, 4283–4290.

[15] O. H. Wheeler in *The Chemistry of Acyl Halides* (Ed.: S. Patai), Wiley, New York, **1972**, pp. 231–251.

[16] L. D. Doerrer, M. L. H. Green, *J. Chem. Soc. Dalton Trans.***1999**, 4325-4329.

[17] M. Kaftory, M. Kapon, M. Botoshansky in *The Chemistry of Organic Silicon Compounds*, *Vol.2* (Eds.: Z. Rappoport, Y. Apeloig), Wiley, Chichester, **1998**, pp. 181-265.

[18] J. D. Epping, S. Yao, M. Karni, Y. Apeloig, M. Driess, *J. Am. Chem. Soc.* **2010**, *132*, 5443–5455.

[19] a) X. Li, X. Cheng, H. Song, C. Cui, *Organometallics* **2007**, *26*, 1039–1043; b) W. Wang, S. Yao, C. Van Wüllen, M. Driess, *J. Am. Chem. Soc.* **2008**, *130*, 9640–9641; c) W. D. Woodul, A. F. Richards, A. Stasch, M. Driess, C. Jones, *Organometallics* **2010**, *29*, 3655–3660; d) J. Li, X. Li, W. Huang, H. Hu, J. Zhang, C. Cui, *Chem. Eur. J.* **2012**, *18*, 15263–15266; e) S. L. Choong, C. Schenk, A. Stasch, D. Dange, C. Jones, *Chem. Commun.* **2012**, *48*, 2504–2506; f) L. Xie, J. Zhang, H. Hu, C. Cui, *Organometallics* **2013**, *32*, 6875–6878.

[20] a) F. Basuli, U. J. Kilgore, D. Brown, J. C. Huffman, D. J. Mindiola, *Organometallics* **2004**, *23*, 6166–6175; b) G. Bai, P. Wei, D. W. Stephan, *Organometallics* **2006**, *25*, 2649–2655; c) H. Hamaki, N. Takeda, N. Tokitoh, *Organometallics* **2006**, *25*, 2457–2464; d) N. C. Tomson, J. Arnold, R. G. Bergman, *Organometallics* **2010**, *29*, 5010–5025; e) Y. Han, H. V. Huynh, *Dalton Trans.* **2011**, *40*, 2141–2147.

[21] a) H. H. Karsch, U. Keller, S. Gamper, G. Müller, *Angew. Chem. Int. Ed.* **1990**, *29*, 295–296; b) C. W. So, H. W. Roesky, P. M. Gurubasavaraj, R. B. Oswald, M. T. Gamer, P. G. Jones, S. Blaurock, *J. Am. Chem. Soc.* **2007**, *129*, 12049–12054; c) S. Inoue, W. Wang, C. Präsang, M. Asay, E. Irran, M. Driess, *J. Am. Chem. Soc.* **2011**, *133*, 2868–2871; d) R. Azhakar, R. S. Ghadwal, H. W. Roesky, H. Wolf, D. Stalke, *Organometallics* **2012**, *31*, 4588–4592; e) K. Hansen, T. Szilvási, B. Blom, E. Irran, M. Driess, *Chem. Eur. J.* **2015**, *21*, 18930–18933; f) H. Cui, J. Zhang, Y. Tao, C. Cui, *Inorg. Chem.* **2016**, *55*, 46–50. For a recent review on the topic of phosphidosilylene, see: g) P. Bag, S. U. Ahmad, S. Inoue, *Bull. Chem. Soc. Jpn.* **2017**, *90*, 255–271.

[22] A. V. Protchenko, A. D. Schwarz, M. P. Blake, C. Jones, N. Kaltsoyannis, P. Mountford, S. Aldridge, *Angew. Chem. Int. Ed.* **2013**, *52*, 568–571.

CHAPTER 7

CONCLUSIONS

In this thesis, the syntheses of amino-functionalised β-diketiminate protio-ligands ("*N*-nacnacH"), and their application in Main Group coordination chemistry are examined. These efforts are designed to probe the hypothesis that incorporating π-donating amino groups into the ligand scaffold would induce changes in the electronic properties of the resulting metal complexes. A modified procedure based on pioneering works by Viehe and Clyburne allows for the isolation of protio-ligands of the form (**1-Ar**)H (Ar = Ph, *o*-Xyl, Dipp). These molecules exist in a diimine configuration in both solution and solid phases, rather than the more common imino-enamine form, as shown by NMR and crystallographic studies. On the other hand, attempts to synthesise (**1-Mes**)H by this route were thwarted by the formation of the cationic spirocycle **3** as the sole product. The critical role played by deprotonation of the *para*-Me group in this unusual transformation is illustrated by the successful synthesis of the corresponding *ortho*-xylyl system, (**1**-Xyl)H. In addition, while the generation of (**1-^{t}Bu**)H *via* this methodology was confirmed by spectroscopic techniques, the low isolated yield – and strictly anaerobic conditions required in this case to prevent rearrangement/isomerisation – precluded further investigation.

Direct metallation of (**1-Ar**)H with ^{n}BuLi or $AlMe_3$ affords the corresponding lithiated (Ar = Ph, *o*-Xyl, Dipp) or aluminated (Ar = Ph, Dipp) *N*-nacnac complexes. In particular, the use of the lithiated ligands as precursors to other sub-valent Main

Group complexes *via* transmetallation has been exploited, leading to the isolation of donor-stabilised monochlorotetrelenes of the form of (**1-Ar**)ECl (Ar = Ph/*o*-Xyl/Dipp for E = Ge and Sn, and Ar = Dipp for E = Si). Notably, (**1-Dipp**)SiCl represents one of the first examples of a β-diketiminate-supported chlorosilylene complex. Spectroscopic studies reveal that, for all the metal complexes, the ^{1}H and ^{13}C NMR resonances associated with the γ-CH group of the ligand backbone are shifted significantly upfield compared to those in their Nacnac analogues – consistent with the π-donor nature of the NMe_2 groups. Furthermore, solid state structural comparisons of the germylene and stannylene species hint at a systematic influence of the steric profile of the *N*-bound aryl groups on the molecular metrics of the respective complexes.

The scope of reactivity studies with *N*-nacnac chlorotetrelenes has been investigated. The generation of cationic species of the type [(**1-Dipp**)E]$^{+}$ *via* chloride abstraction has been demonstrated (for E = Si, Ge, Sn) using the lithium salt of the weakly-coordinating anion $[Al(OR^F)_4]^-$. Anion exchange processes have also been employed to facilitate the formation of heavier Group 14 hydrido- and phosphaketenyl-tetrelene complexes, of the form (**1-Dipp**)EH and (**1-Dipp**)E(PCO) (E = Ge, Sn) respectively. Of particular interest is the photochemical behaviour of (**1-Dipp**)Ge(PCO), which is found to undergo UV-induced P─C bond cleavage and C─C bond insertion to yield a bicyclic *N,P*-heterocyclic germylene **4**. Two plausible reaction pathways are proposed for this transformation, which involve either a

concerted mechanism or a stepwise mechanism *via* a germaphosphinidene intermediate.

With respect to the corresponding silicon chemistry, the availability of the synthetically versatile chloro-silylene (**1-Dipp**)SiCl has allowed access to a monomeric *sila*-acyl chloride (**1-Dipp**)Si(O)Cl *via* mild oxidation. Further reaction *via* nucleophilic substitution affords the *sila*-aldehyde (**1-Dipp**)Si[O(BEt_3)]H and *sila*-ester (**1-Dipp**)Si(O)(O^tBu). This transformation, while near ubiquitous in carbonyl chemistry, has been shown for the first time to be applicable to the Si=O functional group. Notably, the Lewis-acid-free *sila*-acyl chloride and *sila*-ester possess remarkably short Si=O bond distances, which are comparable to those of the structurally-characterised three-coordinate silanones, and presumably implies appreciable multiple bond character in the silicon-oxygen bond.

Interestingly, exchanging the silicon-bound chloride group in (**1-Dipp**)SiCl for a stronger electron-donating substituent R has been found to initiate a ring contraction process, which involves formal reductive C=N bond cleavage within the *N*-nacnac ligand backbone and oxidation of Si^{II} to Si^{IV}, when R = H, O^tBu, $N(SiMe_3)_2$, and $Si(SiMe_3)_3$. This leads to the formation of aza-butadienyl Si^{IV}-complexes of the form (**5-Dipp**)Si(NDipp)R. Computational studies suggest a mechanism which proceeds *via* a single transition state, and involving interaction between the HOMO (a lone pair on the Si^{II} centre) and the LUMO (backbone C=N antibonding orbital) of the six-membered ring (**1-Dipp**)SiR species. While the Si^{IV} configuration (**5-Dipp**)Si(NDipp)R is found to be the most thermodynamically stable form for all

R substituents, a σ-withdrawing group (such as Cl) drastically increases the energy barrier associated with the process – an observation which explains the persistence of (**1-Dipp**)SiCl at ambient temperature and above. Among the systems investigated, (**1-Dipp**)Si{P($SiMe_3$)$_2$} is the only other system not to undergo ring contraction at room temperature. Nonetheless, in line with the calculated (exoergic) energies of formation of the (**5-Dipp**)Si(NDipp)R complexes, the conversion of (**1-Dipp**)SiCl and (**1-Dipp**)Si{P($SiMe_3$)$_2$} to their corresponding aza-butadienyl forms is enabled by prolonged heating, with the identity of the product being unambiguously confirmed by crystallographic studies for the phosphide system.